

**Phenotypic Features  
of the Visual System in Albinism**

Thesis submitted for the degree of  
Doctor of Philosophy  
at the University of Leicester

By

Viral Sheth BSc. (Hons.)  
Ophthalmology Group  
University of Leicester

2018

*In loving memory of my late Father,*

*Mukesh M. Sheth*

## **Abstract**

### **Phenotypic Features of the Visual System in Albinism**

**Author: Viral Sheth**

#### **Purpose**

The main aims were to: 1) characterise the morphology of the iris structures and investigate the diagnostic potential of changes in albinism, 2) investigate visual field changes in albinism and 3) to analyse the relationship between refractive error/iris pigmentation and foveal hypoplasia in infantile nystagmus.

#### **Methodology**

The iris was imaged in 55 individuals with albinism and 45 controls using anterior segment optical coherence tomography (OCT) and segmented using ImageJ software. Visual field assessment using Humphrey field analyser was carried out on 61 individuals with albinism and 32 individuals with idiopathic infantile nystagmus (IIN), and were compared to posterior OCT parameters. Refractive measures were compared to foveal hypoplasia in different groups with nystagmus (albinism=33, IIN=18, *PAX6*=9 and achromatopsia=12) and iris posterior epithelial layer (PEL) thickness in albinism.

#### **Results**

The iris posterior epithelial layer (PEL) in albinism demonstrates significant thinning compared to controls, especially at the ciliary end ( $P<0.001$ ). Ciliary PEL thickness demonstrated 85% sensitivity and 78% specificity in aiding the diagnosis of albinism.

Visual field measurements showed that detection thresholds in albinism were significantly worse than in IIN ( $P<0.001$ ). In albinism the upper nasal visual field quadrant demonstrated poorer detection thresholds compared to other quadrants ( $P<0.05$  for all comparisons). Left eyes had lower detection thresholds than right eyes ( $P<0.0001$ ). Changes in peripapillary retinal nerve fibre layer were not associated with these changes in detection thresholds.

Worse foveal hypoplasia was associated with myopia in achromatopsia but with hypermetropia in albinism. Increasing hypermetropia in albinism was associated with PEL thinning ( $P<0.01$ ).

#### **Conclusion**

The PEL demonstrates significant thinning in albinism which may be used as a diagnostic aid. The cause of lower detection thresholds within the upper nasal visual field and left eyes in albinism is unclear. Hyperillumination appears more important than foveal hypoplasia in the development of refractive error in albinism.

## Acknowledgements

This work would not have been possible without the kindness and participation of the many volunteers who contributed their time to this study; I extend my appreciation to each and every one.

I would like to express heartfelt gratitude to my two principal supervisors, Dr Frank A. Proudlock and Professor Irene Gottlob, for their support, patience and mentorship which have navigated me through the multiple challenges I have encountered along this journey. I also wish to acknowledge their influence in inspiring me to pursue several opportunities which have provided me with many exciting prospects over the past few years.

I thank all of my collaborators and colleagues within the Ophthalmology department at the University of Leicester for their tireless encouragement, enthusiasm, efforts and constant supply of cake! A special acknowledgment must be paid to Dr Sarim Mohammad whom I worked alongside for the initial patient recruitment and to Dr Rebecca Mclean who facilitated in patient recruitment as well as providing me with practical and constructive feedback on my thesis.

I take this opportunity to honour The Ulverscroft Foundation who have funded my research role at the University of Leicester and the Nystagmus Network who have been invaluable in the recruitment of study participants by raising awareness of my research amongst families and supporters.

My final mention is that of my amazing family: firstly, my wife Puja whose perseverance and unconditional love have inspired me throughout this journey; my mother whose motivation, wisdom and prayers have guided me and my sister who has always urged me to be the best version of myself.

*I am just a child who has never grown up. I still keep asking these “how” and “why” questions.  
Occasionally, I find an answer.*

*Professor Stephen Hawking*

# Table of Contents

Chapter 1	Introduction .....	1
1.1	Overview of Thesis .....	2
1.2	Albinism.....	5
1.2.1	The History of Albinism .....	5
1.2.2	What is Albinism?.....	5
1.2.3	Types of Albinism .....	6
1.2.4	Prevalence of Albinism.....	7
1.3	Consequences of Albinism .....	7
1.3.1	Psychosocial Implications.....	7
1.3.2	Cutaneous Implications (Hair and Skin) .....	9
1.3.3	Visual System Implications.....	9
1.4	Mechanism behind Albinism.....	10
1.4.1	Understanding Melanocytes and Melanosomes .....	10
1.4.2	Melanin in the Eye .....	10
1.4.3	Mechanism behind Melanin Biosynthesis .....	11
1.4.4	The Importance of L-DOPA in Retinal Development in Albinism.....	11
1.5	Genotypes in Albinism .....	13
1.5.1	Genetic Classification of Albinism .....	13
1.5.2	Types of Oculocutaneous Albinism (OCA).....	14
1.5.3	Types of Ocular Albinism (OA) .....	22
1.5.4	Hypopigmentation Disorders Associated with Albinism.....	24

1.5.5	FHONDA .....	26
1.6	Phenotypic Characteristics in Albinism .....	28
1.6.1	Pigmentation in Albinism .....	28
1.6.2	Reduced Vision .....	28
1.6.3	Strabismus.....	29
1.6.4	Stereoscopic Vision .....	30
1.6.5	Abnormal Head Posture (AHP).....	31
1.6.6	Abnormal Refractive Errors.....	32
1.6.7	Positive Angle Kappa .....	33
1.6.8	Nystagmus.....	35
1.6.9	Iris Transillumination.....	40
1.6.10	Macular Hypoplasia.....	42
1.6.11	Foveal Hypoplasia .....	43
1.6.12	Optic Nerve Abnormalities.....	45
1.6.13	Misrouting of Optic Nerve/Chiasmal Misrouting.....	47
1.6.14	Visual Field Deficits in Albinism.....	49
1.7	Chiasmal and Post-Chiasmal Abnormalities in Albinism .....	50
1.7.1	The Optic Chiasm and the Optic Tract .....	50
1.7.2	The Lateral-Geniculate Nucleus (LGN) .....	52
1.8	Research Questions and Aims.....	55
Chapter 2	Methodology.....	57
2.1	Patient Recruitment .....	58

2.1.1	Albinism and other Nystagmus-Associated Conditions .....	58
2.1.2	Control Group .....	60
2.1.3	Consent and Ethical Approval .....	60
2.2	Clinical Characterisation of Participants .....	61
2.2.1	Orthoptics Assessment .....	61
2.2.2	Investigation of Nystagmus Type – Examination .....	65
2.2.3	Data Analysis .....	77
Chapter 3	Anterior Segment Imaging in Albinism (Study 1) .....	78
3.1	Introduction .....	79
3.1.1	Iris Structure.....	79
3.1.2	Iris Morphology and Ultrastructure .....	81
3.1.3	Pigmentation in the Iris.....	83
3.1.4	Aims and Rationale for Study 1.....	89
3.1.5	Hypotheses.....	89
3.2	Methodology for Study 1 .....	90
3.2.1	Patient Characteristics .....	90
3.2.2	Anterior Segment Optical Coherence Tomography.....	90
3.2.3	Data Analysis.....	95
3.2.4	Statistical Analysis .....	101
3.3	Iris OCT Results.....	102
3.3.1	Summary of Volunteers Used in this Study.....	102
3.3.2	Differences in Iris Layers between Albinism and Controls.....	103

3.3.3	The Comparison of Iris Layers between Albinism and Controls .....	103
3.3.4	Iris Thickness Compared to Iris Transillumination Grading .....	105
3.3.5	Using PEL Thickness as a Diagnostic Aid for Albinism .....	107
3.3.6	Correlations to Other Phenotypic Features .....	109
3.3.7	Changes in Iris Thickness with Age.....	112
3.4	Discussion.....	113
3.4.1	Structural Differences between Albinism and Controls.....	113
3.4.2	Changes in the Posterior Epithelial Layer (PEL) .....	114
3.4.3	Changes with Age .....	115
3.4.4	A Comparison of Iris Transillumination and Iris Layers.....	116
3.4.5	The Diagnostic Ability of AS-OCT.....	117
3.5	Study Limitations.....	119
3.6	Future Studies .....	119
Chapter 4	Visual Fields in Albinism (Study 2).....	121
4.1	Introduction .....	122
4.1.1	Principles of Visual Field Assessment.....	122
4.1.2	The Importance of Visual Field Assessment.....	123
4.1.3	Visual Field Assessment Techniques .....	124
4.1.4	Previous Studies on Visual Fields in Albinism .....	129
4.1.5	Aims and Rationale for Study 2.....	133
4.1.6	Hypotheses.....	133
4.2	Methodology for Study 2 .....	135

4.2.1	Patient Characteristics .....	135
4.2.2	Additional Examinations for Study 2.....	135
4.2.3	Visual Field - Data Analysis.....	143
4.3	Results .....	144
4.3.1	Participants Summary .....	144
4.3.2	Visual Field Differences between Albinism and IIN .....	144
4.3.3	Nasal/Temporal Differences in Albinism and IIN .....	146
4.3.4	Quadrant Differences in Albinism and IIN .....	149
4.3.5	Right and Left Eye Differences in Albinism and IIN.....	151
4.3.6	Sighting Dominance for Albinism and IIN .....	152
4.3.7	Visual Field Comparisons to VEP Asymmetry and BCVA in Albinism .....	160
4.4	Discussion.....	162
4.4.1	Summary of Findings.....	162
4.4.2	Nasal/Temporal Asymmetry .....	162
4.4.3	Upper Nasal Visual Field Defect in albinism.....	163
4.4.4	Right-Left Eye Differences and Eye Dominance .....	164
4.4.5	Mechanisms behind Visual Field Deficits in Albinism .....	165
4.5	Study Limitations.....	166
4.6	Future Studies/Following Chapter .....	167
Chapter 5 The Comparison of Central and Peripheral Visual Field to Foveal and Optic Nerve		
OCT Parameters in Albinism (Study 3) .....		168
5.1	Introduction .....	169

5.1.1	Foveal Hypoplasia in Albinism.....	169
5.1.2	Optic Nerve findings in Albinism.....	169
5.1.3	Aims and Rationale .....	174
5.1.4	Hypotheses.....	174
5.2	Methodology for Study 3 .....	175
5.2.1	Imaging and Analysis.....	175
5.3	Results.....	183
5.3.1	Foveal OCT Correlation with Central Detection Threshold.....	183
5.3.2	Correlation of Detection Threshold to ppRNFL Thickness .....	185
5.4	Discussion.....	186
5.4.1	The Comparison of Foveal OCT Layers with Central Detection Threshold .....	186
5.4.2	The Correlation of ppRNFL Measures with Peripheral Detection Threshold...	186
5.4.3	Cortical Deficits .....	187
5.5	Study Limitations.....	189
5.6	Future Studies .....	189
Chapter 6 Investigating the Relationship between Foveal Morphology and Refractive Error in Infantile Nystagmus (Study 4).....		190
6.1	Introduction .....	191
6.1.1	General Introduction.....	191
6.1.2	Refractive Error .....	192
6.1.3	Genetic and Environmental Factors Affecting Refractive Errors .....	195
6.1.4	Refractive Error in Albinism .....	195

6.1.5	Aims and Rationale for Study 4 .....	198
6.1.6	Hypotheses.....	198
6.2	Methodology for Study 4 .....	199
6.2.1	Participants and Data Collection .....	199
6.2.2	Refraction.....	199
6.2.3	OCT Imaging and Analysis .....	199
6.2.4	Clinical Grading of Foveal Hypoplasia .....	200
6.2.5	Axial Length Measurement .....	202
6.3	Results.....	203
6.3.1	Patient Demographics.....	203
6.3.2	Foveal Hypoplasia .....	204
6.3.3	Best Corrected Visual Acuity (BCVA).....	207
6.3.4	Refractive Differences between Groups .....	210
6.3.5	The Comparison of Refractive Measures with FHG and FDI.....	214
6.3.6	The Importance of Axial Length on Foveal Hypoplasia and Refractive Error ...	219
6.4	Discussion.....	223
6.4.1	Albinism.....	223
6.4.2	Other Groups.....	227
6.4.3	Intergroup Differences .....	228
6.5	Limitations of study.....	230
6.6	Future Direction .....	230
Chapter 7	Conclusion .....	231

7.1	Principle Findings .....	232
7.2	The Significance of Study Findings .....	234
7.3	Clinical, Scientific and Methodological Advancements.....	242
7.3	Final Thoughts .....	244
7.4	Future Research .....	244
7.5	Publication Plan .....	244
8.0	Appendices .....	246
9.0	References .....	255

## List of Tables

Table 1-1: Genetic details of OCA1-OCA7 .....	13
Table 1-2: The 3 levels of macular transparency. ....	42
Table 2-1: Participant numbers for each separate research study .....	60
Table 2-2: VEP amplitudes acquired for the calculation of lasym. ....	72
Table 3-1: A summary of details for all volunteers used within the study .....	102
Table 3-2: Iris thickness measures and iris transillumination grading in relation to phenotypic characteristics .....	109
Table 3-3: Iris Thicknessmeasures compared to retinal layers. ....	111
Table 3-4: Statistical analysis of change in iris layer thickness with age. ....	112
Table 4-1: Visual field assessment and advantages and disadvantages. ....	128
Table 4-2: Description of visual field annotation .....	140
Table 4-3: Patient demographics for visual field study.....	144
Table 4-4: Level of amblyogenic factors in individuals with albinism without amblyopia .....	157
Table 4-5 : VEP/BCVA compared to visual field .....	161
Table 5-1: Foveal OCT (central and peripheral) correlations with visual field.....	184
Table 5-2: ppRNFL OCT (around optic nerve) correlations with visual field .....	185
Table 6-1: Patient demographics for all 4 groups used in study.....	203

## Table of Figures

Figure 1-1: Animals and plants exhibiting features of albinism.....	6
Figure 1-2: Individuals with oculocutaneous and ocular albinism.....	7
Figure 1-3: Model on melanosome biogenesis.....	10
Figure 1-4: The Pathway of melanin biosynthesis. ....	11
Figure 1-5: Pigmentation in patients with albinism.....	15
Figure 1-6: Images of a patient with temperature sensitive OCA.....	16
Figure 1-7: Individuals demonstrating the phenotype of OCA2.....	17
Figure 1-8: African parents with their two children affected by brown OCA (BOCA).....	18
Figure 1-9: An individual of Chinese descent with OCA4.....	19
Figure 1-10: Phenotype in OCA5.....	20
Figure 1-11: Examples of two individuals with OA. ....	22
Figure 1-12: Types of strabismus.....	30
Figure 1-13: Abnormal head postures associated with nystagmus.....	32
Figure 1-14: Angle kappa. ....	35
Figure 1-15: Nystagmus waveforms commonly seen in infantile nystagmus.....	36
Figure 1-16: Iris transillumination defect seen in albinism.....	41
Figure 1-17: Iris transillumination grading scheme (Summers et al (1988)).....	41
Figure 1-18: The 3 grades of macular transparency (Summers et al (1988)).....	42
Figure 1-19: Illustration of typical and atypical grades of foveal hypoplasia.....	44
Figure 1-20: Optic nerve differences between individuals with albinism and controls.....	46
Figure 1-21: VEP differences in albinism and IIN.....	48
Figure 1-22: Axonal projection – optic nerve and optic tract.....	51
Figure 1-23: Schematic of visual field representation in the visual cortex in albinism and controls.....	54
Figure 2-1: Clinical examination and diagnosis.....	58

Figure 2-2: Precision vision visual acuity testing system (PVVAT). .....	61
Figure 2-3: Orthoptics equipment for assessment .....	62
Figure 2-4: Nine positions of gaze assessed using ocular motility testing.....	62
Figure 2-5: The Frisby stereotest .....	63
Figure 2-6: The Ishihara colour vision test .....	64
Figure 2-7: (A) slit lamp; (B) fundus photo; (C) iris transillumination photo .....	65
Figure 2-8: Eye movement recordings set up .....	66
Figure 2-9: Eye movement recording trace demonstrating horizontal null point width.....	67
Figure 2-10: Eye movement recording analysis .....	68
Figure 2-11: VEP comparison in albinism and IIN .....	69
Figure 2-12: VEP response lateralisation (Apkarian Method).....	70
Figure 2-13: Asymmetry index distributions (above 0.7=albinism) .....	72
Figure 2-14: Schematic diagram of Optical Coherence Tomography .....	74
Figure 2-15: Image of SOCT Copernicus HR: OPTOPOL.....	75
Figure 2-16: OCT demonstrating different types of foveal hypoplasia.....	76
Figure 3-1: The range of iris colours.....	79
Figure 3-2: (A) Structures within the eye. (B) Structure within the iris .....	80
Figure 3-3: Morphological and histological structure of a normal iris.....	81
Figure 3-4: Melanosome and melanocytic distribution in different coloured eyes .....	84
Figure 3-5: Different iris colours and corresponding iris transillumination defect.....	85
Figure 3-6: An illustration of where each scan was taken for the AS-OCT. ....	91
Figure 3-7: Iris scans obtained from AS-OCT (useable and non-useable).....	92
Figure 3-8: Modified Schmitz classification for pigmentation. ....	94
Figure 3-9: Black and white image of a selected iris AS-OCT.....	96
Figure 3-10: Image J programme bar for layer segmentation. ....	96
Figure 3-11: OCT image with the posterior epithelial layer (PEL) converted to white pixels.....	96

Figure 3-12: OCT image with the full iris structure converted to white pixels .....	97
Figure 3-13: Example of images ready to run through a macro for image analysis .....	97
Figure 3-14: Signs of foveal architecture on OCT scan .....	99
Figure 3-15: OCT flattening .....	100
Figure 3-16: Iris layers thickness – albinism compared to controls.....	104
Figure 3-17: Iris transillumination grades compared to the thickness of iris layers.....	106
Figure 3-18: Histogram for PEL Q4 (ciliary quadrant) thickness in albinism and controls.....	107
Figure 4-1: A schematic diagram illustrating the visual pathway and visual field defects .....	122
Figure 4-2: Confrontational visual field testing.....	124
Figure 4-3: Amsler Grid. ....	125
Figure 4-4: Goldman Visual Field. ....	126
Figure 4-5: A visual field example and annotation .....	138
Figure 4-6: Equipment used to conduct a visual field assessment. ....	142
Figure 4-7: Example of how visual field was divided for analysis .....	143
Figure 4-8: Schematic diagrams of the visual field for albinism and IIN.....	145
Figure 4-9: The mean detection threshold for the albinism group compared to IIN .....	146
Figure 4-10: The comparison of nasal and temporal visual fields for albinism and IIN.....	147
Figure 4-11: The mean detection threshold for nasal and temporal visual field .....	148
Figure 4-12: Visual field quadrant split .....	149
Figure 4-13: The mean detection threshold for each quadrant in albinism.....	150
Figure 4-14: The mean detection threshold for each quadrant in IIN .....	151
Figure 4-15: The mean detection threshold - right and left eyes in albinism and IIN. ....	152
Figure 4-16: Dominant and non-dominant eyes in albinism .....	153
Figure 4-17: Dominant and non-dominant eyes in IIN .....	154
Figure 4-18: Visual Acuity plotted against visual field (Right and Left eye) in albinism. ....	155
Figure 4-19: Visual Acuity plotted against visual field (Right and Left eye) in IIN. ....	158

Figure 5-1: Optic nerve differences between individuals with albinism and controls .....	170
Figure 5-2: Optic Nerve comparison to visual field location (Raza and Hood (2015)).....	173
Figure 5-3: OCT Analysis (point measurement and area measurement).....	176
Figure 5-4: Visual field location corresponding to OCT area .....	177
Figure 5-5: OCT Realignment and Motion Correction .....	179
Figure 5-6: ppRNFL analysis using OCT. ....	180
Figure 5-7: Visual field Quadrants compared to ppRNFL sectors. ....	181
Figure 5-8: Optic nerve ppRNFL analysis.....	182
Figure 6-1: Myopia and Hypermetropia.....	193
Figure 6-2: Astigmatism (with the rule and against the rule) .....	194
Figure 6-3: Foveal Hypoplasia Grading Scheme (Thomas et al (2011)) .....	201
Figure 6-4: IOLmaster Biometry – Axial Length .....	202
Figure 6-5: FHG for each group.....	204
Figure 6-6: FDI for each group. ....	205
Figure 6-7: FHG compared to FDI.....	206
Figure 6-8: BCVA for each group.....	207
Figure 6-9: BCVA and FHG for albinism, IIN and <i>PAX6</i> .....	208
Figure 6-10: BCVA and FDI for albinism, IIN and <i>PAX6</i> . ....	209
Figure 6-11: Spherical refractive error for each group. ....	210
Figure 6-12: Cylindrical refractive error for each group .....	211
Figure 6-13: SER for each group.....	212
Figure 6-14: MAM for each group.....	213
Figure 6-15: FHG compared to SER and MAM .....	215
Figure 6-16: FDI compared to SER and MAM. ....	217
Figure 6-17: Correlation between axial length and SER in albinism .....	219
Figure 6-18: Correlation between axial length and FHG in albinism .....	220

Figure 6-19: Correlation between axial length and FDI in albinism .....	221
Figure 6-20: Correlation between axial length and BCVA in albinism. ....	221
Figure 6-21: Correlation between axial length and PEL thickness in albinism. ....	222
Figure 7-1: Visual pathway anomalies in albinism .....	234

## **Abbreviations**

BCVA	Best Corrected Visual Acuity
CSNB	Congenital Stationary Night Blindness
ERG	Electroretinogram
FDI	Foveal Development Index
FHG	Foveal Hypoplasia Grading
GVF	Goldman Visual Field
HPS	Hermansky-Pudlak Syndrome
HVF	Humphrey Visual Field
IIN	Idiopathic Infantile Nystagmus
L-DOPA	Dihydroxyphenalanine
LMM	Linear Mixed Model
MAM	Most Ametropic Meridian
OA	Ocular Albinism
OCA	Oculocutaneous Albinism
OCT	Optical Coherence Tomography
ppRNFL	peripapillary Retinal Nerve Fibre Layer
RGC	Retinal Ganglion Cell
RPE	Retinal Pigment Epithelium
SER	Spherical Equivalent Refractive Error
SITA	Swedish-Interactive Threshold Algorithm
VEP	Visual Evoked Potential
VF	Visual Field

# **Chapter 1**

## **Introduction**

# Chapter 1 Introduction

## 1.1 Overview of Thesis

In this thesis we aim to understand the mechanisms behind three visual abnormalities associated with albinism: the iris transillumination defect, visual fields and abnormal refractive errors.

This first chapter begins by highlighting the impact of albinism and explains the psychological and social implications associated with albinism. We then discuss the mechanisms underlying the cause of albinism including the genetic mutations leading to albinism. Furthermore, we outline the phenotypic features seen in albinism and investigate the abnormal visual pathway in albinism.

The second chapter provides an overview of the methodology applied, the participants examined, the clinical characterisation of all individuals and provides details of equipment used for this clinical characterisation. Each study contains a short methodology section where specific methods and analysis relevant to that chapter are outlined in further detail.

In **Study 1 (Chapter 3)** we report investigation of an area where little work has previously been carried out in albinism even though it is one of the most widely used diagnostic signs: the iris transillumination defect. With the exception of iris transillumination, objective methods now exist to provide quantitative measurements of all of other diagnostic features in albinism (optical coherence tomography (OCT) for foveal hypoplasia and visual evoked potential for chiasmal misrouting). In this study we aim to objectively measure the iris structure in individuals with albinism using optical coherence tomography (OCT) and to assess for differences in iris layers in albinism compared to controls. We investigate the diagnostic potential of anterior segment OCT (AS-OCT) in albinism by comparing the iris in albinism and controls. Finally we correlate the iris abnormalities with other phenotypic features seen in

albinism to assess for any direct relationship between this defect and other features. To our knowledge, this is the first time the iris transillumination defect is being assessed using AS-OCT with the aim of finding the structural cause of this anterior segment anomaly in albinism.

In **Study 2 (Chapter 4)** we investigate visual field (VF) defects in albinism in comparison to idiopathic infantile nystagmus (IIN). We compare albinism to the IIN population as they do not demonstrate iris transillumination or chiasmal misrouting as seen in albinism and both groups predominantly have nystagmus. Our aims were, firstly, to assess if any abnormalities of the VF exist due to albinism itself by comparing results to IIN, secondly, if any defects are present, to ascertain the cause of these defects. To date there are three previous studies examining the VFs in albinism. However, all of these studies are relatively small with fewer than 15 individuals with albinism, and show contradictory findings (St John and Timney 1981, Abadi and Pascal 1993, Hoffmann, Seufert et al. 2007).

In albinism there are profound structural changes in the retina and optic nerve. In **Study 3 (Chapter 5)** we investigate the relationship between foveal and optic nerve (ppRNFL) structural abnormalities measured using OCT and central and peripheral detection threshold derived from the VF measurements.

In **Study 4 (Chapter 6)** we assess the relationship between foveal structure (using posterior OCT measures) and refractive error in albinism. This is compared to other forms of foveal hypoplasia in IIN, *PAX6* mutation and achromatopsia. We also compare the current clinically available foveal hypoplasia grading scheme with an objective measure of foveal hypoplasia for the first time. Previous literature by Healey et al (2013) attempts to compare refractive error in albinism to a heterogeneous group of individuals without albinism (NAIN (non albinotic idiopathic nystagmus)). The key finding from the Healey et al (2013) study was that impaired emmetropisation in nystagmus is likely to be attributed to the whole eye effect in albinism and that the fovea does not play a central role in emmetropisation. In our study we aim to look at 4

phenotypically different groups (albinism, IIN, *PAX6* and achromatopsia) to also look for differences between groups and to see if the foveal effect on refractive error is disease specific.

## 1.2 Albinism

### 1.2.1 The History of Albinism

The term albinism comes from the Latin word 'albus', which means white. The word 'albino' refers to an organism with a complete absence of melanin. The first scientific publication written about albinism was by Sir Archibald Garrod in 1908. Now there are over 4000 peer-reviewed articles published under the search term "albinism"; this number is steadily rising. Albinism has also previously been described in the literature as achromia (Lahiri and Sengupta 1998) and achromatosis (Roudybush 1999).

### 1.2.2 What is Albinism?

Albinism is a congenital defect characterised by the complete or partial absence of pigment within the hair, skin and eyes often due to the absence or a defect of tyrosinase, an enzyme essential for the biosynthetic production of melanin (Gronskov, Ek et al. 2007). Melanin is a universal pigment found in most organisms. In humans, it is the primary determinant of skin colour, hair colour, the stria vascularis of the inner ear and the tissues underlying the iris of the eye (Summers 1996, Sturm and Larsson 2009). Melanin is largely produced by melanocytes and the concentration of melanocytes can range across a wide spectrum.

Albinism not only affects humans, but also animals (Imes, Geary et al. 2006) and plants (Gettys and Wofford 2007) (**Figure 1-1**). Albinism affects animals in a similar way to humans however albinism in plants is caused by a deficiency of the green pigment chlorophyll (Zubko and Day 1998, Gettys and Wofford 2007). Plants require chlorophyll to obtain energy from sunlight for photosynthesis. The condition can be caused by a mutation or by starving the affected leaf of light which stops the substance chlorophyll being produced in the cells, causing a particular part of a plant to be white.

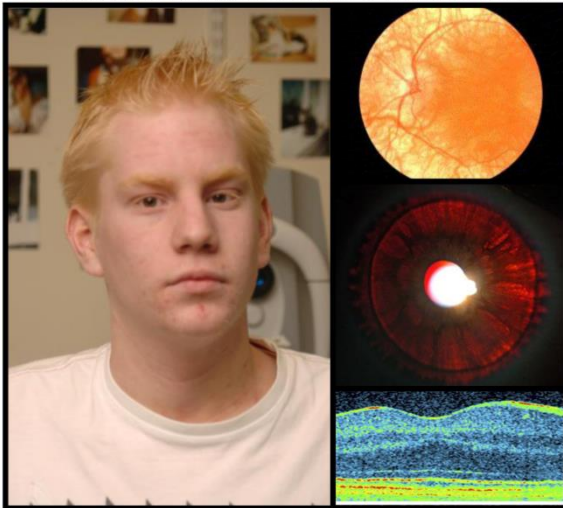


Figure 1-1: Animals and plants exhibiting features of albinism. Pictures taken from Google Images (<https://www.google.co.uk/search?q=albinism+google+images+animals+plants>).

### 1.2.3 Types of Albinism

There are two main types of albinism occurring in humans. Firstly, oculocutaneous albinism (OCA) which affects the hair, skin and the eyes (Gronskov, Ek et al. 2007) and, secondly, ocular albinism (OA) where the melanin deficiency is confined to the eyes and visual system (Lewis 1993). **Figure 1-2** displays the distinct phenotypic differences observed in OCA and OA.

## Oculocutaneous Albinism



## Ocular Albinism

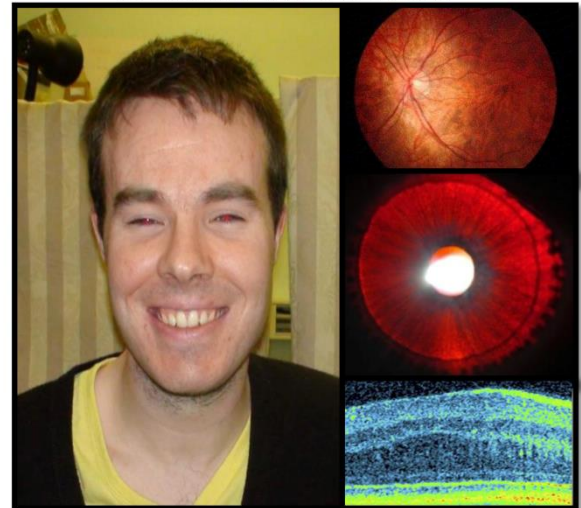


Figure 1-2: Individuals with oculocutaneous and ocular albinism. The images adjacent to these photographs demonstrate macular transparency (top), iris transillumination (middle) and foveal hypoplasia as seen on OCT (bottom).

### 1.2.4 Prevalence of Albinism

The prevalence of all forms of albinism varies considerably worldwide and is dependent upon the ethnicity studied (Gronskov, Ek et al. 2007). The reported prevalence of different genetic sub-types of albinism is discussed in more detail within the genetics section of this chapter (Section 1.5).

## 1.3 Consequences of Albinism

### 1.3.1 Psychosocial Implications

#### 1.3.1.1 Psychological Impact

In addition to medical concerns, people with albinism often struggle with psychological and social challenges. In Nigeria, one study collected written accounts of people with albinism. Individuals with albinism acknowledged that they tend to be more withdrawn from social situations to avoid being noticed. They were more emotionally unstable and had less assertive personalities than people without albinism. They also considered their society to be generally

unkind and rejecting (Ezeilo 1989). The study concludes that there may be the need for a psychological rehabilitation programme for these individuals, particularly in some areas of the world.

### **1.3.1.2 Social Impact**

The social discrimination faced by individuals with albinism stem from their surrounding communities' lack of knowledge, education and awareness. As a result, there are numerous and often harmful myths and superstitions especially common in African societies (Lund 2005). Albinism has, for decades, been coupled with stigma and superstitions. Examples of such beliefs are that a white man impregnated the mother or that the child is the ghost of a European colonist (Cruz-Inigo, Ladizinski et al. 2011). More recently, a notion has emerged that albino body parts are lucky charms and possess supernatural powers. These body parts may be sold for as much as \$75,000 on the black market in certain areas of Africa. As a result there have been over 100 albino murders in Tanzania alone in the past decade (Cruz-Inigo, Ladizinski et al. 2011). A television documentary exhibits the struggles of African albinos: this was aired on BBC2 in the UK on 23/02/2017: <https://www.youtube.com/watch?v=RDGplFVM8mq>.

### **1.3.1.3 Support in the Western World**

Within the western world, there is more support for those living with albinism. This help comes in the form of support groups and forums, and close follow-up by healthcare professionals who aim to improve the symptoms and quality of life for these individuals. Such forums and websites used by many in Europe and the USA include:

<http://www.albinism.org.uk> – U.K

<http://www.albinismo.es/> - Spain

[www.genespoir.org/](http://www.genespoir.org/) - France

<http://www.albinism.eu/> - Germany and Italy (+ other European countries)

[http://www.albinism.org/site/c.fkYIdOUlhJ4H/b.9194783/k.4163/National\\_Organization\\_for\\_Albinism\\_and\\_Hypopigmentation.htm](http://www.albinism.org/site/c.fkYIdOUlhJ4H/b.9194783/k.4163/National_Organization_for_Albinism_and_Hypopigmentation.htm) - U.S.A & Canada

### **1.3.2 Cutaneous Implications (Hair and Skin)**

A lack of melanin predisposes the albinism population to severe skin damage as there is a lack of skin protection against the sun's ultraviolet radiation, leading to skin burns and lesions (Lund 2005). The majority of these lesions are in the most sun-exposed parts of the body such as the face, ears, neck and shoulders. Skin lesions include blisters, solar keratosis, ephelides, lentiginosis, and superficial ulcers. Ultimately squamous cell, and less frequent basal cell, carcinomas may occur (Luande, Henschke et al. 1985, Asuquo, Ngim et al. 2009, 2016).

### **1.3.3 Visual System Implications**

There are numerous visual system implications that face those with albinism; these are explained in **Section 1.6**.

## 1.4 Mechanism behind Albinism

### 1.4.1 Understanding Melanocytes and Melanosomes

Melanocytes are melanin producing cells found at various locations throughout the body (mucosa, cochlear, iris and mesencephalon). Melanosomes are the pigment-bearing organelles of the melanocytes and can be classified into four types based on maturity. Melanosome maturation occurs through sequential maturation and can be defined based upon morphology. Stage I pre-melanosomes lack pigment and contain internal membranous vesicles. Stage II pre-melanosomes are elongated in shape, lack pigmentation and contain intraluminal matrix fibres organised in a striated array. The deposition of black melanin along the matrix fibres begins at stage III. Stage IV melanosomes are characterised by a dense homogenous deposit of melanin that covers all the internal structures of the matrix (Orlow 1998). This important developmental process is illustrated in **Figure 1-3**.

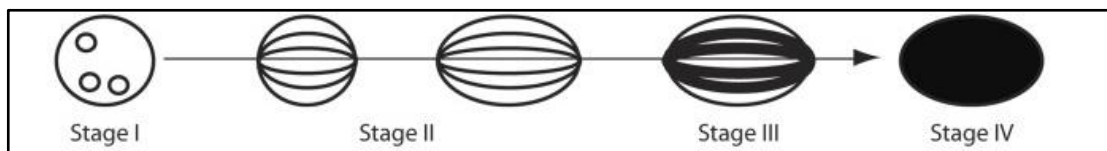


**Figure 1-3: Model on melanosome biogenesis. Image reproduced from Daly et al (2013).**

### 1.4.2 Melanin in the Eye

Melanin, or its precursors, plays an essential role in the development of the visual system. A significant level of pigment production is crucial for the normal development of visual pathways (Jeffery, Schutz et al. 1994). Melanin is the major pigment giving colour to the eyes of mammals (Orlow 1997). Melanin and/or its precursors are very important during ocular development and abnormalities of melanin biosynthesis lead to various visual pathway disorders such as abnormal decussation at the optic chiasm, iris transillumination, foveal

hypoplasia and nystagmus. These visual pathway disorders are covered in more depth in the coming chapters.

### 1.4.3 Mechanism behind Melanin Biosynthesis

Albinism is a defect in the biosynthetic production of melanin that is often caused by an absence or defect of tyrosinase. Tyrosinase is crucial in catalysing reactions within the pathway of melanogenesis (Zhao and Boissy 1994). There are various types of melanin, eumelanin being the most abundant form in humans, and also the most likely form to be deficient in albinism. Eumelanin pigments are the darker pigments that are also responsible for tanning and serve as a protective function from UV light rays from the sun (Levin and Stroh 2011). Pheomelanins are responsible for the blonde, orange and red colours seen in humans and animals, for example, pheomelanins are responsible for the red colour of the lips in humans.

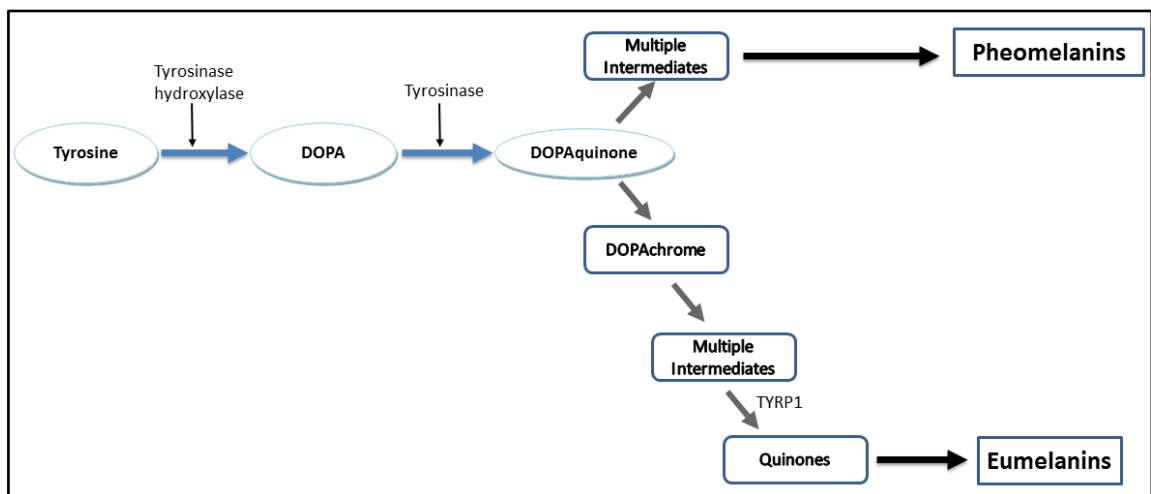


Figure 1-4: The Pathway of melanin biosynthesis.

### 1.4.4 The Importance of Dihydroxyphenalanine (L-DOPA) in Retinal Development in Albinism

Some authors have attributed the alterations in the visual system associated with albinism as a consequence of a lack of L-DOPA and not melanin (Lavado, Jeffery et al. 2006, Lopez, Decatur et al. 2008, Roffler-Tarlov, Liu et al. 2013). In normally pigmented retinal pigment epithelium

(RPE), L-DOPA, an intermediate in the synthetic pathway for melanin, has been hypothesised to regulate the timing of neurogenesis (Roffler-Tarlov, Liu et al. 2013). L-DOPA is absent from the embryonic albino retina and is greatly reduced in the postnatal albino retina compared to pigmented retina (Roffler-Tarlov, Liu et al. 2013). In a recent publication, Roffler-Tarlov et al (2013), suggested that L-DOPA has a very important role throughout the pre and postnatal visual development until the first postnatal month after which its production declines sharply (as found in normally pigmented mice). This time course represents the onset and completion of retinal development (Roffler-Tarlov, Liu et al. 2013). They found the critical period for the production of L-DOPA was within the first 27.5 postnatal days. An arrested production of L-DOPA occurred in the albino mice where there was little or no production of L-DOPA, in comparison to the normally pigmented mice which found a steady increase in L-DOPA production over the first 27.5 days and then a sharp reduction in L-DOPA production thereafter. Over a longer time-course the L-DOPA production over the first 180 days was always more in normals in comparison to their albino counterparts (Roffler-Tarlov, Liu et al. 2013). These studies highlight the importance of intermediate products and their roles in the production of melanin and its effects on the visual pathway.

## 1.5 Genotypes in Albinism

### 1.5.1 Genetic Classification of Albinism

Albinism is divided into two categories: oculocutaneous albinism (OCA) and ocular albinism (OA). OCA refers to hypopigmentation within the hair, skin and the eyes. OA refers to hypopigmentation confined to the eyes only. At present there are seven genes/loci that have been identified in OCA (**Table 1-1**) and one gene associated with OA. Additional genes exist for other hypopigmentation disorders associated with albinism, for example, Hermansky-Pudlak syndrome.

The clinical spectrum of OCA ranges from OCA1A being the most severe type with a complete lack of melanin production throughout life, to the milder forms OCA1B, OCA2, OCA3 and OCA4 which show some pigment accumulation over time (Gronskov, Ek et al. 2007). In addition, newer genes have been identified since 2007 and have been added to genotypes in albinism (OCA5, OCA6 and OCA7) (Montoliu, Gronskov et al. 2014).

<u>Disease Name</u>	<u>Gene Name</u>	<u>Gene Product</u>	<u>Cytogenetic Location</u>	<u>Size</u>	<u>Prevalence</u>
OCA1 (OCA1, OCA1A, OCA1B)	TYR	Tyrosinase (TYR)	11q14.3	(529aa)	1:40,000 (Rare in Africans)
OCA2 (Brown OCA in Africans)	OCA2(P-Gene)	OCA2	15q11.2-q12	(838aa)	1:36,000 in white Europeans 1:3,900– 10,000 in Africans
OCA3 (Rufous OCA)	TYRP1	Tyrosinase-related protein 1 (TYRP1)	9p23	(536aa)	1:8,500 in Africans Rare in white Europeans and Asians
OCA4	MATP	Membrane-associated transporter protein (MATP)	5p13.3	(530aa)	Rare in white Europeans 1:85,000 in Japanese
OCA5	OCA5(locus)*	-	4q24	-	Unknown to date
OCA6	SLC24A5	Solute Carrier Family 24 member 5	15q21.1	(500aa)	Unknown to date
OCA7	LRMDA(C10orf11)	Leucine-rich Melanocyte Differentiation Associated Protein	10q22.2-q22.3	(226aa)	Unknown to date

\* Specific gene has not been identified, only linkage to a region(4q24)

**Table 1-1: Details for OCA1-OCA4 derived and amended from Gronskov et al (2007). Details for OCA5-7 obtained from Montoliu et al (2014) and Gronskov et al (2013).**

## 1.5.2 Types of Oculocutaneous Albinism (OCA)

### 1.5.2.1 OCA1

OCA1 is caused by a loss of function of the enzyme tyrosinase due to mutations of the *TYR* gene. OCA1 is obvious from birth with severe hypopigmentation, white hair, pale skin and light-blue coloured irides (King 2000). OCA1 has a prevalence of approximately 1:40,000 in most populations but is uncommon amongst African-American communities (King 1995). There are different sub-categories of OCA1 each with slightly different characteristics. These are described.

#### 1.5.2.1.1 OCA1A: Tyrosinase-Negative OCA

Individuals with OCA1A have no pigmentation within the hair, skin or the eyes and pigmentation does not develop with time (King 1993). Affected individuals are likely to have full iris transillumination and have severe photophobia. Hair and skin colour tend to be completely white (**Figure 1-5**) with sun exposure being potentially harmful due to the lack of melanin (King 1993).

#### 1.5.2.1.2 OCA1B: Yellow OCA – “Leaky Mutation”

OCA1B differs from OCA1A as tyrosinase mutations still allow the enzyme to work. However, there is minimal (5-10%) enzyme activity and therefore slight pigmentation of the eyes and hair (King 1993). Affected individuals will have the same characteristics as OCA1A at birth but pigmentation slowly develops throughout life and hair colour becomes yellow within their twenties for some of these patients (**Figure 1-5**). The phenotype of these individuals is often variable (King, Pietsch et al. 2003).



**Figure 1-5: Pigmentation in patients with albinism. (A) & (B) Patients with OCA1A which demonstrates no pigment has accumulated and the iris is fully translucent. (C) & (D) Patients with OCA1B which demonstrates a small amount of melanin pigment has slowly accumulated in the hair and the eyes.**

#### **1.5.2.1.3 OCA1MP: Minimal Pigment OCA**

OCA1MP is similar to OCA1A except a very minimal amount of pigment accumulates in the iris alone, but not within skin or hair which remain completely white. It has been argued that OCA1MP should be classified as a subtype of OCA1B because of its subtle phenotypical difference (King, Wirtschafter et al. 1986).

#### **1.5.2.1.4 OCA1TS: Temperature Sensitive OCA**

OCA1TS is a very rare condition and has been reported in humans, Siamese cats and mice (King, Townsend et al. 1991). Individuals with OCA1TS have blue eyes, white hair and white skin at birth. During puberty they develop progressively darker hair around the extremities of the body but retain white hair in areas such as the scalp and axilla (**Figure 1-6**) (King, Townsend et al. 1991, Wang, Waters et al. 2005). A missense mutation in the tyrosinase gene of such patients causes one amino acid replacement which makes the enzyme temperature sensitive, with very low activity at or below 35°C and a loss of activity above 35°C (Giebel, Tripathi et al. 1991).



Figure 1-6: Images of a patient with temperature sensitive OCA. Note the yellow-blond hair, dark eyebrows and strongly pigmented forearm hair. Reproduced from Wang et al (2005).

### 1.5.2.2 OCA2: P-Gene Related Albinism

OCA2 is caused by mutations at the P-locus on chromosome 15q11-12 (Apkarian 1993). The exact function of protein P is unknown but it is essential for the normal colouring of hair, skin and the eyes. It is also likely to be involved in melanin production. The eyes appear well pigmented and hair and skin pigment accumulate with time in OCA2. Compared to all other types of OCA1, whereby the skin never accumulates any pigment, in this type of albinism there is also the possibility that the skin can develop freckles or naevi (**Figure 1-7**). It is described that black albinos in South Africa show up with a fascinating phenotype (Kromberg, Castle et al. 1989). 61% of the albinos with OCA2 within their study developed large, darkly pigmented patches on their skin called ephelides. Ephelides are not present at birth and develop throughout the early years of childhood. It is more likely that parts of the body that are most exposed to the sun are most likely to develop these patches. Albinos who develop these patches, are to some extent, protected against radiation damage caused by the sun and thus carry a lesser risk for skin cancers throughout their lives (Kromberg, Castle et al. 1989). Within families affected with OCA2 either all develop ephelides or none of them will (Kromberg, Castle et al. 1989). OCA2 (OCA2) has an estimated prevalence of 1:36,000 in the USA (Oetting

and King 1999). However, in some parts of Africa it was found to be almost ten times more prevalent at 1:3900 (Kromberg and Jenkins 1982).

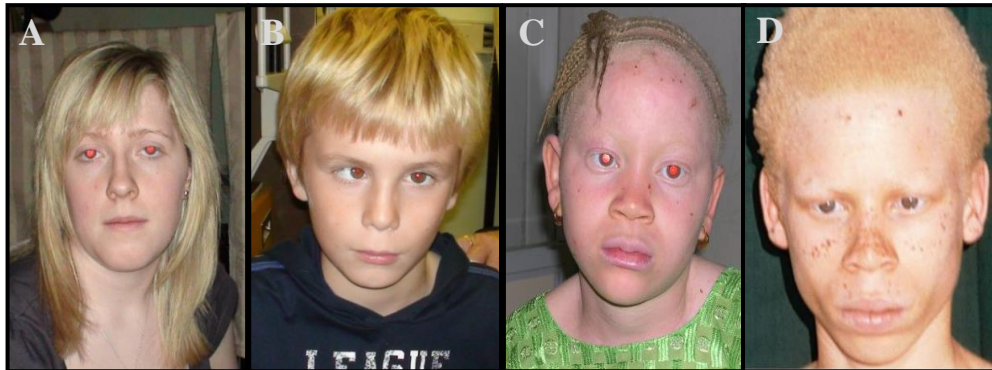
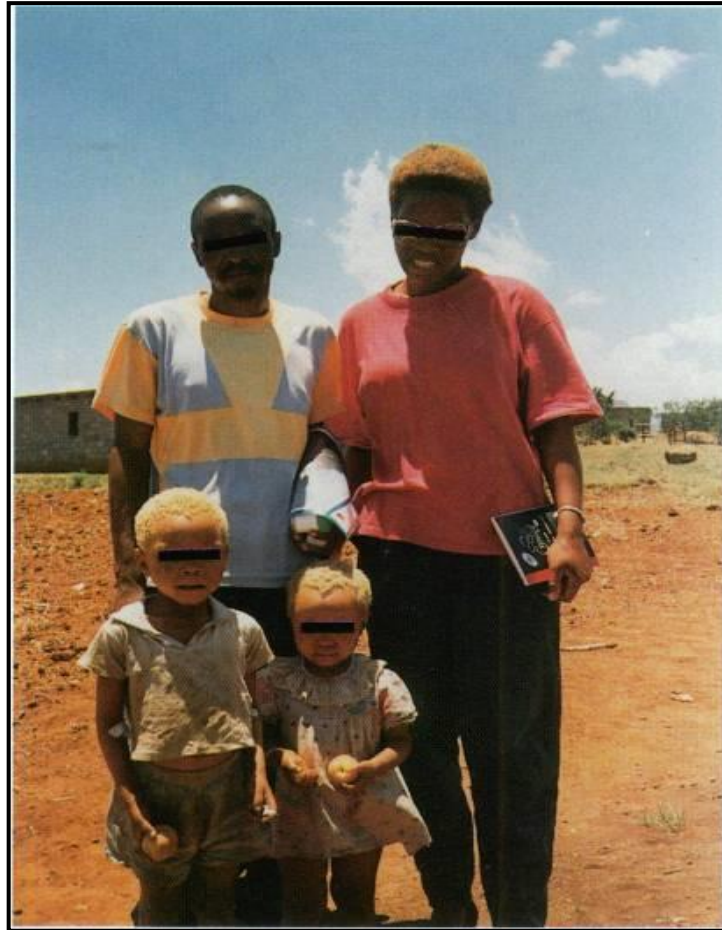


Figure 1-7: (A) & (B) Individuals demonstrating the phenotype of OCA2, eyes accumulate pigmentation and the skin and hair become pigmented with time. Images (C) & (D) African individuals with albinism with ephelides present. Images C & D reproduced from <http://www.dermaamin.com>.

### 1.5.2.3 Brown OCA (BOCA)

Genetic studies shows that BOCA can be caused by a milder mutation of the *P-gene* (Manga, Kromberg et al. 2001). Therefore this is thought to be a variant of OCA2 in African populations. Affected individuals were noted to have creamy coloured skin, light brown hair, and blue-green to brown irides with moderate transillumination defects, nystagmus and reduced retinal pigment (**Figure 1-8**).



**Figure 1-8: African parents with their two children affected by brown OCA (BOCA). Image reproduced from Manga et al (1997).**

#### **1.5.2.4 OCA3: Rufous OCA- TYRP1**

OCA3 is found in African individuals and has been described in the native population of Papua New Guinea (Walsh 1971, Kromberg, Castle et al. 1990). The phenotype for OCA3 is milder than that of OCA1 or OCA2 subtypes, with higher pigmentation levels. Individuals with Rufous OCA are more likely to show a phenotype of a bronze skin colour, ginger coloured hair and blue or brown irides (Manga, Kromberg et al. 1997). OCA3 (TYRP1) has been reported to affect 1:8500 in Africa, but is very rare in Asian and Caucasian populations (Gronskov, Ek et al. 2007).

### 1.5.2.5 OCA4: MATP Gene

OCA4 results from mutations of the *MATP* gene and is considered one of the most common forms within the Japanese population (**Figure 1-9**). 18 out of 75 (24%) unrelated Japanese patients with nystagmus were positive for *MATP* gene and diagnosed with OCA4; this is a large percentage considering all other potential diagnoses related to nystagmus (Inagaki, Suzuki et al. 2004). The phenotypic and clinical features of OCA4 reported within the Japanese patients are similar to OCA2. It is therefore not possible to diagnose OCA4 based upon clinical findings alone (Gronskov, Ek et al. 2007). Currently the only method of diagnosing these patients is through the use of genetics. The exact prevalence is yet to be reported.



**Figure 1-9: An individual of Chinese descent with OCA4. Image reproduced from <http://www.kacaras.eu/en/photos/albinism-in-asia/2.html>**

### 1.5.2.6 OCA 5: Non Syndromic OCA Mapped to Chromosome 4q24

This type of albinism was found when investigating the cause of albinism in a consanguineous Pakistani family. They found the phenotype within this family was linked to chromosome 4q24 (Kausar, Bhatti et al. 2013). The phenotype of individuals from this family presented with golden coloured hair, nystagmus, photophobia, white skin, decreased visual acuity and foveal

hypoplasia (regardless of their sex or age). To date only one family has been reported with OCA5. **Figure 1-10** shows the different phenotypes that can be seen with OCA5.



**Figure 1-10: Individuals affected with OCA5. Image reproduced and amended from Kauser, Bhatti et al (2013).**

#### **1.5.2.7 OCA6: *SLC24A5* Gene**

In 2013, a Chinese team of researchers (Wei, Zang et al. 2013) reported that they found a mutation in *SLC24A5* in a family affected with OCA. Mutations in *SLC24A5* have previously been associated with pigment variants in zebrafish (Lamason, Mohideen et al. 2005), mice (Vogel, Read et al. 2008) and humans (Lamason, Mohideen et al. 2005). The phenotype of individuals with this mutation showed lighter coloured hair which darkens with age, iris transillumination, photophobia, foveal hypoplasia, reduced visual acuity, nystagmus and with no defects in platelet dense granules which are all characteristic traits of non-syndromic autosomal recessive OCA (Wei, Zang et al. 2013). The mutation has been found in other ethnic origins, thus is not restricted to the Chinese population. A single-nucleotide polymorphism (SNP) in *SLC24A5* (*rs 1426654*) encoding an alanine or threonine at position III was detected (AlaIII or ThrIII). ThrIII is present in almost all normal individuals of European origin, while AlaIII is present in African/Asian populations. ThrIII is associated with lighter pigmented skin. Thus suggesting an important role of this SNP in the establishment of human pigmentation (Lamason, Mohideen et al. 2005).

### **1.5.2.8 OCA7: LEUCINE-RICH MELANOCYTE DIFFERENTIATION-ASSOCIATED PROTEIN (*LRMDA*) - *C10orf11***

This gene was found in a consanguineous family from the Faroe Islands, Denmark. All individuals affected with OCA7 had variable visual acuity, high hypermetropia and against-the-rule astigmatism. Visual symptoms were nystagmus, iris transillumination and chiasmal misrouting. Hair colour ranged from white to dark brown. Interestingly, photophobia was not a major problem in individuals with albinism affected with this gene (Gronskov, Dooley et al. 2013, Montoliu, Gronskov et al. 2014).

### 1.5.3 Types of Ocular Albinism (OA)

Ocular albinism (OA) is defined phenotypically when only the eyes and visual system are affected (Lewis 1993, Rosenberg and Schwartz 1998) but not skin and hair. However, more recently, this definition has been questioned with various authors stating there is some degree of reduced pigment within the skin and hair. OA is reported as being less prevalent than OCA (Rosenberg and Schwartz 1998). There are two main types of OA described in the literature (X-linked ocular albinism (GPR143)) and autosomal recessive ocular albinism.



**Figure 1-11: Individuals with ocular albinism, both with tanned skin, dark hair and dark eye brows.**

#### 1.5.3.1 X-Linked Ocular Albinism

X-linked ocular albinism has been described in the literature under various different names, these include: XLOA, Nettleship-Falls ocular albinism, OA1 and ocular albinism type 1. In essence, all these synonyms describe the same condition.

The locus for X-linked ocular albinism is located on the short arm of the chromosome Xp22-3 (Bergen, Samanns et al. 1990, Schnur, Nussbaum et al. 1991). *GPR143* (OA1) is the solitary gene currently known to be associated with ocular albinism (Podkrajsek, Kranjc et al. 2012). Patients classically present with reduced visual acuity, nystagmus, strabismus, photophobia, iris transillumination, hypopigmentation of the retina, foveal hypoplasia and misrouting of

optic nerve fibres at the chiasm (Podkrajsek, Kranjc et al. 2012). Skin and hair pigmentation are generally spared.

X-linked ocular albinism characteristically runs through a family whereby males are affected and females are carriers that often demonstrate a mud-splattered fundus and occasionally iris transillumination (Charles, Green et al. 1993). The incidence of X-linked ocular albinism was found to be 1 in 50,000 in the USA population (King 1995). This type of OA is particularly interesting as its phenotype can vary hugely between different ethnicities and populations. Investigations in X-linked ocular albinism include: a study on British Caucasian X-linked ocular albinism sufferers (Charles, Moore et al. 1992, Charles, Green et al. 1993); American Caucasians (Lam, Fingert et al. 1997); two black families (O'Donnell, Green et al. 1978); three Finnish Caucasian families (Lauronen, Jalkanen et al. 2005) and seven Japanese families (Shiono, Tsunoda et al. 1995). It is worth noting that all of these populations have not been genetically determined and were presumed to be X-linked ocular albinism from phenotypic features and thus results must be treated with caution.

### **1.5.3.2 Autosomal Recessive Ocular Albinism (AROA)**

AROA has also been described in the literature most recently by Hutton and Spritz (2008) but currently no gene for this type of ocular albinism has been identified. Hutton and Spritz (2008) conducted genetic analysis of 36 individuals diagnosed clinically with AROA which actually revealed abnormalities in the *TYR* gene, *P*-gene and *TYRP1* gene (all OCA genes) for 27/36 individuals assessed (Hutton and Spritz 2008). Interestingly the other 9 individuals in this study with clinical AROA could not be genetically determined, this could be for 2 reasons. Firstly, due to the possibility that a novel gene for AROA is unknown and yet to be found or, secondly, due to these falling within OCA5-OCA7 as well as other OCA mutations which were unknown at the time of this publication. To date, in 2018, there is still no genetically determined cases of AROA with a novel gene described.

## **1.5.4 Hypopigmentation Disorders Associated with Albinism**

### **1.5.4.1 Organelle Defects**

#### **1.5.4.1.1 Hermansky Pudlak Syndrome**

Hermansky Pudlak Syndrome (HPS) is a rare autosomal recessive disorder which comprises of a triad of oculocutaneous albinism, haemorrhagic diathesis due to a platelet storage pool deficiency and the accumulation of ceroid-like material in the reticulo-endothelial system and surrounding other tissues (Izquierdo, Townsend et al. 1995). To date, there are eight forms of HPS that exist (Dessinioti, Stratigos et al. 2009), each with a very different phenotype. Distinct diagnosis can only be made via genetics. The phenotypic variability can depend upon age and the racial background of an individual. The majority of research carried out concludes that the highest incidence of HPS is within Puerto Rico (Witkop, Nunez Babcock et al. 1990, Santiago Borrero, Rodriguez-Perez et al. 2006). There is generally a reduction in life expectancy of patients with HPS.

#### **1.5.4.1.2 Chediak-Higashi Syndrome**

This is another rare autosomal recessive disorder characterised by OCA, silver hair, bleeding tendencies, severe immune deficiency and can also present with large, recurrent pyogenic infections as well as progressive sensory or motor neurological defects (Reddy, Babu et al. 2011). Familial consanguinity is often determined if this diagnosis is made (Carnide, Jacob et al. 1998, Reddy, Babu et al. 2011).

#### **1.5.4.1.3 Griscelli Syndrome**

Griscelli Syndrome is a rare autosomal recessive disorder that can be distinguished by pigmentary dilution of the skin, silver-grey coloured hair, large clumps of pigment within hair shafts and the accumulation of large and end-stage melanosomes in the centre of melanocytes (Menasche, Ho et al. 2003). The syndrome is linked with defects of the Rab27a-MLph-Myo5A

protein complex formation in melanocytes. There are 3 main sub-types, each with a very different phenotype.

## **1.5.4.2 Neural Crest Defects**

### **1.5.4.2.1 Waardenburg Syndrome (WS)**

This is a group of rare genetic disorders most often characterised by varying degrees of deafness, minor defects in structures arising from the neural crest and pigmentation deficits. At least four types of WS have been identified with further subtypes in each category (Gad, Laurino et al. 2008, Dessinioti, Stratigos et al. 2009). The genes that cause WS are involved in the development and production of different cells, including the pigment producing melanocytes. Melanocytes are not only essential for pigmentation but also play a significant role in the function of the middle ear, which is also affected here.

### **1.5.4.2.2 Hirschsprungs Disease**

Hirschsprungs Disease (HSCR) is also known as congenital aganglionosis megacolon. It has been found previously in patients with Waardenburg syndrome as they develop heterochromia, megacolon and deafness (Cheng, Au et al. 2001).

### **1.5.4.2.3 Tietz Syndrome**

This is yet another rare autosomal dominant disorder characterised by reduced pigmentation, blue eyes, congenital deafness associated with WS and the absence of nystagmus. It arises from mutations of the MITF gene. Although this is similar to WS2, affected individuals do not have heterochromic irides or patchy pigmentation (Smith, Kelley et al. 2000).

### **1.5.4.2.4 Pie-Baldism**

Pie-Baldism is a rare autosomal dominant disorder with congenital de-pigmented patches of the mid-forehead, chest, abdomen and extremities, where no melanocytes are found. Melanocytes in the eye and ear are rarely affected (Boissy and Nordlund 1997). Pie-Baldism

has been linked to inactivity mutations or deletions of the C-kit gene, which is mapped on chromosome 4q12 located on chromosome 8q11. These mutations instigate a reduction in receptor tyrosinase-kinase signalling and impaired melanoblast development, thereby inhibiting melanogenesis (Boissy and Nordlund 1997). Mutations of C-kit that have been identified in pie-bald patients range from gross deletion to missense defects and all are inherited as autosomal dominant traits (Dessinioti, Stratigos et al. 2009).

### **1.5.5 FHONDA (Foveal Hypoplasia, Optic Nerve Decussation and Anterior Segment Dysgenesis)**

The FHONDA phenotype comprises of foveal hypoplasia, optic nerve decussation defects and anterior segment dysgenesis in the absence of iris transillumination and other pigmentary defects usually seen in albinism. Two Asian families have been identified with the FHONDA phenotype (Al-Araimi, Pal et al. 2013). Initially these two families were thought to have different phenotypic characteristics to one another as Pal et al (2004) did not initially observe optic nerve decussation with the family they assessed (F1) (Pal, Mohamed et al. 2004). Van Genderen et al (2006) did not observe anterior segment dysgenesis within the family they assessed (F2) (van Genderen, Riemsdag et al. 2006). When both families (F1 and F2) were reassessed by Al-Araimi et al (2013), family F1 was in fact identified as having chiasmal misrouting and family F2 was found to have either Axenfelds anomaly or posterior embryotoxin (both forms of anterior segment dysgenesis). Both families had reduced vision (20/120 to 20/400), nystagmus and abnormal refractive errors (Al-Araimi, Pal et al. 2013). Interestingly, the combination of foveal hypoplasia and optic nerve decussation defects are usually found in albinism. However in this study of patients with FHONDA, none are reported to have hair, skin or eye pigmentation defects which would indicate FHONDA is not a variant of albinism or caused by a defect in the melanin biosynthesis pathway. The gene mutated in this

disorder was found to be within a 3.1mb interval containing 33 genes on chromosome 16q23.3-24.1(Al-Araimi, Pal et al. 2013).

To further identify the mutated gene in FHONDA, Poulter et al (2013) used Sanger sequencing to screen all 33 genes with the FHONDA locus for both families and identified mutations in SLC38A8 for both families. Poulter et al (2013) assessed a further 12 individuals with a similar phenotype from other families and found that 5 of the 12 individuals had mutations within this gene (Poulter, Al-Araimi et al. 2013). Despite the above findings there remains controversy as to whether pigmentation deficiency occurs in FHONDA as pigmentation in albinism can often be very subtle (especially in OA). This has led to some authors postulating that FHONDA is in fact mild albinism (Michaelides, Jeffery et al. 2012), especially given the fact that anterior segment dysgenesis has previously been observed in albinism (Shiono, Tsunoda et al. 1995).

## 1.6 Phenotypic Characteristics in Albinism

As outlined in the previous section, individuals with albinism display a broad range of deficits including pigmentation defects, reduced visual acuity, strabismus, reduced stereopsis, abnormal head postures, abnormal refractive errors, positive angle kappa, nystagmus, iris transillumination, foveal hypoplasia, macular hypoplasia, optic nerve abnormalities and misrouting of the optic nerves at the chiasm (Summers 1996, Gronskov, Ek et al. 2007). These phenotypic characteristics are covered in more detail in this section.

### 1.6.1 Pigmentation in Albinism

The degree of skin and hair pigmentation varies with the type of albinism but is, in general, reduced compared to the normal population (King and Summers 1988). The clinical spectrum of pigmentation abnormalities ranges with OCA1A being the most severe having an absolute lack of melanin production within the whole body throughout life, whereas milder forms OCA1B, OCA2, OCA3 and OCA4 demonstrate some pigment accumulation over time (Gronskov, Ek et al. 2007). Individuals with OA generally have a good level of pigmentation throughout the skin and hair; however, ocular features are similar to those with OCA.

### 1.6.2 Reduced Vision

Individuals with albinism are likely to have reduced vision. All visual acuity measures in this section are provided as Snellen equivalent (6/6 is equal to normal vision). Those with OCA1 mainly have visual acuity between 6/30 and 6/120; although some individuals have achieved visual acuity of 6/18 or better in previous literature (King 2000). Visual acuity in OCA2 is generally better than that in OCA1, though there is often a degree of overlap. Visual acuity in OCA2 commonly falls between 6/9 and 6/120, typically 6/30 – 6/60 (King and Oetting 2003). Visual acuity was found to be between 6/18 and 6/60 in a previous study for those with OCA3 (King, Lewis et al. 1985). Visual acuity for individuals affected with OCA4 is 6/9 – 6/120, similar

to OCA2 (Rundshagen, Zuhlke et al. 2004, Suzuki and Hayashi 2005). Visual acuity for those with OCA5, OCA6 and OCA7 have been reported in very few individuals, therefore ranges are difficult to ascertain. A reduction in Visual acuity is often a consequence of various phenotypic features associated with albinism.

### 1.6.3 Strabismus

Strabismus is defined as a condition whereby the visual axes of the eyes are not parallel and thus each eye appears to be looking in different directions (**Figure 1-12**). In divergent strabismus (exotropia) the visual axis will demonstrate one eye turning out. If the visual axis converges (esotropia), the visual axis will demonstrate one eye turning in (Ansons and Davis 2000). One consequence of strabismus is that amblyopia (reduced vision) may develop in the non-dominant eye (Ansons and Davis 2000).

Strabismus often occurs in albinism. Various literature explain differences in percentages of patients affected by strabismus who have albinism. Brodsky and Fray (1997) found that of 82 patients with infantile nystagmus, 30 had albinism. From these 30 patients, 16 (53%) had strabismus (8 esotropia, 6 exotropia and 2 superior oblique palsy) (Brodsky and Fray 1997). More recent literature found 71.2% (37/52) of albinism subjects demonstrated strabismus, of which 73% (27/37) had esotropia and 27% (10/37) exotropia (Kumar, Gottlob et al. 2010).

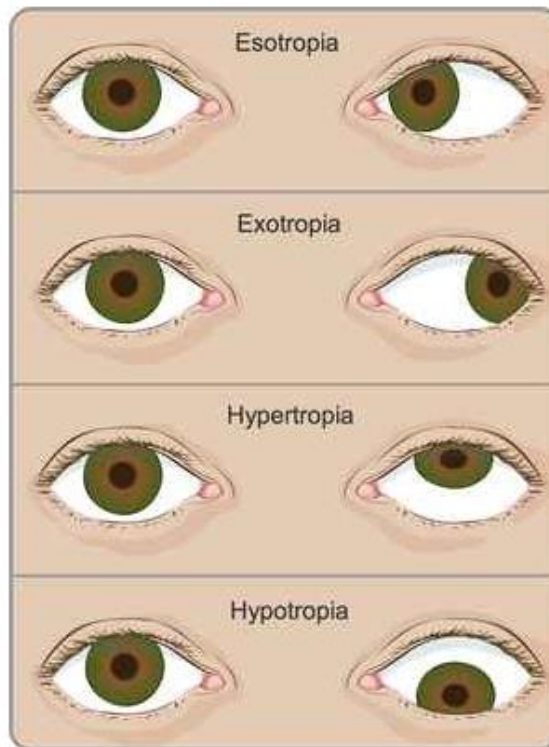


Figure 1-12: Types of strabismus shown are either horizontal (esotropia or exotropia) or vertical (hypertropia or hypotropia). Sometimes a horizontal strabismus can exist with a vertical strabismus. Illustration reproduced from <https://www.nuh.com.sg/eye/>

## 1.6.4 Stereoscopic Vision

Stereoscopic vision allows perception of depth when separate images from each eyes are successfully combined into one image in the brain.

A study by Lee et al (2001) retrospectively assessed the stereovision in 45 patients with albinism. They divided the cohort into three categories: those with no detectable stereopsis (NDS) n=26, course stereopsis (CS) n=10, and fine stereopsis (FS) n=9. The Titmus Fly test was used to assess the level of stereopsis. The individuals with albinism who demonstrated stereopsis were found to have better visual acuity, normal pigmentation, less iris transillumination, less foveal hypoplasia and less nystagmus (5 patients in the FS group did not show nystagmus) (Lee, King et al. 2001). It has been suggested that reduced stereopsis is due to the chiasmal misrouting that is present in albinism (Lee, King et al. 2001).

A more recent study by Kumar et al (2010) compared the stereoscopic vision in albinism and *FRMD7-IIN* and found within the albinism group, only 19.2% demonstrated stereopsis using the Lang test compared to 93.4% in the *FRMD7-IIN* group (Kumar, Gottlob et al. 2010).

### 1.6.5 Abnormal Head Posture (AHP)

The ocular causes of AHP include nystagmus (Kumar, Gottlob et al. 2010), strabismus (Helveston 1990), ptosis (Fiergang, Wright et al. 1999), high refractive errors (Havertape and Cruz 1998), various nerve palsies (Nucci, Kushner et al. 2005) and other rare forms of incomitant strabismus, for example, congenital fibrosis of extraocular muscles (CFEOMs) (Coymans, Al-Zuhaibi et al. 2010). Most patients with albinism will have nystagmus and/or strabismus. An AHP is often used by individuals with albinism to try and keep the eyes within the “null zone” and achieve the sharpest visual acuity (**Figure 1-13**). The null zone is the area where the nystagmus intensity is at its least and visual acuity is at its best. Generally an AHP is recorded whilst a patient is conducting a vision test or during reading. A maximal AHP is usually seen when the patient is making the most visual effort, for example when attempting to read small print (Stevens and Hertle 2003).

Anderson et al (2004) assessed 35 patients with albinism to investigate the efficacy of spectacle wear. In general they found wearing glasses increased the AHP compared to when not wearing them (Anderson, Lavoie et al. 2004). A previous study had hypothesised that patients with foveal hypoplasia and albinism may not benefit from an AHP (Shallo-Hoffmann, Faldon et al. 1999). However, a more recent study by Kumar, Gottlob et al (2010) assessed 52 patients with albinism and 80 patients with *FRMD7-IIN*; 47 of 52 (90.4%) patients with albinism demonstrated an AHP. They found an AHP over more than 5° in over half of the patients with albinism compared to only 15% of the *FRMD7-IIN* group. Interestingly, 15% of the albinism group had an AHP of greater than 15° compared to none of the *FRMD7-IIN* group (Kumar,

Gottlob et al. 2010). **Figure 1-13** gives examples of individuals with abnormal head postures pre and post-surgery.

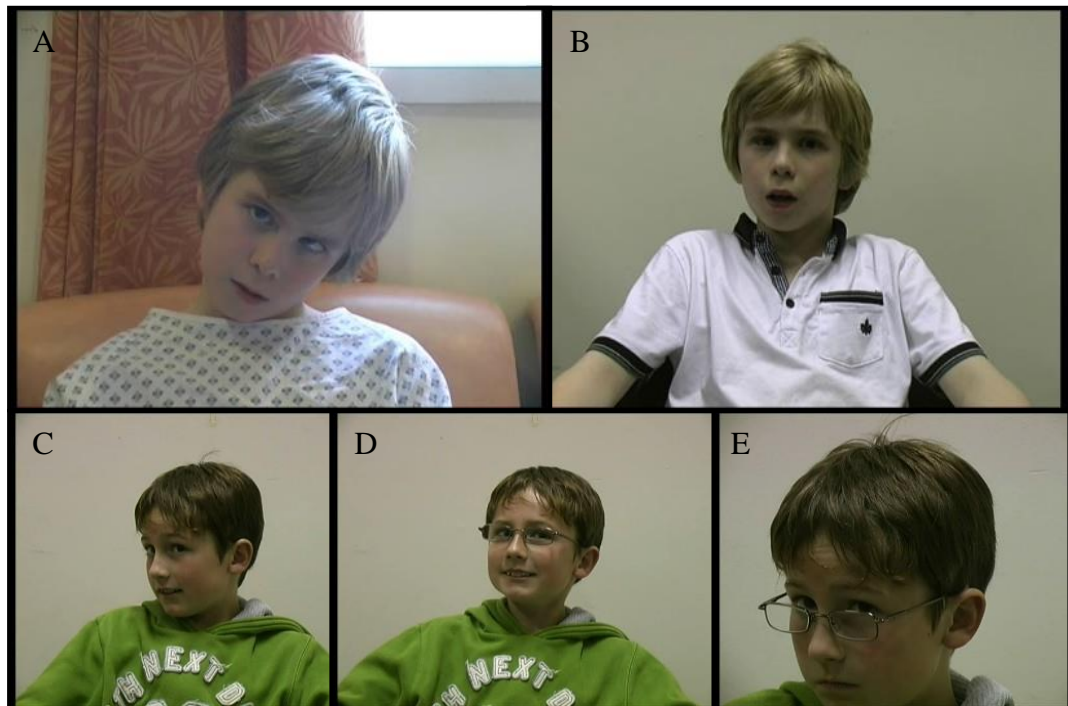


**Figure 1-13: Abnormal head postures. (A) Individual pre-surgery with a left head tilt. (B) Same individual post-surgery with  $<5^\circ$  face turn to the right. (C) Individual with a  $>15^\circ$  face turn to the right. (D) The same individual with glasses and a reduced AHP. (E) The same individual altering the head posture to where he feels he can see optimally.**

## 1.6.6 Abnormal Refractive Errors

A refractive error occurs when there is failure of the eye to correctly focus rays of light from an object onto the fovea. A refractive error is defined as the difference between the focal length of the lens and cornea and the length of the whole eye resulting in spherical refractive errors such as myopia (short-sightedness), hypermetropia (long-sightedness) and/or astigmatism (shape of eyeball or cornea) (Williams, Verhoeven et al. 2015).

High refractive errors are often encountered in humans with albinism (Dickinson and Abadi 1984, Wildsoet, Oswald et al. 2000, Anderson, Lavoie et al. 2004, Yahalom, Tzur et al. 2012).

There is debate between authors as to whether individuals with albinism predominantly show hypermetropia (Loshin and Browning 1983, Dickinson and Abadi 1984, Wildsoet, Oswald et al.

2000) or myopia (Dickinson and Abadi 1984). With-the-rule astigmatism (vertical meridian is steeper than the horizontal meridian) is commonly found in albinism according to previous literature (Wildsoet, Oswald et al. 2000).

Recent literature by Healey et al (2013) compared the refractive error in albinism to the grade of foveal hypoplasia (subjectively graded). Surprisingly, no correlation was observed for this comparison alone, the authors only found a relationship between foveal hypoplasia and refractive error when grouping all patients within their study together (albinism, IIN, isolated foveal hypoplasia and *PAX6* mutation) (Healey, McLoone et al. 2013). These findings were of particular interest especially as there were a number of limitations in this study, particularly in relation to the patient cohorts used. For example, the albinism group in this study only demonstrated grade 3-4 foveal hypoplasia thus wasn't representative of the spectrum of foveal hypoplasia seen in albinism (Thomas, Kumar et al. 2011), also the group used to compare the albinism group with was three separate nystagmus associated groups put together (IIN, isolated foveal hypoplasia and *PAX6* patients) in NAIN (non-albinotic idiopathic nystagmus). These conditions can have a very different phenotype and thus should not be grouped together.

These limitations are discussed fully in **Chapter 6** of this thesis and provided us motivation to conduct our own study looking at refractive status in four separate conditions associated with nystagmus (albinism, IIN, *PAX6* mutation and achromatopsia) and compare these to foveal hypoplasia (graded subjectively as well as objectively). All four conditions have a very different phenotype and are therefore considered as separate groups.

### **1.6.7 Positive Angle Kappa**

Angle kappa is determined by the intersection between the line of sight, detected clinically by the corneal light reflex and the pupillary axis, defined as the axis that passes through the

centre of the pupil and perpendicular to the central cornea (Merrill, Lavoie et al. 2004) (**Figure 1-14**). A positive angle kappa corresponds to a corneal light reflex nasally from the centre of the pupil. In a previous study by Brodsky and Fray (2004), a positive angle kappa was found in at least one eye in 95% of patients with albinism and in both eyes for 71.4% of the same patients, compared to 33% in at least one eye for idiopathic nystagmus and 16.6% in both eyes (Brodsky and Fray 2004). In a study carried out by Merrill, Lavoie et al (2004) it was found that 99.6% of albinism patients demonstrated a positive angle kappa. The clinical significance of this is that an exotropia will appear larger or an esotropia will appear smaller due to the corneal light reflex being displaced nasally.

The cause for an abnormally positive angle kappa is poorly understood. Merrill, Lavoie et al (2004) and Brodsky and Fray (2004) attempted explanations in their studies. Brodsky and Fray (2004) suggest that the involvement of the anomalous decussation of the optic axons in albinism could play a part in causing this structural anomaly. They also state infantile nystagmus can demonstrate a latent nystagmus component when one eye is occluded. In latent nystagmus a nasally directed drift is followed by a temporally directed saccade that overshoots the fovea and situates the image onto the temporal retina immediately after cessation of the fast phase. This produces a corresponding positive angle kappa (Brodsky and Fray 2004). In addition, Merrill, Lavoie et al (2004) suggest the refractive status of a patient can often increase the chances of the appearance of a positive angle kappa. They also hypothesise that this increase in positive angle kappa is due to foveal hypoplasia with a preferred fixation point at an eccentric location (Merrill, Lavoie et al. 2004).

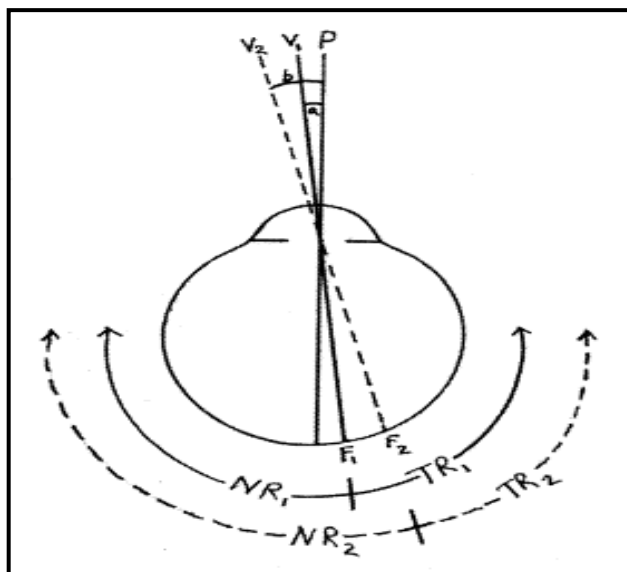


Figure 1-14: Explanation of angle kappa. This right eye is viewed from above. a = normal positive angle kappa; b = abnormal positive angle kappa; F1 = normal fovea; F2 = abnormal fovea; NR1 = normal nasal retina; NR2= abnormal nasal retina; P= pupillary axis; TR1= normal temporal retina; TR2= abnormal temporal retina; V1= normal visual axis; V2= abnormal visual axis. Reproduced from Brodsky and Fray (2004).

## 1.6.8 Nystagmus

Nystagmus is an involuntary to and fro oscillation of the eyes. Nystagmus, and other spontaneous abnormal eye movements that disrupt steady fixation pose a common diagnostic challenge for clinicians (Leigh and Zee 2006). In a previous survey, carried out in Leicestershire, UK, the prevalence of nystagmus was estimated to be 24 in 10,000 (Sarvananthan, Surendran et al. 2009). However, the prevalence varies worldwide.

Different types of nystagmus exist, with the differences being in waveform, axis and oscillation. The bilateral involuntary oscillations are conjugate and occur principally on the horizontal plane, although torsional and vertical eye movements have also been recorded in albinism (Collewijn, Apkarian et al. 1985).

Dell'Osso and Daroff (1975) characterised the waveforms of individuals with infantile nystagmus into three distinct groups: pendular, jerk and dual jerk waveforms (Dell'Osso and Daroff 1975). These distinct waveforms can be seen in **Figure 1-15**.

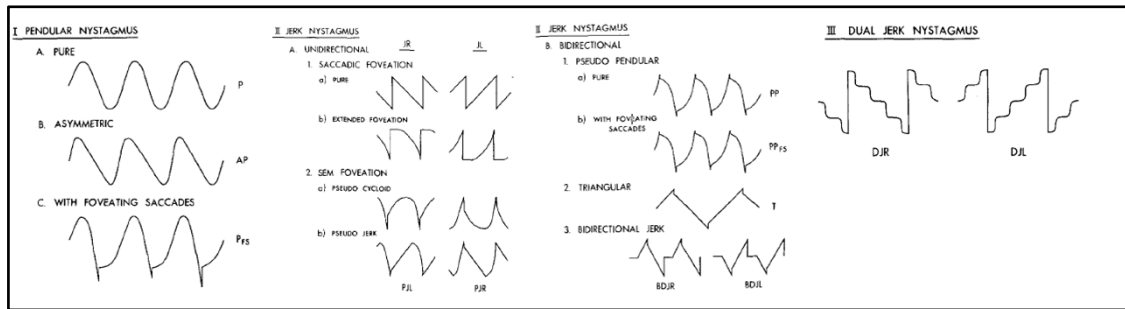


**Figure 1-15: The different types of waveforms commonly seen in infantile nystagmus. I=Pendular nystagmus, II=Jerk nystagmus and III=Dual Jerk nystagmus. Reproduced from Dell'Osso and Daroff (1975).**

Nystagmus is almost always present in patients with albinism. A study by Timms et al (2006), found even though some patients diagnosed with albinism did not demonstrate nystagmus, they did in fact have square wave jerks (back to back saccades) on examination (Timms, Thompson et al. 2006). Nevertheless there have been cases reported where patients have all other signs of albinism with the exception of nystagmus.

Previous studies have attempted to determine the association between the nystagmus phenotype and genotype in patients with albinism using DNA testing (Collewijn, Apkarian et al. 1985, Abadi and Pascal 1994). Abadi and Pascal (1994) assessed thirty-two patients with albinism and nystagmus and characterised the type of nystagmus based upon a diagnosis of TNOCA (tyrosinase-negative oculocutaneous albinism), TPOCA (tyrosinase-positive oculocutaneous albinism), XLOA (X-linked ocular albinism) and AROA (autosomal recessive ocular albinism). It is important to note that TNOCA and TPOCA are no longer used when characterising individuals with albinism. From these 32 patients with TNOCA and TPOCA, 12 (37.5%) exhibited periodic alternating nystagmus (PAN). Periodic alternating nystagmus consists of involuntary oscillations of the eyes with cyclical changes of nystagmus direction (Thomas, Crosier et al. 2011). Abadi and Pascal (1994) concluded there was no clear link between type of albinism and type of nystagmus except for two patients diagnosed with AROA

who both had PAN. However this finding could have been due to such a small cohort (n=2) (Abadi and Pascal 1994). A larger cohort would be required to strengthen this theory further.

Another study by Abadi and Pascal (1994) further agrees with the previous findings as the authors assessed monozygotic twins with TNOCA. Both individuals carried an identical genetic make-up. Both siblings were tested and eye movement recordings assessed. Twin A demonstrated left beating jerk nystagmus with extended foveation, whereas twin B exhibited right beating jerk nystagmus with extended foveation. Both the amplitude and frequency of nystagmus also differed between the patients. These findings demonstrate how patients with an equivalent genetic make-up can have different nystagmus characteristics and suggest that environmental factors also have a part to play.

This is further supported by the previous work of Dell'Osso (1985) who reviewed eye movement records collected over a twenty year span to look at the relative incidence of each congenital nystagmus waveform or combination of waveforms in one hundred individuals. From this data he postulated that due to various families with congenital nystagmus displaying higher than expected probabilities of similar waveform, heredity played a significant role in determining nystagmus characteristics (Dell'Osso 1985). Factors such as convergence, fixation and also emotional state can influence the nystagmus characteristics (Abadi and Pascal 1994).

### **1.6.8.1 Nystagmus Types not related to Albinism**

#### **1.6.8.1.1 Idiopathic Infantile Nystagmus**

Idiopathic infantile nystagmus (IIN) was previously termed congenital idiopathic nystagmus. Individuals with IIN can be singletons or familial. In IIN there is no obvious pathology on ophthalmological examination. Inheritance patterns for familial types are autosomal recessive, autosomal dominant and X-linked. Mutations of the *FRMD7* gene are now known to be a cause of X-linked IIN (Tarpey, Thomas et al. 2006). Thomas et al (2008) reported phenotypical

differences between individuals with *FRMD7* IIN and non-*FRMD7* IIN. The main differences between the groups were that the *FRMD7* IIN group had considerably fewer individuals with abnormal head posture and also less nystagmus in primary position (Thomas, Proudlock et al. 2008). Similarities between the groups included good visual acuity, good stereopsis and low incidence of strabismus. Kumar et al (2011) compared nystagmus characteristics in IIN and albinism and found no significant differences for the groups for nystagmus amplitude or nystagmus foveation. Interestingly, they discovered that nystagmus associated with albinism was significantly more likely to be jerk nystagmus rather than pendular compared to IIN (Kumar, Gottlob et al. 2011).

## **1.6.8.2 Infantile Nystagmus Due to Retinal Disease**

### **1.6.8.2.1 Achromatopsia**

Achromatopsia is characterised by reduced visual acuity, hypo-reflective zone on OCT, nystagmus and a decreased or complete loss of colour vision due to reduced function of cone photoreceptors. Electroretinogram (ERG) testing is useful to diagnose achromatopsia by demonstrating an extinguished photopic response (including the 30Hz flicker response). Genetic analysis of mutations of known genes has high diagnostic value (Kohl S 2004).

### **1.6.8.2.2 Congenital Stationary Night Blindness (CSNB)**

Congenital stationary night blindness (CSNB) is characterised by reduced visual acuity, defective dark adaptation, refractive errors, nystagmus, normal colour vision and normal fundus examination (Boycott KM 2000). The ERG in CSNB displays a negative ERG with a reduced scotopic b wave amplitude (Miyake, Horiguchi et al. 1994).

### **1.6.8.3 PAX6 Mutation**

Mutations in the *PAX6* gene can cause a multitude of ocular manifestations which are likely to reduce the visual potential of an affected individual. A study by Hingorani et al (2009) found

that these ocular malformations can include aniridia, nystagmus, foveal hypoplasia, corneal and anterior segment abnormalities, cataracts, optic nerve hypoplasia and glaucoma (Hingorani, Williamson et al. 2009).

#### **1.6.8.4 Manifest Latent Nystagmus**

Manifest latent nystagmus (MLN) is a term used to describe nystagmus which increases under monocular viewing compared to binocular viewing conditions and changes direction depending on which eye is fixing. It is almost always associated with infantile squint syndrome (Abadi and Scallan 2000).

## 1.6.9 Iris Transillumination

Iris transillumination is a common sign noted in patients who have albinism. Unless retro illumination is performed using slit lamp biomicroscopy in a dark room, this sign can easily be missed. It is invariably present in individuals affected with albinism, and is used as a major diagnostic feature (Summers 1996). Iris transillumination can cause photophobia. Various types of transillumination of the iris can occur without albinism, for example with pseudo exfoliation syndrome (Trantow, Mao et al. 2009) and pigment dispersion syndrome (Yip, Sothornwit et al. 2009). Occasionally, diffuse iris transillumination can also occur with other conditions affecting the iris, after intraocular surgery and also as a side effect of specific medications (Willermain, Deflorenne et al. 2010). Due to the high incidence of iris transillumination in conditions not associated with albinism, a clinician must ensure there is sufficient other evidence to be able to make an accurate diagnosis of albinism.

**Figure 1-16** displays photos of a marked iris transillumination defect of a patient with albinism and no iris transillumination in a control. **Figure 1-17** displays a subjective iris transillumination grading scheme created by Summers et al (1988) with photos produced by Seo et al (2007) to aid grading the iris transillumination defect seen in albinism.

Prior to commencing our study, anterior segment – optical coherence tomography (AS-OCT) imaging of iris abnormalities in albinism had not been reported. Consequently, **Study 1 (Chapter 3)** of this thesis consists of imaging the iris using OCT to assess structural differences between individuals with albinism and controls. This was then used to assess the diagnostic potential of AS-OCT in albinism.

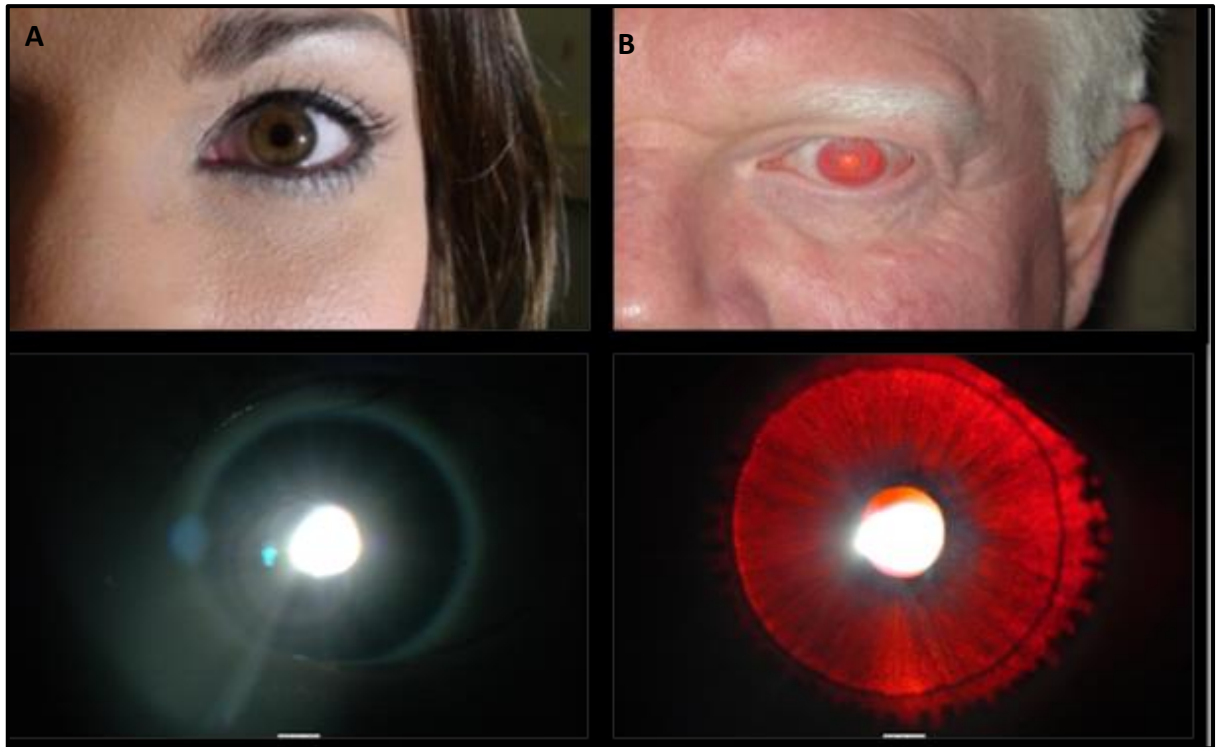


Figure 1-16: (A) Control patient with no iris transillumination. (B) Patient with albinism and the full iris transillumination defect.

Iris Transillumination Grade	Description
Grade 1	Marked amount of iris pigment, minimal punctuate transillumination
Grade 2	Moderate amount of iris pigment; diffuse iris transillumination, often irregular in location
Grade 3	Minimal amount of iris pigment; almost complete transillumination
Grade 4	No iris pigment; full iris transillumination

Figure 1-17: Iris transillumination grading scheme as created by Summers et al (1988). Photos produced by Seo et al (2007).

## 1.6.10 Macular Transparency

Individuals with albinism are likely to show varying degrees of macular transparency, which is generally due to the lack of pigment within the fundus (Summers 1996). Macular transparency is determined by assessing the level of visibility of choroidal vessels in the macula. The easier it is to see these vessels the poorer the level of pigmentation within the fundus. Macular transparency grading was more readily used before the invention of OCT. Since OCT has been introduced the degree of foveal hypoplasia is now the preferred method of assessment used by clinicians.

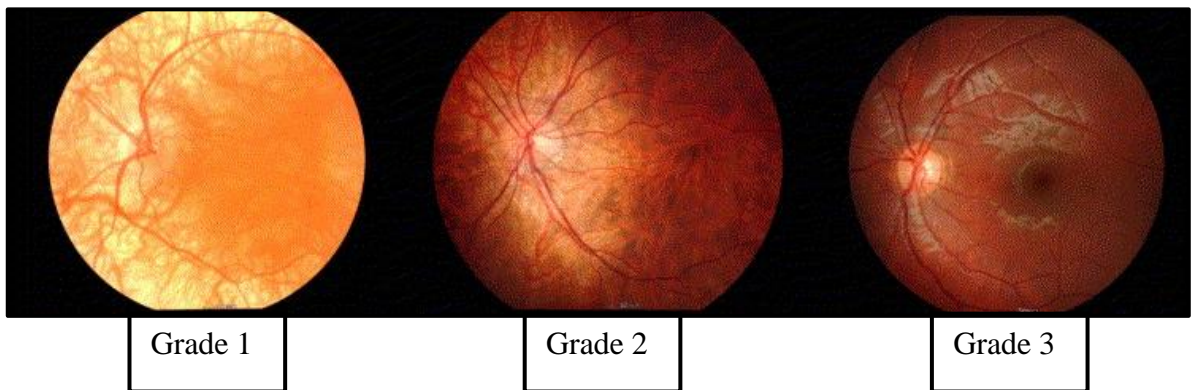


Figure 1-18: The 3 grades of macular transparency. Reproduced from Summers et al (1988).

Macular transparency	Description
Grade 1	Choroidal vessels easily visible in the macula
Grade 2	Choroidal vessels visible in the macula, but indistinct because of translucent-appearing retinal pigment epithelium
Grade 3	Choroidal vessels not visible in the macula because of the opaque quality of the pigment epithelium

Table 1-2: The 3 Grades of macular transparency. Reproduced from Summers et al (1988).

### 1.6.11 Foveal Hypoplasia

The fovea is the site where the highest numbers of cone photoreceptor cells are found and it is the region of the retina that provides the sharpest visual acuity (Tick, Rossant et al. 2011). The macula of individuals with albinism using slit lamp bio-microscopy show an absent or reduced foveal reflex and hypoplastic fovea. Disturbance during the foveal maturation process can lead to foveal hypoplasia.

Optical coherence tomography (OCT) has been used to explore varying degrees of foveal hypoplasia in conditions associated with nystagmus. Numerous recent studies have shown that OCT can be used as a diagnostic tool when assessing foveal hypoplasia (Seo, Yu et al. 2007, Mohammad, Gottlob et al. 2011, Thomas, Kumar et al. 2011).

Thomas et al (2011) have created a subjective grading scheme for foveal hypoplasia which is readily used to sub-divide foveal hypoplasia into grades of severity (Thomas, Kumar et al. 2011). This is shown in **Figure 1-19**.

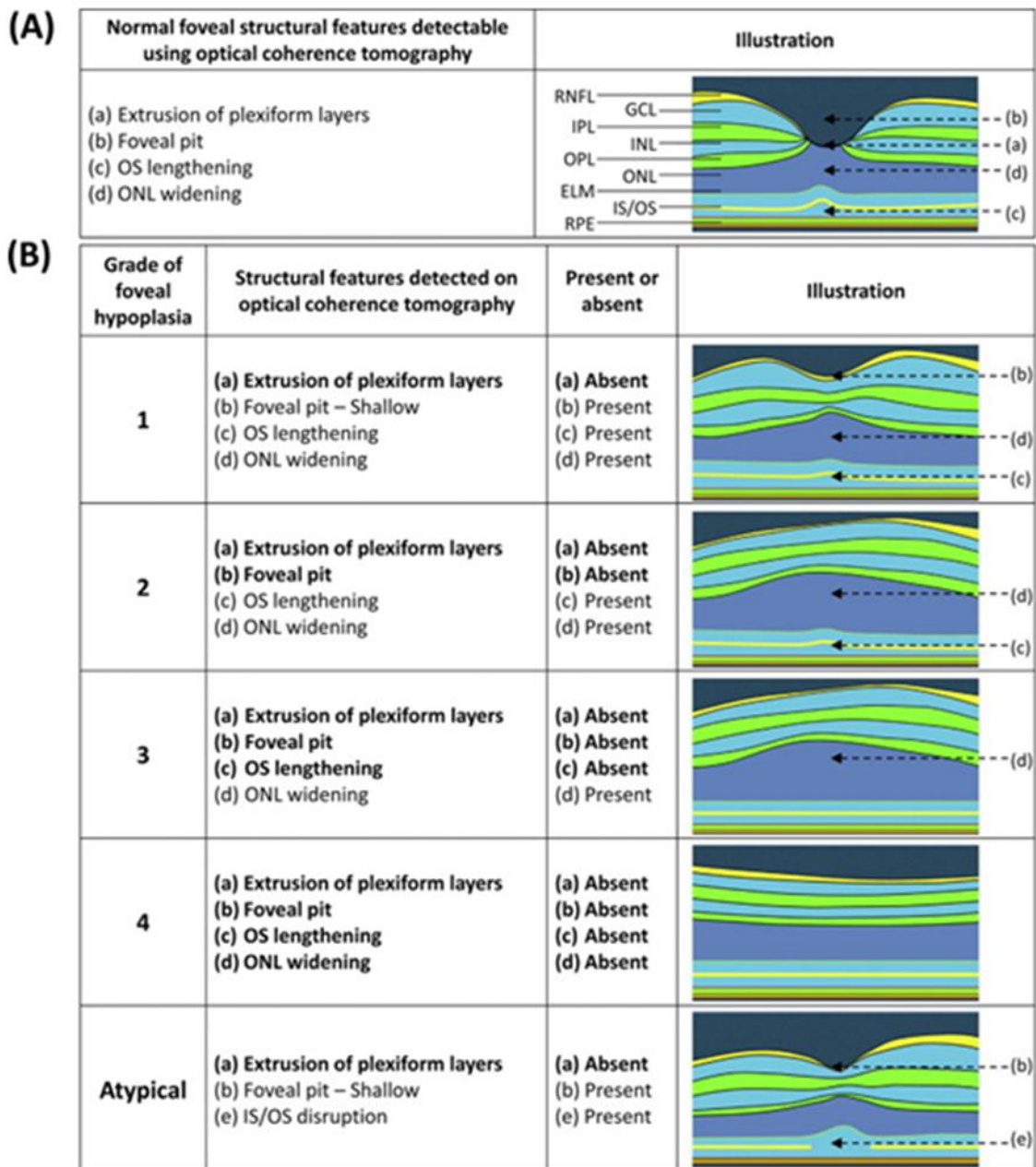


Figure 1-19: (A) Illustration showing the unique features of a normal fovea on optical coherence tomography. (B) Illustration of typical and atypical grades of foveal hypoplasia. Image reproduced from Thomas et al (2011).

## 1.6.12 Optic Nerve Abnormalities

Previous literature assessing the optic nerve in albinism has demonstrated various abnormalities. Käsmann-Kellner et al (2003) assessed anatomical differences in the optic nerve, optic chiasm and optic tract using standardised clinical and MRI evaluation. They found ten out of seventeen individuals with albinism demonstrated signs of dysplasia of the optic nerve head. This included individuals with smaller optic nerves, different angles of optical entry into the chiasm and smaller chiasm height and width (Kasman-Kellner, Schafer et al. 2003). Chong et al (2009) assessed the foveal structure in albinism using OCT and interestingly also discovered several patients within their study had elevated optic nerves (Chong, Farsiu et al. 2009). Furthermore, Schmitz et al (2003), using MRI, also found variations in size and shape in the optic nerve and found the optic nerve to be smaller in albinism, they also found smaller chiasmatic widths and smaller optic tracts in albinism (Schmitz, Schaefer et al. 2003).

More recently, Mohammed et al (2015) conducted a large study to compare the optic nerves in albinism and healthy controls using OCT. They found a number of differences between the optic nerve structure in albinism and controls. The principal findings from this literature were as follows:

1. The optic discs were significantly elongated horizontally and found smaller cup to disc ratios in the albinism group compared to the control group (**Figure 1-20A**).
2. The nasal and temporal rim areas were significantly larger in the albinism group compared to the controls which leads to the cup volume being significantly smaller in albinism compared to controls (**Figure 1-20B**).
3. The peri-papillary RNFL (ppRNFL) was also significantly thinner in the albinism group compared to controls, especially in the temporal quadrant (**Figure 1-20C**).

The author concluded that ocular mal-development in albinism is not limited to the fovea alone and the optic nerve is also involved (Mohammad, Gottlob et al. 2015).

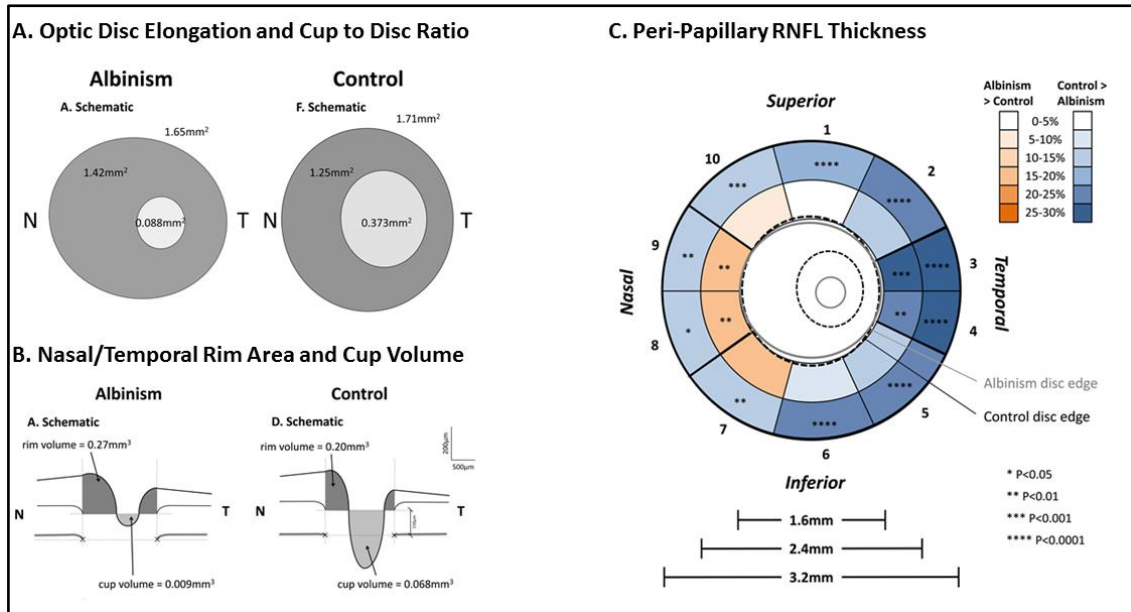


Figure 1-20 : Optic nerve differences between individuals with albinism and controls. (A) Shows optic disc elongation and the cup to disc ratio. (B) Shows the nasal/temporal rim areas and the optic cup volume. (C) Shows the peri-papillary RNFL (ppRNFL) thickness differences. Reproduced from Mohammad et al (2015).

### 1.6.13 Misrouting of Optic Nerve/Chiasmal Misrouting

In the normal population, the nasal retina projects to the contralateral hemisphere whereas the temporal retina projects ipsilaterally. A line of decussation that divides between the nasal and temporal fibres normally coincides with the vertical meridian running through the fovea (Hoffmann, Seufert et al. 2007). In cases of albinism and albinism-associated defects a higher percentage of fibres from the temporal retina crosses the midline at the optic chiasm. Thus the line of decussation is shifted towards the temporal retina (Guillery, Okoro et al. 1975).

Increased crossing of the optic nerve fibres at the chiasm is one of the most consistent findings in albinism in all species. In humans, it has been found to be highly specific and asymmetries in visual evoked potentials are a very helpful diagnostic tool for albinism (Apkarian, Reits et al. 1983), although the degree of asymmetry varies from patient to patient (Hoffmann, Lorenz et al. 2005).

The gold standard method of assessing the presence of this asymmetry/misrouting of the optic nerve is using visual-evoked potentials (VEP). Creel (1971) was the first to explore and demonstrate abnormal visual projections in humans with albinism using VEP. Prior to this, abnormal decussation in albino rats was reported (Lund 1965). Misrouting of the optic nerve can be determined with VEPs by detecting the contralateral predominance in the responses to monocular stimulation (Creel, Witkop et al. 1974, Apkarian, Reits et al. 1983, Apkarian, Reits et al. 1984). There are two methods of conducting VEPs whereby the stimulus used can be either (i) flash or (ii) pattern-onset. Apkarian (1992) has suggested that flash stimuli can be used for children aged below three years and permits both flash and pattern-onset for children between three and six years of age (Apkarian 1992). However Kriss et al (1990) argues that flash VEP is better than pattern-onset stimulation when detecting asymmetry in children aged up to eleven years old (Kriss, Russell-Eggitt et al. 1990). **Figure 1-21** shows the asymmetric VEP results produced when comparing an individual with albinism to an individual with IIN. The average traces from the 5-channel VEP go in the opposite directions in albinism when left and

right eyes are stimulated whereas the peaks in IIN do not, this is highlighted on **Figure 1-21** with the arrows.

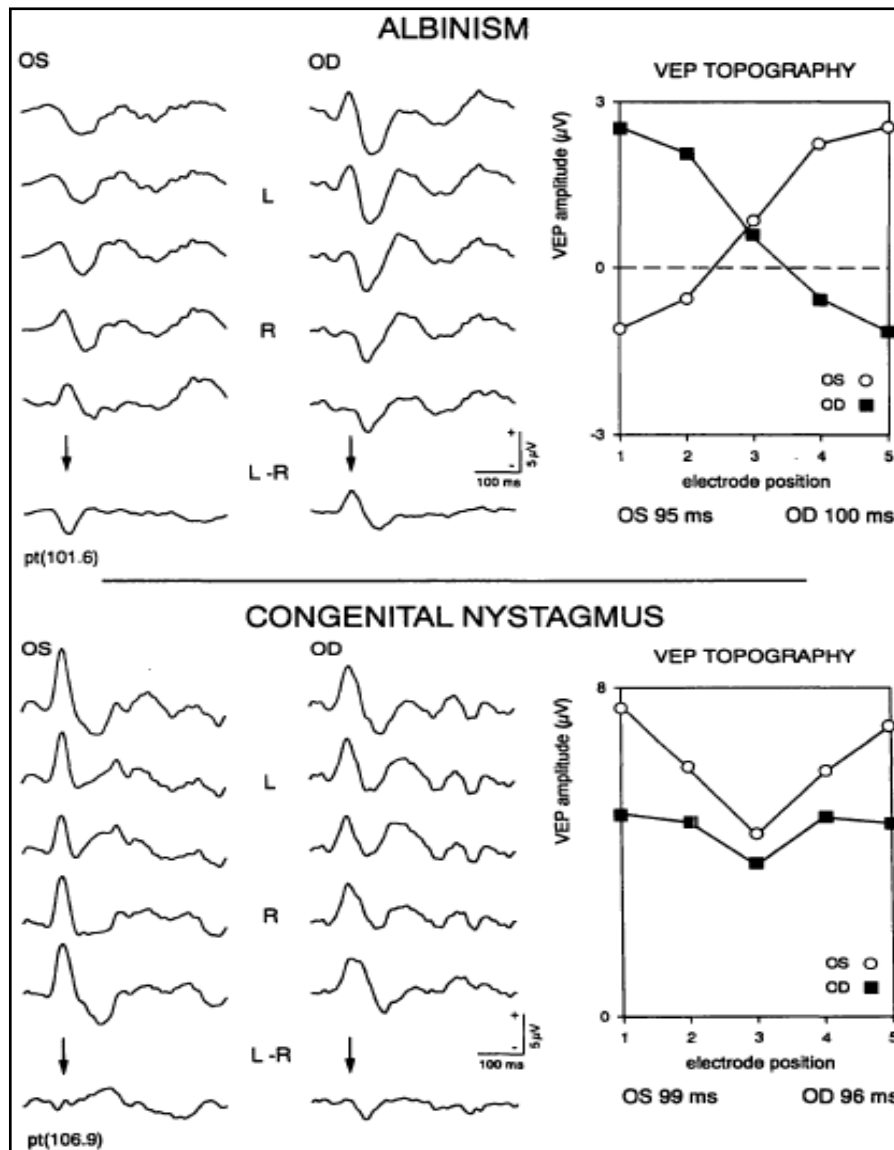


Figure 1-21: A VEP trace for a patient with albinism (top) and a VEP trace for a patient with congenital idiopathic nystagmus (bottom). It is clear to see the abnormal crossing seen in albinism as illustrated by the arrows showing peaks in different directions for each eye when comparing the averaged peaks. Image reproduced from Apkarian and Shallo-Hoffman (1991).

### **1.6.14 Visual Field (VF) Deficits in Albinism**

Previous literature describing VF deficits in albinism is controversial. St John and Timney (1981) found 9 out of 13 individuals with albinism had constricted VFs compared to controls using a tangent screen. They also found that the contrast sensitivity was reduced in albinism compared to a control group. Interestingly, a small subset of their patients with albinism demonstrated a difference in nasal/temporal contrast sensitivity (St John and Timney 1981). Abadi and Pascal (1993) assessed the VFs in albinism, IIN and controls using Goldman visual field testing. However, they did not find constricted fields but found 5/11 of their subjects exhibited their peak contrast sensitivity away from the fovea demonstrating areas of reduced contrast sensitivity compared to controls. Abadi and Pascal (1993) also found that the detection threshold was worst in their albinism group compared to the IIN group and controls (Abadi and Pascal 1993). Hoffmann et al (2007) assessed the VFs in albinism and controls using the Octopus 101 (static perimetry) and compared this to chiasmal misrouting (VEP) that is seen in albinism. Hoffmann et al (2007) did not find a relationship between chiasmal misrouting and VF contrast sensitivity. They also assessed for nasal/temporal asymmetries in their group, however no nasal/temporal differences were found (Hoffmann, Seufert et al. 2007).

The three studies mentioned above used different methods for assessing the VFs in albinism and all report different findings. In the previous studies by St John and Timney (1981) and Hoffmann et al (2007), neither study had a control group with other nystagmus forms without albinism. As all of their participants had nystagmus, the effect of nystagmus on their findings cannot be ruled out. All of the aforementioned studies had also used a small number of participants with albinism ( $n < 15$ ). There is also controversy in whether nasal/temporal asymmetry exists in the VFs in albinism, with St John and Timney (1981) finding nasal/temporal VF differences in a subset of their study population with albinism, whereas Hoffmann et al (2007) found no nasal/temporal asymmetry in their cohort of patients with albinism.

## 1.7 Chiasmal and Post-Chiasmal Abnormalities in Albinism

### 1.7.1 The Optic Chiasm and the Optic Tract

As previously mentioned, one of the main diagnostic features in individuals with albinism is the abnormal decussation of the optic nerves at the optic chiasm (**Section 1.6.13**). In albinism there is an abnormal projection of the temporal retina to the visual cortex contralateral to each eye. The projection, in addition to the normal projection from the nasal retina, provides a cortical hemisphere with visual input from more than the normal hemi-field of visual space (Hoffmann, Tolhurst et al. 2003). In previous models of albinism in the ferret there have been various theories proposed as to what happens with this additional visual input: an extensive debate discusses whether there is re-organisation of the thalamo-cortical connections to give a standardised true albino pattern, whether it gives the abnormal input an exclusive cortical representation (Boston pattern) or whether it is suppressed (Midwestern pattern).

The retinofugal fibres within the mammalian visual organisation make a binary decision to either cross the chiasmal midline and project to the contralateral hemisphere or remain uncrossed and project to the ipsilateral hemisphere. The percentage of fibres that remain uncrossed varies between different species (Neveu and Jeffery 2007). The optic chiasm contains two spatially distinct retinal trajectory patterns that probably represent the course of the crossed and uncrossed fibres. These appear to be largely different with uncrossed fibres confined laterally and crossed projections found more centrally (Neveu and Jeffery 2007). However, caution should be taken with this assumption when comparing different species affected by albinism. **Figure 1-22** illustrates the structural differences existing between rodents and humans unaffected by albinism.

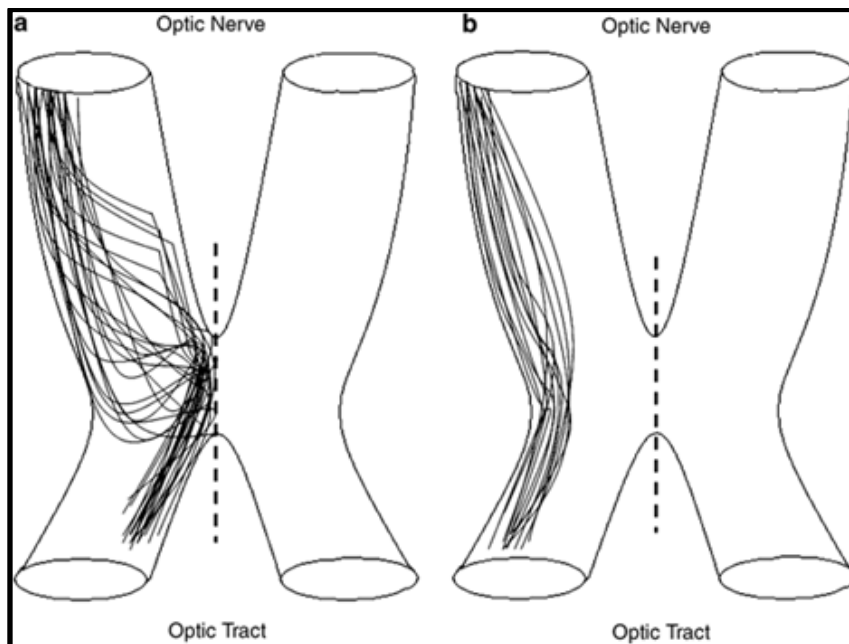


**Figure 1-22: Schematic drawings showing two distinct forms of axon projection to the ipsilateral optic tract and chiasm formation. (a) Representative pattern of chiasm formation in the rodent, where axons that form the ipsilateral projection interact with axons from the other eye at the chiasmal midline (dashed line), before innervating the ipsilateral optic tract. (b) Representative pattern of chiasm formation in the marsupial and man, where axons that form the ipsilateral projection maintain a lateral course through the optic chiasm into the ipsilateral optic tract. Reproduced from Neveu et Jeffrey (2007).**

The optic tract in individuals with albinism is predominantly filled with fibres from the contralateral side due to the abnormal decussation found at the chiasm (Guibal and Baker 2009). Current literature suggests that in pigmented carnivores and rodents, retinal ganglion cells in the temporal retina with ipsilateral coursing axons are more likely to be generated at earlier stages than cells with crossing projections from the same retinal region (Priour and Rebsam 2017). Uncrossed axons from the temporal retina have been found to reach the chiasm at earlier stages than neighbouring cells in the temporal retina with crossed axons (Priour and Rebsam 2017).

In all mammals, timing of the retinal ganglion cell outgrowth has been linked to fibre reorganisation along the retinofugal pathway (Guibal and Baker 2009). Guibal et Baker (2009) aimed to assess differences in the optic tract between pigmented and unpigmented (albino)

ferrets using light and electron microscopy. The main findings were that, when comparing the axons within the tract, the large diameter axons were confined to the superficial layers in normal ferrets but are found throughout superficial and deep layers within the albino ferrets. The study also revealed the large diameter axons were poorly myelinated in comparison to small diameter axons which were thickly myelinated. These deep abnormal axons were found to originate from the contralateral retina (Guibal and Baker 2009).

## **1.7.2 The Lateral-Geniculate Nucleus (LGN)**

The LGN is normally organised so it receives visual information from both the contralateral and ipsilateral eyes to create a visual image. However, in albinism, most of this information comes from the contralateral eye alone due to the structural abnormality found at the chiasm. In albino carnivores and primates, regions of the dorsal LGN (dLGN) that should have been occupied by terminals from the temporal retina of the ipsilateral eye now receive input from the temporal retina of the contralateral eye. This characteristic is demonstrated in Siamese cats (Guillery and Kaas 1971), ferrets (Thompson, Morgan et al. 1993), monkeys (Guillery, Hickey et al. 1984) and humans (Hoffmann, Tolhurst et al. 2003).

The functional consequence of this anomaly appears to take three major forms in albinism which shall be discussed below.

### **1.7.2.1 Cortical Representation Patterns**

#### **1.7.2.1.1 True Albino/ Interleaved Representation**

The alteration in retinal projection in albino mammals has dramatic effects on the visuotopic organisation within the visual cortex. Even if re-routing at the chiasm has no effect on the geniculocortical projection in albinos, the visuotopic map would be abnormal. There would be a strong representation of both the contralateral and ipsilateral hemi-fields in the same part of the cortex. This projection pattern is termed “true albino” and has been reported in albino cats

(Schmolesky, Wang et al. 2000), albino monkeys (Guillery, Hickey et al. 1984) and albino humans (Guibal and Baker 2009). An interesting finding made by Schmolesky et al (2000) was that the representation of the ipsilateral hemi-field in albino cats was weaker in the cortex rather than the dLGN, indicating some cortical suppression may be taking place (Schmolesky, Wang et al. 2000).

#### **1.7.2.1.2 Midwestern Pattern/ Interleaved Suppressed Representation**

This projection pattern consists of a full cortical suppression of the aberrant input from the contralateral eye in albinism. This was exhibited in one of twelve Siamese cats (Shatz 1977) and five of five albino ferrets (Garipis and Hoffmann 2003).

#### **1.7.2.1.3 Boston Pattern/ Contiguous Representation**

Here there is a functional input from both the temporal and nasal contralateral retina in the striate cortex. Input from the misrouted contralateral temporal retina passes through a different cortical location so that the mapping is novel. The geniculocortical projections are rearranged to generate a continuous and coherent mapping of the VF far into the ipsilateral hemi-field. The Boston pattern has been found in eleven of twelve Siamese cats (Shatz 1977) as well as twenty-two of twenty-five albino ferrets (Akerman, Tolhurst et al. 2003).

Hoffman et Dumoulin (2015) proposed a novel nomenclature intended for future use. They proposed the use of contiguous representation (formerly known as the Boston pattern), interleaved representation (previously referred to as the true albino pattern) and interleaved suppressed representation (known as the Midwestern pattern) (Hoffmann and Dumoulin 2015). Hoffman et Dumoulin (2015) consider this broader classification to be more appropriate as it would allow for these chiasmatic abnormalities to be discussed in conditions other than albinism. **Figure 1-23** elucidates the three representations that we associate with albinism and how these compare to the VF representation in controls (Hoffmann and Dumoulin 2015).

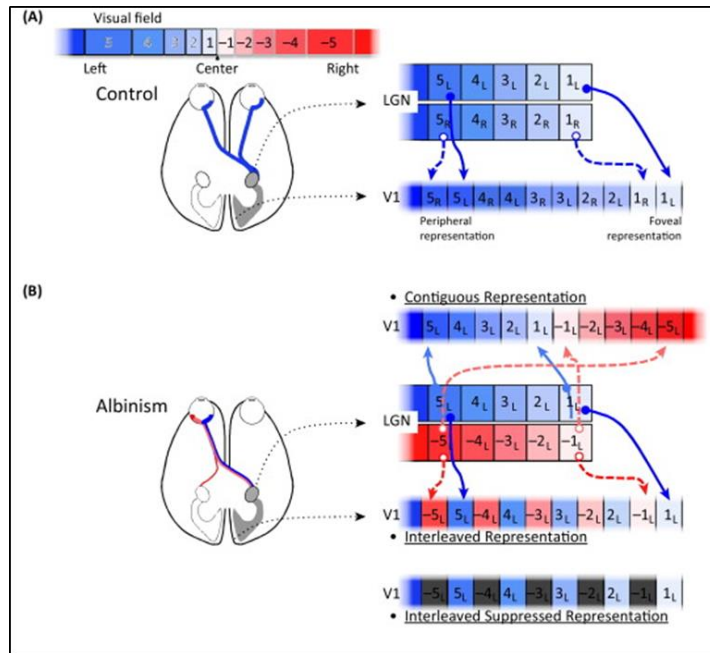


**Figure 1-23: Visual field representations in the visual cortex in (A) control and (B) albinism.** (A): The binocular input to the right lateral geniculate nucleus (LGN) is organised in retinotopic maps of the left visual field (colour coded blue; positive numbers) that are separate for each eye (fields with positive numbers, subscript indicates L – left, R – right eye input). (B): For the central visual field, the right LGN receives monocular input from the nasal (i.e. left hemi-field, colour coded blue) and the temporal hemi-retina (i.e. right hemi-field, colour coded red) of the contralateral (left) eye. Consequently, in addition to the normal input from the contralateral visual field (positive numbers) there is input from the ipsilateral visual field (negative numbers). Three different projections from the LGN to V1 were inferred from animal models of albinism: i) Contiguous Representation (Boston Pattern) requires a re-ordering of the geniculostriate projection (note the inversion of the geniculostriate projection for the additional input of the ipsilateral hemifield, i.e. broken light red lines whilst the unbroken blue lines indicate the projection of the normal input of the contralateral hemi-field); ii) Interleaved Representation (former True Albino Pattern) indicates geniculostriate projections that are equivalent to those found in controls, although they operate on partially abnormal input, that is, the representation of the ipsilateral visual field (broken red lines). This cortical organisation indicates the conservation of the normal geniculostriate projection scheme despite abnormal LGN input. iii) The same conservative geniculostriate projection is inferred for the Interleaved Suppressed Representation (former Midwestern Pattern cortical organisation depicted below Interleaved Representation), except that the abnormal representation of the ipsilateral visual field is suppressed (indicated by dark grey fields with negative numbers). Reproduced and amended from Hoffman et Dumoulin (2015).

### 1.7.2.2 Superior Colliculus and Pre-Tectum

Creel et al (1982) found uncrossed retinal projection to the superior colliculus and pre-tectum is reduced in albinism (Creel, Hendrickson et al. 1982) which indicates that it may cause problems with visuo-motor integration in orientating reflex and facilitating shifts in gaze.

## 1.8 Research Questions and Aims

Below are the main aims for studies conducted as part of this thesis:

### **Study 1: Anterior Segment Imaging in Albinism**

- Compare anterior-segment OCT imaging in albinism and controls to look specifically at the iris transillumination defect structurally
- Assess the efficacy of anterior segment OCT (AS-OCT) in the diagnosis of albinism
- Correlate iris thickness measures in albinism with other phenotypic features associated with albinism (e.g. foveal hypoplasia and pigmentation)

### **Study 2: Visual Fields (VF) in Albinism and idiopathic infantile nystagmus (IIN)**

- Evaluate the VF deficits in albinism and IIN using a large sample size
- Assess nasal/temporal asymmetries in VF in order to correlate to VEP
- Assess quadrant differences in VF
- Assess VF differences in right and left eyes in albinism and IIN

### **Study 3: Central and Peripheral VF correlations with foveal and optic nerve (RNFL) measures**

- Compare central VF measures to foveal thickness at the fovea and peripheral retina in albinism using OCT
- Compare central and peripheral VF measures to retinal nerve fibre layer thickness around the optic nerve using OCT

### **Study 4: Assessing the relationship between foveal structure and refractive error in infantile nystagmus**

- Determine whether any relationships exist between refractive error and foveal hypoplasia in different groups of infantile nystagmus (albinism, IIN, *PAX6* and achromatopsia)

- Assess objective and subjective measures of foveal hypoplasia and how these compare to refractive errors and best corrected visual acuity
- Assess whether relationships exist between axial length and pigmentation with foveal structure and refractive error

These general aims and research questions are further elaborated in each study chapter.

# **Chapter 2**

## **Methodology**

## Chapter 2 Methodology

This chapter details the recruitment of all patients, their clinical characterisation and also an overview of the equipment used. In addition, each of the four studies has a separate methods section to explain the approaches that were used specifically for each study. All participant recruitment, assessment and analysis within this thesis was conducted by the author (VS) unless described otherwise.

### 2.1 Patient Recruitment

#### 2.1.1 Albinism and other Nystagmus-Associated Conditions

All patients were recruited from specialised neuro-ophthalmology clinics at the Leicester Royal Infirmary (NHS), from the Nystagmus Network UK or from databases created in the ophthalmology department at the University of Leicester. **Figure 2-1** is a flow chart explaining the testing procedure for the diagnosis and characterisation for all patients used as participants within the studies.

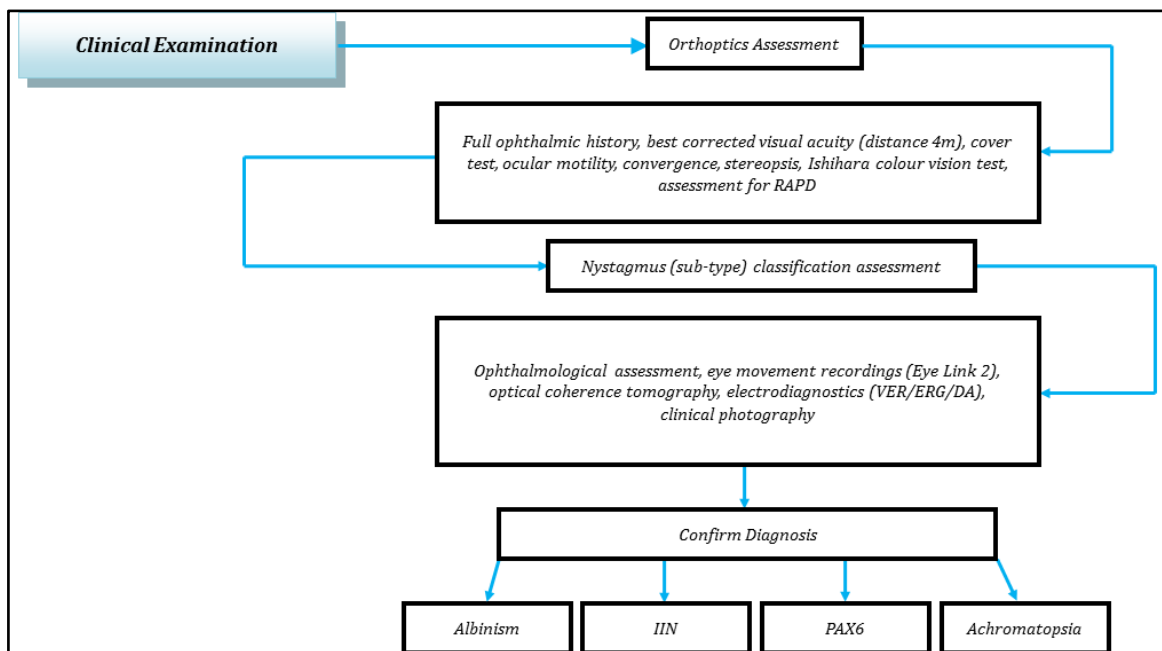


Figure 2-1: Flow chart illustrating the stages of clinical examination and diagnosis.

## **2.1.1.1 Inclusion/Exclusion Criteria**

### **2.1.1.1.1 Albinism**

The diagnosis of albinism was based on the coexistence of 3 key signs: foveal hypoplasia, chiasmal misrouting (VEP) and iris transillumination. All individuals with albinism used in the studies also had nystagmus.

### **2.1.1.1.2 IIN**

The diagnosis of IIN was made when an individual had nystagmus and no other ophthalmological or neurological disorders related to nystagmus. This included no iris transillumination, normal anterior segment and fundus assessment, normal electrophysiology testing (VEP/ERG) and no signs related to any other nystagmus associated diagnosis.

### **2.1.1.1.3 PAX6 Mutations**

*PAX6* has a broad phenotype. The diagnosis of *PAX6* is made when an individual has nystagmus, foveal hypoplasia and anterior segment anomalies (e.g. aniridia, corneal opacities, cataracts, etc.). All participants with *PAX6* mutations used in our study were genetically confirmed.

### **2.1.1.1.4 Achromatopsia**

The diagnosis of achromatopsia is made when an individual has nystagmus, a hypo-reflective zone on OCT assessment, reduced/absent colour vision and extinguished photopic response on electroretinography (ERG). All participants with achromatopsia used in our study were genetically confirmed.

### **2.1.1.1.5 Exclusion Criteria**

Individuals used in the aforementioned groups (albinism, IIN, *PAX6* and achromatopsia) were assessed to ensure they did not have any other eye disease or general health problems (for example, neurological disease, diabetes). If they did then they were excluded from the study.

## 2.1.2 Control Group

Control participants were recruited from volunteer colleagues at the Leicester Royal Infirmary and University of Leicester. Participants were not genetically related to an individual with nystagmus. All participants had no previous history of eye disease and performed normally in orthoptics and ophthalmological examinations. Controls were only used in **Study 1** to assess the differences in iris structure between patients with albinism and the controls. Further details of the control group used and their demographics are discussed in **Chapter 3 (Study 1)**.

	Study details	Albinism (n)	IIN (n)	PAX6 (n)	Achromatopsia (n)	Controls (n)
Study 1	Iris OCT in Albinism	55	-	-	-	45
Study 2	Visual Fields in Albinism and IIN	61	32	-	-	-
Study 3	Visual Field and OCT Correlations	61*	-	-	-	-
Study 4	Refractive Error compared to foveal hypoplasia	33	18	9	12	-

\*=99 eyes for foveal correlations and 71 eyes for optic nerve correlations from 61 individuals with albinism

[Table 2-1: Participant numbers for each study.](#)

## 2.1.3 Consent and Ethical Approval

Informed consent was taken from all individuals prior to assessment. The assessment adhered to the tenets of declaration of Helsinki and was approved by the local ethics committee. The participant information sheet and consent forms can be found within Appendix A.

## 2.2 Clinical Characterisation of Participants

All patients enrolled for each study underwent a series of clinical examination as discussed in this section.

### 2.2.1 Orthoptics Assessment

#### 2.2.1.1 Best Corrected Visual Acuity (BCVA)

Best corrected logMAR visual acuity was assessed under monocular and binocular conditions. Precision Vision Visual Acuity Testing (PVVAT v3.8. Precision Vision, Illinois, USA) was used to assess best corrected visual acuity. The system is based on an iMac with a monitor resolution of 1680x1050 pixels, colour depth of 32 bit, and screen size of 51cm. The computerised visual acuity system allows for the randomisation of letters. The individual was seated 4 metres away from the screen and asked to read one letter at a time, starting at the top of the chart with the largest sized letters and working their way down to the smaller sized letters. If they required any form of refractive correction it was advised that they use this during testing. They were given a maximum of two attempts at each letter.



Figure 2-2 : Precision vision visual acuity testing system (PVVAT).

### 2.2.1.2 Cover Test

Each participant was asked to fixate on a target whilst ocular deviation was assessed at near (33 cm) and at distance (4 metres). This allows for the detection of strabismus.



Figure 2-3: From top: a pen torch, occluder and a Snellen stick as used for the cover test, ocular motility and convergence.

### 2.2.1.3 Ocular Motility

Ocular motility was tested in the nine positions of gaze. Any change in nystagmus intensity or direction was assessed upon covering each eye to determine if participants had latent nystagmus. The presence and position of a null zone (quietest zone of nystagmus) was also examined at different positions of gaze.

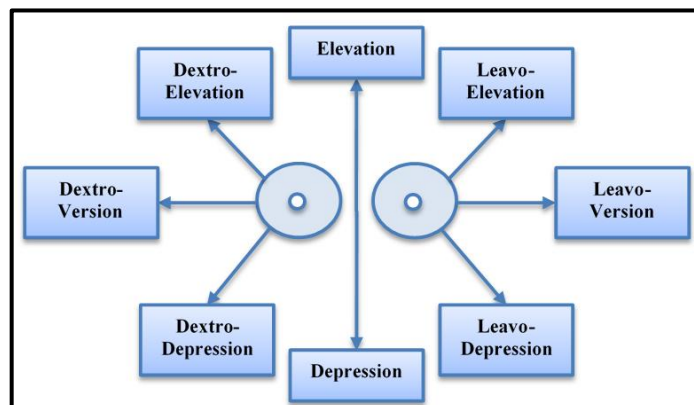


Figure 2-4: Nine positions of gaze assessed using ocular motility testing.

### 2.2.1.4 Convergence

Convergence was tested to determine if nystagmus dampened down on convergence.

### 2.2.1.5 Stereo-Acuity

The Frisby stereotest was used to assess for stereovision in all patients with nystagmus who did not demonstrate a manifest strabismus. The Frisby stereotest consists of three different sized plate thicknesses: 6mm; 3mm; and 1.5mm. It is performed at distances between 30 to 80cm from the patient. The 1.5mm plate at 80cm would be the most difficult.

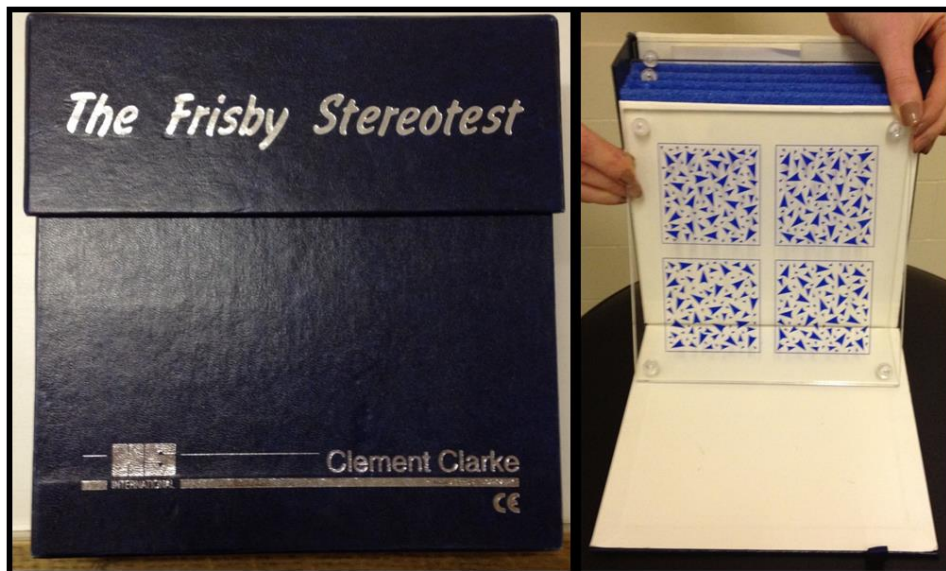


Figure 2-5: The Frisby stereotest and the test plate used whilst assessing the stereoacuity.

### 2.2.1.6 Colour Vision

This was assessed using the Ishihara test for colour blindness and was tested on all patients to assess for different types of colour vision defects. Abnormal colour vision raises suspicion of achromatopsia. **Figure 2-6** displays an example of test plates from the Ishihara colour vision test.

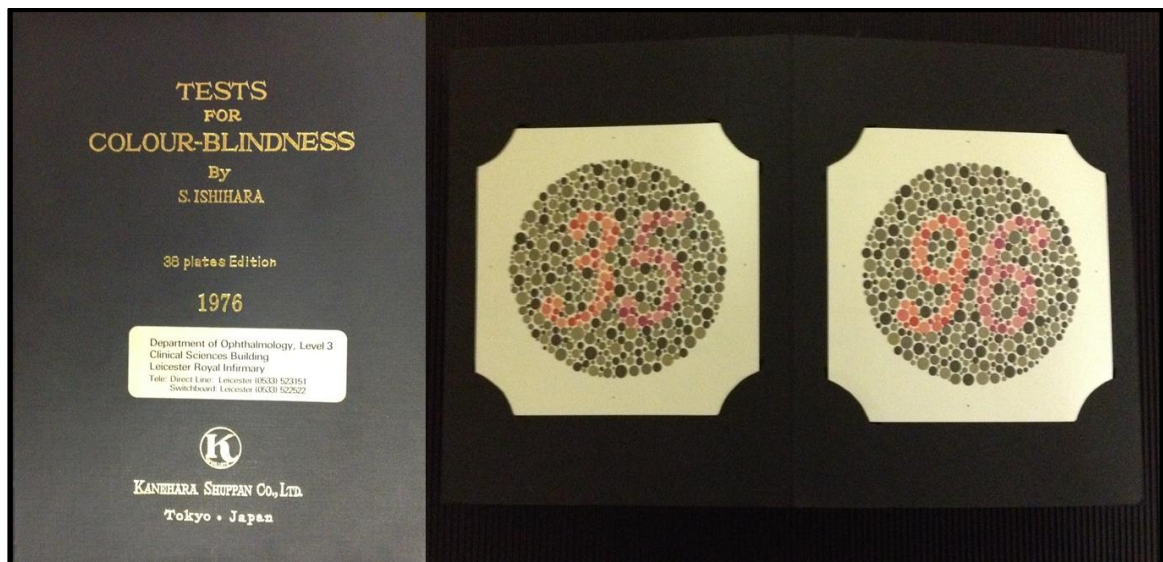


Figure 2-6: The Ishihara test used to assess colour blindness.

## 2.2.2 Investigation of Nystagmus Type (Albinism, IIN, *PAX6* and Achromatopsia)

### 2.2.2.1 Ophthalmological Examination: Slit Lamp Biomicroscopy

The slit lamp allows anterior and posterior assessment of the eye. The posterior assessment allows visualisation of the fundus and provides further detail of the foveal and optic nerve structure and if either are abnormal. Macular transparency, foveal hypoplasia and optic nerve hypoplasia may also be seen during this assessment.

Patients with nystagmus had an anterior segment assessment and Summers's classification of iris transillumination was used for individuals with albinism (Summers, Knobloch et al. 1988). Iris transillumination was classified between Grade 1 and Grade 4 by ophthalmologists in the case of albinism. Anterior structures were assessed to check for eye features often present with *PAX6* such as aniridia or congenital cataracts.

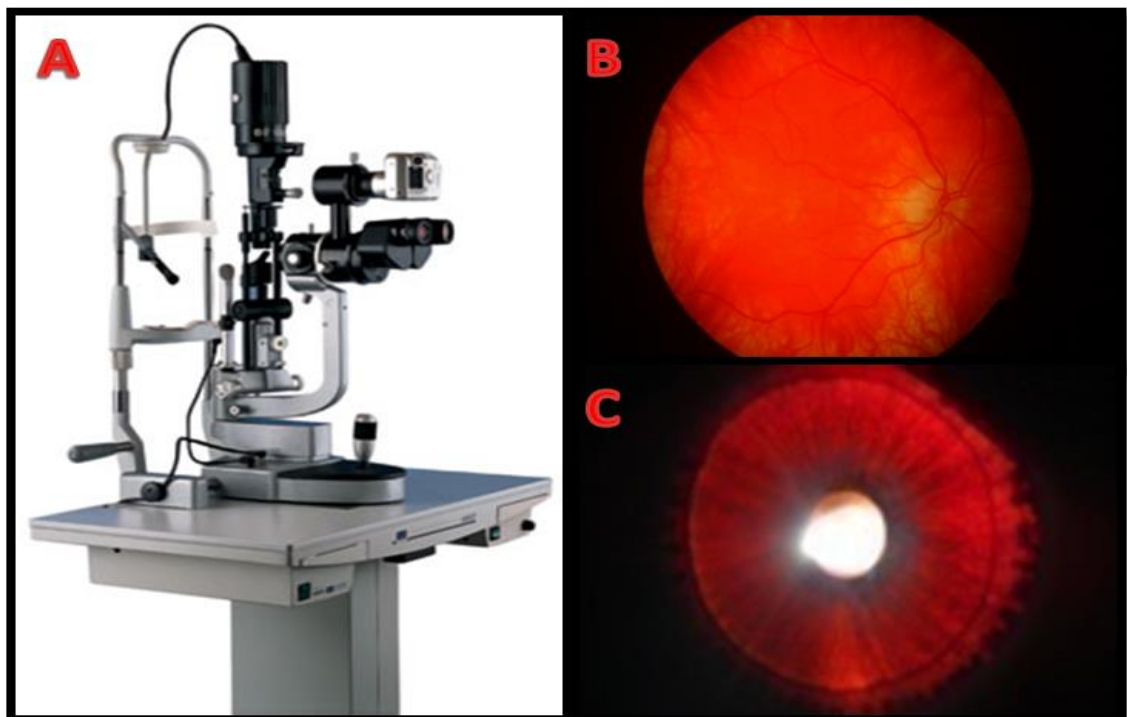


Figure 2-7: (A) The slit lamp biomicroscope, (B) fundus image seen when assessing the posterior segment in albinism and (C) the iris transillumination defect seen in albinism.

## 2.2.2.2 Eye Movement Recordings

### 2.2.2.2.1 Eye Movement Assessment

A high resolution infrared video-oculography device (Eye Link II pupil tracker, SR Research, Osgoode, Canada) with a sample rate of 500Hz in horizontal and vertical dimensions was used to record eye movements in all individuals with nystagmus. Each individual with nystagmus completed the same protocol of eye movement recordings by viewing a target (1° diameter black) on a projection screen (1.5m wide by 1.125m high; 1024x768 pixels; Epsom UK Ltd, Hemel Hempsted, UK) at 1.2m. The eye movement tests included: manual calibration, null point width (NPW), fixation (binocular and monocular), saccades, smooth pursuit and OKN (optokinetic nystagmus) responses. Only NPW was used for analysis as NPW allows characterisation of the null zone (where nystagmus movement is at its quietest). During the NPW test, the black dot is fixated as it moves from -30 degrees to +30 degrees on the horizontal plane. The target moves 3° every 8 seconds. There are several steps taken to analyse NPW data; these are shown in **Section 2.2.2.2.2**. Data was collected by the author, but nystagmus intensity analysis was initially done by FAP and RJM (40 individuals) and VS (10 individuals).

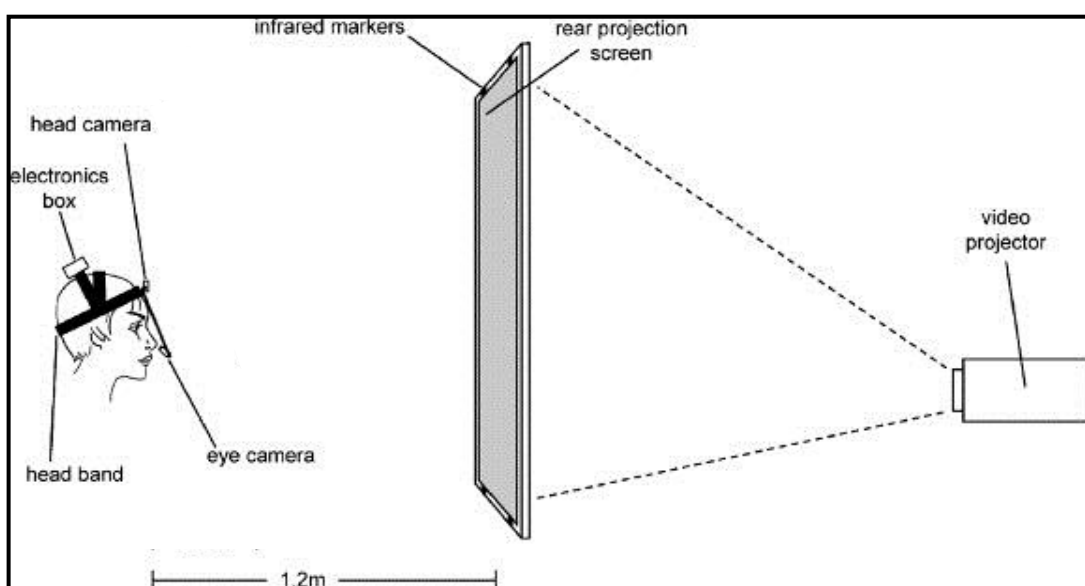
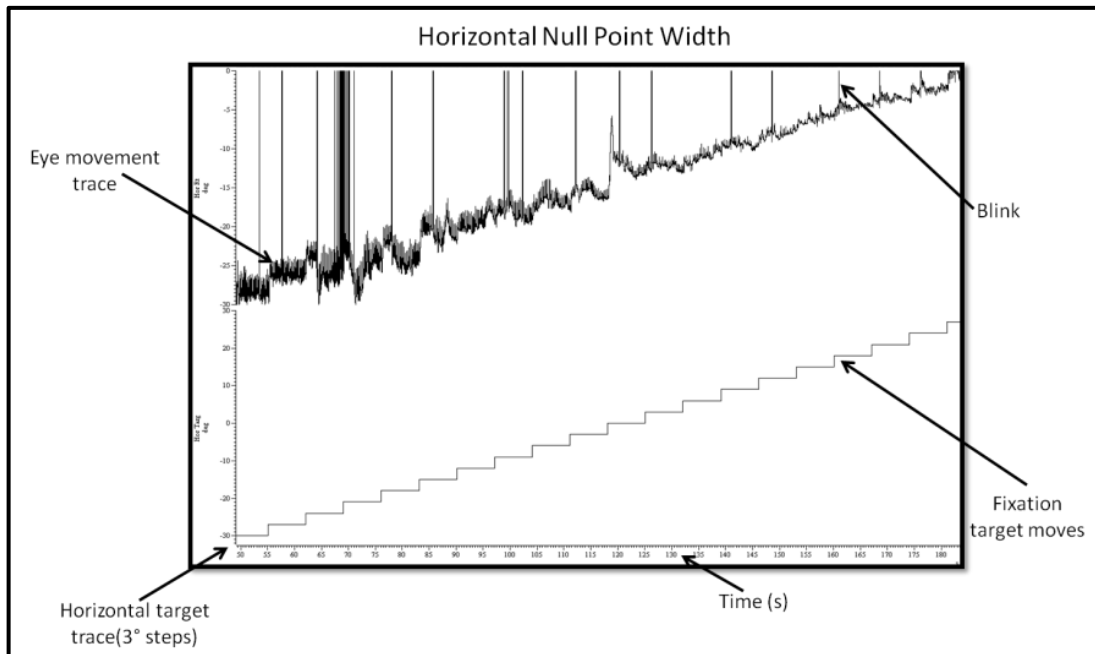


Figure 2-8 : Set up for eye movement recordings. Modified from Proudlock, Shekhar and Gottlob (2004).

### 2.2.2.2.2 Eye Movement Analysis

The eye movement analysis was used for correlations in **Study 1**.

#### EMR Analysis: Nystagmus Intensity (VS, RJM and FAP)



**Figure 2-9: Eye movement recording trace demonstrating horizontal null point width.**

#### Step-by-step guide of EMR analysis

**Step 1:** All EDF (raw data) files need to be converted into SMR files to allow the file to be opened in Spike 2 (Cambridge Electronic Design Limited, Cambridge, UK). Just one eye needs to be analysed because infantile nystagmus is conjugate.



**Step 2:** The EMR data is then calibrated using a line of best fit of the mean foveation position against the target position. The foveation position is calculated using a Spike 2 script (developed by FAP). Using this script, the velocity and position thresholds can be adjusted by the user to allow foveation to be identified.



**Step 3:** Once the data is “cleaned” and all foveation positions have been calculated, the data can be smoothed (manually by user) to aid the detection of peaks and troughs to calculate nystagmus cycle amplitudes and frequencies.



**Step 4:** The results from this analysis were exported into text files which were then imported into Excel using a batch import process (Visual Basic macro written by FAP) to allow the automated calculation of the intensity (frequency x amplitude). An Excel template calculated the average of the parameters across all gaze positions and also at the null zone as identified by the user. The null zone was calculated for each person as the lowest value after performing a five point smooth of the intensity curve. **Figure 2-10** outlines the recorded data and smoothed points. The intensity plot is created by multiplying the amplitude and frequency.

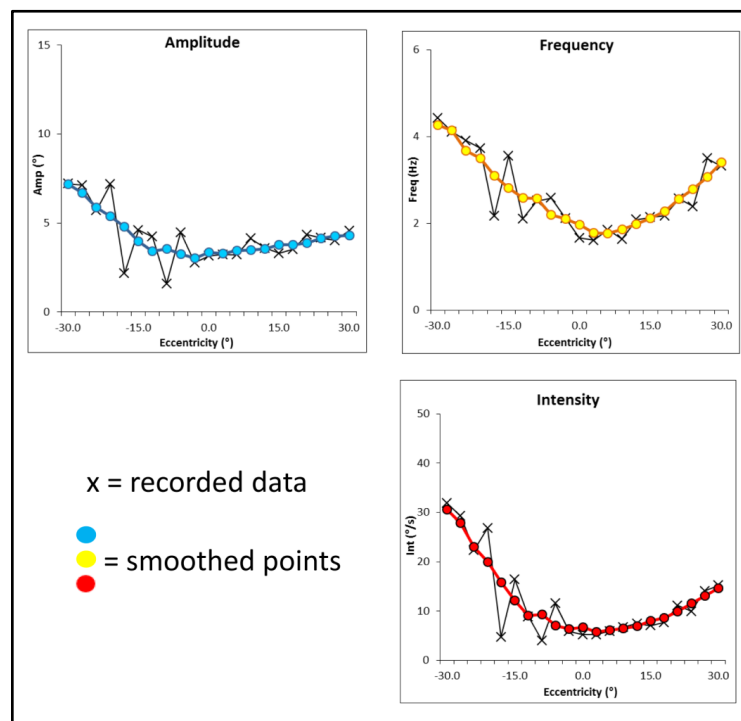


**Figure 2-10:** Graphs showing the amplitude, frequency and intensity of nystagmus after they have been manually smoothed by the user. The intensity plot is used for analysis purposes and is created by multiplying the amplitude and frequency.

## 2.2.2.3 Electro-Diagnostic Testing

### 2.2.2.3.1 VEP and ERG Assessment

Misrouting of the optic nerve for confirming the diagnosis of albinism is through either pattern-onset or flash visual-evoked potentials (VEP). The examination takes approximately forty minutes. Patients with albinism demonstrate a contralateral pre-dominance in VEP response to monocular stimulation. The fibres separate at the optic chiasm and misroute to the lateral geniculate nucleus, causing anomalous projections at the occipital cortex in all patients with albinism. **Figure 2-11** displays the set up for a five channel VEP.

Electroretinography (ERG) was obtained from all patients to assess for achromatopsia or congenital stationary night blindness. Patients with suspicion of Åland Island disease or congenital stationary night blindness underwent dark adaptometry (DA) to rule out abnormal dark adaptation which would suggest these diagnosis. Patients with IIN demonstrated normal VEP and ERG responses. Electro-diagnostic testing was carried out in accordance with the International Society for Clinical Electrophysiology of Vision Standards (Odom, Bach et al. 2010). All electrodiagnostic testing was carried out by the electrophysiology department at the Leicester Royal Infirmary.

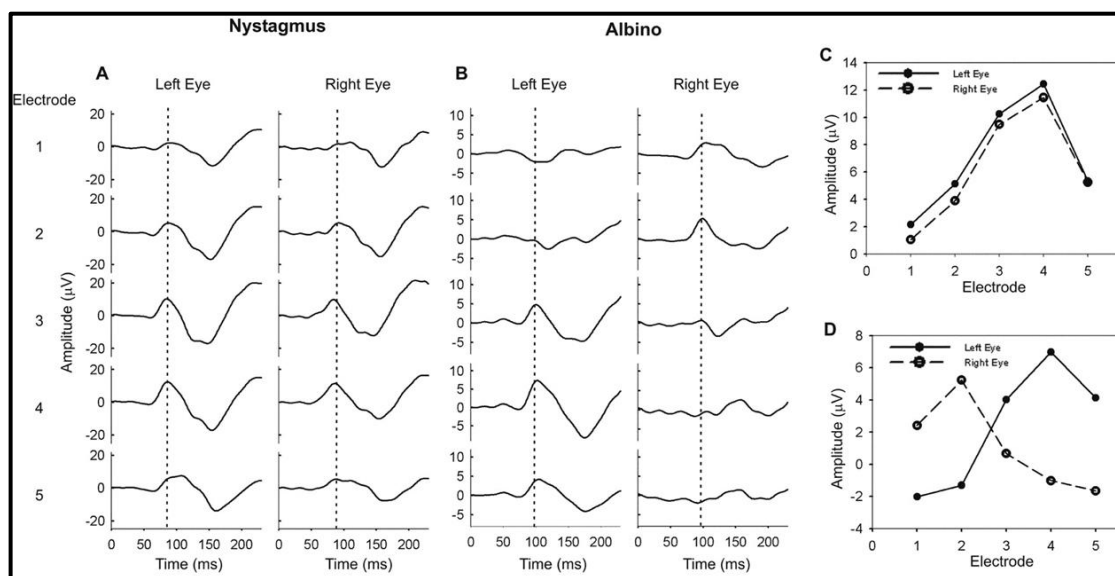


**Figure 2-11: VEP recordings in non-albinism with nystagmus (A) and in albinism (B). The graphs illustrate recordings for each electrode placed across the occiput and are displayed**

from left hemisphere (electrode 1) to right hemisphere (electrode 5). The vertical dotted line shows the time at which the peak amplitude measurements were made. The peak amplitude as a function of electrode position for the left and right eyes are plotted in (C) and (D) for non-albinism and albinism, respectively. Crossed asymmetry is noted in (D). Image reproduced from von dem Hagen et al (2008).

### 2.2.2.3.2 VEP Analysis – Apkarian Method – Quantifying VEP Asymmetry

The Apkarian VEP analysis method (Apkarian and Shallo-Hoffmann 1991) was used in correlations for **Study 1** and **Study 2**.

This method quantifies VEP asymmetry using a derived parameter called Intra-Hemispheric Asymmetry Index (IASym). A step-by-step demonstration of how to calculate the IASym is shown below. The lowest value from either eye is used as the baseline. The lowest value was converted to zero and all other numbers were adjusted accordingly. Firstly, the response lateralisation ( $R_{LAT}$  and  $L_{LAT}$ ) for each eye is calculated. This is determined by plotting a graph of the electrode positions against the VEP amplitudes ( $\mu\text{v}$ ).

**Right Eye**

**Left Eye**

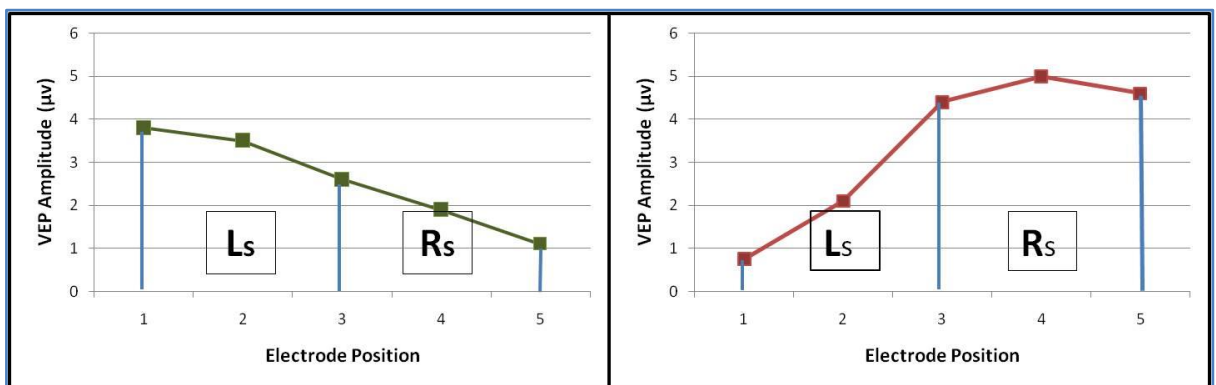


**Figure 2-12: VEP response lateralisation.** The area below electrode points 1-3 (Ls) is a quantification of left hemispheric stimulation. The area below electrode points 3-5 (Rs) is a quantification of right hemispheric stimulation. This is before the lowest value is converted to 0.

Each graph is then divided into two hemispheric sections ( $L_s = \sum$  electrode positions 1-3,  $R_s = \sum$  electrode positions 3-5) and the response lateralisation is worked out separately for each eye based upon the following calculations:

$$L_s > R_s \quad \longrightarrow \quad LAT = R_s / L_s$$

$$L_s \leq R_s \quad \longrightarrow \quad LAT = 2 - (L_s / R_s)$$

Once the response lateralisation (LAT) is calculated for each eye, the lasym is calculated using

the formula: 
$$lasym = L_{LAT} - R_{LAT}$$

According to Apkarian et al (1991), a lasym of over 0.7 is characteristic of albinism as shown in

**Figure 2-13** (Apkarian and Shallo-Hoffmann 1991).

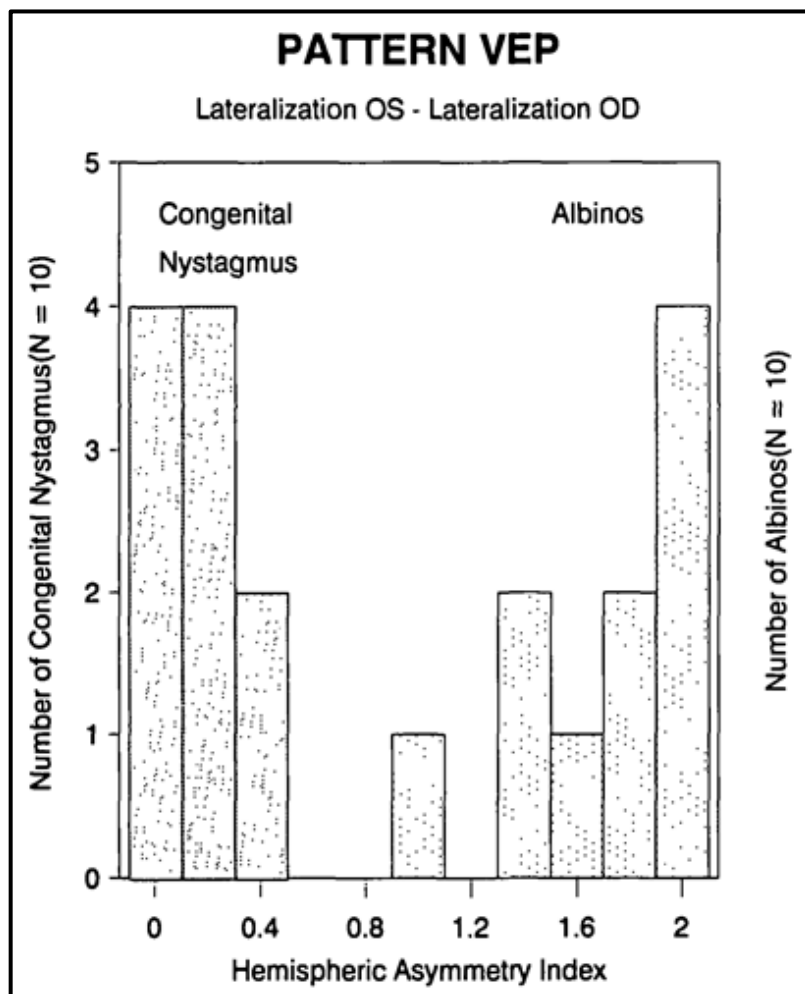


Figure 2-13: Asymmetry index distributions for patients with idiopathic nystagmus (left of graph) and age-matched albinos (right of graph). Values greater than 0.7 indicate asymmetry in albinism. The two groups show no overlap. Reproduced from Apkarian and Shallo-Hoffman (1991).

### Example lasym Calculation

**NOTE:**  $L_s > R_s \longrightarrow LAT = R_s/L_s$   
 $L_s \leq R_s \longrightarrow LAT = 2 - (L_s/R_s)$

Data acquired for example:

Electrode Position	1	2	3	4	5
Right eye amplitude	7.9	8.5	5.0	1.4	0.8
Left eye amplitude	0.00	1.6	5.1	9.7	8.6

Table 2-2: Amplitudes acquired for the calculation of lasym.

#### Right Eye Response Lateralisation

$$R_{LAT} = L_s = 7.9 + 8.5 + 5.0 = 21.4$$

$$R_s = 5.0 + 1.4 + 0.8 = 7.2$$

Therefore:  $L_s > R_s \longrightarrow R_{LAT} = R_s/L_s = 7.2/21.4 = 0.337$

$$R_{LAT} = 0.337$$

#### Left Eye Response Lateralisation

$$L_{LAT} = L_s = 0.00 + 1.6 + 5.1 = 6.70$$

$$R_s = 5.1 + 9.7 + 8.6 = 23.4$$

Therefore:  $L_s \leq R_s \longrightarrow L_{LAT} = 2 - (L_s/R_s) = 2 - (6.70/23.4) = 1.714$

$$L_{LAT} = 1.714$$

#### Intra-Hemispheric Asymmetry Calculation

$$I_{asym} = L_{LAT} - R_{LAT}$$

$I_{asym} = 1.714 - 0.337 = 1.38$  (2d.p) – Over 0.7, therefore classified as albinism

## 2.2.2.4 Optical Coherence Tomography (OCT)

OCT has been completed on all patients and controls used within the studies. The use of OCT has been paramount in measuring structures in the anterior and posterior segments of the eye as well as assisting in the diagnosis of the conditions outlined in this thesis.

OCT has been used in studies 1, 3 and 4 of this thesis and its principles are therefore explained further. OCT of the fovea and optic nerve were carried out on all participants to aid with diagnosis.

In **Study 1**, anterior segment OCT (AS-OCT) was used to image the iris structure in albinism for the first time. We also compared AS-OCT to foveal OCT measures to assess for relationships between these structures. In **Study 3** we correlate central VF with foveal OCT and peripheral visual field with ppRNFL around the optic nerve using OCT. In **Study 4** we correlated refractive status to foveal structures measured using OCT.

Principles of OCT, assessment using OCT and how this aided our diagnosis are explained here. As analysis modes are different for each study these are described within each separate chapter.

### 2.2.2.4.1 History of Optical Coherence Tomography

Optical coherence tomography (OCT) is a high resolution, non-invasive imaging technique which generates three dimensional (3D) images based upon magnitude, phase, frequency shift and polarisation of light back scattered or back reflected from the sample (Fercher 2010). It now has mainstream use in ophthalmology and has also found use in cardiology and gastroenterology (Fercher 2010). More recently, OCT has also begun to be used in interventional cardiology to help diagnose coronary artery disease (Bezerra, Costa et al. 2009).

OCT was first demonstrated in 1991 (Huang, Swanson et al. 1991) and the first in-vivo OCT images were published in 1993 (Fercher, Hitzinger et al. 1993, Swanson, Izatt et al. 1993).

#### 2.2.2.4.2 Principles of OCT

**Figure 2-14** shows a schematic diagram of the components comprising an OCT device. Spectral Domain-OCT (SD-OCT) uses light from a broadband coherent light source such as a super luminescent diode (SLED) which is directed towards the target organ, the eye in this case. The light is then either reflected, absorbed or dispersed by the target organ. The dispersed and absorbed light is not directly reflected to the reference arm and is thus not detected. The interference pattern of the reflected light is then detected by the spectrometer. The interference spectrum acquired is analysed by a computer to produce a reflectivity profile. This is what is referred to as an “A-scan”. A series of continuous A-scans are produced to create a B-scan. A series of B scans create a 3D image. The scanning speed of our high resolution ( $3\mu\text{m}$  axial resolution in tissue) OCT is 52,000 measurements per second. This allows an accurate measurement of retinal structures in patients with eye movement disorders such as nystagmus (Thomas, Kumar et al. 2011). Anterior segment OCT allows visualisation of structures such as the iris whereas posterior segment OCT allows imaging of the fovea and optic nerve.

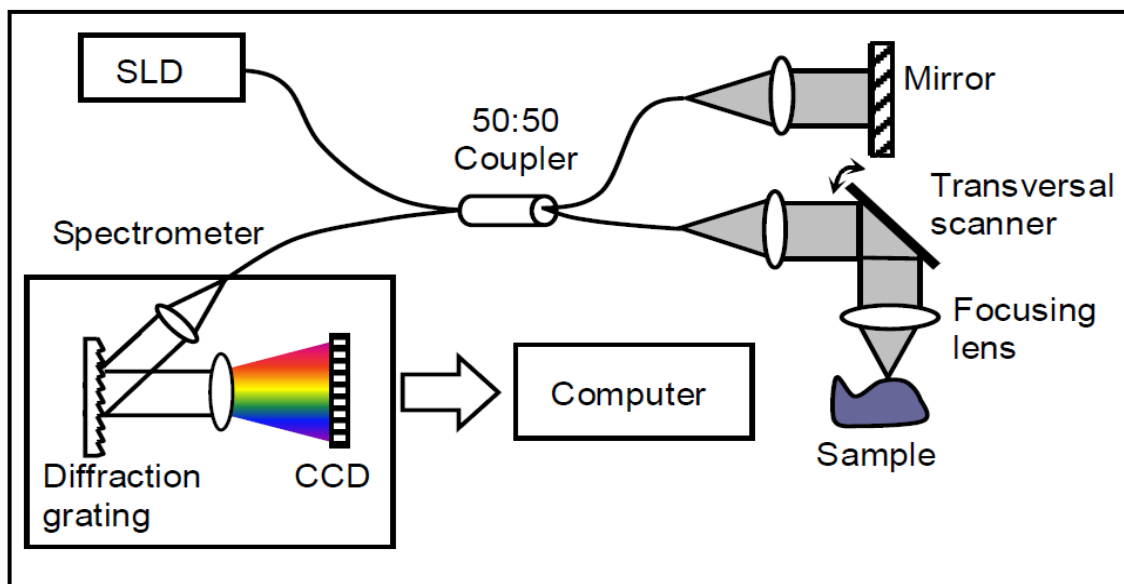


**Figure 2-14: Schematic diagram of Optical Coherence Tomography and the principles behind the instrument. Reproduced from Peng et al (2006).**



**Figure 2-15: Image of SOCT Copernicus HR: OPTOPOL used in our study for posterior and anterior OCT imaging.**

#### **2.2.2.4.3 Posterior Segment Optical Coherence Tomography**

Posterior segment OCT is used to image the fovea, optic nerve and any fundal area of interest. It is used in ophthalmology in conditions such as glaucoma, age related macular degeneration and retinitis pigmentosa. OCT appears to be finding use in most eye related conditions. In the current set of studies we were interested in imaging the fovea and optic nerve to assess for foveal hypoplasia and optic nerve abnormalities in our participants.

##### **2.2.2.4.3.1 Posterior OCT Image Acquisition for Participants**

A high resolution (3 $\mu$ m axial resolution) spectral domain OCT (SOCT Copernicus HR: OPTOPOL Technology S.A, Zawierci, Poland) was used to acquire all foveal and optic scans. The scanning protocol for the fovea and optic nerve was a 7mm X 7mm scan comprising of 743 A scans and 75 B scans.

##### **2.2.2.4.3.2 Diagnosis using OCT**

OCT was used on all individuals in our study to provide improved diagnosis in conjunction with eye movement recording, electrodiagnostics (VEP/ERG) and slit lamp assessment (anterior and

posterior examination). **Figure 2-16** shows how foveal hypoplasia can differ amongst different groups with nystagmus.

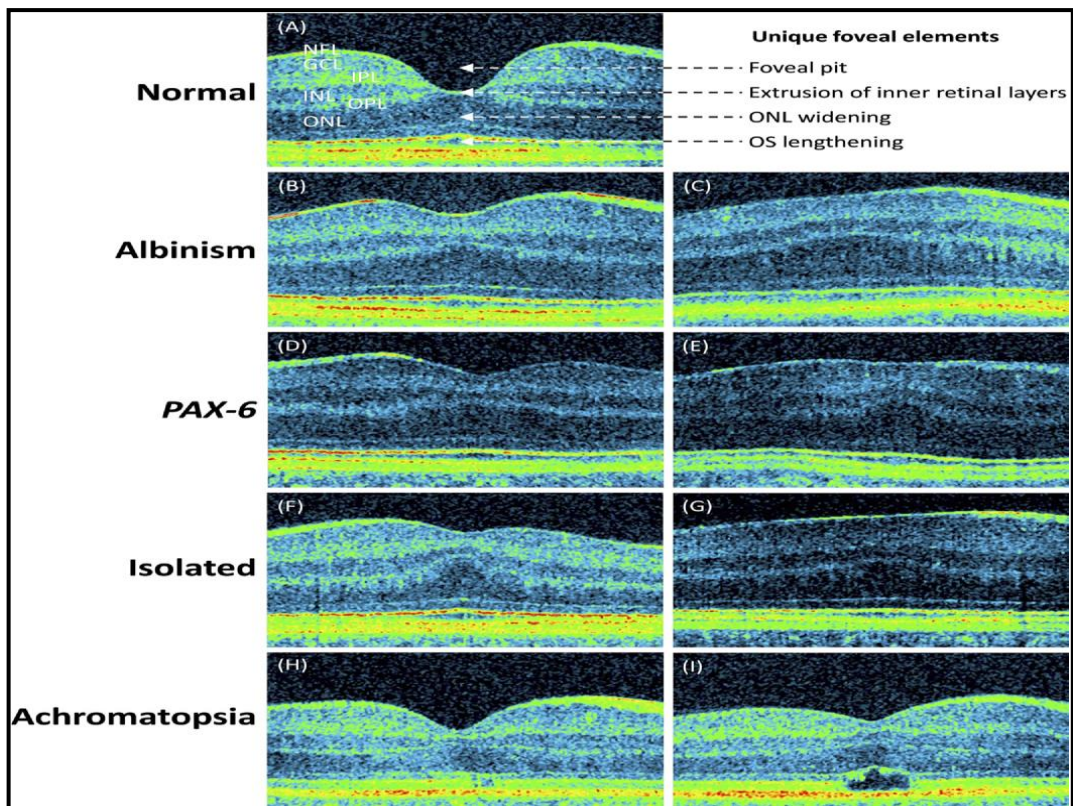


**Figure 2-16:** (A) Optical coherence tomography scan showing a normal fovea with description of the normal foveal elements. Optical coherence tomography scans showing the spectrum of foveal hypoplasia seen in various conditions, including: (B, C) albinism, (D, E) associated with *PAX6* mutations, (F, G) isolated cases, and (H, I) an atypical form of foveal hypoplasia seen in achromatopsia. Reproduced from Thomas et al (2011).

#### 2.2.2.4.4 Anterior Segment Optical Coherence Tomography (AS-OCT)

AS-OCT has been previously extensively used to study and diagnose glaucoma with the ability to image iridocorneal angles and anterior structures (Wang, Sakata et al. 2010). AS-OCT was conducted for **Study 1** in individuals with albinism and controls to image the iris transillumination defect in albinism and compare this to controls who do not demonstrate this sign to assess for structural differences in the iris.

#### **2.2.2.4.4.1 Anterior Segment OCT image acquisition in albinism and controls**

The same OCT with an anterior lens attachment was used to obtain all anterior AS-OCT scans for **Study 1**. Full details of AS-OCT image acquisition and analysis are described in the methods section of **Study 1**.

#### **2.2.2.5 Clinical Photography**

Images were taken by the Leicester Royal Infirmary clinical illustration department.

Photographs were taken, where possible, of each individual's iris transillumination and full patient-profile photographs were also taken to allow the level of pigmentation to be assessed. All photographs were taken under the same lighting conditions and in the same room location.

### **2.2.3 Data Analysis**

The data for each study was analysed separately, if there are any studies where the data analysis is similar to previous studies this has been outlined.

# **Chapter 3**

## **Anterior Segment Imaging in Albinism (Study 1)**

# Chapter 3 Anterior Segment Imaging in Albinism (Study 1)

## 3.1 Introduction

The iris is named from Iris, the Greek goddess of the rainbow and messenger of the gods. The iris can simply be referred to as the colour of one's eye and can be one of many colours, ranging from light blue to dark brown (**Figure 3-1**).



**Figure 3-1: The range of iris colours from light blue to brown. Reproduced from Sturm and Frudakis (2004)**

### 3.1.1 Iris Structure

The iris is a thin, contractile, pigmented diaphragm with a central aperture; the pupil. It is suspended in the aqueous humour between the cornea and lens. The periphery of the iris, which is attached to the anterior surface of the ciliary body, is named the ciliary zone. The pupil is surrounded by the pupillary margin of the iris, the pupillary zone. The iris, measuring about 21mm in diameter, is thickest about 2mm from the pupillary margin and is the thinnest

at the ciliary margin (Snell and Lemp 1989). **Figure 3-2** shows the basic structures within the eye (A) and a front, back and cross sectional view through the iris (B).

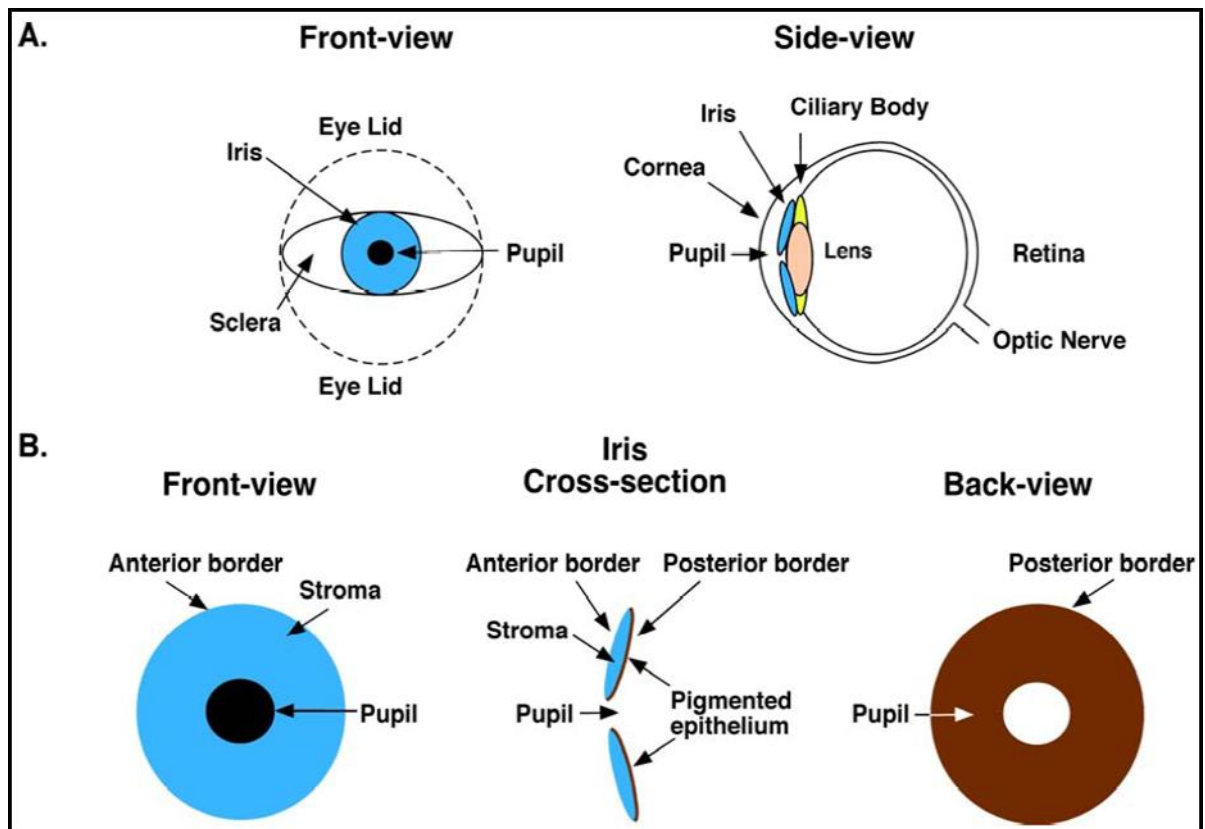


**Figure 3-2: (A) Structures within the eye. (B) Structure within the iris. Reproduced from Sturm and Frudakis (2008).**

The iris has 5 distinguishable layers, starting with the most anterior; the anterior border layer (ABL), the stroma, the pupillary constrictor muscle, the iris dilator muscle and the posterior pigmented epithelium (**Figure 3-2A**). The most important structures for the appearance of eye colour are the anterior border layer and the stroma (Eagle 1988, Imesch, Bindley et al. 1996, Wilkerson, Syed et al. 1996). The histological cross section of the iris and its structures are shown below (**Figure 3-2B**).

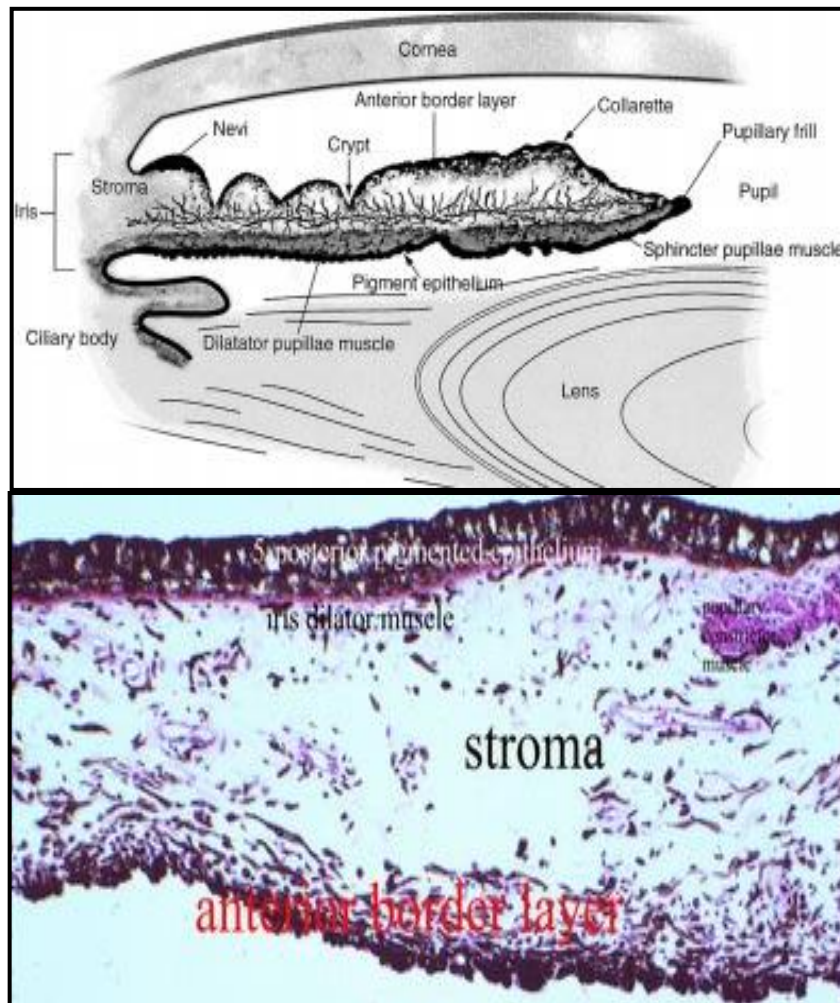


Figure 3-3: (Top): Morphological structure of the iris and surrounding structures (<http://math.ipm.ac.ir/scc/vision/iris/Iris-Recognition.html>). (Bottom): Histological structure of the iris of a normally pigmented individual. (<http://www.images.missionforvisionusa.org/anatomy/2005/10/iris-histology.html>).

## 3.1.2 Iris Morphology and Ultrastructure

### 3.1.2.1 The Anterior Border Layer (ABL)

The ABL is the most anterior portion of the iris and is composed of two principal cell types: melanocytes and fibroblasts with associated collagen (Freddo 1996). The fibroblasts of the ABL exhibit a smooth, generally flattened profile with branching processes radiating from their cell bodies. These processes tend to support the functions of other structures, such as blood vessels and melanocytes. The fibroblasts lack a basal lamina and contain an abundance of mitochondria, endoplasmic reticulum, ribosomes, golgi apparatus and cytoplasmic filaments

(Freddo 1996). Melanosomes of the ABL are more cylindrical in shape (type I and II) compared to melanosomes within the posterior epithelial layer (type III and IV). Type I and II melanosomes are termed as pre-melanosomes due to their shape and reduced melanin volume. The density of melanosomes in melanocytes within the ABL is greater than that of the stroma but less than that of the posterior epithelial layer (McCartney, Spalton et al. 1985). It has been reported that there is a constant number of melanocytes in the ABL of all irides, irrespective of iris colour. However, darker irides have more abundant and larger melanin granules and the cytoplasmic volume of melanocytes is also increased (Eagle 1988).

There are three main junction types (intercellular) that join the ABL and the stroma: these are gap junctions, intermediate junctions and discontinuous light junctions (Raviola, Sagaties et al. 1987).

### **3.1.2.2 The Iris Stroma**

Various cell types within the iris stroma have been described including fibroblasts, melanocytes, mast cells, clump cells, macrophages and lymphocytes (Freddo 1996). Although the iris stroma contains both fibroblasts and melanocytes, the cell density in the stroma is less. The fibroblasts and melanocytes within the stroma are situated within a collagen and acidic glycosaminoglycan extra-cellular matrix (Sames and Rohen 1978).

### **3.1.2.3 The Pupillary Sphincter**

Within the pupillary region, the circularly orientated smooth muscle cells of the iris sphincter are present. This muscle is separated from the underlying iris epithelium by a thin strip of iris stroma (Freddo 1996). Light microscopy shows that it is composed of spindle shaped cells that are orientated parallel to the pupillary margin so when it contracts, the pupil constricts.

### 3.1.2.4 The Dilator Muscle

The cells of this layer of the iris have two distinct components; the muscular basal part (anterior) and the epithelial apical portion (posterior). When the pupillary dilator contracts the pupil dilates (Snell and Lemp 1989).

### 3.1.2.5 The Posterior Epithelial Layer (PEL)

The shape of the posterior pigmented epithelial cells can vary and is dependent upon the state of contraction. The cytoplasm of the posterior epithelial layer is densely packed with Type III and Type IV melanosomes. These melanosomes are larger than those found in the stromal melanocytes due to maturation (McCartney, Spalton et al. 1985). In this layer there are also mitochondria, rough endoplasmic reticulum and Golgi apparatus but they are not fully mature (Freddo 1996).

## 3.1.3 Pigmentation in the Iris

### 3.1.3.1 Iris Colour

The colour of an individual's iris is determined by the quantity and size of melanocytes and melanin enclosed by the anterior border layer and the stromal layer (Sturm and Frudakis 2004, Sturm and Larsson 2009). In the brown iris there is an abundance of melanocytes and melanosomes in the anterior border layer and the stroma, whereas in the blue iris these layers contain very little melanin. **Figure 3-4** is a simplified illustration of this theory.

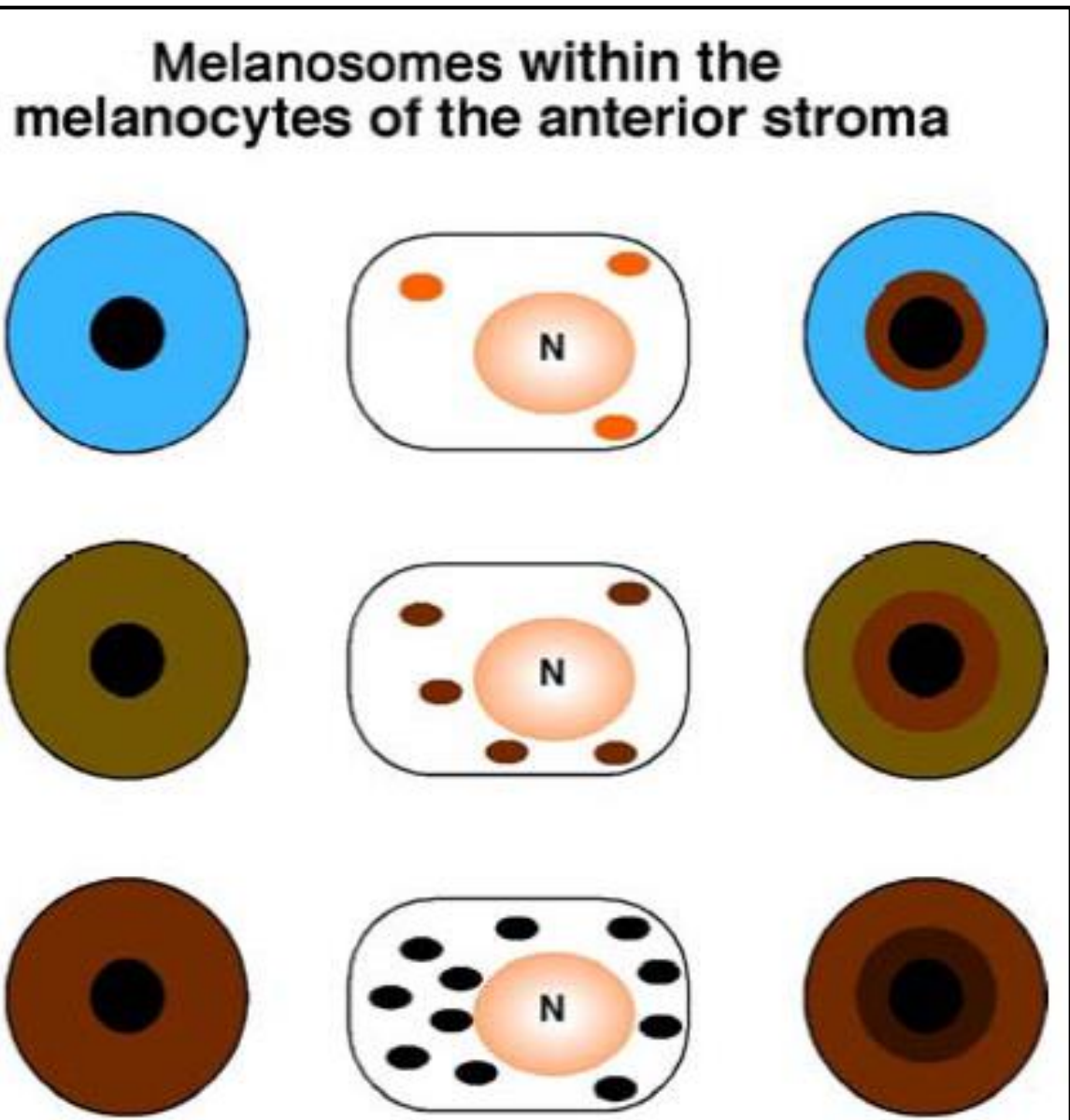
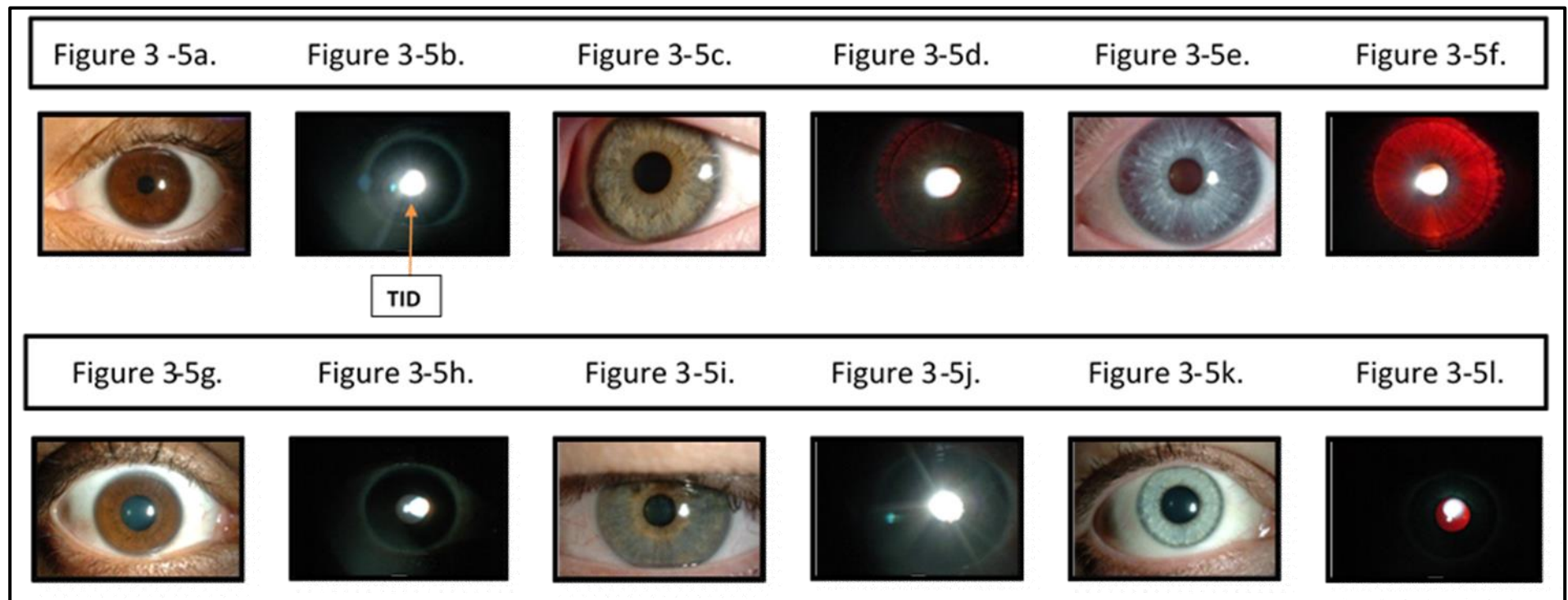


Figure 3-4: Darker eyes are shown to have an increased number of melanosomes within their melanocytes. On the left are iris colours (blue, green and brown) and the melanocytic distribution for these colours, on the right are the same iris colours but with a darkly pigmented peripupillary iris ring that can also occur. Reproduced from Sturm and Frudakis (2004).

An example of iris photos and iris transillumination is shown in **Figure 3-5**. The range of iris colours shown in **Figure 3-5** demonstrate that iris transillumination can occur in all iris colours present in albinism.



**Figure 3-5:** The variation in iris colour and the corresponding iris transillumination defect for each iris. Figures 3-5a to 3-5f are the iris and iris transillumination photos of individuals with albinism. Figures 3-5g to 3-5l are photos of the controls. Figures 3-5a and 3-5g show brown irides, Figures 3-5c and 3-5i show green irides and Figure 3-5e and 3-5k demonstrate blue irides.

### 3.1.3.2 The Structure and Function of Melanocytes and Melanosomes in Albinism

A general introduction to melanocytes and melanosomes can be found in **Section 1.4.1**.

Currently very little is known about the structure and function of melanocytes and melanosomes when considering the iris transillumination defect seen in albinism.

Previous studies which describe the mechanisms behind the iris transillumination defect and reduced melanin within the iris are all based on microscopy (Fulton, Albert et al. 1978, McCartney, Spalton et al. 1985, Akeo, Shirai et al. 1996). In the first study, Fulton et al (1978) evaluated the eyes of a 13 year old boy with albinism and found he did not have any form of Type III or IV melanosome (Fulton, Albert et al. 1978). McCartney et al (1985) describe assessment of the iris from a 63 year old individual with albinism who had a reduced percentage type IV mature melanosome (stromal melanosomes: 19% type II, 61% type III, and 20% type IV in albinism) compared to a normal individual (<1% type II, 29% type III, and 70% type IV in controls) in this study the mean cell area of the mature melanosomes (type III and IV) was also significantly reduced in the individual with albinism compared to the control. McCartney et al (1985) describe that melanosomes in the posterior epithelial layer of their albinism patient are only 36% of the area in controls whereas stromal melanosomes are 60% of area in controls. McCartney et al (1985) suggest that the greater proportion of pre-melanosomes and smaller size of mature melanosomes in both the stroma and posterior epithelial layer explains the iris transillumination defect seen in their patients with albinism (McCartney, Spalton et al. 1985).

A major difference found in literature from McCartney et al (1985) and Fulton et al (1978) is the age of the patient they studied; 62 and 13 years old respectively. This leaves ambiguity over the time frame for the Type III and Type IV melanosome to mature in the younger patient.

The third study by Akeo et al (1996) assessed a foetus of 19 weeks gestation using skin biopsy did not find any type IV melanosomes within the iris structure (Akeo, Shirai et al. 1996).

The posterior epithelial layer is packed with melanin in normal individuals as the Type I and Type II (pre-melanosome) develop into Type III and IV melanosome which contain melanin due to the abundance of tyrosine. However those with albinism lack tyrosinase, which decreases the number of Type III and Type IV melanosome and thus melanin and pigment within the iris (McCartney, Spalton et al. 1985).

In the three previous studies describing the morphological structure of melanosomes within the iris of individuals with albinism all included patients of different ages and the type of albinism was not specified. This is important since an individual with OCA1A who has a total lack of pigment will not acquire pigment later in life, whereas a patient with OCA2 may develop pigmentation throughout life.

### **3.1.3.3 The Importance of Melanin (Biological and Imaging)**

Melanin regulates homeostasis in melanocytes, however this is disrupted in albinism (Drager 1985). A previous study by Iwai-Takekoshi et al (2016) reports that the consequences of a lack of melanin in albinism can lead to abnormal melanosomal distribution, perturbations in the formation of junctional complexes and even abnormal cell shapes with anomalous cell function. This deficit of melanin is likely to have a cascading effect on retinal maldevelopment (Iwai-Takekoshi, Ramos et al. 2016).

A recent investigation by Wilk et al (2017) assessed the effect of melanin on the appearance of hyper-reflective outer retinal bands using OCT in humans with and without albinism. This study describes the difficulty in separating retinal layers below the cone outer segment layer from each other, e.g. the ROST (rod outer segment tips), COST (cone outer segment tips) and RPE. This makes it very difficult to explicitly isolate the RPE for analysis on OCT images. Specifically

the authors describe differences in relative reflectance and thickness between the RPE and Bruch's membrane bands between normal subjects and patients with albinism, suggesting that the level of melanin may change the appearance of these layers on OCT images and influence thickness measurements. They also find greater difficulty in separating out the outer retinal bands accurately in controls compared to the albinism group. They postulate that this is due to higher levels of melanin in the outer retina of controls reducing the ability for differences in signal intensity to be delineated (Wilk, Huckenpahler et al. 2017). These observations raise caution over the interpretation of thickness measurements of layers that are normally melanin dense, in the case of our study, the posterior epithelial layer of the iris as well as the retinal pigment epithelium.

### 3.1.4 Aims and Rationale for Study 1

Anterior segment OCT has not been applied to a cohort of individuals with albinism to look at the iris transillumination defect or to assess whether this can be used to aid diagnosis of this condition. We aim for the first time to assess the iris structure in individuals with albinism in comparison to controls.

### 3.1.5 Hypotheses

These are the main research hypotheses to be addressed in **Study 1**:

- The irides of individuals with albinism are thinner than those of control individuals.
- All layers of the iris are affected in individuals with albinism.
- The iris anterior segment OCT can be used to diagnose albinism.
- Iris thickness in individuals with albinism are correlated to other phenotypic characteristics such as retinal OCT (using posterior OCT), visual acuity and skin and hair pigmentation.
- The iris layers increases in thickness with age in albinism and controls.

## 3.2 Methodology for Study 1

### 3.2.1 Patient Characteristics

The study population for this study consisted of 55 participants with albinism (mean age=35.9 years, SD±13.6 years) and 45 control individuals (mean age=33.2 years, SD±13.6 years). The participants were diagnosed with albinism using clinical criteria discussed in the methodology chapter.

### 3.2.2 Anterior Segment Optical Coherence Tomography

An ultra-high resolution (3µm axial resolution) spectral domain OCT (SOCT Copernicus HR: OPTOPOL Technology S.A., Zawierci, Poland) was utilised with a telecentric anterior lens attachment to acquire sectional scans of the iris. These iris scans were obtained in a completely darkened room where the only light source was an LED lamp with 12 LEDs (Rula LED lamp). The illuminance was measured using the IL1700 International Light Research Radiometer (with 4271 filter, input optic W1595). The LED lamp produced an illuminance of 1850 Lux<sup>-1</sup>. The light source was placed in front of the non-imaged eye at 45 degrees from the optical axis at a distance of 100mm; this distance was measured for each participant using a ruler. The LED was then switched on one second before each iris scan was taken to allow sufficient time for the light to constrict the pupil of the imaged eye through consensual light response.

The iris scans were acquired using a volumetric raster scan programme (4.37x4.37 mm, 743 A-scans x 50 B-scans, 3µm axial resolution: 0.014 seconds per B-scan). Three iris scans were obtained from the nasal and temporal sides of each eye, as shown in **Figure 3-6**. To ensure that all the scans have the relevant features required for analysis the pupil edge was imaged through to the ciliary end of the iris. Only those images with a quality index of 5 or above were

used for analysis. Quality index refers to the clarity of image obtained and the ability to discriminate layers within it based on signal to noise ratio.

### 3.2.2.1 Image Acquisition

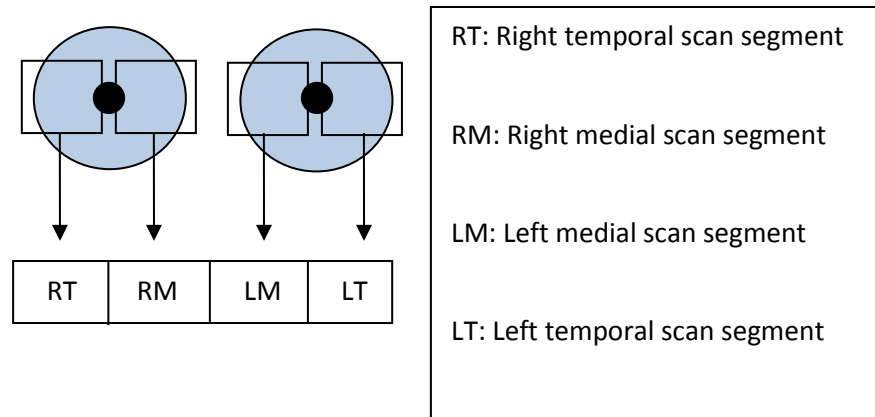


Figure 3-6: An illustration of location at which each scan was taken for the AS-OCT.

### 3.2.2.2 Image Selection

Figure 3-7 represents iris images collected from patients with albinism and controls. Beside each iris scan a tick or cross indicates whether the iris scan has been used within this study. Images A, B and C were analysed. Images D, E and F were discarded. Image D shows an example of an iris OCT image where only half of the imaging area has been filled with the iris; consequently this was not selected for analysis. Image E is an example of an iris OCT with a quality index of less than 5 and thus it was not used for evaluation. A low quality index indicates a high level of noise within the image. Image F has a quality index above 5; however, the pupillary portion of the iris has been cut off and it has therefore not been chosen for further analysis. Images were viewed immediately once a scan was taken. For poor quality scans, we repeated the scan protocol until an analysable image of a satisfactory calibre was obtained.

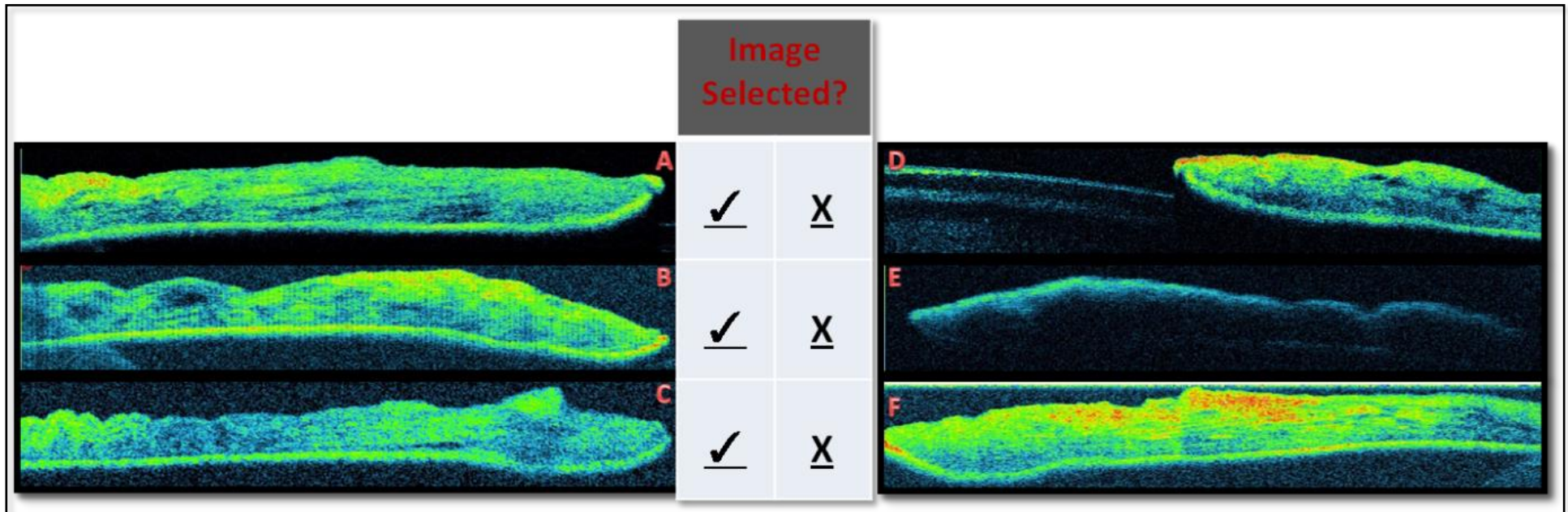
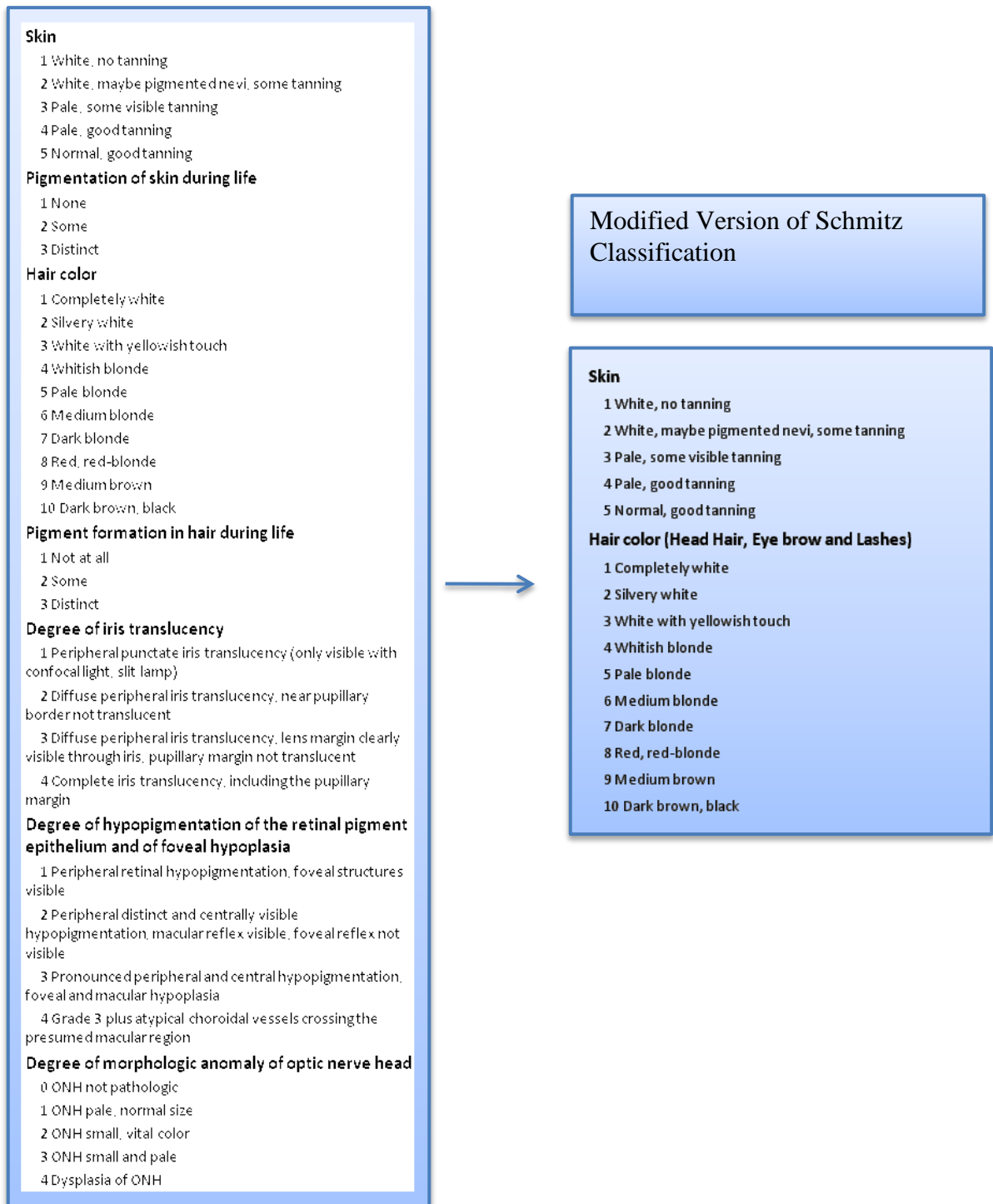


Figure 3-7: Iris scans obtained from AS-OCT. Images A, B and C were useable. Images D, E and F were discarded.

### 3.2.2.3 Pigmentation Scale

This was objectively assessed in all patients by clinical examination, photos and videos. Skin and hair pigmentation were assessed using a modified version of the classification of phenotypes in albinism (Schmitz, Schaefer et al. 2003). **Figure 3-8** shows the full classification system used by Schmitz et al (2003) for skin and hair pigmentation (left) and the modified version used for our study (right). A score of 1 to 10 was used for hair pigmentation and a score of 1 to 5 was used for skin pigmentation. For hair pigmentation, a score of 1 describes hair that is totally white, whereas a score of 10 indicates dark brown hair or black hair. The score was averaged for head hair, eyebrows, and eye lashes. For skin pigmentation, a score of 1 indicates the skin was white and cannot tan, whereas a score of 5 indicates normal tanning. The measurements were then correlated to the iris OCT measurements.



**Figure 3-8: On the left is the original Schmitz classification (2003) for grading the severity of a patient with albinism. On the right is a modified version that has been simplified to consider skin and hair pigmentation only for our study.**

## 3.2.3 Data Analysis

### 3.2.3.1 Iris Transillumination

This was one of the main clinical outcome measures for this study. Professor Irene Gottlob and Dr Anil Kumar, who both have a vast experience in assessing individuals with albinism graded the iris transillumination for the patients diagnosed with albinism between grades 1 and 4. All iris transillumination assessments were carried out in a completely darkened clinic room.

### 3.2.3.2 Anterior Optical Coherence Tomography

The highest quality OCT scans were used for each segment (nasal and temporal from each eye) based upon the following criteria: quality index of image; horizontal sectioned scan; pupillary border distinguished; and ability to recognise layers within the iris. Once these images were identified, they were analysed using Image J software (National Institute of Health, Bethesda, MD; available at <http://rsweb.nih.gov/ij/>; accessed November 29 2012). The B-scans were exported as jpeg images, where each pixel had a physical dimension of  $1.955\mu\text{m} \times 1.955\mu\text{m}$  (lateral scaling resampled from  $5.88\mu\text{m}$  to  $1.955\mu\text{m}$  pixel width) and the image generated was 1020 pixels high and 2236 pixels wide. The images were orientated so that the pupillary end of the iris was on the left of the image with the images cropped up to the inner pupillary border of the iris. Images were visually examined and the posterior epithelial layer (PEL), stroma and anterior border layer (SAB) and total thickness of iris were manually identified. The stroma and anterior border could not be distinguished automatically or manually, thus were combined in a layer termed the stroma anterior border (SAB) layer. A step-by-step guide of the image analysis is shown. All anterior segment OCT imaging and analysis was completed by the author (VS).

**Step 1:** Image identified

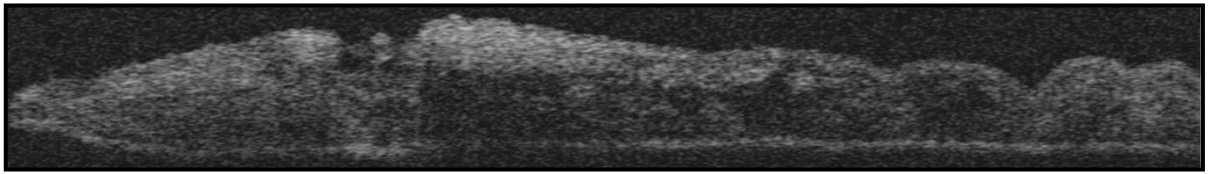


**Figure 3-9:** Black and white image of a selected iris OCT.



**Step 2:** Open image with Image J ready to convert into white pixelated image.

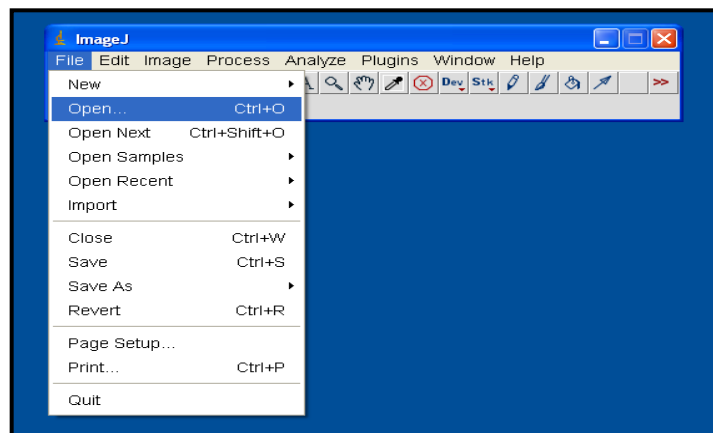


**Figure 3-10:** Image J programme bar where the image is opened for layer segmentation.

**Step 3:** Select “polygon selections” from the tab, manually pick out the posterior epithelial layer (PEL) and then save image for analysis.

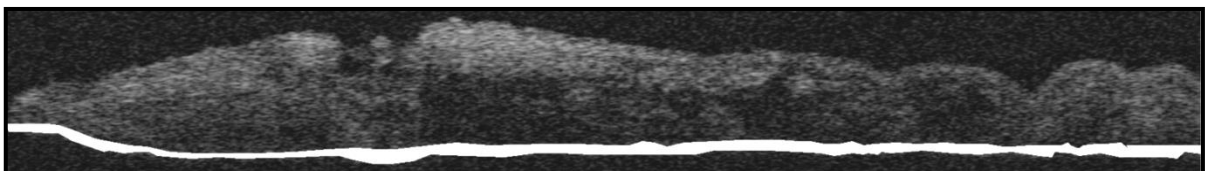


**Figure 3-11:** Original iris OCT image with the posterior epithelial layer (PEL) converted into white pixels.



**Step 4:** Using “polygon selections” from the tab manually pick out the whole iris profile and then save this for image analysis.



**Figure 3-12:** OCT image with the full iris structure converted to white pixels



**Step 5:** Two images are ready to be analysed, both must be converted into text files (.txt) before being imported for analysis. Grayscale values from the 2 images were then imported into an Excel (Microsoft Corporation, Redmond, WA) macro (1 pixel grayscale value into each cell) from which the white pixels were counted to sum the mean thicknesses for the PEL, total iris thickness, and SAB (difference between the total iris thickness and PEL). After observing iris profiles in pilot analysis, we determined that averaging every 50-pixel intervals (equivalent to 97.75  $\mu\text{m}$ ) was sufficient to resolve the variations in thickness along the iris profiles. 36 intervals which equated to 1800 pixels (3519  $\mu\text{m}$ ) from the inner rim of the iris were included in the analysis. These were further divided into 4 quartiles for further analysis (450 pixels, 879.75  $\mu\text{m}$ ).

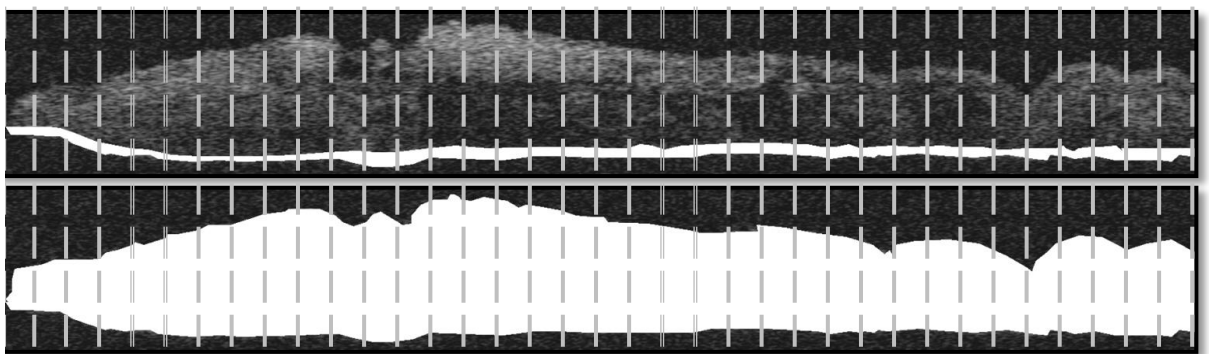


**Figure 3-13:** Example of images ready to run through a macro, the thickness is averaged for each of the 36 intervals.



**Step 6:** Repeat the previous steps for each iris OCT image (100 subjects in total, therefore 400 iris OCTs).



**Step 7:** Once all black and white iris images have been created, they were imported into an Excel macro which identifies all white pixels using a threshold measure to provide the thickness of each layer (total iris thickness and PEL thickness). To obtain the SAB thickness, the PEL thickness is subtracted from the total iris thickness.



**Step 8:** Image analysis complete. Verify all results to ensure there are no anomalous results from human error.

### 3.2.3.3 Retinal OCT Image Analysis (Author and SM)

Data for retinal OCT correlations were collected as a collaborative effort by the author and SM.

A sub-set of this data was published by Mohammed et al (2011). Foveal analysis was carried out by the author and SM.

#### Step-by-step guide of image analysis

**Step 1:** Firstly, identify the B-scan at the centre of the fovea. To help find the fovea one must look for signs of foveal architecture such as the foveal pit, doming of the outer nuclear layer, lengthening of the cone outer segment (OS layer) and thinning of the inner retinal layers. This is often difficult in individuals with foveal hypoplasia.

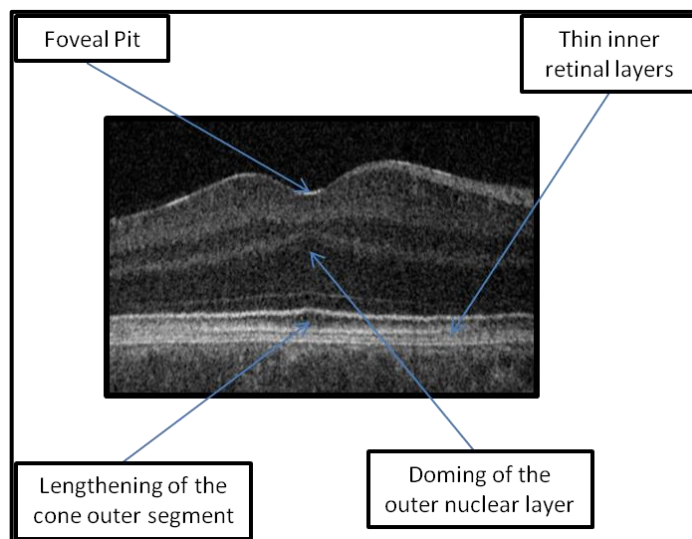


**Figure 3-14: Signs of foveal architecture shown on OCT scan.**



**Step 2:** Once the B-scan at the centre of the fovea is identified, the scan was flattened using the software package provided by the manufacturer of the SD-OCT equipment (Optopol) (Figure 3-15). Once this process is complete each file is to be saved as a bitmap file ready for analysis.

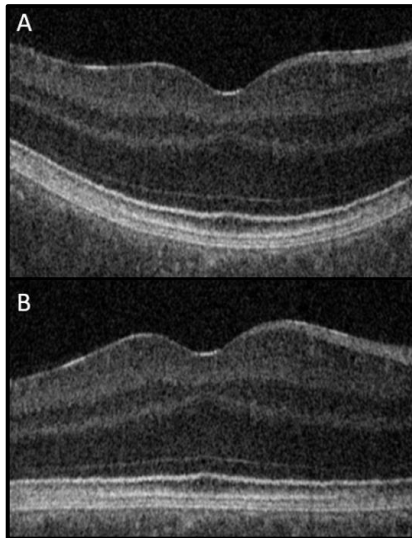


**Figure 3-15: (A) singular B-scan as obtained before flattening. (B) Singular B-scan after flattening.**



**Step 3:** Each bitmap file is then opened up within Image J and the retinal layers are manually delineated and defined by placing points along the retinal border which are fitted with a cubic spine. Once analysis is completed each saved file is placed within an Excel macro (Microsoft Corp.,) which produces automated analysis of each retinal layer at the fovea.



**Step 4:** Once analysis is complete, all foveal layers are quantified. These layers included the retinal nerve fibre layer, ganglion cell layer, inner plexiform layer, inner nuclear layer, outer plexiform layer, outer nuclear layer, inner segment of photoreceptor layers, outer segment of photoreceptor layers and retinal pigmented epithelium.

### 3.2.4 Statistical Analysis

A linear mixed model (LMM) is a mixed paradigm which allows the comparison of both fixed effects and random effects. LMMs assume normality of residuals which was confirmed for the data analysed. The group (albinism or control), side (nasal or temporal) and eye (left or right) were included as the fixed factors.

Profiles of irides were divided into four quartiles  $Q_1$  to  $Q_4$ . Quartiles ( $Q_x$ ) in medial and temporal irides were compared between albinism and control groups using unpaired t-tests (p-values adjusted using Bonferroni correction).

Iris thickness (total iris thickness and PEL thickness) was compared to iris transillumination grading using a Kruskal-Wallis test due to non-normality of the data.

The effect of age on iris layer thickness was investigated using univariate analyses, using the interaction term between group (albinism or control) and age to investigate a difference in the effect of age between the groups. Statistical analysis was performed using SPSS software version 16.0 (SPSS, Inc., Chicago, IL).

Linear regression analysis was used to calculate correlation co-efficient and explore whether statistically significant correlations between iris thickness measurements and the following parameters were evident: (i) iris transillumination grading; (ii) retinal measurements at the fovea; (iii) nystagmus intensity; (iv) best corrected visual acuity (BCVA); (v) VEP asymmetry; (vi) skin pigmentation; (vii) hair pigmentation (scalp hair, lashes and brow). For analysis we averaged the right and left eyes iris OCT measures.

### 3.3 Iris OCT Results

#### 3.3.1 Summary of Volunteers Used in this Study

	Albinism	Control
N	55	45
Male: Female	32:23	20:25
Mean Age ( $\pm$ SD)	35.9 ( $\pm$ 16.3)	33.2( $\pm$ 13.6)
<b>Ethnicity</b>		
Caucasian	51	43
*Asian	2	2
African-American	2	0
<b>**Iris transillumination grading</b>		
Grade 1	19	-
Grade 2	19	-
Grade 3	12	-
Grade 4	5	-
Pupil Size during test in mm ( $\pm$ SD)	2.32 ( $\pm$ 0.39)	2.28 ( $\pm$ 0.33)

\* Asians of Indian origin only

\*\* Based on Summers classification grading (**Figure 1-17**)

Table 3-1: A summary of details for all volunteers used within the study.

### 3.3.2 Differences in Iris Layers between Albinism and Controls

The mean iris thickness (averaged for left and right eyes and nasal and temporal irides) was 10.7% thicker in controls (mean thickness,  $379.3 \pm 44.0 \mu\text{m}$ ) compared to the albinism group (mean thickness,  $342.5 \pm 52.6 \mu\text{m}$ ,  $F=18.3$ ,  $P<0.001$ ). The SAB layers was 5.8% thicker in controls (mean thickness,  $315.1 \pm 43.8 \mu\text{m}$ ) compared to the albinism group (mean thickness,  $297.7 \pm 50.0 \mu\text{m}$ ,  $F=4.18$ ,  $P=0.044$ ). The PEL showed the largest percentage difference between groups and was 44.0% thicker in controls (mean thickness,  $64.1 \pm 11.7 \mu\text{m}$ ) compared to the albinism group (mean thickness,  $44.5 \pm 13.9 \mu\text{m}$ ,  $F=76.2$ ,  $P<<0.001$ ). Two patients in the albinism group with full iris transillumination (grade 4) did not demonstrate a PEL, possible reasons for this will be discussed further in the discussion section.

LMM's indicated no significant differences between left and right eyes for any comparison and PEL, SAB and total iris thicknesses were consistent between right and left eyes (intraclass correlation coefficient 0.91 for PEL and total iris thickness and 0.86 for SAB layer). Consequently, iris profiles were averaged across left and right eyes and divided into four quartiles for each medial and temporal segment for further analysis.

### 3.3.3 The Comparison of Iris Layers between Albinism and Controls

**Figure 3-16** shows the mean (A) total, (B) SAB and (C) PEL layer thicknesses along the whole profile of medial and temporal irides (averaged across right and left eyes) with the statistical comparisons between albinism and control groups for each quartile (unpaired t-test adjusted with Bonferroni correction).

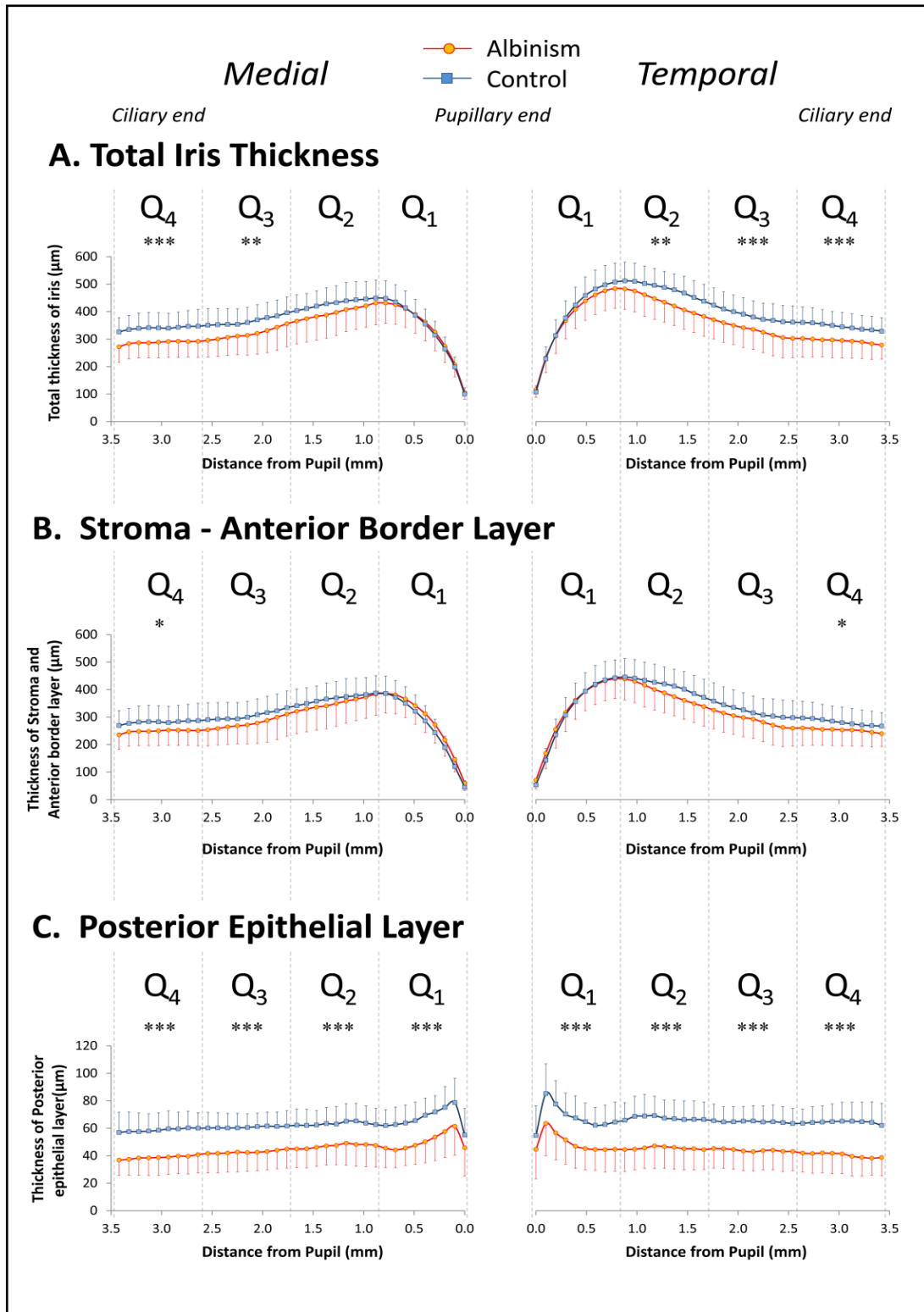


Figure 3-16: Mean iris layer thicknesses for the 53 albinism participants and 45 controls for medial and temporal irides where (A) is the total thickness (B) is the stromal and anterior border layer thickness (SAB), and (C) is the posterior epithelial layer (PEL) thickness. The values are averaged for right and left eyes. The grey dashed lines show the division of quartiles with Q1 being the most pupillary quartile and Q4 the most ciliary quartile. The number of asterisks above each quartile box represents the level of significance (\* $P < 0.05$ , \*\* $P < 0.01$ , \*\*\* $P < 0.001$ ).

There was no significant difference in the total iris thickness of the pupillary iris ends between albinism and control groups (Q<sub>1</sub>). However the ciliary ends were significantly thinner in albinism patients. This difference was more obvious in the temporal iris (unpaired t-tests with Bonferroni correction: for medial: Q<sub>3</sub> and Q<sub>4</sub>, P=0.0033 and P<<0.0001, respectively; for temporal: Q<sub>2</sub>, Q<sub>3</sub> and Q<sub>4</sub>, P=0.0019, P=0.0006 and P<<0.0001, respectively) (**Figure 3-16A**). The SAB layer (**Figure 3-16B**) showed a similar trend to total iris thickness although significant differences between albinism and control groups were only observed for the most ciliary quartile (Q<sub>4</sub>: medial: P=0.011; temporal: P=0.030). The PEL (**Figure 3-16C**) showed highly significant differences along the whole iris profile (P<<0.0001 for all quartiles) with the albinism group demonstrating a thinner PEL compared to the control group. The most statistically significant differences were found in Q<sub>4</sub>.

Both total iris thickness and SAB temporal segments were thicker than medial segments for pupillary iris end in both albinism (P<0.001 for Q<sub>1</sub> and P<0.05 for Q<sub>2</sub>) and control groups (P<0.001 for all Q<sub>1</sub> and Q<sub>2</sub> comparisons). In contrast PEL temporal segments were thicker than medial segments for the ciliary iris end (Q<sub>4</sub>) in controls only. These differences can be further delineated from **Figure 3-16**.

### 3.3.4 Iris Thickness Compared to Iris Transillumination Grading

**Figure 3-17** shows graphs for the individual (A) total, and (B) PEL layer thicknesses for each grade of iris transillumination compared to controls. For total iris thickness there was a large overlap in total iris thickness between controls and patients with albinism for all grades of transillumination (**Figure 3-17A**). The transillumination grading group 4 was the only group that was significantly different to controls for total iris thickness (Kruskal-Wallis test: P<0.05). However, there were no significant differences between any transillumination grading group and controls for the SAB layer (Kruskal-Wallis: P=0.48). For PEL (**Figure 3-17B**), all



### 3.3.5 Using PEL Thickness as a Diagnostic Aid for Albinism

Since we found the PEL was the most affected layer of the iris when comparing controls to individuals with albinism, we assessed whether the iris AS-OCT PEL measurement can be used as a diagnostic aid. From **Figure 3-16** PEL Q4 (the most ciliary quartile of the iris) was found to demonstrate the most significant difference between the groups. This was used to create a histogram to demonstrate the thickness of the PEL at Q4 for individuals with albinism and controls.

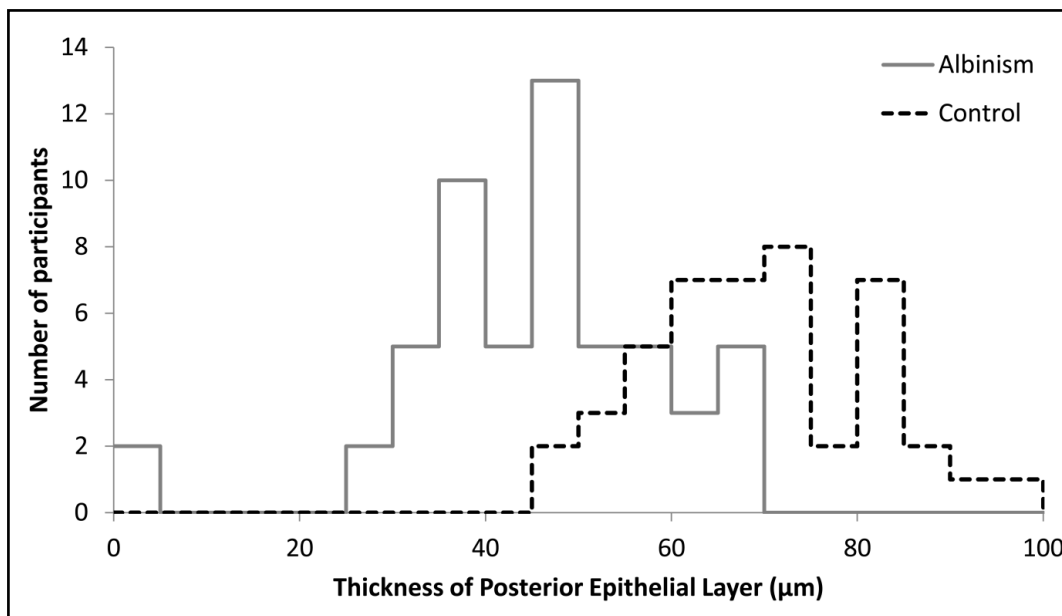


**Figure 3-18: Histogram showing the distribution of posterior epithelial layer (PEL) thickness for the most ciliary quartile (Q4). The participants with albinism are indicated with a grey solid line. The control participants are indicated in dotted black.**

Using a threshold of 55 µm for Q4 of the PEL yielded a sensitivity of 85% and specificity of 78% for the detection of albinism using the anterior segment approach. Our high percentage of sensitivity (85%) and high percentage of specificity (78%) show that this test would be best used as a diagnostic aid rather than a diagnostic test. We analysed the patients who had iris thickness above the threshold of 55 µm. For the 5 individuals with albinism who had PEL

thicker than 65  $\mu\text{m}$ , two had grade 1 iris transillumination, two patients were categorised to have grade 2 and one grade 3, and none had grade 4 iris transillumination.

An interesting observation was made when analysing the best-corrected visual acuity (BCVA) of these patients. The BCVA amongst these 5 patients with albinism ranged from 0.18 to 0.44 logMAR with a mean of 0.27 Log MAR, considerably better than the mean for the entire group of patients with albinism (mean=0.53 logMAR).

### 3.3.6 Correlations to Other Phenotypic Features

Phenotypical Characteristic	Outer Segment of Photoreceptor		Retinal Pigment Epithelium		Nystagmus Intensity		BCVA		VEP Asymmetry		Skin Pigmentation		Hair Pigmentation	
	(n=49)		(n=49)		(n=50)		(n=55)		(n=45)		(n=48)		(n=48)	
Mean ± Standard Deviation	31.99 ± 6.52		30.41 ± 3.87		10.45 ± 8.24		0.53 ± 0.25		1.25 ± 0.59		2.20 ± 0.40		3.50 ± 2.50	
Iris Parameter	<i>p</i>	<i>r</i>	<i>p</i>	<i>r</i>	<i>p</i>	<i>r</i>	<i>p</i>	<i>r</i>	<i>p</i>	<i>r</i>	<i>p</i>	<i>r</i>	<i>p</i>	<i>r</i>
Total Iris Thickness	0.986	-0.003	0.111	0.231	0.233	-0.172	<b>0.002</b>	-0.416	0.931	-0.013	<b>0.041</b>	0.296	<b>0.035</b>	0.306
Posterior Epithelial Layer	0.787	-0.04	0.289	0.154	<b>0.039</b>	-0.293	<b>0.001</b>	-0.453	0.941	-0.011	<b>0.042</b>	0.294	<b>0.043</b>	0.294
Transillumination grading	0.388	-0.126	0.459	0.108	0.153	0.205	0.132	0.206	0.566	-0.88	<b>0.004</b>	-0.406	<b>0.000</b>	-0.531

Table 3-2: shows the Level of significance (*p*) and correlation coefficients (*r*) for iris thickness measures and transillumination grading in relation to other phenotypic characteristics. BCVA=best-corrected visual acuity; SD=standard deviation; VEP=visual evoked potential. The number of participants for whom data were available is indicated. Figures in bold indicate statistical significance ( $P < 0.05$ ).

**Table 3-2** shows correlations for thickness measures and transillumination grades against phenotypic characteristic. Although iris transillumination grading was strongly correlated to skin and hair pigmentation, it was not significantly correlated to any other phenotypical feature. In contrast, both total iris thickness and PEL were strongly correlated to BCVA and PEL was also significantly correlated to nystagmus intensity. Interestingly VEP asymmetry was not correlated to iris or PEL thickness or transillumination grading measurements. In addition, there were no significant correlations between any retinal layer thickness measurements at the fovea and either iris/PEL thickness or transillumination grading (statistical analysis for outer segment layer and retinal pigment epithelium shown in **Table 3-2**. **Table 3-3** categorises correlations with foveal layers.

<i>Retinal Layer (Processing Layers)</i>	<i>Nerve Fibre Layer</i>		<i>Ganglion Cell Layer</i>		<i>Inner Plexiform Layer</i>		<i>Inner Nuclear Layer</i>		<i>Outer Plexiform Layer</i>	
	<i>p</i>	<i>r</i>	<i>p</i>	<i>r</i>	<i>p</i>	<i>r</i>	<i>p</i>	<i>r</i>	<i>p</i>	<i>r</i>
Iris Parameter										
Total Iris Thickness	0.221	-0.178	0.270	-0.161	0.554	-0.087	0.227	-0.176	0.090	-0.247
SAB	0.300	-0.151	0.247	-0.168	0.390	-0.126	0.358	-0.134	0.057	-0.276
PEL	0.312	-0.147	0.905	-0.017	0.427	0.116	0.169	-0.199	0.865	0.025

<i>Retinal Layer (Photoreceptor Layers)</i>	<i>Outer Nuclear Layer</i>		<i>Inner Segment Layer</i>		<i>Outer Segment Layer</i>		<i>Retinal Pigment Epithelium</i>	
	<i>p</i>	<i>r</i>	<i>p</i>	<i>r</i>	<i>p</i>	<i>r</i>	<i>p</i>	<i>r</i>
Iris Parameter								
Total Iris Thickness	0.098	0.239	0.172	0.198	0.986	-0.003	0.111	0.231
SAB	0.085	0.248	0.108	0.232	0.713	-0.054	0.156	0.206
PEL	0.815	0.034	0.653	-0.066	0.787	-0.040	0.289	0.154

Table 3-3: shows the level of significance (p) and correlation coefficients (r) for iris thickness measures for each retinal layer. There are no statistically significant findings for this analysis.

### 3.3.7 Changes in Iris Thickness with Age

The effect of age on changes in iris thickness is interesting as certain types of albinism demonstrate increased pigmentation with age. **Table 3-4** shows the changes in iris layer thickness with age in the albinism cohort and controls. The interaction between age and group is also shown to highlight significant differences in the rate of change in iris thickness with age in the albinism and control groups.

<i>Iris Parameter</i>	<i>Albinism</i>		<i>Control</i>		<i>Interaction</i>	
	<i>p</i>	<i>F</i>	<i>p</i>	<i>F</i>	<i>p</i>	<i>F</i>
Total Iris Thickness	<b>0.030</b>	4.974	0.082	3.181	0.870	0.027
Stroma Anterior Border Layer	<b>0.035</b>	4.687	0.229	1.492	0.152	0.697
Posterior Epithelial Layer	0.426	0.643	<b>0.044</b>	4.313	0.433	0.620

**Table 3-4: Statistical analysis of change in iris layer thicknesses with age using a univariate analyses. The level of significance (p) and the F-statistic (F) are shown separately for albinism and control groups. The interaction between group and ages is also shown when including data from both groups into the model.**

The statistical analyses revealed a significant effect of age on total iris thickness and the SAB layer in the albinism group. Also, age had a significant effect of the PEL thickness in the control group, although the change in total iris thickness did not reach significant levels. None of the effects were highly significant ( $P < 0.01$ ), and the interaction terms were not significant, indicating that there were no significant differences between the albinism and control groups with respect to the rate of change in iris thickness with age.

## 3.4 Discussion

### 3.4.1 Structural Differences between Albinism and Controls

In this study, we describe for the first time in-vivo structural deficits of the iris associated with albinism in a large cohort of patients (n=55) using OCT imaging. The PEL showed the most significant differences, being 44.0% thicker in controls compared with individuals with albinism, with the differences being observed along the whole iris from pupillary to ciliary ends. In contrast, a small deficit was observed in SAB thickness. The SAB was 5.8% thicker in controls compared with participants with albinism, with the most significant differences being observed at the ciliary ends of the iris.

Although differences in iris structure have been described in a small number of individuals with albinism using light and electron microscopy (Fulton, Albert et al. 1978, McCartney, Spalton et al. 1985), this is the first study to describe in-vivo iris structure in albinism using OCT. The cohort used in the study was also of a sufficient size to be representative of the wide phenotypical variations in iris structure associated with albinism.

In the only previous anatomic study of the iris in an adult with albinism, McCartney et al (1985) describe the ultra-structure in a 62-year-old individual with OCA leading to marked transillumination and blue irides. They found melanin containing cells in both the stroma and the PEL. However, there was a difference in the proportion of early (types I and II) and mature melanosomes (types III and IV) in the stroma. Stromal melanosomes consisted of 19% type II, 61% type III, and 20% type IV in albinism in comparison with <1% type II, 29% type III, and 70% type IV in a control iris. The proportion of early and mature melanosomes was not reported for the PEL (McCartney, Spalton et al. 1985).

Our results demonstrate that the largest differences in total layer thicknesses caused by albinism are observed in the PEL rather than the SAB layer. This could be due to a reduction in size of melanocytes in the PEL compared with the SAB layer. Although there are no reported data on PEL melanocyte size differences due to albinism, McCartney et al (1985) report that type III and IV melanosomes in posterior epithelial cells in albinism measure only 36% of the area of melanosomes in the posterior epithelial layer in controls. A similar finding was observed in stromal melanosomes in albinism measuring 60% of the area of stromal melanosomes in the stroma in controls (McCartney, Spalton et al. 1985). Another important factor is the composition of the PEL and SAB layers. The PEL consists of a double layer of tightly fused cubical melanocytes (Eagle 1988), so changes in melanocyte cell volume are likely to have a dramatic effect on the PEL layer thickness. In contrast, in addition to melanocytes, the SAB layer consists of fibroblasts, collagenous proteins, glycosaminoglycan's, macrophages, and mast cells (Rittig, Lutjen-Drecoll et al. 1990, McMEnamin 1997). These SAB cell types are responsible for the distinctive patterns and colouring of the iris and its role in immunologic defence (McMenamin 1997).

### **3.4.2 Changes in the Posterior Epithelial Layer (PEL)**

The PEL is derived from the same embryological structure as the RPE, the external optic vesicle. This makes the PEL a candidate as a source of substitute cells for the RPE for transplantation into sub-retinal space to treat retinal degenerative diseases (Abe, Yoshida et al. 2007). The similar embryological origin of the PEL and RPE could provide clues as to why these two layers are particularly important in the developmental abnormalities observed in both the anterior and posterior segments of the eye in albinism. However, we found no correlation between PEL thickness and RPE thickness. One possible reason for this lack of correlation may be attributed to the difficulty in segmenting retinal layers below the outer segment layer using OCT, as described by Wilk et al (2017) (Wilk, Huckenpahler et al. 2017).

McCartney et al (1985) suggest that the greater proportion of pre-melanosomes and smaller size of mature melanosomes in both the stroma and PEL explains the transillumination defect seen in their patient (McCartney, Spalton et al. 1985). We observed greater differences in the ciliary end of the SAB layer, which matches the partial iris transillumination patterns that exist in many patients in whom spots or a ring of transillumination can be observed around the ciliary outer edge of the iris (Summers, Knobloch et al. 1988). The differences we observed in the PEL compared with the SAB may indicate that transillumination deficits are mainly due to abnormalities in the PEL rather than the SAB.

Of note, two participants in this study with no observable PEL on OCT showed complete iris transillumination (grade 4). It is likely that these patients possess a PEL layer with unpigmented melanocytes (i.e. with no type III or IV melanosomes) that cannot be detected using OCT. OCT requires a difference in reflectance of light for delineation of different layers which were not possible in these two cases.

### **3.4.3 Changes with Age**

The absence of type III and IV melanosomes has been described in 2 other microscopy studies of the irides of a 13-year-old child (Fulton, Albert et al. 1978) and a foetus at 20 weeks gestation (Akeo, Shirai et al. 1996). The difference in the pattern observed in adulthood has been explained by the slow conversion of tyrosine to dopamine in the absence of tyrosinase, leading to the late development of mature melanosomes. This matches the change in pigmentation observed in most OCA subtypes, which slowly increases with time (Gronskov, Ek et al. 2007). We observed no changes in PEL layer thickness (the most affected layer in albinism) with respect to age in albinism, although it appears to increase in size with age in controls. However, the SAB layer (and total iris thickness) did significantly increase in size with the age of participants in albinism, although there was no significant difference in the rate of change between participants with albinism and controls. This suggests that these age-related

changes in iris layer thicknesses were not related to abnormal pigmentation in albinism.

Investigation of the effect of age on iris layer thicknesses was not the primary aim of this study and would require further investigation using a cohort with a representative group in each age band.

### **3.4.4 A Comparison of Iris Transillumination and Iris Layers**

The relationship between the iris transillumination grading and iris thickness measurements was not significant for total iris thickness and SAB layer thickness. There also was no significant relationship between PEL thickness and transillumination grading for grades 1 to 3, although all of these 3 grades showed lower mean PEL thicknesses compared to normal values. This could be due to the classification scheme of Summers et al (1988) relying on subjective grading that could vary between assessors. However, the strong correlation between subjective iris transillumination grading and grading of skin and hair pigmentation argue that the scaling used by Summers et al (1988) is a sensitive measure in the study cohort. Another possibility is that iris thickness measurements (e.g. PEL thickness) do not represent transillumination because they do not capture the whole transillumination defect, which can often be punctated in appearance, or thickness measurements do not give an indication of the level of pigmentation. Because OCT provides a measure of the tissue light reflectance, it may be possible to use intensity measurements of the image as a measure of pigmentation level in future studies. Currently, image intensity is a highly variable measurement that depends greatly on the equipment setup and the resulting quality of the image recorded. However, future developments in OCT recording and analysis could lead to this being feasible.

In contrast to the transillumination grading system by Summers et al (1988) both iris and PEL thickness were correlated to BCVA. This may suggest that OCT thickness measurements may offer a more clinically relevant measure of transillumination defects than the classification

scheme by Summers et al, 1988. Currently, we cannot determine whether the association between iris and PEL thickness and BCVA is causative (i.e. thinner iris and PEL leads to more stray light going into the eye leading to deterioration in BCVA). Alternatively, the link between PEL thickness and BCVA could be associated with nystagmus intensity, which was also correlated to PEL thickness and BCVA. Of note, iris and PEL thickness were not correlated to the level of foveal hypoplasia (quantified using the analysis of retinal layers at the fovea), one of the main causes of deterioration in BCVA.

### **3.4.5 The Diagnostic Ability of AS-OCT**

The detection of albinism can be problematic (Gronskov, Ek et al. 2007, Zuhlke, Stell et al. 2007, Hutton and Spritz 2008). In the study cohort, we found that PEL thickness was able to detect albinism with 85% sensitivity and 78% specificity. These figures should be interpreted with caution because one of the inclusion criteria of the study cohort was the presence of a transillumination defect on slit-lamp examination.

A significant level of mutations in the population with albinism is currently undetected in OCA and OA. For example, Gronskov et al (2007) have estimated that 50% of OCA mutations are undetected (Gronskov, Ek et al. 2007), whereas Zuhlke et al (2007) estimate that 30% to 40% of OCA mutations are undetected (Zuhlke, Stell et al. 2007). Hutton and Spritz (2008) have also suggested that 25% of patients with OA cannot be genetically diagnosed (Hutton and Spritz 2008). This is the reason why phenotypical diagnostic signs are currently needed for diagnosis, however, there is a long-standing debate about the sensitivity and specificity of VEP in albinism, with various authors stating differing detection rates. Apkarian and Shallo-Hoffmann (1991) report a 100% detection rate when comparing individuals with albinism with those who have IIN (Apkarian and Shallo-Hoffmann 1991), whereas Soong et al (2000) found a 71% sensitivity and 86% specificity when comparing VEP in controls with patients with albinism (diagnosis based on genetics in 9 of 21 patients, nystagmus, and iris transillumination)(Soong,

Levin et al. 2000). More recently, Hoffman et al (2005) found a 97% sensitivity and 100% specificity when comparing VEP in albinism (diagnosis based on clinical findings) against controls (Hoffmann, Lorenz et al. 2005). As none of these studies included a full cohort of genetically proven individuals with albinism, sensitivity and specificity results for VEPs should be considered with caution.

The use of phenotypical signs is not without problems. For example, foveal hypoplasia with chiasmal misrouting has been reported in patients suspected as non-albino, such as those with incomplete congenital stationary night blindness (Ung, Allen et al. 2005), Kartagener's syndrome (van Genderen, Riemsdag et al. 2006) and FHONDA (Al-Araimi, Pal et al. 2013) . We demonstrate that OCT measurements of PEL could be used as an additional objective marker for the diagnosis of albinism.

### 3.5 Study Limitations

A possible weakness of the study is that diagnosis was based on phenotype only. This meant that the sensitivity and specificity measurements could not be compared with a genetically determined population, this could be looked at in the future if genetic diagnosis was confirmed in our cohort of participants. Another limitation within the study was that only a single B-scan was used for analysis rather than a 3-dimensional volumetric analysis to avoid realignment problems caused by nystagmus. One must bear in mind that the iris transillumination defect is often irregular in appearance and in location within iris thus the horizontal OCT scan may not have picked up a true representation of the defect.

### 3.6 Future Studies

AS-OCT could potentially be useful in assessing objective changes in iris pigmentation during clinical trials. Clinical trials are beginning to emerge in albinism. In 2014, Summers et al assessed the efficacy of oral L-DOPA in human with albinism (Summers, Connett et al. 2014). An ongoing trial is currently taking place investigating the role of oral nitisinone in humans with albinism following the success of the study by Onajafe et al (2011) showing an improvement in pigmentation within mice (Onajafe, Adams et al. 2011). In light of this, Wang et al (2018) have recently devised a novel iris transillumination grading scheme (8 point scale) to use within this trial (Wang, Brancusi et al. 2018). AS-OCT could also potentially be used to objectively measure the iris differences pre- and post- treatment to help understand the efficacy of this treatment modality in humans with albinism.

In order to accurately validate iris AS-OCT measures, studies would be required to demonstrate the degree of reproducibility. Reproducibility can be assessed by test-retest analysis between repeated measurements close in time to ensure no biological change has occurred as well as by comparing repeated acquisition and analysis by different examiners.

To our knowledge, this is the first time AS-OCT has been used to measure iris thickness with a view to investigate pathology and clinically aid the diagnosis of albinism.

Future improvements in technology are likely to lead to faster acquisition, better realignment of B-scans, deeper penetration, and higher resolution of images, this could lead to segmentation of iris layers by automatic routines that could be implemented in a clinical setting. Further to this, volumetric segmentation throughout the whole iris in albinism could be a real possibility. The possibility of using adaptive optics to image iris structures with higher lateral resolution also requires further investigation. For example, adaptive optics could allow imaging of melanocytes, opening up the possibility of tracking pigment accumulation in some types of albinism.

# Chapter 4

## Visual Fields in Albinism (Study 2)

# Chapter 4 Visual Fields in Albinism (Study 2)

## 4.1 Introduction

### 4.1.1 Principles of Visual Field (VF) Assessment

A VF assessment indicates pathological connections within the visual pathway. A problem along the visual pathway (from the optic nerve through to the visual cortex) can result in a VF defect. **Figure 4-1** illustrates corresponding localisations of VF defect and cortical lesions.

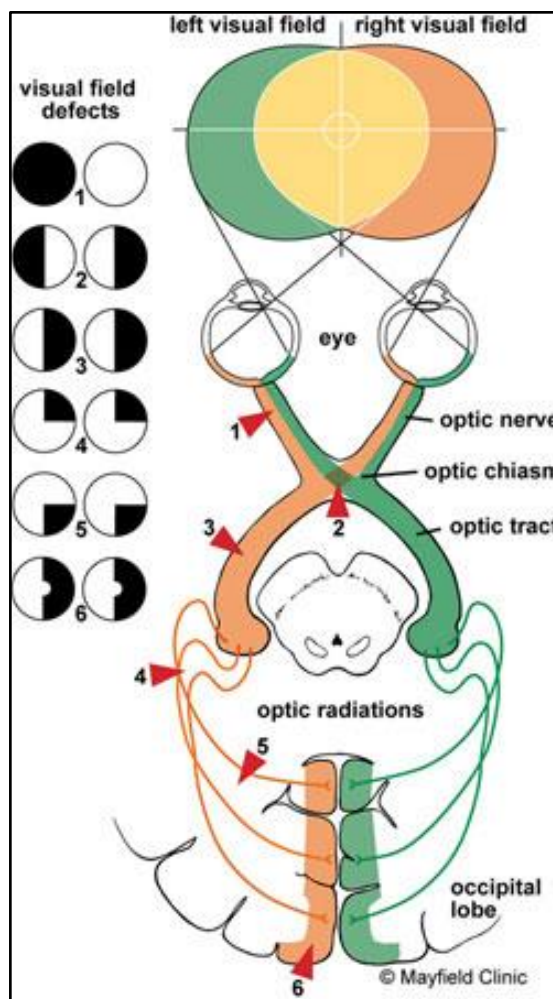


Figure 4-1: A schematic diagram illustrating the visual pathway (right) and visual field defects (left). Each red triangle matches to the visual pathway lesion corresponding to the visual field defect with the same number. Image reproduced from <http://www.mayfieldclinic.com>

## 4.1.2 The Importance of Visual Field Assessment

The rationale behind VF testing is to provide information essential to aid the diagnosis of ocular disease, such as the early detection of glaucoma (De Moraes, Juthani et al. 2011), evaluate neurological disease and to monitor its progression. Disorders can be detected during VF testing due to diminished sensitivity in the peripheral VF. VF assessments are often one of the most important clinical procedures in evaluating the status of the afferent pathways for locations outside the macular region of the retina.

There are two main types of perimetry; kinetic and static. Kinetic perimetry includes tests like the Goldman visual field (GVF) assessment and the Tangent screen; static perimetry is more likely to be automated using methods such as the Humphrey visual field (HVF) assessment. Kinetic perimetry refers to a VF test which uses a target which is moved by an assessor (or semi-automatically in some VF machines) (Nowomiejska, Vonthein et al. 2010)) until it appears in the patient's VF. This is repeated at different points around the VF and the point at which the patient sees the target is recorded. Using kinetic perimetry is advantageous in patients who have difficulty with automated machines, who require full 180° VF assessment or those with learning difficulties. They are often used in neuro-ophthalmological examination as they are accurate in delineating the location of the VF defect, for example a hemianopia. Static perimetry assesses threshold throughout the VF, the intensity of the target is increased or decreased in a staircasing method until a threshold value is calculated.

Static perimetry is more likely to be automated. Currently the majority of VFs in clinical practice are automated due to advantages such as fast speed of assessment, quantitative measures and the ability to quantitatively monitor progression from one visit to another. In some instances, for example when a quick assessment is required (e.g. at the bedside), a confrontation VF which involves asking the patient whether they can see in different areas of

their VF can be performed. Over the past 20-30 years, departments across the world have moved to a more automated approach.

### 4.1.3 VF Assessment Techniques

VF assessment has helped diagnose various ophthalmological defects over the past 150 years. Over this time the testing strategies and instrumentation have changed vastly, although the underlying principles remain similar. This chapter will outline the methods of VF assessment.

#### 4.1.3.1 Confrontational Visual Field Testing

Confrontational visual field assessment is undertaken when a quick examination of any VF defect is required. There are many methods of confrontational visual field: the most commonly used approach is whereby the patient fixates on the examiners eye and confirms when the examiner's finger is seen as it is brought in from outer positions. This is performed in all areas of the patient's VF to check for any possible defects. It is usually assessed unilaterally (**Figure 4-2**).



**Figure 4-2:** The photo shows an example of confrontational visual field testing in an adult. Image reproduced from [avserver.lib.uthsc.edu](http://avserver.lib.uthsc.edu)

### 4.1.3.2 Amsler Grid

The Amsler grid provides qualitative analysis of visual disturbance in patients. An individual looks at the grid at 33cm and is asked to fixate on a central spot of the grid unocularly. The individual is then asked, whilst maintaining central fixation, whether there are any regions with lines missing, blurred, distorted, bent or irregular. The test is routinely used to examine patients with macular disease, macular scars, macular degeneration and other retinal disorders.

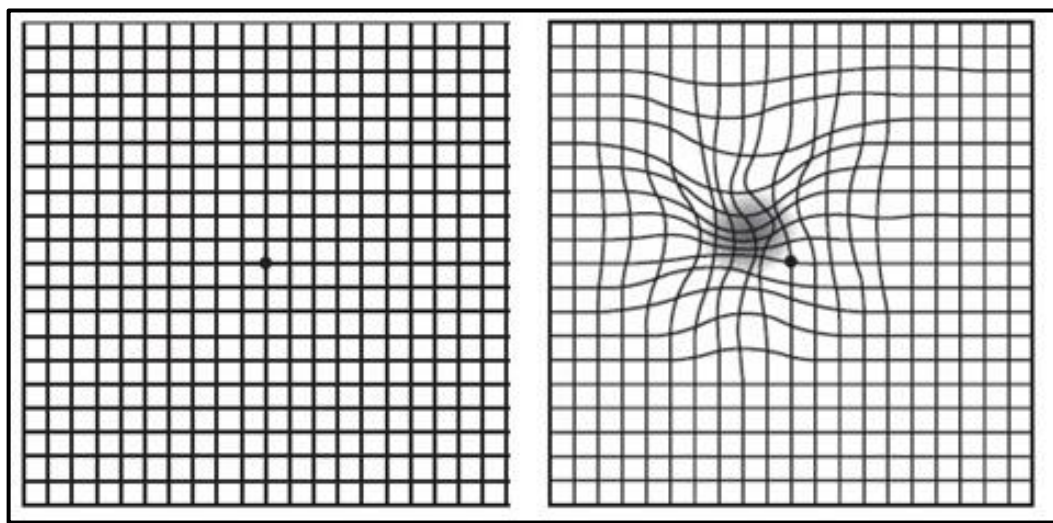


Figure 4-3: (Left) Amsler grid viewed when the patient has no underlying eye condition. (Right) Amsler grid when a patient has an eye condition for example age-related macular degeneration. Image reproduced from <http://www.asrs.org>.

### 4.1.3.3 Tangent Screen/Bjerrum Screen

This is another form of manual perimetry. The Tangent/Bjerrum screen is made of black felt and is often mounted on a wall. The test is usually performed at a distance of 1 metre. A light source is used to ensure illumination is constant. With this test an individual fixates a central target and a stimulus is slowly moved from the periphery towards the centre of the screen along a meridian until the stimulus is detected. This is repeated along all meridians and eventually an isopter (curve representing areas of equal visual acuity in the field of vision) is plotted. This is performed unocularly. Scotomas, areas of low sensitivity or non-seeing areas surrounded by normal visual field regions, are also drawn.

#### 4.1.3.4 Goldman Visual Field (GVF)

The GVF machine is a hemispheric bowl of controlled illumination (10.0 candelas/m<sup>2</sup> (measure of light density)) onto which a small bright stimulus is projected (size and brightness can be altered). Unlike the Amsler grid and tangent screen the GVF can evaluate the full VF. The test is conducted unilaterally with a patient fixating on a central target whilst the examiner moves a target in from the periphery. When the target is seen in the field of vision this is noted on the chart. This is then repeated for all positions and a VF is plotted. Testing on the GVF machine can also be performed on co-operative children as young as 5 years of age.



Figure 4-4: (Left) shows the examiners view of the Goldman Visual field test. The examiner can control all required measures and plot the patient's visual field. (Right) shows the patients view during the test and where they place the chin during the test.

#### 4.1.3.5 Automated Visual Field Testing/Static Perimetry

In the 21st century automated VF assessment has become mainstream and now constitutes a large part of the ophthalmological examination. For static perimetry the Humphrey visual field (HVF) analyser is one the most used automated machines on the market. Measurements usually consist of single detection thresholds taken at 54 points along 24-30° of the field of

vision for each eye. A staircase procedure is used to measure threshold sensitivity. A staircasing method starts with high intensity stimulus which is then reduced until the observer makes an error at which point the staircase reverses and the intensity increases again until the patient responds correctly causing another reversal. The values for the last reversals are then averaged to provide a threshold reading. There are many different types of staircase procedures. The SITA (Swedish Interactive Threshold Algorithm) model produces threshold estimates and also estimates on the certainty to which the threshold is known at each point. The SITA method is a staircasing method that was developed to shorten test duration without compromising its sensitivity (Bengtsson, Olsson et al. 1997, Bengtsson, Heijl et al. 1998, Roggen, Herman et al. 2001). The SITA test optimises the determination of perimetry thresholds by continuously estimating what the expected threshold is based on the patient's age and neighbouring thresholds. The SITA algorithm is similar to the full-threshold algorithm. However, the number of stimuli produced are 29% less in normals (Bengtsson, Olsson et al. 1997).

### 4.1.3.6 Advantages and Disadvantages of Visual Field Tests

Method of Visual Field Assessment	Advantages	Disadvantages
VF by Confrontation	<ul style="list-style-type: none"> <li>• Simple for patient and clinician</li> <li>• Rapid and reliable</li> <li>• Can perform at bedside</li> </ul>	<ul style="list-style-type: none"> <li>• Inability to detect subtle VF defects</li> <li>• Easy for patients to pretend problem</li> <li>• No option to monitor progression</li> </ul>
Amsler Grid	<ul style="list-style-type: none"> <li>• Quick and easy to perform</li> <li>• Useful in identifying small scotomas</li> <li>• Can monitor progression of disease</li> </ul>	<ul style="list-style-type: none"> <li>• Inability to detect subtle VF defects</li> <li>• More suited to assess maculopathies</li> </ul>
Tangent Screen	<ul style="list-style-type: none"> <li>• Simple for patient and clinician</li> <li>• Can monitor progression of disease</li> </ul>	<ul style="list-style-type: none"> <li>• Strong dependence of results on skill and technique of perimetrist</li> <li>• Lack of standardization</li> <li>• No normative age values for comparison</li> <li>• Difficult to monitor patient fixation</li> </ul>
Goldman Perimetry (Kinetic Perimetry)	<ul style="list-style-type: none"> <li>• Utilised to assess the whole VF (up to 180°)</li> <li>• Can monitor progression</li> </ul>	<ul style="list-style-type: none"> <li>• Long testing time (approx. 30 minutes)</li> <li>• Limited quantitative information</li> <li>• Strong dependence of results on skill and technique of examiner</li> </ul>
Automated Perimetry (Static Perimetry)	<ul style="list-style-type: none"> <li>• Measurements provide quantitative data throughout the full VF</li> <li>• Very quick and easy to set up and perform</li> <li>• Fixation, false positives and false negatives recorded</li> <li>• Test duration approx. 10 minutes for both eyes</li> <li>• Accurate results due to stair-case procedures</li> <li>• Provides age-matched raw data, total deviation and pattern deviation</li> <li>• Automated calibration</li> <li>• Long term monitoring of disease/progression</li> </ul>	<ul style="list-style-type: none"> <li>• Automated perimeters take up space</li> <li>• Takes longer for those with VF defects</li> <li>• Difficult to assess when fixation is poor, e.g. in nystagmus</li> </ul>

**Table 4-1: Showing each type of visual field assessment and its advantages and disadvantages. VF=Visual Field, SITA=Swedish Interactive Threshold Algorithm.**

#### 4.1.4 Previous Studies on Visual Fields in Albinism

As previously described the visual system is structurally different in albinism. In particular, part of the temporal retina projects abnormally to its contralateral hemisphere (Creel, Witkop et al. 1974, Schmitz, Kasmann-Kellner et al. 2004, Hoffmann, Seufert et al. 2007). Previous literature is controversial as to whether or not VFs in individuals with albinism are affected due to the projection abnormality found in albinism. There are 3 main studies which have previously investigated albinism and VFs:

***St John and Timney (1981):*** As early as 1981, St John and Timney assessed 13 individuals with albinism (12 OCA and 1 OA) and 15 controls using a 1m<sup>2</sup> tangent screen viewed at 50cm to assess the VFs and, in addition, contrast sensitivity was assessed with sine wave gratings. This study found that the VFs in 9/13 individuals with albinism were constricted in size compared to the controls. The largest VFs in albinism were very similar to that of a control; however the worst VFs were severely constricted in albinism. Contrast sensitivity comparison between the groups found that on average the contrast sensitivity of the albinism group was well below that of the control group. In the control group the contrast sensitivity was the same in the nasal and temporal retina and lower than in the central retina (as expected).

The albinism group was divided into two groups, those who performed better (Group 1) and those who performed worse (Group 2) on VF testing. There was actually no differences between the functions for each eye and therefore data from both eyes of the subjects were pooled together for analysis. There were no differences for all retinal positions for those in Group 1. In contrast, for those in Group 2 the average sensitivity in the central retina was better than the nasal retina, and the nasal retina was better than the temporal retina (central retina>nasal retina>temporal retina). Within the discussion section for this study, the authors state the most striking aspect of the data is that this small proportion of individuals with albinism show their most severe VF loss in the temporal retina (nasal VF), this corresponds to

findings expected with the chiasmal misrouting seen in albinism as the fibres from the temporal retina cross over erroneously.

Although this study created a good foundation for future research into the assessment of VFs in albinism there are various aspects of this study that were not clarified. There is no clear description of the inclusion or exclusion criteria for albinism patients or specifically how all patients were diagnosed. The type of test used was a tangent screen for which it is often very difficult to know what is normal for each age group, it is highly subjective and significantly relies on the examiner. In addition, there is no mention of the level of VEP crossing in these patients so it is impossible to correlate the VF abnormality with the level of abnormal VEP crossing. This study was descriptive providing no possibility for future comparison.

**Abadi and Pascal (1993)** published a study assessing light-spot detection thresholds in humans with albinism. This study involved 11 individuals with oculocutaneous albinism (age range 13-60 years old), 6 with IIN (age range 16-47) and 6 controls (age range 18-24 years old) who were all assessed using GVF) testing. Each GVF session commenced with a 5 minute adaptation period and then each eye was assessed separately with a refractive lens placed in front of the eye and the fellow eye occluded. Retinal sensitivity thresholds were determined for the central 30° of the VF. From 0-20°, measurements were taken at 2° intervals and between 20-30°, at 5° intervals. For all of the central VF measurements the subjects were instructed to fixate in the centre of the perimeter. An ascending method of limits was used to determine the threshold in this case. The fixation was monitored through a built-in telescope. If there were large eye movements then threshold measurements were repeated. Biochemical tests, clinical testing, family history questioning and personal tanning experience were used as a diagnostic test for patients with albinism. The patients with albinism had poor visual acuity in this study compared to those with IIN. Those with albinism had visual acuity ranging from 0.42 to 0.94 logMAR compared to those with IIN who had visual acuity ranging from 0.12 to 0.80 logMAR.

The authors found that contrast sensitivity was best in controls (average -0.60 log units) followed by the IIN group (-0.70 to -1.90 log units) followed by the albinism group (-0.90 to -2.10 log units). The 11 subjects with albinism demonstrated a great diversity of incremental sensitivities at the 0° location. An interesting point to note from this study was that for controls the peak contrast sensitivity was always found at the fovea. In contrast, only 5 out of 11 patients with albinism and 4 out of 6 patients with IIN demonstrated their peak contrast sensitivity at the fovea. The authors postulate this could indicate a misplaced fovea in albinism (Abadi and Pascal 1993).

Most recently, **Hoffmann et al. (2007)** assessed 15 individuals with albinism (21-71 years old) and 6 controls (22-29 years old) carrying out VF testing using automated static white on white perimetry (OCTOPUS 101 Perimeter, Haag-Streit, Koeniz, Switzerland) and comparing to previously conducted visually evoked potentials (VEPs). Individuals with albinism appear to have been previously diagnosed with albinism, have chiasmal misrouting on VEP and visual acuity ranging from 0.1-0.6 (average 0.2 logMAR). The VEPs indicated the misprojection was limited to the central part of the retina and its extent varied between subjects. The line of decussation was shifted by 2°-15° from the retinal midline into the temporal retina (median 8°). For the Octopus 101 assessment of VF in this study all participants wore their prescribed refractive correction and positioned their heads straight during assessment. The percentage of false positives and false negatives never exceeded 17%. For a direct comparison with age matched controls, reference data supplied by the Octopus 101 was used.

The main findings from this study was firstly that there was no evidence of selective defects that correspond with the projection abnormality of the temporal retina (i.e. no significant reduction in nasal VF in comparison to temporal VF). In patients with albinism, the contrast sensitivity of the abnormally projecting area of the temporal retina was not selectively reduced, however, the contrast sensitivity was reduced around the blind spot. In this study

there were no differences between nasal and temporal contrast sensitivity as found in a subset of individuals with albinism in the St John and Timney (1981) study. Further to their findings, the authors postulate that a light spot detection threshold test is not sensitive enough to demonstrate the chiasmal abnormality. They felt a more complex task was needed which requires an integration of information from neighbouring representations in the visual cortex (Hoffmann, Seufert et al. 2007).

These three studies used different methods and presented different findings. When comparing the findings in all three studies, the oldest study by St John and Timney (1981) is the only one to demonstrate a nasal/temporal asymmetry in a small subset of their patients with albinism. Neither of the other studies found this. Hoffman et al (2007) was the only study to consider the degree of anomalous crossing in comparison to nasal and temporal VFs, however this did not produce any significant findings. Interestingly none of the studies found differences between left and right eyes and all pooled data from both eyes together for their comparisons. Interestingly, a recent study by Mohammad et al (2015) found a difference in peripapillary RNFL thickness in right and left eyes in albinism so differences between eyes should be considered when comparing data in albinism (Mohammad, Gottlob et al. 2015).

In all aforementioned studies the sample size was relatively small with fewer than 15 subjects with albinism.

## 4.1.5 Aims and Rationale for Study 2

The main aim of this study is to address the discrepant questions raised from these previous studies by using a larger sample of carefully diagnosed participants with a range of visual deficits caused by albinism or IIN. Specifically, we will assess asymmetries in nasal and temporal VF, quadrant differences (i.e. comparing superior and inferior field deficits) and we will also compare differences between the left and right eye.

We will also compare the relationship between nasal/temporal VF asymmetry and severity of the crossing abnormality at the chiasm assessed using VEP and visual acuity.

A second element to the study will be the comparison of VF abnormalities to structural deficits within the eye using OCT. This will be covered in **Study 3**.

## 4.1.6 Hypotheses

These are the main hypotheses to be addressed in **Study 2**:

### **Detection Threshold Differences**

- Detection thresholds are worse in albinism compared to IIN

### **Nasal/Temporal VF and Quadrant Deficits**

- Nasal VF is less sensitive than temporal VF in albinism but not IIN
- Vertical as well as horizontal VF asymmetries exist in albinism

### **Right and Left eye Differences**

- The detection threshold is better in the dominant eye compared to the non-dominant eye

### **VF Asymmetry in Relation to VEP and BCVA**

- The degree of asymmetry on VF is related to degree of chiasmal misrouting measured using VEP
- The degree of asymmetry on VF is related to visual acuity

## 4.2 Methodology for Study 2

### 4.2.1 Patient Characteristics

61 individuals with albinism (mean age=32.4 years, SD=13.6 years) and 32 individuals with IIN (mean age=33.9 years, SD=14.0 years) were used in the study. In the albinism group 65 individuals were recruited; however two participants were excluded due to abnormal intraocular pressure, one participant had excessive false positives (66%) during VF assessment and one participant had a VF defect secondary to stroke. Within the IIN group 34 individuals were recruited. Two participants were excluded. One had a macular hole noticed on OCT and the other had the wrong preliminary diagnosis (participant had CSNB). All participants were recruited from paediatric and adult ophthalmology clinics at the Leicester Royal infirmary. Informed consent was given by each individual before examination and for participants under the age of 16 years of age (n=4) parental/guardian consent was obtained.

The diagnosis of albinism and IIN was confirmed using the diagnostic criteria outlined in **Chapter 2**.

### 4.2.2 Additional Examinations for Study 2

#### 4.2.2.1 The Assessment of Eye Dominance – Sighting Dominance

The assessment of eye dominance was carried out after analysing our initial set of results. We used sighting dominance to determine the dominant eye. The method used for sighting dominance was the Miles test (hole in hand method) that allows the determination of which monocular view of a distant object matches the binocular view. This test is carried out by the patient extending both arms and bringing them together to create a small opening, then with both eyes open you view a distant object. The patient then alternates closing each eye to see

which eye viewing (left or right) matches that of binocular viewing – this is classed as the dominant eye.

#### **4.2.2.2 Visual Field Examination**

The VF was assessed in each individual with nystagmus using the Humphrey field analyser (HFA, Humphrey Instruments, Inc., San Leandro, CA) which is a form of static perimetry. The program used was a SITA (Swedish Interactive Threshold Algorithm) Fast 24-2 method which determines the threshold for 24° around the fixation point.

Light spot detection thresholds were obtained for 54 locations around a 24° radius from the fixation point. All subjects who required refractive correction were provided the correct lens over each eye during the test, this ensured spectacle frames did not obstruct the VF. Fixation monitoring was turned off as nystagmus causes continuous ‘loss of fixation’, this was monitored by VS during examination to ensure fixation was maintained to the best ability for each participant. A false positive response occurs if a patient responds when no stimulus is being presented. False negative errors are recorded when a patient cannot see a brighter stimulus in the same spot where they had previously seen a dimmer stimulus.

The current Humphrey criteria for good reliability for false positive and false negative responses are 33% as recommended by Humphrey Instruments, Inc. (San Leandro, CA). Data from various studies have argued that this is too high and recommend 20% as a more appropriate cut off (Vingrys and Demirel 1998, Newkirk, Gardiner et al. 2006). A study by Newkirk et al (2006) found in some patients with glaucoma, mean deviation (MD) improving from baseline by more than 6 decibels when a 33% false positive error was introduced (Newkirk, Gardiner et al. 2006). False positive and false negative errors were observed for each participant and anybody who had either of these above 20% was not included within our study. As described above, only 1 participant was excluded due to this.

As we required a direct comparison to age-matched healthy controls we used the reference data within the HFA which provides averages from the machine for age. The total deviation results, which are used for our analysis, represents the patient's field of vision after correction for age. Retinal sensitivity decreases with age, and this analysis makes that adjustment by correcting the data at each point based on a normative age matched Humphrey database. The results at each point is in decibels and the minus (-) or plus (+) represent the performance in comparison to an individual with no eye problems of the same age. The reason why the total deviation is used over other measures is because it accounts for a change at each location in comparison to the pattern deviation which follows patterns around the location point.

#### **4.2.2.2.1 The Relevance of Information from Visual Fields**

**Figure 4-5** shows a VF print out and all the relevant information available for analysis purposes.

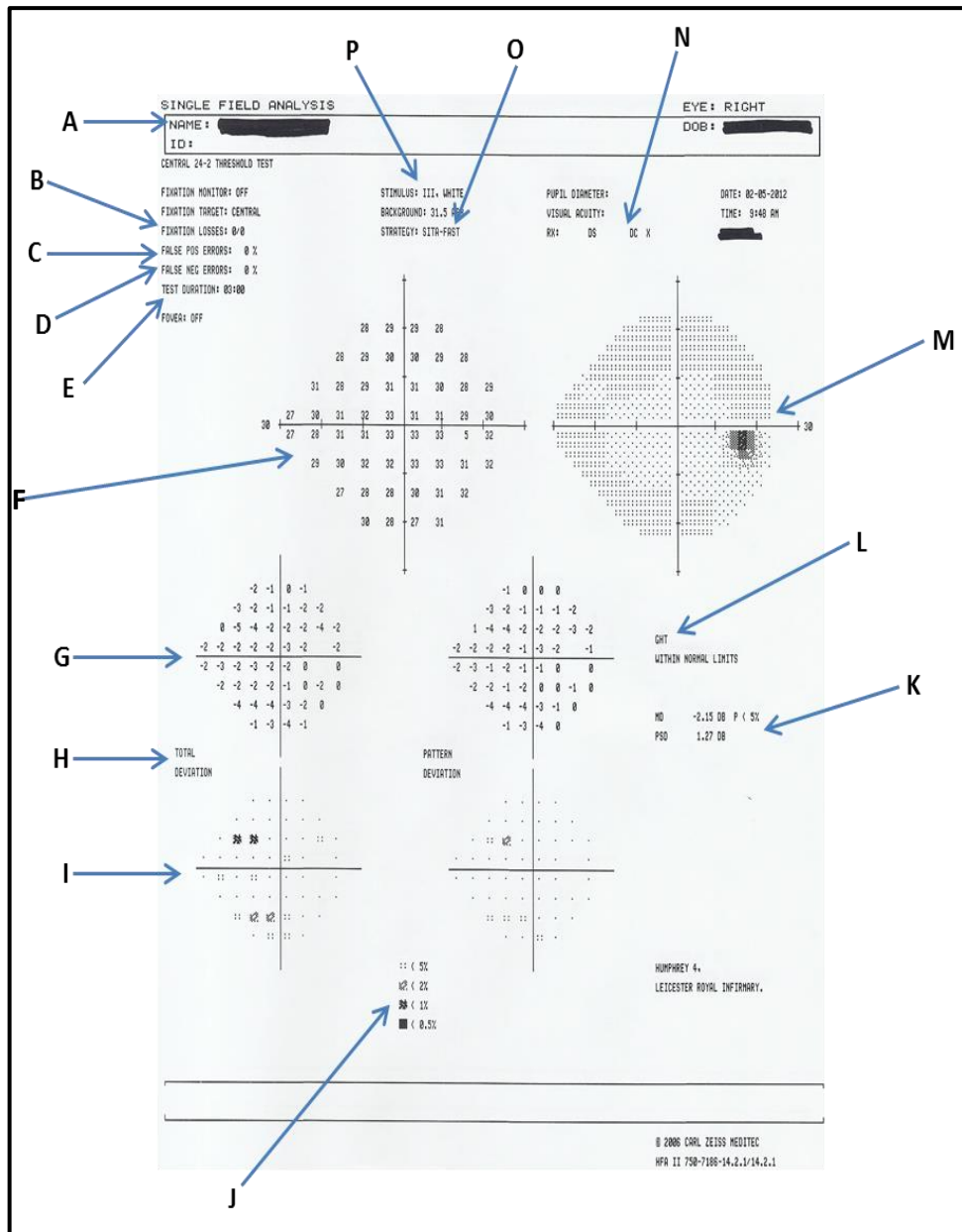


Figure 4-5: An example of a visual field assessment. A detailed description of each annotation is given below (A-P).

#### 4.2.2.2.1.1 Interpretation of Visual Field:

<b>Letter</b>	<b>Heading</b>	<b>Description</b>
<b>A</b>	<b>Name</b>	Patient's full name documented here
<b>B</b>	<b>Fixation losses</b>	The HVF analyser assesses fixation losses throughout the test to verify the plausibility of the test and how much an individual has been looking away from the central "fixation" point. A high percentage (usually over 20%) is classed as "low reliability".
<b>C</b>	<b>False positive errors</b>	The HVF keeps a track of all the times the patient responded to a stimulus which was not present. A high false positive score suggests the patient has been "second-guessing" throughout the test and responding despite a lack of stimuli. SITA tests also use patient response time as a guide for false positives.
<b>D</b>	<b>False negative errors</b>	The HVF senses the number of times that a light brighter than the threshold for that point is presented and missed. A high false negative score suggests either the patient is confused or trigger happy.
<b>E</b>	<b>Test duration</b>	This indicates how long the test takes. As a general rule the weaker a visual field the longer the time needed for completion.
<b>F</b>	<b>Threshold at each point</b>	This is the threshold at each point on the visual field assessment. The higher the number the "dimmer" the light seen.
<b>G</b>	<b>Deviation from normal</b>	The HVF analyser has integrated values of normality for each age range and therefore calculates the deviation from normal for each point. The difference is shown in decibels.
<b>H</b>	<b>Total deviation from the norm</b>	Title stating what is in I
<b>I</b>	<b>Total deviation from the norm</b>	This is a diagrammatic demonstration of the total deviation from the norm; the further away from the norm, the darker the shade
<b>J</b>	<b>Percentage of population comparison</b>	Each percentage is a calculation of the population that have these deficits at this age.
<b>K</b>	<b>Global indices</b>	Provides MD (mean deviation) and PSD (pattern standard deviation) readings.
<b>K*</b>	<b>Mean deviation (MD)</b>	Statpac determines each patient's visual field averages as the decibels above/below the normal reference fields (age-calculated).

<b>K*</b>	<b>Pattern standard deviation (PSD)</b>	Measures to what extent the shape of the visual field differs from the normal reference field (age-calculated), i.e. how smooth the hill of vision is (low PSD=smooth hill, high PSD=irregular hill).
<b>L</b>	<b>Test Performance</b>	This will tell you whether the examination is within normal limits or outside normal limits for a comparison to a normal individual of the same age.
<b>M</b>	<b>Diagrammatic visual field</b>	Shows the visual field diagrammatically and outlines any problematic areas in darker shades(excluding blind spot)
<b>N</b>	<b>Refraction</b>	The patient's refraction is termed as either sphere or cylinder
<b>O</b>	<b>Test Type</b>	This will tell you the type of test carried out (e.g. SITA FAST or SITA STANDARD)
<b>P</b>	<b>Stimulus size and type</b>	Size III is standard. Comparisons can only be made and probability values assigned using a Size III stimulus. Stimuli range from Type I (smallest) to Type V (largest). Type V is only used with very poor vision.

**Table 4-2: Annotation described from Figure 4-5 (A-P). HVF=Humphrey visual field, MD=Mean deviation, PSD=Pattern standard deviation.**

#### 4.2.2.2.2 Step by Step VF Assessment

Below is a step-by-step guide as to how a Humphrey visual field (HVF) was carried out on all individuals:

**Step 1:** Patient identified with correct diagnosis and consent is taken.



**Step 2:** Prepare examination room with appropriate lighting and calibration (important as the intensity of light is affected by surrounding lighting conditions).



**Step 3:** Input the individual's details into the HVF machine, ensuring the refraction is also examined and put into the machine as this will automatically decipher the correct lens required whilst assessing the VF.



**Step 4:** Provide the patient with concise instructions throughout testing:

The test is completed unilaterally: place an adhesive patch over one eye. Ensure the patient fixates their vision on the yellow coloured light (fixation target) ahead of them throughout the test.

Ensure the patient is sat still and correctly positioned on the VF machine, taking particular care of the posture. Ask the individual to place their head against the head rest and chin against the chin rest and ensure each eye is looking through the lens placed directly in front.

Provide the patient with the buzzer and explain this must be clicked when a flashing stimulus is seen. Explain to the patient that they must not look at the dots as they appear, they must fixate on the yellow/orange dot in front of them throughout.



**Step 5:** During the test gaze-tracking monitors the individuals position of gaze. The fixation is also automatically monitored, however due to the nystagmus this will not be possible in the majority of patients and so this setting is switched off. It is crucial to manually assess the fixation to confirm it has remained steady throughout, providing a valid and fair test. Throughout the test the HVF machine attempts to locate the blind spot. If the blind spot map fails it is important to repeat the mapping. If this fails again, then it is advised to turn the blind spot monitor off as it is likely that it is not being located due to the nystagmus.



**Step 6:** Repeat all steps using the fellow eye. Print results and file so they are ready for analysis.

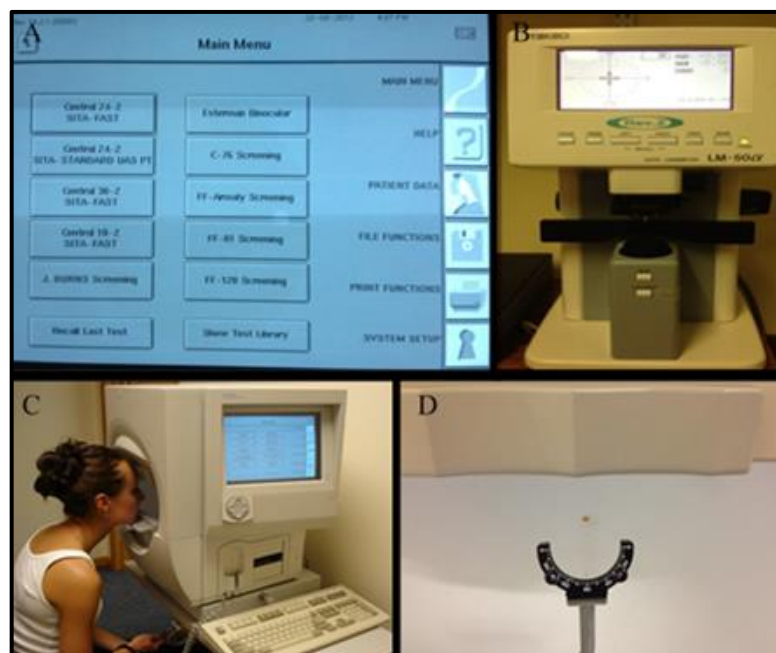


**Figure 4-6:** Equipment used to conduct a visual field assessment. (A) Opening menu and choice of tests: Central 24-2 SITA-FAST used for this study. (B) Focimeter to assess the strength of refractive correction. (C) Patient correctly positioned on visual field machine. (D) The lens holder and the yellow/orange stimulus that must be fixated on for the duration of the test.

### 4.2.3 Visual Field - Data Analysis

VF data was manually entered into an Excel database (Microsoft Inc.) outlining each of the 54 points of the VF. For analysis, the VF was divided into 5 areas: the macular region (central 6° of the visual field which corresponds to the foveal area measurement), upper nasal VF, upper temporal VF, lower nasal VF and lower temporal VF. We did not use the horizontal measurements around the blind spot due to nystagmus. Nystagmus within our patients was predominantly horizontal which meant that the blind spot may be accentuated horizontally. Data at the blind spot and the points immediately adjacent to it were not included in any analysis. The VF was divided in 5 separate areas as shown diagrammatically in **Figure 4-7** and only these points were used in analysis.

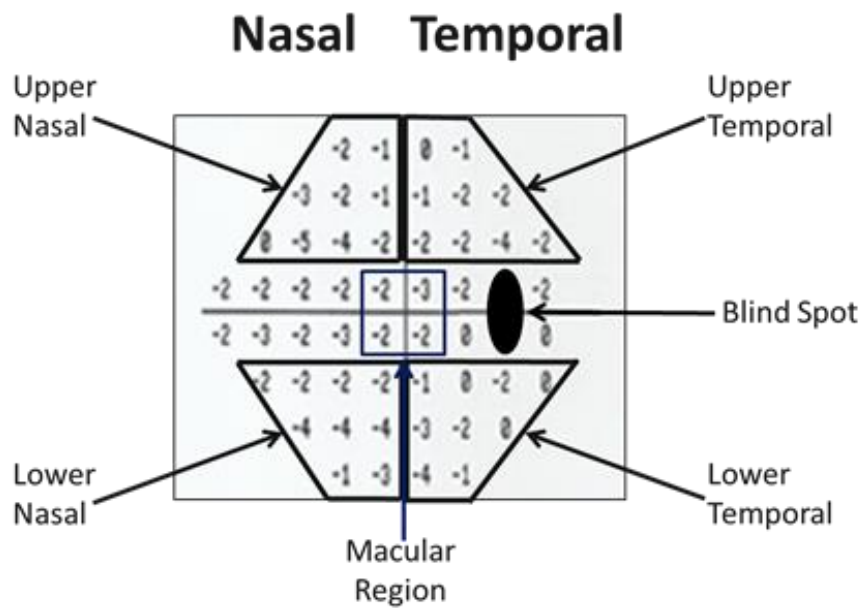


**Figure 4-7:** Data showing the total deviation from an aged matched normal with no eye condition in decibels. The visual field was divided into quadrants and a macular region.

## 4.3 Results

### 4.3.1 Participants Summary

Patient details are shown in **Table 4-3**.

	Albinism	IIN
<b>Participants (n)</b>	<b>61</b>	<b>32</b>
<b>Male: Female (n)</b>	<b>44:17</b>	<b>24:8</b>
<b>Mean Age (Years)</b>	<b>32.4</b>	<b>33.9</b>

**Table 4-3: Patient demographics for visual field study.**

### 4.3.2 Visual Field Differences between Albinism and IIN

**Figure 4-8** is a schematic diagram for the right and left eyes of the albinism and IIN groups. The darkness of each square indicates the deviation of the performance of detection threshold in that area ( $6^\circ$ ) compared to normal values. On visual inspection of the VFs for individuals with albinism and IIN an obvious difference can be seen when comparing these profiles. Overall the albinism group shows darker shades of grey than the IIN group which indicates this group performed worse in the detection threshold task (HVF).

A cursory view of the images suggests differences between right and left eyes and also between various quadrants of the VF.

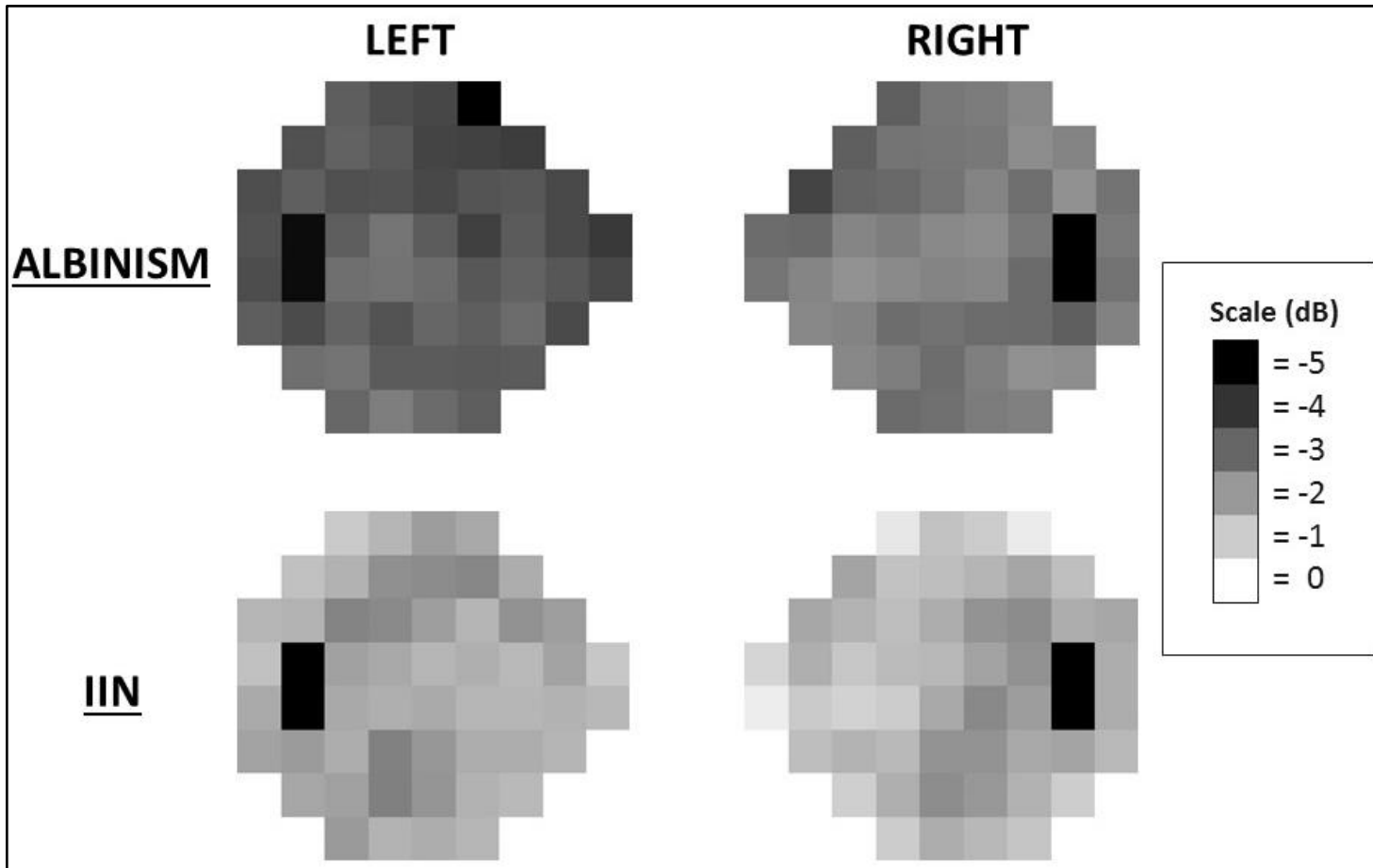


Figure 4-8: Schematic diagrams of the visual field for albinism and IIN. Each square represents 6° of the visual field. The darker each 6° square the poorer the detection threshold and the lighter each square the better the detection threshold. The blind spot is represented with the 2 black squares on the horizontal line temporally to the centre.

The mean detection threshold for the albinism group (right and left eyes combined) was -3.06 decibels (SE=0.17) in comparison to the IIN group (right and left eyes combined) where the mean detection threshold was -1.60 decibels (SE=0.14). All data was normally distributed. Using an unpaired t-test to compare these groups we found that the albinism groups mean detection threshold (for both eyes) was significantly worse than the IIN group's mean detection threshold ( $P < 0.001$ ; mean difference=1.465, 95% CI=0.9239 to 2.005).

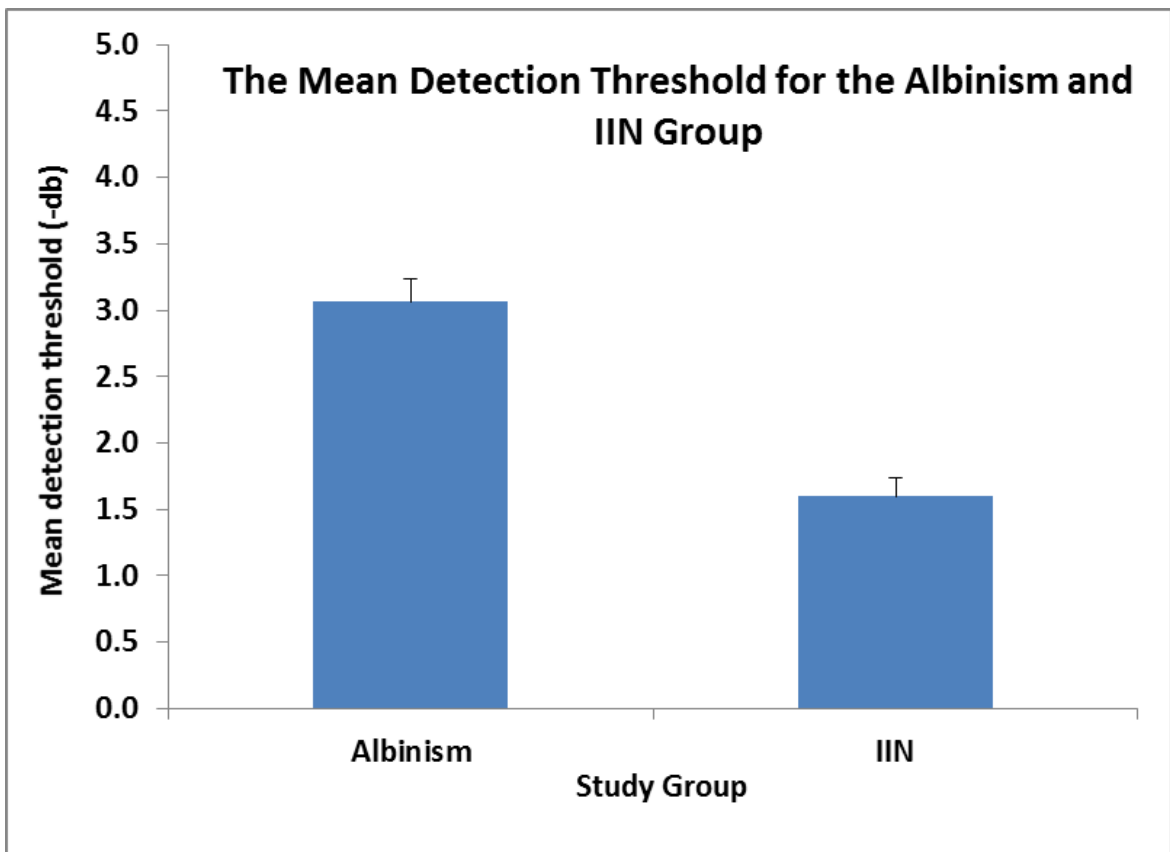


Figure 4-9: The mean detection threshold for the albinism group compared to the IIN group. The error bars show the standard error of the mean. The mean detection threshold for the albinism group was significantly worse than the IIN group.

### 4.3.3 Nasal/Temporal Differences in Albinism and IIN

There are inconsistent findings in the literature for nasal/temporal differences in VFs in albinism. St John and Timney (1981) found a subset of their albinism patients demonstrated nasal/temporal differences in their VFs compared to Hoffman et al (2007) who found no

nasal/temporal VF differences. Accordingly, we investigated nasal and temporal VFs asymmetries in our data set.

We divided the VF into temporal VF (red trapezoid shapes) and nasal VF (green trapezoid shapes) as shown in **Figure 4-10**.

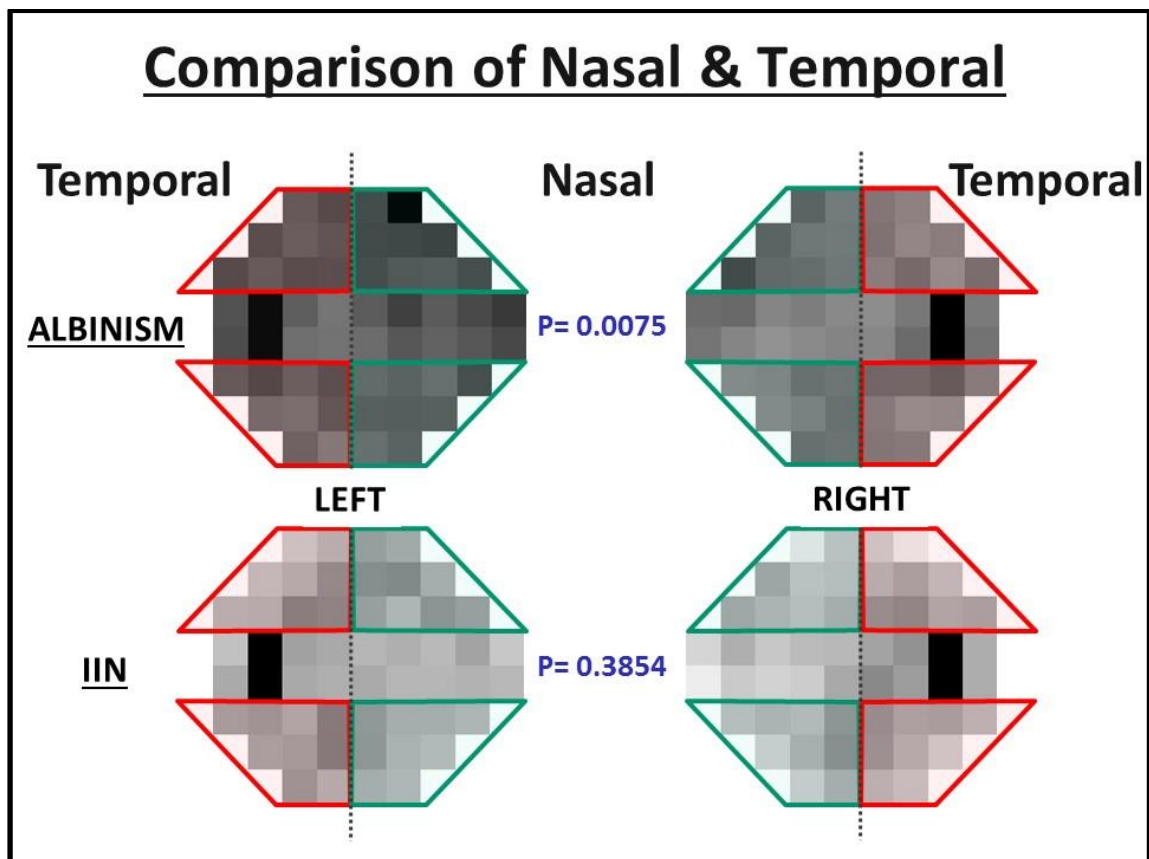


**Figure 4-10:** The comparison of nasal and temporal visual fields for albinism and IIN.

When we compared the nasal and temporal detection thresholds in the albinism and IIN groups (right and left eyes averaged together) we found significant differences. Statistical analysis in the albinism group revealed that the mean nasal detection threshold (-3.21 decibels (SE=0.17)) was significantly worse than the mean temporal detection threshold (-2.97 (SE=0.18), ( $P=0.0075$ ; mean of difference=0.2421, 95% CI=0.06599 to 0.4183).

In the IIN group the mean nasal detection threshold was -1.62 (SE 0.21) and the mean temporal detection threshold was -1.69 (SE 0.19) demonstrating no significant differences (P=0.3854; mean of difference=-0.07047, 95% CI=-0.2316 to 0.09065).

Figure 4-11 shows bar graphs of these comparisons.

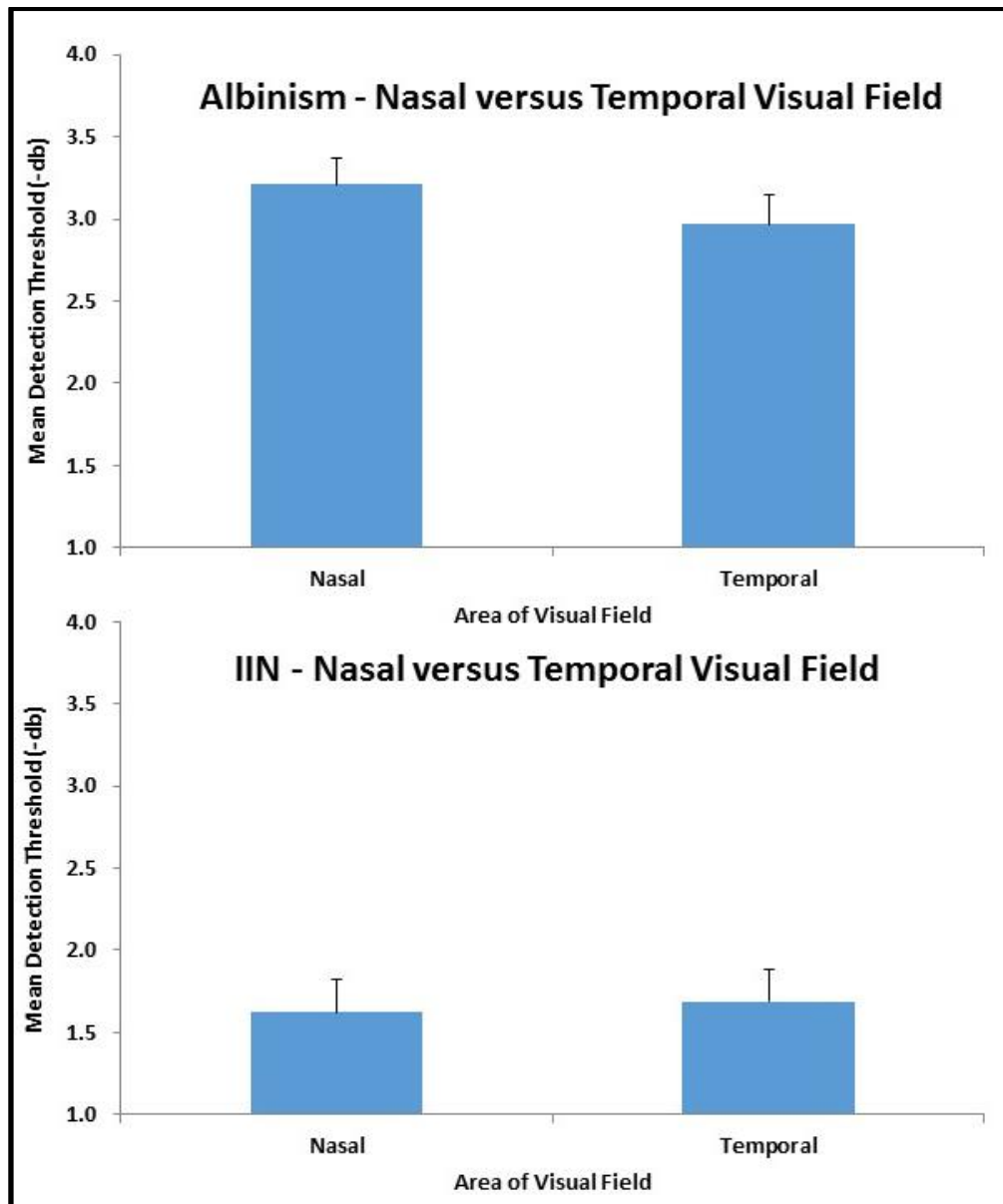


Figure 4-11: The mean detection threshold for nasal and temporal area of the visual field in albinism (top) and IIN (bottom). The error bars show the standard error of the mean.

### 4.3.4 Quadrant Differences in Albinism and IIN

In a further analysis we compared each VF quadrant for both groups as shown in **Figure 4-12** to explore horizontal and vertical differences in VF.

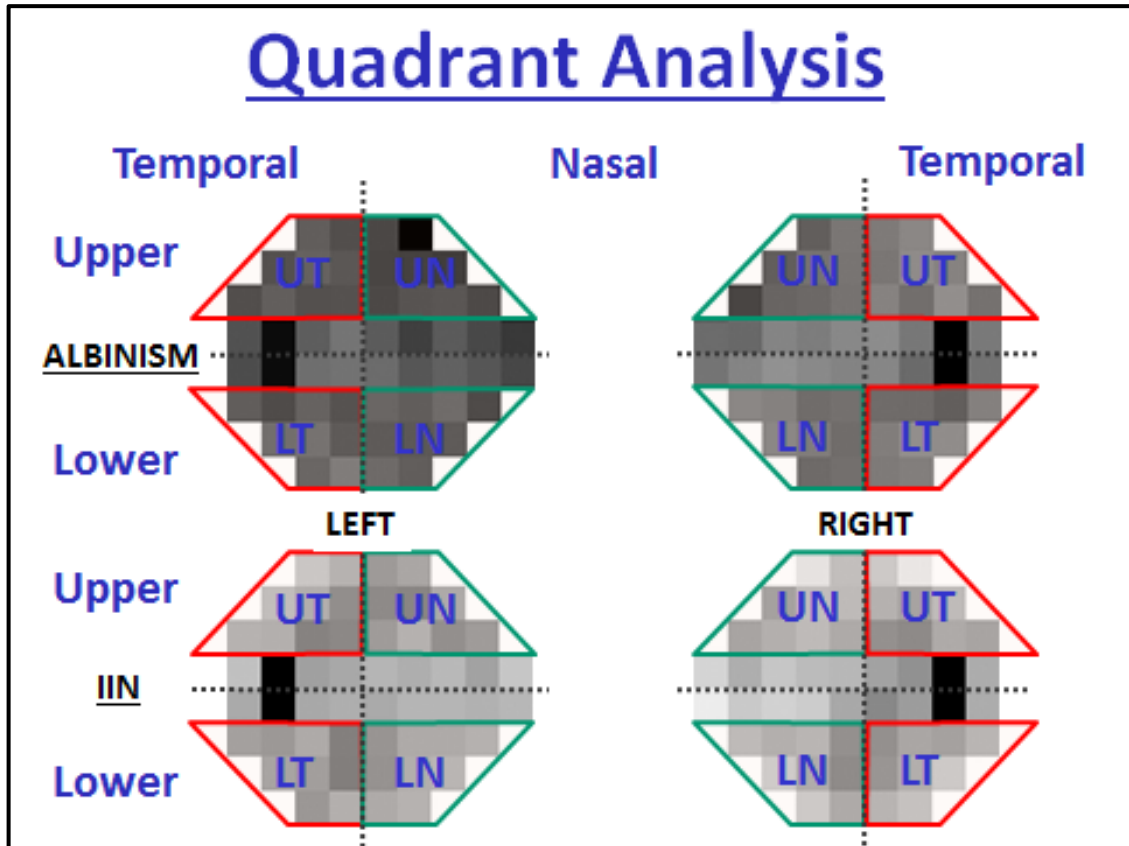


Figure 4-12: Quadrant analysis and how the visual field was divided.

#### 4.3.4.1 Quadrant Analysis for the Albinism Group

**Figure 4-13** shows the detection threshold for each separate quadrant in a bar chart format for the albinism group for the right and left eye (top). This figure also provides the comparison of all quadrants statistically using a LMM. When assessing the bar chart it is visible that the upper nasal VF shows the worst total deviation for the right eye in albinism in comparison to all other quadrants with the same pattern seen for the left eye.

Linear mixed models indicated significant differences between the four quadrants ( $P < 0.001$ ,  $F = 28.5$ ). Posthoc comparisons (with Bonferroni adjustment) show that the upper nasal VF was significantly poorer than the upper temporal field ( $P = 0.004$ ), lower temporal field ( $P = 0.013$ ) and lower nasal fields ( $P = 0.02$ ).

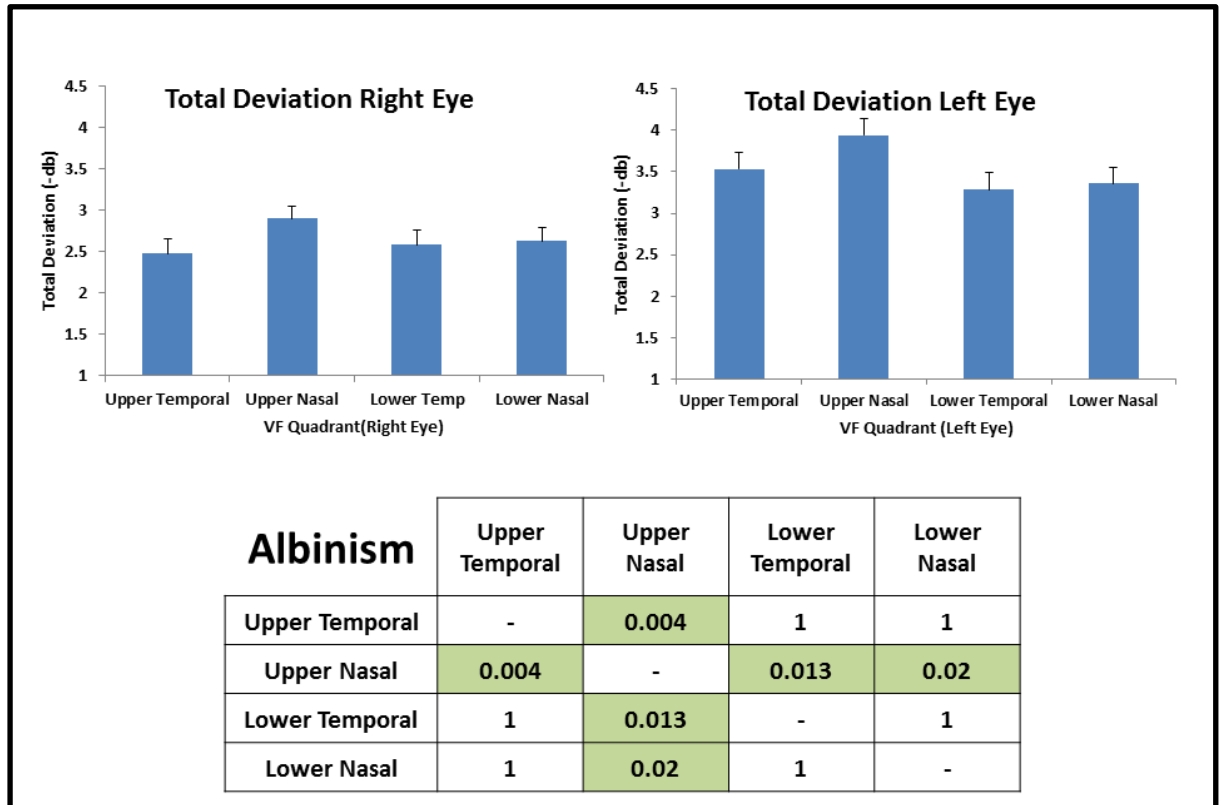


Figure 4-13: The mean detection threshold (-db.) for each quadrant of the visual field for the right eye and the left eye in albinism (top). The error bars show the standard error of the mean. A statistical comparison (LMM) was made of all quadrants with both eyes together showing the upper nasal visual field was significantly different to all other quadrants.

#### 4.3.4.2 Quadrant Analysis for the IIN Group

Figure 4-14 shows the detection threshold for each separate quadrant in a bar chart format for the IIN group for the right and left eye (top). The comparison of all quadrants statistically is shown below. When comparing the quadrants statistically using a LMM we did not find any significant differences between any quadrants for the IIN group.

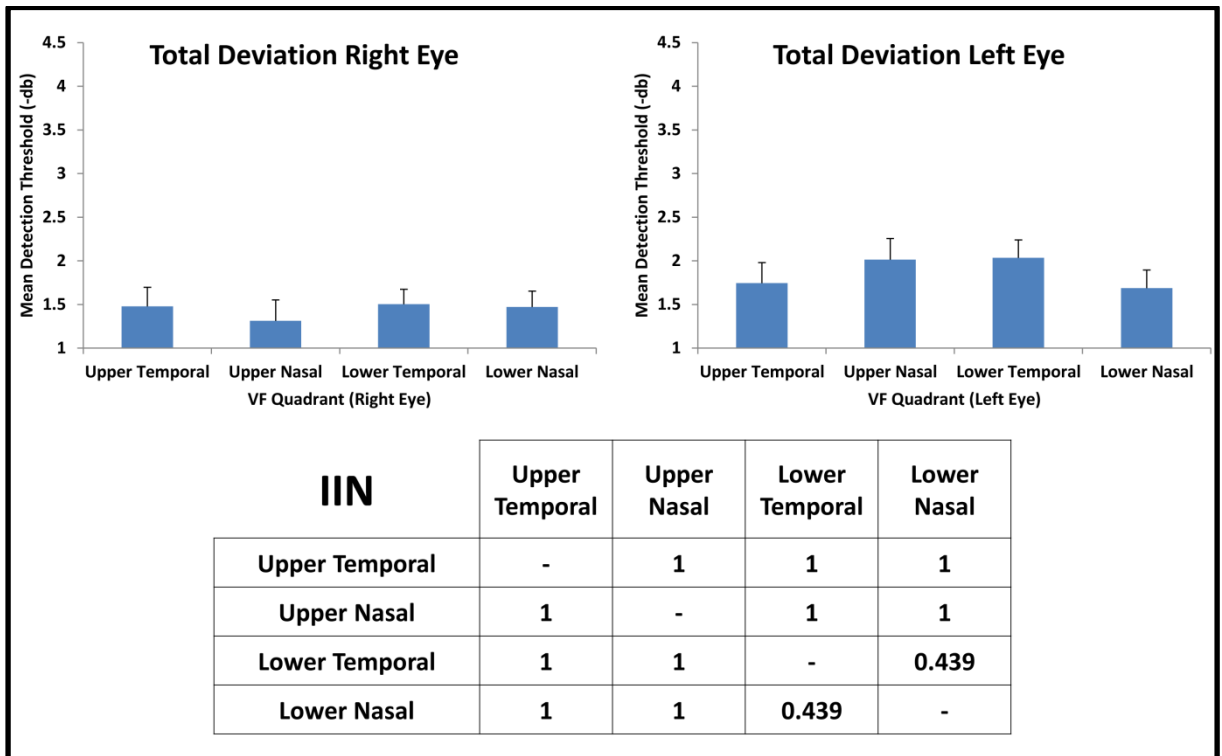


Figure 4-14: The mean detection threshold (-db.) for each quadrant of the visual field for the right eye and the left eye (top). The error bars show the standard error of the mean. A statistical comparison (LMM) was made of all quadrants with both eyes together, there were no significant differences.

### 4.3.5 Right and Left Eye Differences in Albinism and IIN

Distinct differences can be observed between the right and left eyes when examining the schematic diagram. Both graphically and in statistical models we further analyse right and left eye differences in both groups and discuss this further (4.3.6 and 4.3.7).

For the albinism group the mean detection threshold for the four quadrants for the right eye was -2.61 decibels (SE 0.21) compared the mean detection threshold for the left eye which was markedly lower at -3.52 decibels (SE 0.26) (**Figure 4-15**). As the data was normally distributed, using a paired t-test to compare the eyes statistically we found a significant difference between the eyes ( $P < 0.0001$ ; mean difference = -0.9031, 95% CI = -1.323 to -0.4828).

In the IIN group the mean detection threshold for the right eye was -1.41 decibels (SE 0.26) compared to the left eye which was -1.79 decibels (SE 0.28). Statistical analysis also

demonstrated a significant difference ( $P=0.0111$ ; mean difference= $-0.3788$ , 95% CI= $-0.6649$  to  $-0.09263$ ) (Figure 4-15).

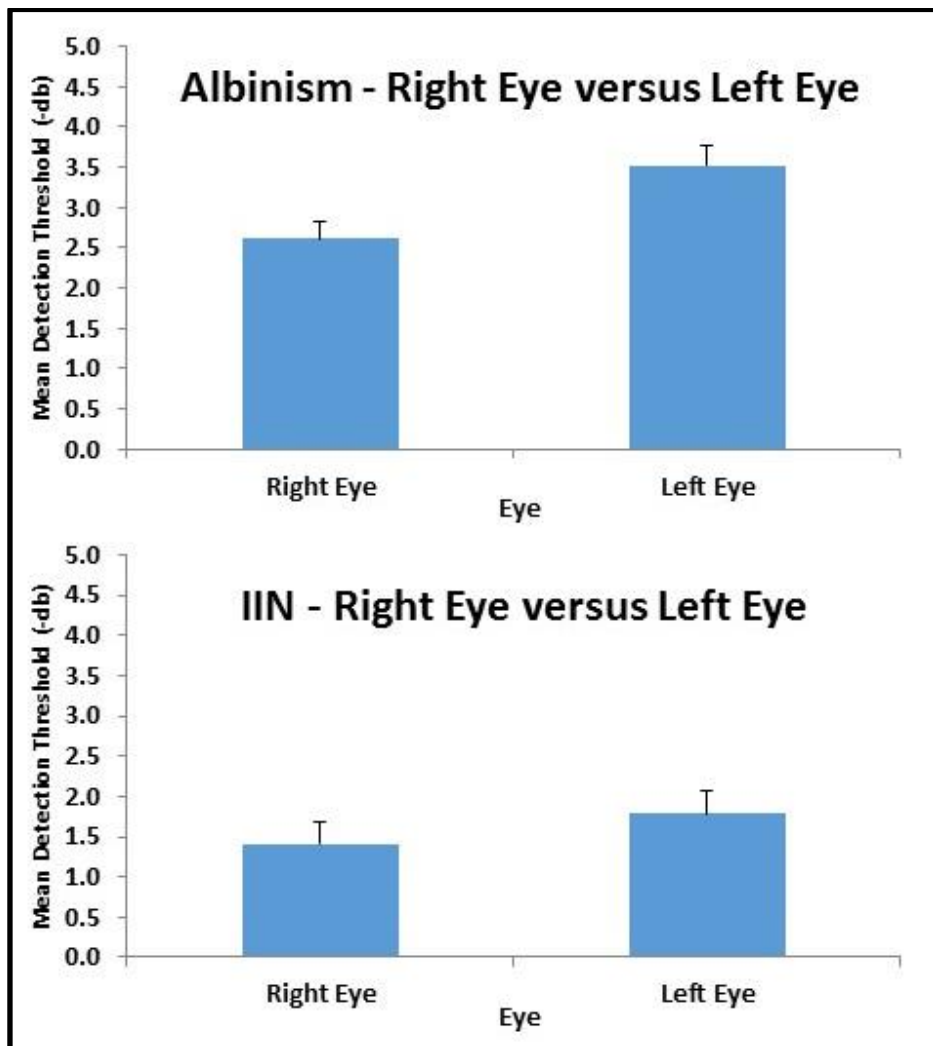


Figure 4-15: The mean detection threshold comparisons for the right and left eyes in albinism and IIN. The error bars show the standard error of the mean.

#### 4.3.6 Sighting Dominance for Albinism and IIN

Due to the obvious differences between detection thresholds in left and right eyes in albinism and IIN, we compared sighting eye dominance for both groups and assessed differences in the detection threshold for dominant and non-dominant eyes.

### 4.3.6.1 Eye Dominance for Right and Left Eyes in Albinism

Figure 4-16 shows the detection threshold for the albinism group for the right and left eye when dividing the groups into right dominant and left dominant. In the albinism group there were 35 individuals who were right eye dominant and 24 individuals who were left eye dominant. We were unable to determine eye dominance on 2 individuals with albinism.

For those in whom the right eye was dominant, the mean detection threshold for the right eye (-2.34 decibels, SE=0.26) was significantly better than the left eye (-3.92 decibels, SE=0.33) ( $P < 0.0001$ ). When the left eye was the dominant eye, the mean detection threshold for the left eye (-3.00 decibels, SE=0.39) was worse than the right eye (-2.83 decibels, SE=0.37), although not statistically significant ( $P = 0.29$ ).

In the linear mixed models these differences were evident by including an interaction term for eye x dominance which was significant ( $P < 0.001$ ,  $F = 11.29$ ).

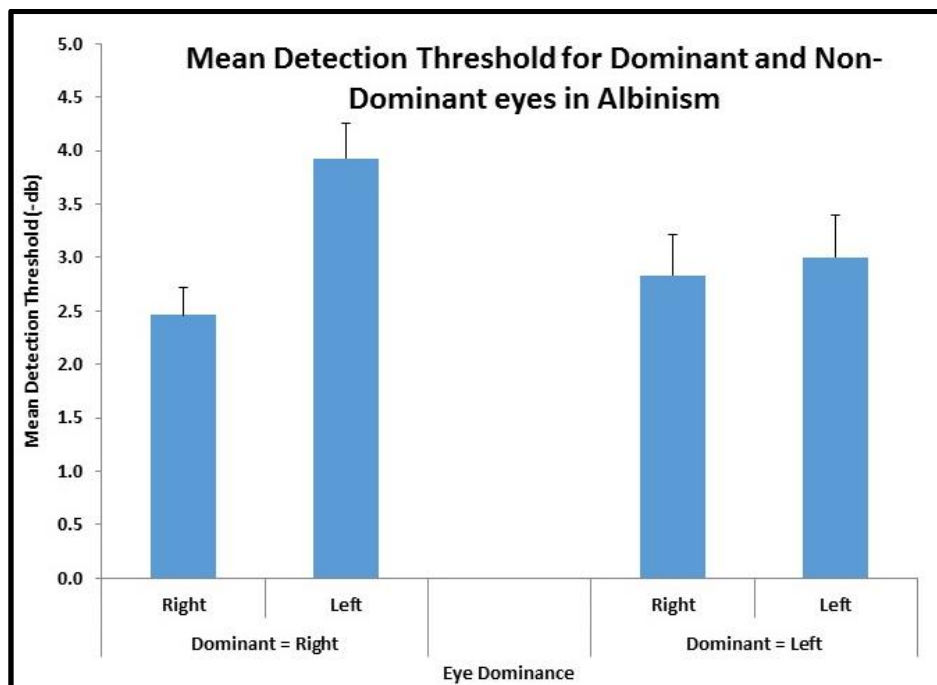


Figure 4-16: The mean detection threshold for the dominant and non-dominant eye in albinism. On the left hand side is a bar chart showing the mean detection threshold for the right and left eye when the right eye is the dominant eye. On the right hand side is a bar chart showing the mean detection threshold for the right and left eye when the left eye is the dominant eye. The error bars show the standard error of the mean.

### 4.3.6.2 Eye Dominance for Right and Left Eyes in IIN

Figure 4-17 shows the detection threshold for the IIN group for the right and left eye when dividing the groups into right dominant and left dominant. In the IIN group there were 17 right eye dominant individuals and 13 individuals who were left eye dominant. We were unable to determine dominance on 2 individuals with IIN.

In the IIN group when the right eye is dominant, the mean detection threshold for the right eye (-0.90 decibels, SE=0.34) was significantly better than the mean detection threshold for the left eye (-1.73 decibels, SE=0.41) ( $P=0.0002$ ). When the left eye is dominant, the mean detection threshold for the left eye (-2.03 decibels, SE=0.43) is slightly worse compared to the right eye (-2.00 decibels, SE=0.35) although the differences were not significant ( $P=0.90$ ).

In the IIN group the interaction term for eye x dominance in the statistical models was also significant ( $P=0.02$ ,  $F=6.51$ ).

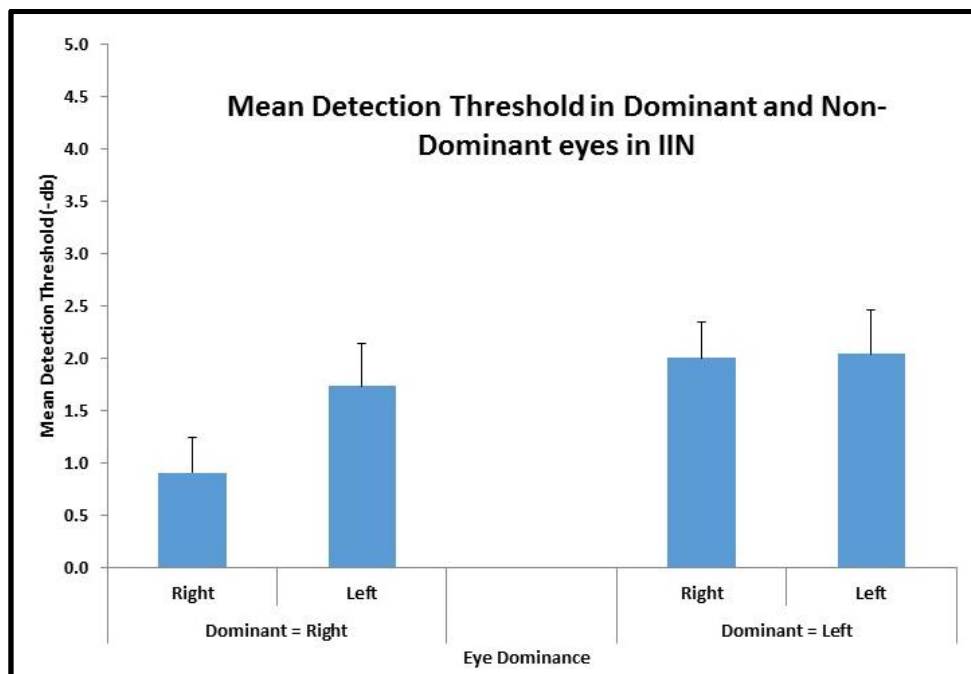


Figure 4-17: The mean detection threshold for the dominant and non-dominant eye in IIN. The left hand side shows the mean detection threshold for the right and left eye when the right eye is the dominant eye. The right hand side shows the mean detection threshold for the right and left eye when the left eye is the dominant eye. The error bars show the standard error of the mean.

### 4.3.6.3 Is a Difference in Visual Acuity Between the Eyes Associated with a Difference in Detection Threshold Between the Eyes?

Because albinism is associated with amblyogenic factors such as strabismus and anisometropia we have investigated relationship between amblyopia (differences in visual acuity between two eyes) and difference in VF sensitivity. We have also analysed these amblyogenic factors (strabismus and anisometropia) in the albinism group without amblyopia (<1 logMAR line difference).

#### 4.3.6.3.1 Albinism

**Figure 4-18** shows the difference in visual acuity between left and right visual acuity (LVA and RVA) plotted against the difference in VF sensitivity (average of four quadrants, excluding macular area) between the two eyes. The dominant eye was separated for this analysis.

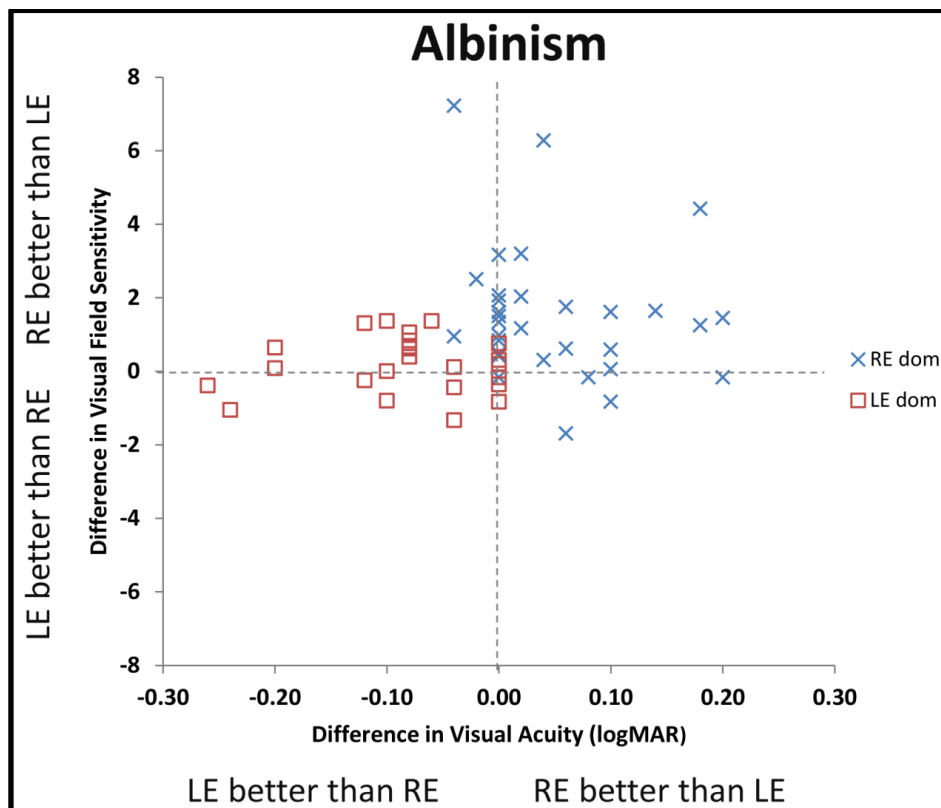


**Figure 4-18:** The difference in visual acuity plotted for both when the LVA is better than the RVA and vice versa against the visual field sensitivity when one eye is better than the other for albinism.

In the individuals with albinism who are right eye dominant (sighting dominance), the right visual acuity dominance (visual acuity better in right eye) shows a better VF sensitivity in the right eye. This pattern was not as clear when looking at those who were left eye dominant (sighting dominance), as left visual acuity dominance (visual acuity better in left eye) was confirmed however the VFs did not demonstrate this exclusively (some individuals demonstrated the right VF was better than the left VF even though the left eye was dominant and LVA better).

There was no obvious trend and no positive slope on the graph (right and left eye dominant data put together). This regression analysis found no significant relationship between difference in visual acuity and difference in VF in albinism ( $P=0.116$ ;  $r=0.207$ , 95% CI=-0.867 to 7.68).

#### **4.3.6.3.1.1 Do non-amblyopic individuals demonstrate amblyogenic factors?**

An interesting observation from the graph below reveals the individuals with albinism in our study only show amblyopia up to a maximum of 0.26 logMAR difference. A large number did not demonstrate a clinically significant difference between the two eyes (i.e. difference in visual acuity  $<0.1$  logMAR,  $n=41$  of 59 (69.5%)), with 20 showing equal visual acuity between the two eyes.

100% of the individuals with albinism who have a difference in visual acuity of  $>0.05$  logMAR ( $n=28$ ) show eye dominance in the same direction as the amblyopia. Interestingly, those who have little or no differences in visual acuity ( $\leq 0.05$  logMAR,  $n=31$ ) show predominantly right eye dominance (71.0% show right eye dominance).

#### **4.3.6.3.1.2 Amblyogenic factors**

Of the 41 individuals who did not demonstrate mild amblyopia or worse (defined as  $>0.1$  logMAR line difference), we assessed our records for results on strabismus and refractive

correction. 2/41 patients had missing data. We constructed a table showing the level of amblyogenic factors amongst the remaining 39 patients.

Interestingly, we found a very high incidence of amblyogenic factors in the patients who did not have clinical amblyopia. In total, 33/39 (85%) demonstrated either strabismus or anisometropia (difference in refractive error between the eyes). When dividing these further with eye dominance a similar pattern is seen. This is shown in **Table 4-4**. These findings indicate the differences seen between the eyes is not likely to be amblyopia.

	Right Eye Dominant		Left Eye Dominant		Total
	Equal VA	Subclinical Amblyopia	Equal VA	Subclinical Amblyopia	
<b>n</b>	<b>14</b>	<b>11</b>	<b>5</b>	<b>9</b>	<b>39</b>
<b>Anisometropia</b>	<b>4(29%)</b>	<b>2(18%)</b>	<b>0(0%)</b>	<b>1(11%)</b>	<b>7(18%)</b>
<b>Strabismus</b>	<b>7(50%)</b>	<b>9(82%)</b>	<b>4(80%)</b>	<b>8(89%)</b>	<b>28(72%)</b>
<b>Either</b>	<b>10(71%)</b>	<b>10(91%)</b>	<b>4(80%)</b>	<b>9(100%)</b>	<b>33(85%)</b>

**Table 4-4: Level of amblyogenic factors in individuals with albinism without clinical amblyopia (<0.1 logMAR line difference). (Right and Left eye dominant shown separately) VA=Visual Acuity.**

#### 4.3.6.3.1.3 Bilateral amblyopia

Bilateral amblyopia is defined as a bilateral reduction in visual acuity for both eyes worse than 0.2 logMAR (6/9.5 Snellen equivalent) (Taylor, Powell et al. 2012) and commonly there is a single cause for bilateral reduction in vision (e.g. congenital cataracts which may cause form deprivation amblyopia). Historically, amblyopia is defined as not being associated with retinal abnormalities although recent OCT findings have also highlighted some retinal changes such a reduction in pit depth in the horizontal meridian in amblyopic patients compared to non-amblyopic participants (Bruce, Pacey et al. 2013). In our patients with albinism it is difficult to separate the exact cause for the bilateral reduction of vision. Factors that clearly lead to a loss in high spatial frequency vision such as foveal hypoplasia, nystagmus and iris transillumination

are difficult to separate out from amblyopia that might result from these factors leading to form deprivation.

#### 4.3.6.3.2 IIN

**Figure 4-19** shows the difference in visual acuity between left and right visual acuity (LVA and RVA) plotted against the difference in VF sensitivity (average of four quadrants, excluding macular area) between the two eyes.

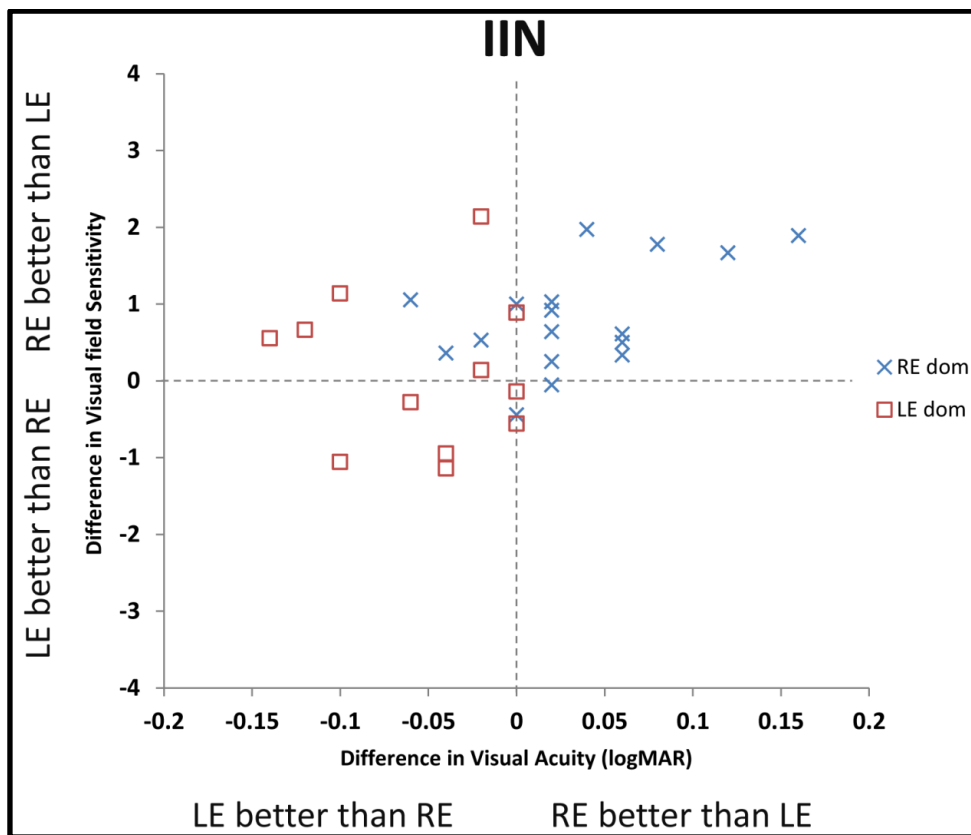


**Figure 4-19:** The difference in visual acuity plotted for both when the LVA is better than the RVA and vice versa against the visual field sensitivity when one eye is better than the other for IIN.

In the individuals with IIN who are right eye dominant (sighting dominance), generally the right visual acuity dominance (visual acuity better in the right eye) shows a better VF sensitivity in the right eye. This pattern again was more ambiguous for those who were left eye dominant

(sighting dominance) as left visual acuity dominance shows no preference for VF sensitivity in the two eyes.

When conducting a regression analysis for individuals with IIN (right eye dominant and left eye dominant together) we found a significant relationship between the difference in visual acuity and the difference in VF sensitivity ( $P=0.018$ ;  $r=0.43$ , 95% CI=1.108 to 10.685).

We see these eye differences follow through even when we consider eye dominance, visual acuity dominance and VF dominance. It appears patterns for the right eyes in albinism and IIN follow an expected path (e.g. right eye sighting dominance leads to RVA dominance and right eye VF dominance). However this is not the case for the left eye in albinism or IIN (e.g. left eye sighting dominance leads to LVA dominance but a mixture of right/left eye VF dominance).

### 4.3.7 Visual Field Comparisons to VEP Asymmetry and BCVA in Albinism

Previous literature from Hoffman et al (2007) found no relationship between level of asymmetry seen on VEP compared to temporal and nasal VF asymmetries in 15 individuals with albinism. We have explored this issue again as well as comparing the upper nasal VF abnormalities in albinism to VEP patterns. We used the asymmetry index (AI) as our measure of VEP asymmetry as outlined in **Chapter 2** (methodology). We also compared VF deficit to BCVA (best corrected visual acuity from either right or left eye) to assess for any relationship between level of visual acuity and VF differences encountered. Pearson's Correlations are shown in **Table 4-5**.

Nasal/Temporal VF differences for each eye was calculated to give this entity a value using this equation:

$$\text{Nasal/Temporal Asymmetry} = \frac{\text{Nasal}}{\text{Nasal+Temporal}}$$

The upper nasal VF deficit compared to other quadrants was also calculated using the equation:

$$\text{Upper Nasal VF Deficit} = \frac{\text{Upper nasal detection threshold}}{\text{Sum of all other quadrants detection threshold}}$$

Correlations are shown on the next page.

**Correlations**

		AI (VEP)	BCVA
NT asymmetry right eye	Pearson Correlation	0.043	-0.136
	Sig. (2-tailed)	0.777	0.303
	n	46	59
NT asymmetry left eye	Pearson Correlation	0.300*	-0.059
	Sig. (2-tailed)	0.043	0.658
	n	46	59
Degree of Upper Nasal Field deficit Right eye	Pearson Correlation	-0.067	-0.16
	Sig. (2-tailed)	0.657	0.225
	n	46	59
Degree of Upper Nasal Field deficit Left eye	Pearson Correlation	0.336*	-0.119
	Sig. (2-tailed)	0.022	0.367
	n	46	59

**Table 4-5 : Pearson’s correlations are shown for comparisons of VEP asymmetry index (AI) and BCVA compared to nasal/temporal asymmetry and upper nasal quadrant asymmetry measure seen in albinism (eye separately). NT=Nasal/Temporal, AI=Asymmetry Index, BCVA=Best Corrected Visual Acuity.**

There were no significant correlations between VEP asymmetry and VF (nasal/temporal) asymmetry for the right eye (P=0.777, r=0.043). However, the VEP asymmetry and VF (nasal/temporal) asymmetry for the left eye revealed a significant positive correlation (P=0.043, r=0.300).

There is no significant correlation between VEP asymmetry and upper nasal quadrant asymmetry for the right eye (P=0.657, r=-0.067). However the left eye shows a significant positive correlation between VEP asymmetry and upper nasal quadrant asymmetry (P=0.022, r=0.336).

There were no significant correlations for all comparisons with BCVA.

## **4.4 Discussion**

### **4.4.1 Summary of Findings**

We describe for the first time a novel visual field deficit found in albinism, with the detection threshold in the upper nasal VF quadrant being significantly worse compared to the other three quadrants (the upper temporal, lower nasal and lower temporal) of the VF. This is the first time this type of VF defect has been reported in albinism and could underlie the significant nasal/temporal differences reported in previous studies and in our study as well.

Another novel finding was that the average detection threshold for the left eye was significantly worse than the right eye, more so in albinism compared to IIN. Reasons for this were investigated with eye dominance proving a decisive factor in both albinism and IIN. When assessing the relationship between visual acuity eye differences and VF difference between the eyes, there was no significant relationship underlying the differences in albinism. However, in IIN a significant relationship was found for both eyes.

We also demonstrated significant correlations between level of VEP asymmetry using Apkarian's method and nasal/temporal asymmetry and upper nasal quadrant differences for the left eye. There were no significant correlations for the right eye.

### **4.4.2 Nasal/Temporal Asymmetry**

We found a significant difference between the nasal and temporal VF for the albinism group ( $P=0.0075$ ), however this difference was not found within the IIN group ( $P=0.3854$ ). This agrees with previous findings by St John and Timney (1981) who found nasal/temporal asymmetry in a sub group (worst affected participants) of their albinism patients. On the contrary, other authors have found no differences exist using other methods of VF assessment (Abadi and Pascal 1993, Hoffmann, Seufert et al. 2007). Abadi and Pascal (1993) using Goldman visual field

(kinetic perimetry), and Hoffman et al (2007) using Octopus visual field (static perimetry) found no nasal/temporal asymmetry within their albinism groups. However, all of these previous studies used a smaller number of patients with albinism (maximum n=15) in comparison to that used in our current study (61 individuals with albinism and 32 with IIN).

We believe our findings suggest that chiasmal misrouting is further represented within the visual pathway and that it has an effect on VF and detection threshold. We correlated VEP asymmetry with nasal/temporal asymmetry and found a weak but significant positive correlation for the left eye ( $P=0.043$ ) but not the right eye ( $P=0.777$ ). As the left eye had a significantly worse detection threshold it is possible that only the most affected eye was sensitive enough to detect this asymmetry. St John and Timney (1981) describe this nasal/temporal defect may only be visible in the most severely affected patients.

### **4.4.3 Upper Nasal Visual Field Defect in Albinism**

We found the detection threshold in the upper nasal VF was significantly poorer in comparison to all other quadrants in the albinism group.

The VEP asymmetry was also correlated to the upper nasal VF detection threshold for the left eye ( $P=0.022$ ): this was more significant than the VEP and nasal/temporal detection threshold correlations indicating that there appears a vertical element to the asymmetry. There was no significant correlation for the comparison of VEP asymmetry to upper nasal VF detection threshold for the right eye ( $P=0.657$ ).

A previous study by Bhansali et al (2014) in pigmented and albino mice highlight a possible reason for the upper nasal visual field deficit observed in our participants with albinism. They describe the timing of melanin formation in pigmented mice coincides with the onset of retinal ganglion cell production, and postulate, therefore, that defects in melanin biosynthesis in albinism influence the pace of retinal ganglion cell formation and specification of retinal

ganglion cell population. They also demonstrate that the ventrotemporal retinal ganglion cells are specifically affected in albino mice causing an imbalance in ipsilateral and contralateral projecting retinal ganglion cells (Bhansali, Rayport et al. 2014). The closest equivalent retinal area in humans is likely to be the inferior temporal retina which would be associated with the upper nasal visual field deficits we see in humans with albinism. However, this comparison should be treated with caution as the pathway of retinal ganglion cells and their axons along the optic tract take a very different route in mice compared with humans (see page 50).

A study by Mohammad et al (2015) also found a nasal/temporal as well as a subtle vertical difference in ppRNFL thickness between albinism and controls. Individuals with albinism were found to have significantly thinner ppRNFL temporally compared to nasally when compared to controls. They also found significant differences in vertical ppRNFL thickness (superior thinner than inferior) between albinism and controls. These specific thinning patterns in ppRNFL are likely to be due to localised loss of specific retinal ganglion cells entering the optic nerve (Mohammad, Gottlob et al. 2015).

Cortical reorganisation that takes place in albinism may provide a further insight into a possible reason for this finding (theories discussed in **Section 1.7.2.4**). This would indicate the changes noted are related more to higher order processing.

#### **4.4.4 Right-Left Eye Differences and Eye Dominance**

The detection threshold for the right and the left eye in albinism shows the left eye in albinism performed significantly worse than the right eye ( $P=0.0001$ ), this was same in IIN ( $P=0.01$ ).

There is very little evidence in the literature of right-left asymmetry noted within albinism and IIN. However, a study by Mohammed et al (2015) found the ppRNFL was actually significantly thicker in an annulus 2.4 to 3.2mm diameter around the optic nerve in the right eyes of individuals with albinism compared to the left eyes ( $P=0.001$ ) (not related to eye dominance).

This may indicate that the thickness of ppRNFL could possibly be related to our findings of eye differences and this is explored further in **Chapter 5 (Study 3)**. Within the literature there are a number of studies highlighting right and left eye differences also exist in normals and is based on laterality that we see in the general population (Seyal, Sato et al. 1981, Choi, Kim et al. 2014).

#### **4.4.5 Mechanisms behind VF Deficits in Albinism**

In explaining the specific VF deficits (nasal/temporal asymmetry and upper nasal VF<other quadrant asymmetry), refractive errors, nystagmus or iris transillumination are unlikely to lead to localised VF defects described in our patients as both are likely to cause an overall reduction in visual sensitivity rather than specific VF defects we have observed. The localised VF defects we have encountered are most likely caused by:

1. Localised retinal abnormalities
2. Projection abnormalities – misrouting of the optic nerves at the chiasm affecting connectivity through to the LGN
3. Reduced cortical input and/or cortical reorganisation

In the following chapter OCT has been used to investigate whether structural changes in the retina provide any clues to these localised VF areas of interest to assess for any significant associations which may improve our understanding as to the origin of these defects.

## 4.5 Study Limitations

This study was carried out both prospectively and retrospectively with the aim of acquiring a large dataset of patients with albinism and IIN. Participants were either recruited on their first clinic appointment or patient's results were obtained as VFs were completed as part of a baseline prior to a trial carried on the effects of medication on nystagmus. Using this method of patient recruitment it was decided to conduct the VF in the same way for all patients. However, this resulted in all participants having the right eye tested first, followed by the left eye. Interestingly, even though a process of 'learning' could have aided the performance of the left eye, the left eye actually performed significantly worse in the albinism and IIN group. There was also the potential of participants becoming fatigued during their VF examination and thus performing worse when their second eye was assessed.

We must also consider the degree of nystagmus. This was not analysed for our dataset as this was not the primary aim of our study. Further analysis looking at the eye movement measures (frequency, amplitude and intensity) in comparison to VF detection threshold could provide further evidence as to why certain individuals performed better than others. Although this could be a potential cause, previous literature has stated that the nystagmus is similar in both albinism and IIN (Kumar, Gottlob et al. 2011). Similar to iris transillumination and refractive errors, nystagmus is unlikely to lead to localised changes in VF but may interact with localised changes with motion sensitivity in the retina caused by albinism or IIN.

Another limitation of our study was the presence of positive angle kappa in our patient groups. Previous work by Brodsky and Fray (2004) found 95% (20/21) of his albinism patients had a positive angle kappa in at least one eye in comparison to 33% (4/12) in IIN (Brodsky and Fray 2004). In response to a previous study looking at the VFs in albinism (Hoffmann, Seufert et al. 2007), Brodsky (2008) postulated that the consequence of a positive angle kappa is that visual field perimetry would show a larger area of temporal field and a smaller area of nasal field in

humans with albinism than in individuals without albinism (Brodsky 2008). A positive angle kappa would also have implications for our study because any area of crossed temporal retina that lies nasal to the fixation point would correspond to temporal rather than nasal VF using our method of static perimetry.

## **4.6 Future Studies/Following Chapter**

As a follow on from this study, we compare foveal and optic nerve OCT's on all patients to VF measures. This is to compare central VF to foveal abnormalities and VF quadrant patterns to RNFL thickness around the optic nerve. In glaucoma it has been found that RNFL changes around the optic nerve often impact upon an individual's VF (Galvao Filho, Vessani et al. 2005, Horn, Mardin et al. 2009, Bussel, Wollstein et al. 2014). Previous literature by Mohammed et al (2015) has also described specific changes in ppRNFL in albinism compared to controls so there is a possibility that these changes may be related to localised VF changes.

# Chapter 5

## The Comparison of Central and Peripheral Visual Field to Foveal and Optic Nerve OCT Parameters in Albinism (Study 3)

# Chapter 5 The Comparison of Central and Peripheral Visual Field to Foveal and Optic Nerve OCT Parameters in Albinism (Study 3)

## 5.1 Introduction

Following on from **Chapter 4**, we investigate how the structure of the fovea and ppRNFL thickness around the optic nerve relate to VF (detection threshold) changes. We aim to provide an insight into the cause of VF deficits found in albinism.

### 5.1.1 Foveal Hypoplasia in Albinism

Previous literature has distinguished relationships between foveal hypoplasia and visual acuity in albinism. A study by Mohammed et al (2011) identified a highly significant correlation between the cone outer segment layer and visual acuity (Mohammad, Gottlob et al. 2011). From this finding it is clear that structural changes in the retina relate to functional measures of vision. It would be of particular interest to investigate whether foveal layers have any correlation to VF (detection threshold) to indicate whether retinal deficits underlie the central VF deficits.

### 5.1.2 Optic Nerve Findings in Albinism

#### 5.1.2.1 Optic Nerve Structure

Mohammad et al (2015) have assessed the optic nerve structure in albinism using OCT and also compared ppRNFL distribution around the optic nerve in this cohort to controls. (Mohammad, Gottlob et al. 2015). This is illustrated in **Figure 5-1**.

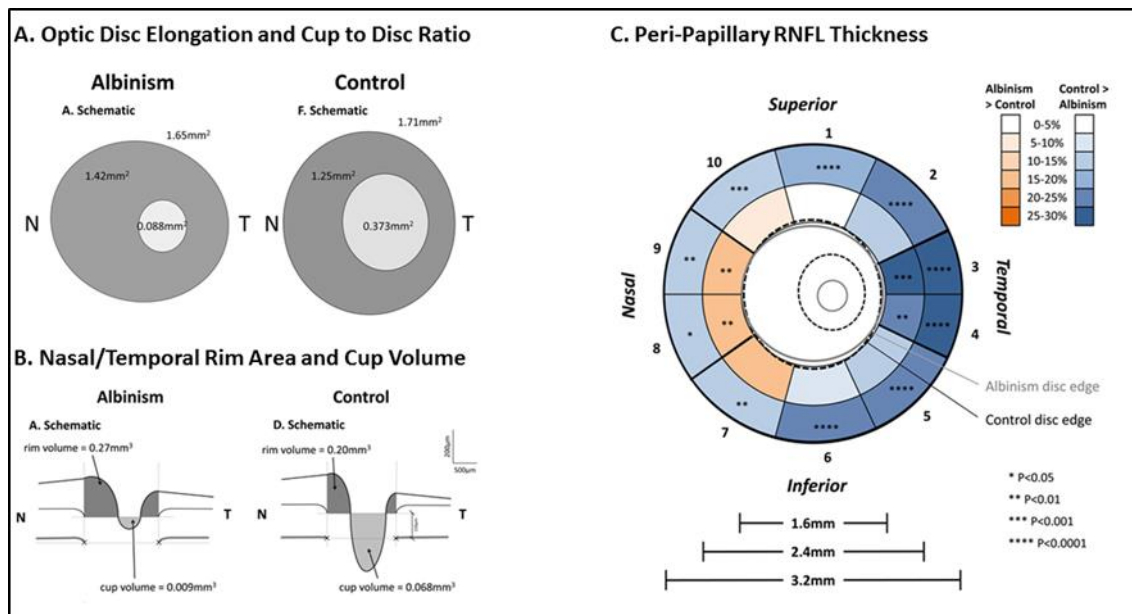


**Figure 5-1: Optic nerve differences between individuals with albinism and controls. (A) Shows optic disc elongation and the cup to disc ratio. (B) Shows the nasal/temporal rim areas and the optic cup volume. (C) Differences in peri-papillary RNFL (ppRNFL) thickness. Reproduced from Mohammad et al (2015).**

The authors found the optic disc was significantly elongated horizontally in the albinism cohort ( $P<0.001$ ) compared to age matched controls. A highly significant difference was found when comparing the area of optic cup in the albinism cohort ( $0.088\text{mm}^2$ ) to the area of the optic cup in controls ( $0.373\text{mm}^2$ ) ( $P<0.001$ ). The optic cup in albinism was only 23.7% the size of the optic cup in controls. Interestingly, 39.4% of eyes in the albinism group did not demonstrate a measureable optic cup. The ppRNFL was significantly thinner in the albinism cohort compared to controls ( $P<0.001$ ) especially within the temporal area.

### 5.1.2.2 Retinal Nerve Fibre Layer (RNFL)

The RNFL is made up of axons of retinal ganglion cells (RGC). The axons are organised into bundles which extend from the periphery of the retina to the optic nerve. These bundles usually have a very specific course so that the RGC pass into localised areas of the optic nerve.

The areas more densely populated with RGC are the origin of thicker ppRNFL for example around the papillomacular fibres which originate from the macular region.

This study compares the ppRNFL thickness around the optic nerve to the corresponding areas on the VF (separate quadrants) to assess whether structural deficits in ppRNFL relate to functional deficits in VF.

When associating the VF (detection threshold) results to the ppRNFL thickness around the optic nerve, it is important to remember that VF results are inverse of the area it corresponds to around the optic nerve. Hence the upper nasal VF would correspond to the structure of ppRNFL at the inferior temporal area of the optic nerve.

### **5.1.2.3 Previous Analysis Methods for RNFL and VF Location**

There appears a longstanding debate on the exact relationship between VF locations and corresponding regions of the ppRNFL around the optic nerve. Attempts were made to assess this relationship in humans using histology (Wirtschafter, Becker et al. 1982) and computerised methods (Garway-Heath, Poinoosawmy et al. 2000) with limited success. Garway-Heath et al (2000 & 2002), Harwerth et al (2007 & 2010), Wheat et al (2012) and Medeiros et al (2012) propose methodologies used within their studies assessing individuals with glaucoma (Garway-Heath, Poinoosawmy et al. 2000, Garway-Heath, Holder et al. 2002, Harwerth, Vilupuru et al. 2007, Harwerth, Wheat et al. 2010, Medeiros, Zangwill et al. 2012, Wheat, Rangaswamy et al. 2012).

**Figure 5-2** demonstrates theories on the relationship between localised VF area and OCT ppRNFL area (RGC thickness) used in previous studies. Garway-Heath et al (2000 and 2002) based their estimations on anatomy and have divided the VF up into six localised segments based on this. Harwerth et al (2007 and 2010) attributed their estimations on ppRNFL OCT and

VF comparisons in glaucoma and Wheat et al (2012) followed this up with a further correction for a simplified VF comparison to RNFL area.

Initially, Harwerth et al (2007) divided the ppRNFL into ten segments around the optic nerve, they revised this considerably though due to participant variability on VF performance and because the optic nerve supplies far more than 24° around the fovea, which is all that is recorded on the VF. To reduce error they felt a generalised model was most suitable (Harwerth et al (2010) model). Wheat et al (2012) followed this up with a further point correction which allowed disease progression to be taken into account from the glaucoma data and allow a significant correlation to be found between RNFL area and VF performance. Medeiros et al (2012) simplified this again by splitting the optic nerve and VF into 2 segment for the purpose of their study to reduce further error.

These studies indicate the likelihood of high participant variability when conducting a VF examination and also expose the difficulty in correlating specific areas of ppRNFL around the optic nerve to VF.

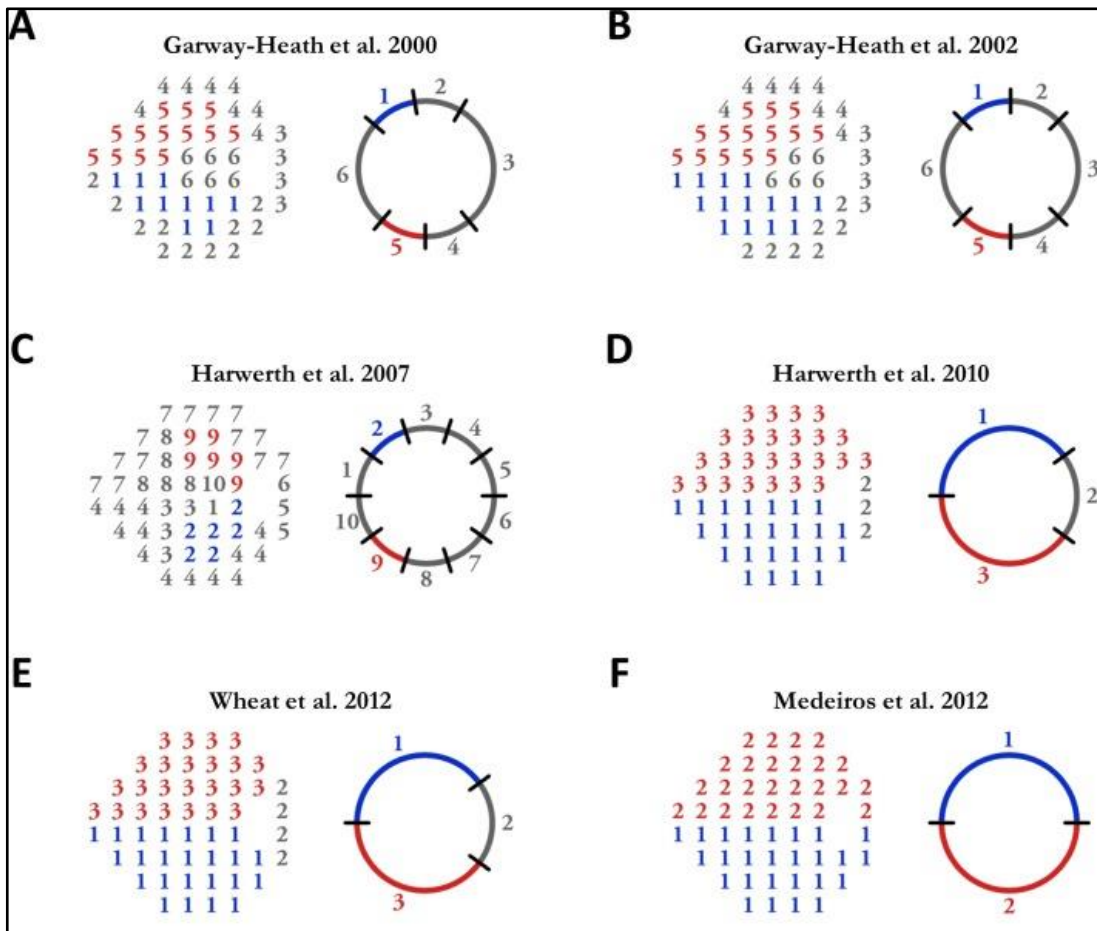


Figure 5-2: The prediction of visual field locations and their relationship to the specific area of the optic nerve when considering retinal ganglion cell entrance into the optic nerve. Reproduced from Raza and Hood (2015).

The OCT Copernicus divides the ppRNFL thickness into ten measurements around the optic nerve. We then grouped the equivalent ppRNFL anatomical areas as shown by Garway-Heath et al (2002) to best match our pre-determined VF quadrants and macular area. An explanation of methodology is discussed within **Section 5.2.1.2.4**.

## 5.1.3 Aims and Rationale

The main aims of this study are to address whether there are structure to function correlations between OCT (fovea and optic nerve) measures and our novel VF findings to aid our understanding of the outcomes from **Study 2**.

### 5.1.3.1 Aim 1

To correlate central VF detection threshold to foveal thickness at the fovea and macular region in albinism.

### 5.1.3.2 Aim 2

To correlate central and peripheral detection threshold (VF) to retinal nerve fibre layer thickness around the optic nerve in albinism.

## 5.1.4 Hypotheses

These are the two main hypotheses to be addressed in **Study 3**:

- The degree of foveal hypoplasia will correlate with central VF detection threshold
- The nasal/temporal VF asymmetry and upper nasal VF defect will correlate with ppRNFL differences around the optic nerve

## 5.2 Methodology for Study 3

All participants who were enrolled into the VF study (**Chapter 3**) also had OCT imaging (fovea and optic nerve).

### 5.2.1 Imaging and Analysis

#### 5.2.1.1 Foveal OCT Imaging

Foveal OCT imaging has been described in the methods section (**Chapter 2**).

For analysis a point measurement was used (see **Chapter 2** for description) as well as a macular area measurement (explained in **Section 5.2.1.1.1**). 99 eyes with albinism were included within the analysis.

##### 5.2.1.1.1 Foveal OCT Analysis

The retinal layers were subdivided into inner retina (4 layers) and outer retina (4 layers). The inner retina comprised of the retinal nerve fibre layer (RNFL), ganglion cell layer (GCL), inner plexiform layer (IPL) and the inner nuclear layer (INL). The outer retina was made up of the outer plexiform layer (OPL), the outer nuclear layer (ONL), the inner segment (IS) and the outer segment (OS). All foveal scans were analysed at the fovea (0°) and an area analysis from -892µm to +892 µm (central 6° of VF). Each foveal layer was manually delineated using an Image J custom written script (National Institutes of Health, Bethesda, MD; available at: <http://rsbweb.nih.gov/ij/>; accessed November, 2013). The text file output generated by the script was then imported into an Excel macro (Microsoft corp.,) to provide thickness measures of each separate foveal layer at the fovea and an area measure of the macular region. This foveal analysis method is shown in **Figure 5-3**.

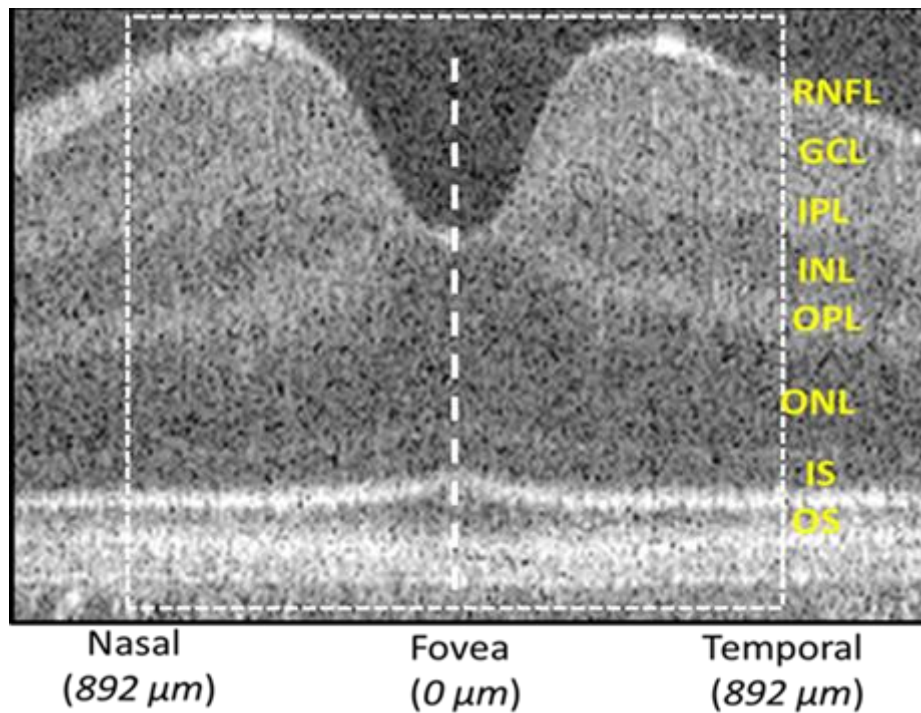


Figure 5-3: Analysis for each foveal OCT image. A point thickness measure was taken at the fovea as shown by the hatched line. An area layer thickness measure is taken within the hatched box as shown (892μm nasally to 892 μm temporally). Retinal nerve fibre layer (RNFL), ganglion cell layer (GCL), inner plexiform layer (IPL) and the inner nuclear layer (INL). The outer retina was made up of the outer plexiform layer (OPL), the outer nuclear layer (ONL), the inner segment (IS) and the outer segment (OS).

The association between the macular region from VF and OCT area is shown **Figure 5-4** on the next page.

### 5.2.1.1.2 Association between Macular Region (VF) and OCT

Figure 5-4 illustrates the VF area that corresponds to the OCT measure (central 6° from the VF corresponds to the same macular region on the OCT). Correlations were performed between the detection threshold for the macular region (4 points averaged) and fovea point measurements and the macular region OCT thickness measurements.

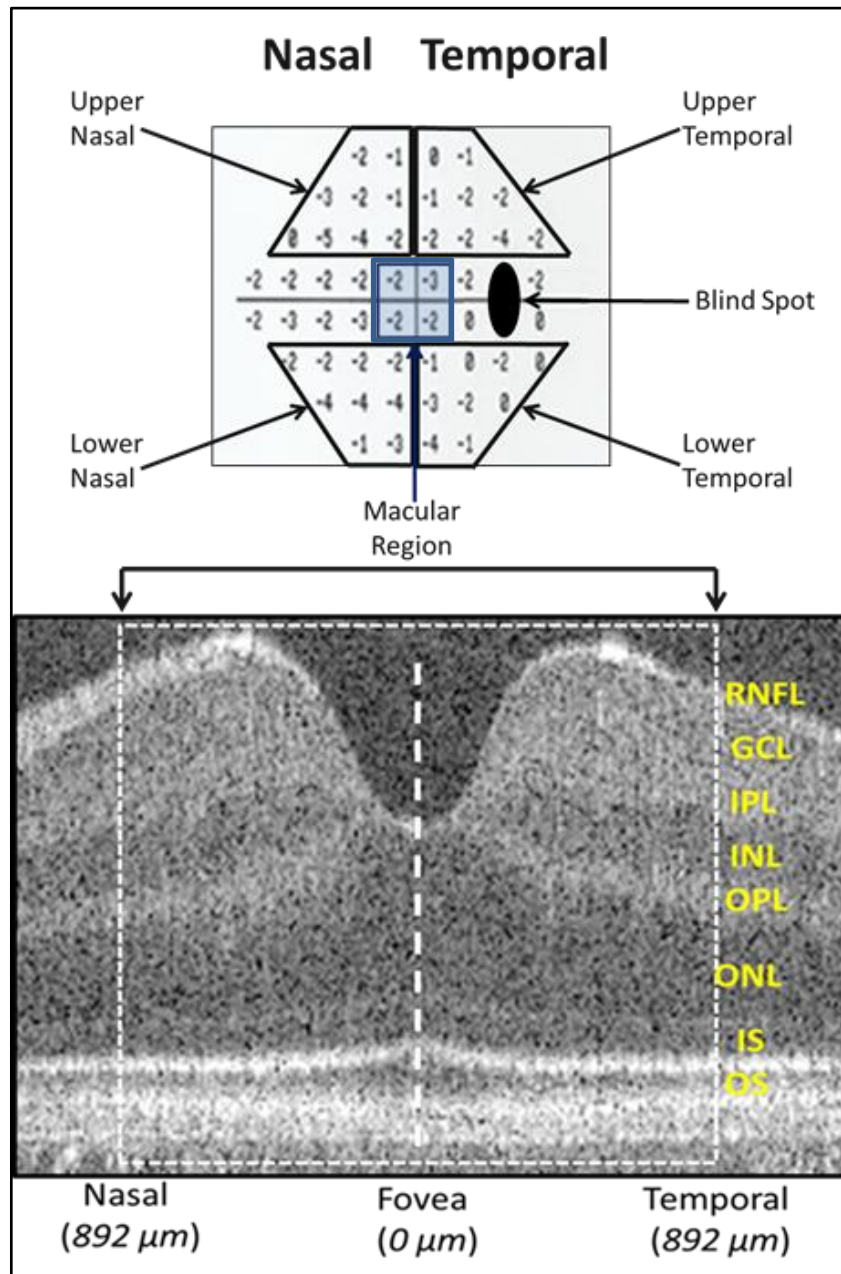


Figure 5-4: The macular region (blue box) on the visual field results and its corresponding area on the OCT image (hatched box).

### 5.2.1.2 ppRNFL OCT Imaging

The scanning protocol was a 7mm X 7mm scan comprising of 743 A scans and 75 B scans. 71 eyes with albinism were used in the analysis. Optic nerve scans for some participants were not used due to missing areas of scan and the inability to motion correct the full ppRNFL area around the optic nerve for analysis.

#### 5.2.1.2.1 ppRNFL Analysis

ppRNFL analysis was carried out on all scans if the full extent of the optic nerve could be distinguished. Due to nystagmus and motion artefact seen en-face it was important to realign all B-scans for accurate automated analysis. Firstly we obtained all scans for patients within our dataset. We then realigned all B-scans as shown below (**Section 5.2.1.2.2**). The realignment of B-scans was performed by author (VS) (56/71) and by Zhanhan Tu (15/71) on the albinism images. RNFL analysis was done by author (VA) for 56/71 eyes in albinism. Data previously analysed by SM was also used to complete the dataset (15/71 eyes) (Mohammad, Gottlob et al. 2015).

#### 5.2.1.2.2 Motion Correction/Realignment of B-scans

The OCT images for all participants with albinism required realignment of the B-scans due to nystagmus. This realignment was done by comparing OCT scans with the contours of retinal vessels and disc margins from fundus photographs. A macro made in image J was used. (<http://imagej.nih.gov/ij/>; provided in the public domain by the National Institutes of Health, Bethesda, MD, USA). The macro allowed each B-scan to be shifted horizontally until it matched the fundus photo. Realignment of B-scans was not possible in all scans. An example of the process is shown in **Figure 5-5**.

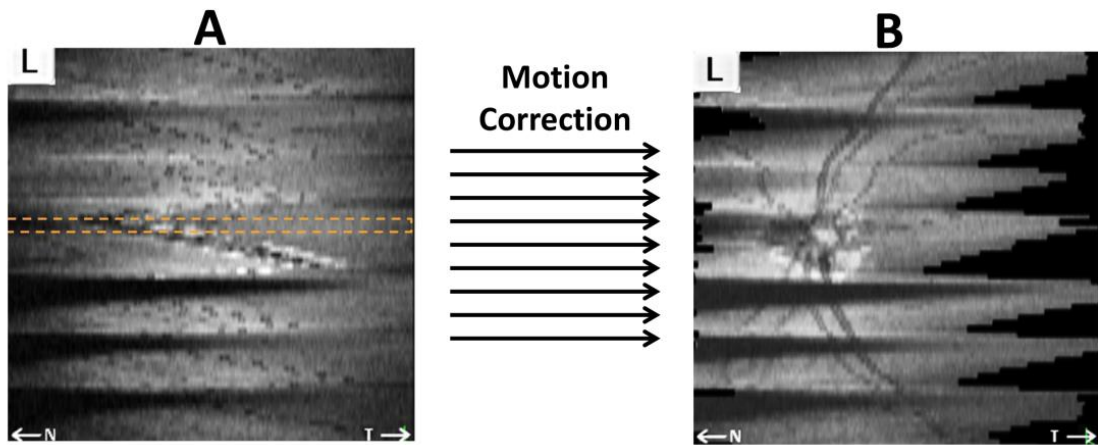


Figure 5-5: This image shows how image A required realignment of each individual B-scan by moving each B-scan in the correct position so the optic nerve and its branching vessels could be seen in the realigned image (image B). The realignment of B-scans was not possible for a large number of scans due to a high frequency nystagmus and thus an inability to accurately realign the B-scan to allow full optic nerve RNFL analysis.

### 5.2.1.2.3 ppRNFL Analysis

Once the realignment of B-scans is complete, the next step is to apply automated ppRNFL analysis. The SOCT Copernicus software attempts to automatically detect ppRNFL thickness but due to infrequent problems in the analysis every B-scan was double checked and the measurement adjusted manually if required. The ppRNFL thickness was measured around the annulus 2.4 to 3.2mm in diameter which was subsequently divided into ten segments (using the GDx Nerve Fiber Analyzer protocol, Carl Zeiss Meditec). This process is shown in **Figure 5-6** on the next page.

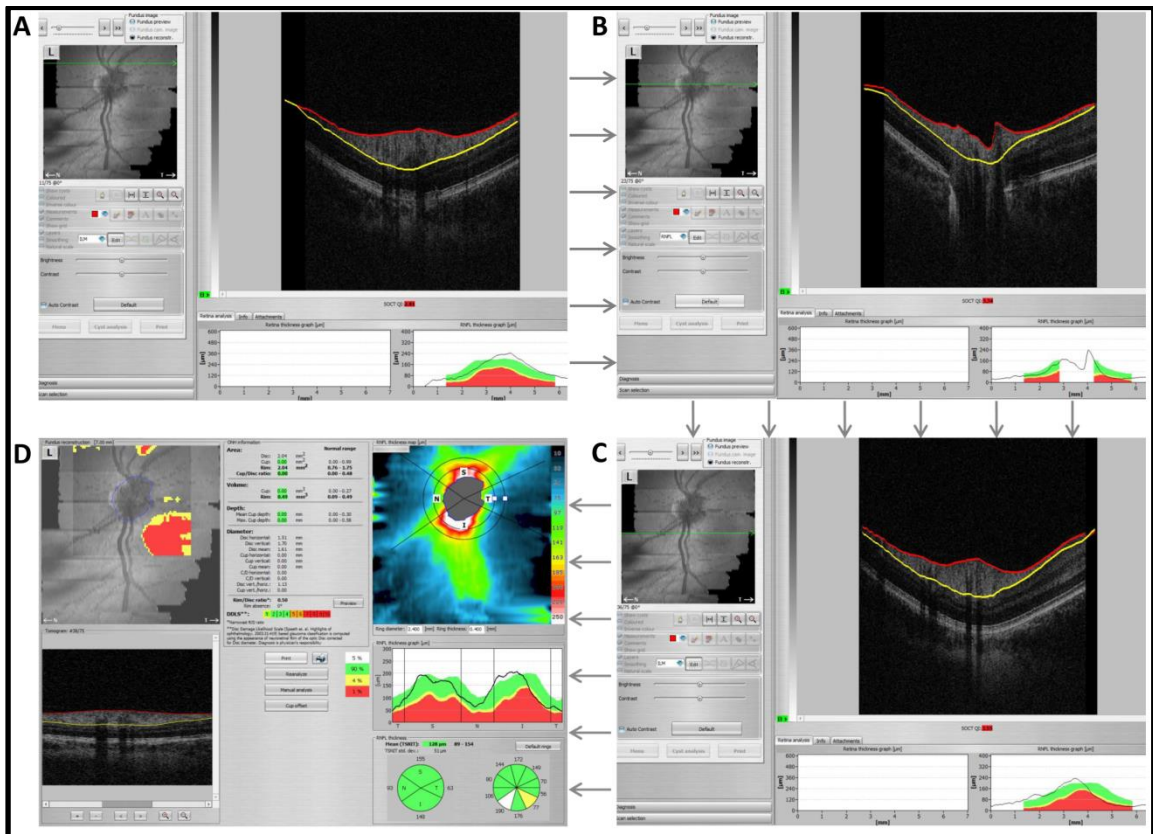


Figure 5-6: RNFL analysis: Images A, B and C show the RNFL analysis and image D shows the final results. (A) Shows the RNFL analysis for the superior area of the optic nerve (B) shows the RNFL analysis for the central cut through the optic nerve and (C) shows the RNFL analysis for the inferior portion of the optic nerve. The red and yellow lines measure the thickness of the RNFL and can be manually adjusted when required. Image (D) provides the full RNFL analysis. For RNFL analysis we were interested in the area at the bottom right of (D) which shows the RNFL thickness for superior, inferior, nasal and temporal RNFL.

### 5.2.1.2.4 RNFL Area compared to VF Location

The next step of the analysis is to correlate the correct quadrant of the VF to its corresponding area around the optic nerve. The automated RNFL analysis divides the RNFL thickness into ten separate sectors (Figure 5-7). These were divided according to the scheme shown in Figure 5.8 to compare with the four differently located quadrants and the macula.

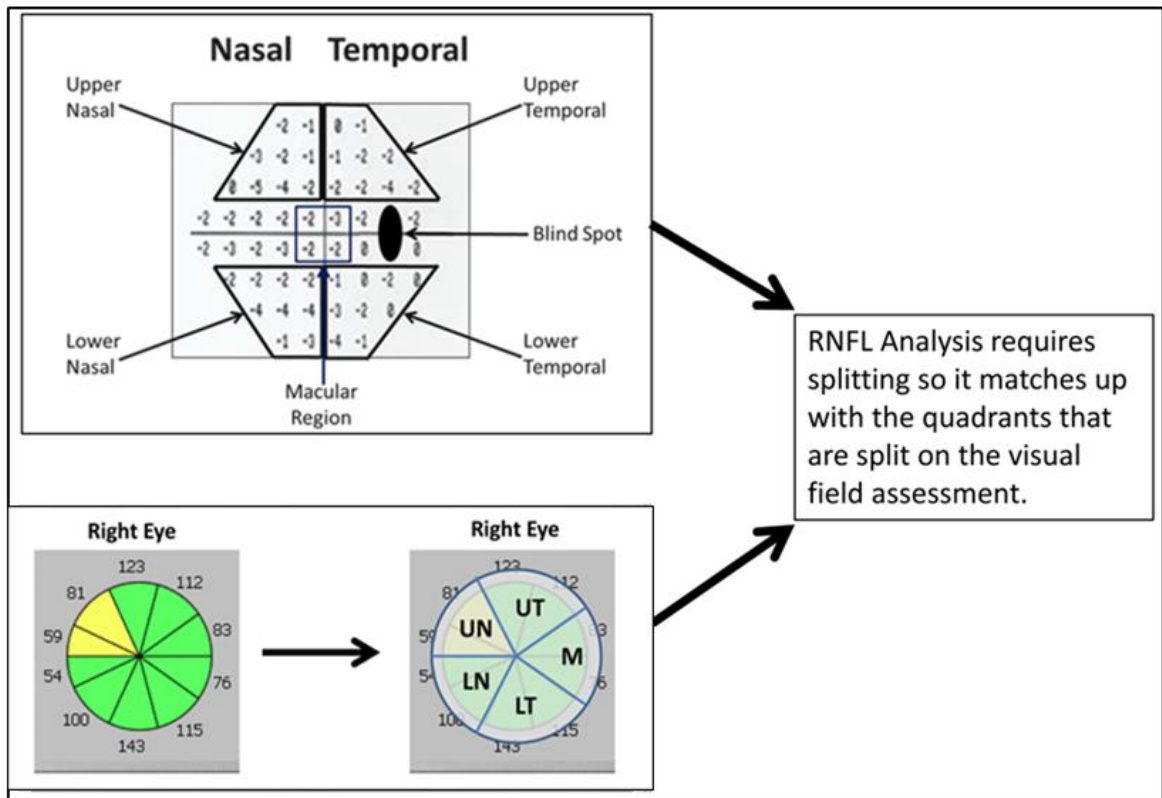


Figure 5-7: Top=Visual field divided into different quadrants. Bottom=ppRNFL analysis from SOCT Copernicus and how this was divided for correlations.

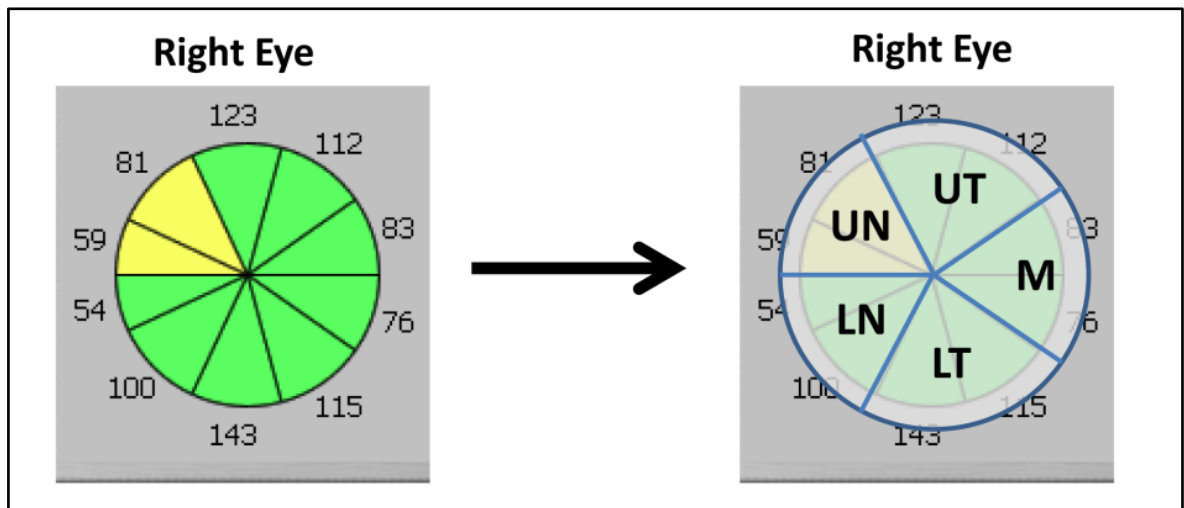


Figure 5-8: The ppRNFL was split into separate areas which correspond to entrance of retinal ganglion cells into the optic nerve. UT=upper temporal, UN=upper nasal, LN=lower nasal, LT=lower temporal and M=Macula. Note: this is opposite to the visual field.

### 5.2.1.3 Statistical Tests Used

As the data was normally distributed we used a linear regression analysis and Pearson correlation for foveal and ppRNFL correlations with VF parameters. Right and left eyes were treated separately for ppRNFL comparisons.

## 5.3 Results

### 5.3.1 Foveal OCT Correlation with Central Detection Threshold

#### 5.3.1.1 Correlations in Albinism

We correlated the central detection threshold (4 points averaged) to 8 foveal layers at the fovea (point measurement) and the macular region (area measurement) for 99 eyes in albinism (right and left eye combined). For the inner retinal layers we found significant negative correlations for the RNFL at the fovea ( $P=0.002$ ) and in the macular region ( $P=0.001$ ) as well as the INL at the fovea ( $P=0.005$ ). For the outer retinal layers there were significant positive correlations for the ONL at the fovea ( $P=0.001$ ) and in the macular region ( $P=0.003$ ) and the OS at the fovea ( $P=0.005$ ).

These correlations demonstrate thicker inner retinal layers are associated with poorer detection thresholds and thicker outer retinal layers are associated with better detection thresholds.

Pearson's correlations are shown in **Table 5-1**.



### 5.3.2 Correlation of Detection Threshold to RNFL Thickness for Right and Left Eye

Correlations are shown for albinism groups in right and left eyes. We found no significant correlations between detection thresholds in four VF quadrants and corresponding ppRNFL segments for the right and left eyes. The ppRNFL adjacent to the macula correlated with central foveal detection threshold ( $P=0.034$ ,  $r=0.358$ ) and upper temporal VF ( $P=0.037$ ,  $r=0.355$ ) in the left eye only (Table 5-2).

Visual Field Area		Optic Nerve RNFL Segment				
		Macula RNFL n=36	Upper Temporal RNFL n=36	Upper Nasal RNFL n=36	Lower Nasal RNFL n=36	Lower Temporal RNFL n=36
Upper Temporal	p	0.849	0.62	0.352	0.874	0.49
	r	-0.033	0.085	-0.16	0.027	-0.119
Upper Nasal	p	0.862	0.196	0.929	0.769	0.856
	r	-0.03	0.22	-0.015	-0.051	-0.031
Lower Temporal	p	0.779	0.407	0.093	0.951	0.485
	r	0.049	0.143	-0.284	0.011	-0.12
Lower Nasal	p	0.641	0.858	0.354	0.364	0.395
	r	-0.08	0.031	-0.159	0.156	-0.146
Nasal	p	0.711	0.434	0.549	0.7	0.546
	r	-0.064	0.134	-0.103	0.066	-0.104
Temporal	p	0.964	0.475	0.16	0.904	0.452
	r	0.008	0.123	-0.239	0.021	-0.13
Central Fovea	p	0.574	0.235	0.565	0.904	0.888
	r	0.097	0.203	-0.099	-0.021	0.024
Total VF Average	p	0.881	0.445	0.291	0.804	0.484
	r	-0.026	0.131	-0.181	0.043	-0.121

Visual Field Area		Optic Nerve RNFL Segment				
		Macula RNFL n=35	Upper Temporal RNFL n=35	Upper Nasal RNFL n=35	Lower Nasal RNFL n=35	Lower Temporal RNFL n=35
Upper Temporal	p	0.037	0.18	0.419	0.886	0.113
	r	0.355	0.232	0.141	-0.025	0.273
Upper Nasal	p	0.261	0.414	0.275	0.351	0.258
	r	0.195	0.143	0.19	0.162	0.196
Lower Temporal	p	0.201	0.337	0.961	0.395	0.891
	r	0.221	0.167	0.009	-0.148	0.024
Lower Nasal	p	0.234	0.3	0.428	0.724	0.785
	r	0.207	0.18	0.138	0.062	0.048
Nasal	p	0.218	0.323	0.319	0.502	0.466
	r	0.214	0.172	0.173	0.117	0.127
Temporal	p	0.07	0.215	0.648	0.589	0.363
	r	0.31	0.215	0.08	-0.095	0.159
Central Fovea	p	0.034	0.147	0.837	0.338	0.332
	r	0.358	0.25	-0.036	-0.167	0.169
Total VF Average	p	0.114	0.247	0.457	0.958	0.395
	r	0.272	0.201	0.13	0.009	0.148

Table 5-2: (Top) Right eye ppRNFL and visual field quadrant correlations. (Bottom) Left eye ppRNFL and visual field quadrant correlations.

## 5.4 Discussion

### 5.4.1 The Comparison of Foveal OCT Layers with Central Detection Threshold

We found significant negative correlations for the RNFL thickness at the fovea ( $P=0.002$ ,  $r=-0.314$ ) and macular region ( $P=0.001$ ,  $r=-0.326$ ) as well as for the INL at the fovea ( $P=0.005$ ,  $r=-0.279$ ) when compared to VF detection threshold. These findings were of interest as they highlight that a thicker inner retina at the fovea and the macular region is associated with worse central detection threshold in albinism. This finding allows us to postulate that as foveal hypoplasia increases the central detection threshold in albinism worsens. Similar findings have previously been found when considering visual acuity in albinism (Mohammad, Gottlob et al. 2011).

We correlated the outer retinal layers (fovea and macular region) against the central detection threshold and found significant positive correlations for the ONL at the fovea ( $P=0.001$ ,  $r=0.318$ ) and the macular region ( $P=0.003$ ,  $r=0.297$ ) and the OS layer at the fovea ( $P=0.005$ ,  $r=0.28$ ). The ONL is comprised of the cell bodies of rods and cones, indicating that increased numbers of these cells centrally is associated with better detection threshold. Thicker cone outer segments at the fovea are associated with better VF detection thresholds. This concurs with previous findings which found the cone OS layer to be the best OCT layer to predict visual acuity in albinism (Mohammad, Gottlob et al. 2011). This can be explained by the specialisation of cone receptors at the fovea which are usually thinner and taller. Hence, greater specialisation is associated with better detection thresholds.

### 5.4.2 The Correlation of ppRNFL Measures with VF Detection Threshold

We correlated the ppRNFL around the optic nerve (5 segments (macula ppRNFL, upper temporal ppRNFL, upper nasal ppRNFL, lower nasal ppRNFL and lower temporal ppRNFL)) with the detection thresholds for quadrants and macular area on the VF. We correlated each eye separately since

Mohammad et al (2015) found that the ppRNFL thickness was significantly thicker in the right eyes in albinism compared with the left eyes ( $P=0.001$ ) (Mohammad, Gottlob et al. 2015). We found no significant correlations for any comparison of VF quadrant or macula area to ppRNFL segment for the right eye. For the left eye we found a significant positive correlation for the macula ppRNFL area and central foveal VF area ( $P=0.034$ ,  $r=0.358$ ) and macula ppRNFL area and upper temporal VF quadrant ( $P=0.037$ ,  $r=0.355$ ). However, we found no significant correlations for any VF quadrants to the equivalent ppRNFL segments in the right eye.

One possible explanation for the lack of association between ppRNFL and VF quadrants could be that the exact route of ppRNFL fibres entering the optic nerve in albinism is unknown and so assumptions are made about the VF locations and their projections into the optic nerve. Our structural comparisons are based on anatomy and previous work in glaucoma on how ppRNFL corresponds to VF location.

### **5.4.3 Cortical Deficits**

Our findings from this chapter demonstrate that VF deficits are not associated with selective structural ppRNFL deficits.

Another explanation could be the differences in connectivity that are observed in the LGN and the visual cortex in albinism and the cortical reorganisation occurring. Within the normal visual system, the spatial layout of the retina and visual scene is preserved which gives rise to VF maps. There is ample literature providing evidence that these maps are altered in albinism (Guillery, Hickey et al. 1984, Schmolesky, Wang et al. 2000, Hoffmann, Tolhurst et al. 2003, Hoffmann and Dumoulin 2015). There is a longstanding debate discussing various types of VF representation in albinism from work that has been carried out on animals (Siamese cats, albino cats, ferrets and monkey) (Shatz 1977, Guillery, Hickey et al. 1984, Schmolesky, Wang et al. 2000, Garipis and Hoffmann 2003) and humans

(Hoffmann, Tolhurst et al. 2003) (different types of cortical reorganisation are discussed in **Section 1.7.2.6**).

Possibly, the cortical reorganisation leads to localised areas of reduced cortical stimulation or greater inhibition although the mechanisms behind this are unclear.

## 5.5 Study Limitations

As mentioned in the previous chapter, a positive angle kappa in albinism means we cannot be sure that the correct VF quadrant is being correlated to the correct area of ppRNFL around the optic nerve. With a positive angle kappa there is likely to be an increase in temporal VF representation and a reduction in nasal VF representation and therefore, the areas picked off for the VF corresponding to the ppRNFL segments may differ.

Another major limitation of the study is the difficulty in RNFL segmentation during analysis, despite automated analysis on a good quality scan (Q.I.>5), manual segmentation is often required. Manual segmentation for the nasal side (away from bundles) is especially difficult as the reflectivity on this side is poorer. This may lead to the estimated ppRNFL thickness for this area to be reduced compared to the temporal area.

An additional weakness to this study is the inability to precisely compare ppRNFL area which matches the corresponding VF area. In our study we had four readily created quadrants and Copernicus OCT provided automated analysis on ten separate sector ppRNFL measures. We were required to choose a model of analysis to match the Copernicus OCT ppRNFL data available.

## 5.6 Future Studies

Foveal OCT correlations with VF detection threshold provide further evidence of foveal layers offering a very useful objective measure in predicting visual loss caused by retinal abnormalities. Although useful, the relationship between ppRNFL differences in albinism and functional deficits requires further work. This study provides an important reference point for the assessment of structural abnormalities in albinism using OCT imaging.

To assess whether in fact these VF deficits are cortical in origin, rather than based on ppRNFL structure around the optic nerve, we require further research into the cortical structure in albinism and how our subjective measures compare to the objective cortical measures.

# Chapter 6

## Investigating the Relationship between Foveal Morphology and Refractive Error in Infantile Nystagmus (Study 4)

# Chapter 6 Investigating the Relationship between Foveal Morphology and Refractive Error in Infantile Nystagmus (Study 4)

## 6.1 Introduction

### 6.1.1 General Introduction

In earlier chapters we have assessed phenotypic features in albinism (such as iris abnormalities and VF changes) in comparison to other groups (e.g. IIN or controls). In this chapter we explore the relationship between refractive error and foveal hypoplasia in albinism and other nystagmus associated conditions such as IIN, *PAX6* and achromatopsia. The motivation for this comes from an investigation by Healey et al (2013) where the authors describe a relationship between refractive error and grade of foveal hypoplasia (Thomas et al (2011)) in individuals with nystagmus (Healey, McLoone et al. 2013). The principal finding from the Healey et al (2013) study was that impaired emmetropisation in nystagmus is likely to be attributed to the whole eye effect in albinism and they suggest the fovea does not play a central role in this.

There were a number of limitations to the study, particularly in relation to the patient cohort:

- All 33 participants with albinism displayed a narrow range of foveal hypoplasia (grades 3-4) which does not reflect the range described in previous publications with albinism (Thomas, Kumar et al. 2011). This narrow range of foveal hypoplasia limited the power of the correlation analysis.
- Additionally, they included 17 patients with “non-albinotic idiopathic” nystagmus (NAIN). This was a heterogeneous group of individuals with different forms of nystagmus (IIN, isolated foveal hypoplasia and *PAX6*) each with a different phenotype. The majority of the group (14/17) demonstrated a narrow range of foveal hypoplasia, mainly of milder forms (grades 0-1) and only 3/17 had severe (grade 3). The patients who had either no foveal

hypoplasia or grade 1 foveal hypoplasia are likely to be patients with IIN or isolated foveal hypoplasia. This NAIN group with severe foveal hypoplasia (only 3 patients) showed no correlation with refractive error.

There are various other eye conditions with foveal hypoplasia where higher than normal refractive errors have been found such as achromatopsia (Haegerstrom-Portnoy, Schneck et al. 1996) and *PAX6* mutations (Hewitt, Kearns et al. 2007, Hingorani, Williamson et al. 2009).

The purpose of our study is to compare foveal hypoplasia to refractive error in a larger group of participants with albinism compared to Healey et al., as well as other carefully diagnosed conditions associated with nystagmus (IIN, *PAX6* and achromatopsia). We also compare the current clinically available subjective foveal hypoplasia grading (FHG) scheme to an objective measure of foveal hypoplasia (foveal development index (FDI)). This has allowed us to discriminate the degree of foveal hypoplasia on a continuous scale rather than being limited to four grades.

## 6.1.2 Refractive Error

Next is a brief overview of the nature and origin of refractive errors.

A refractive error occurs when there is failure of the eye to correctly focus rays of light from an object onto the fovea. This causes any perceived image to appear blurred. A refractive error is the difference between the focal length of the lens and cornea and the length of the whole eye resulting in spherical refractive errors namely myopia (near or short-sightedness) or hypermetropia (far or long-sightedness) and/or cylindrical refractive errors i.e. astigmatism (shape of eyeball or cornea) (Williams, Verhoeven et al. 2015).

### 6.1.2.1 Spherical Refractive Error

**Myopia:** In myopia an image is focused to a point in front of the retina either due to excessive refraction at the cornea, lens or more commonly from an eyeball that is too long (axial myopia).

Myopia can be corrected with a concave lens (negative power) which allows an image to be focused onto the retina (Snell and Lemp 1989). This is shown in **Figure 6-1**.

**Hypermetropia:** In hypermetropia, the opposite occurs to myopia where the image is focused to a point behind the retina due to less than the required amount of refraction at the cornea or an

eyeball that is too short (axial hyperopia). Hypermetropia can be corrected with convex lenses (positive power) (Snell and Lemp 1989). This is also demonstrated in **Figure 6-1**.

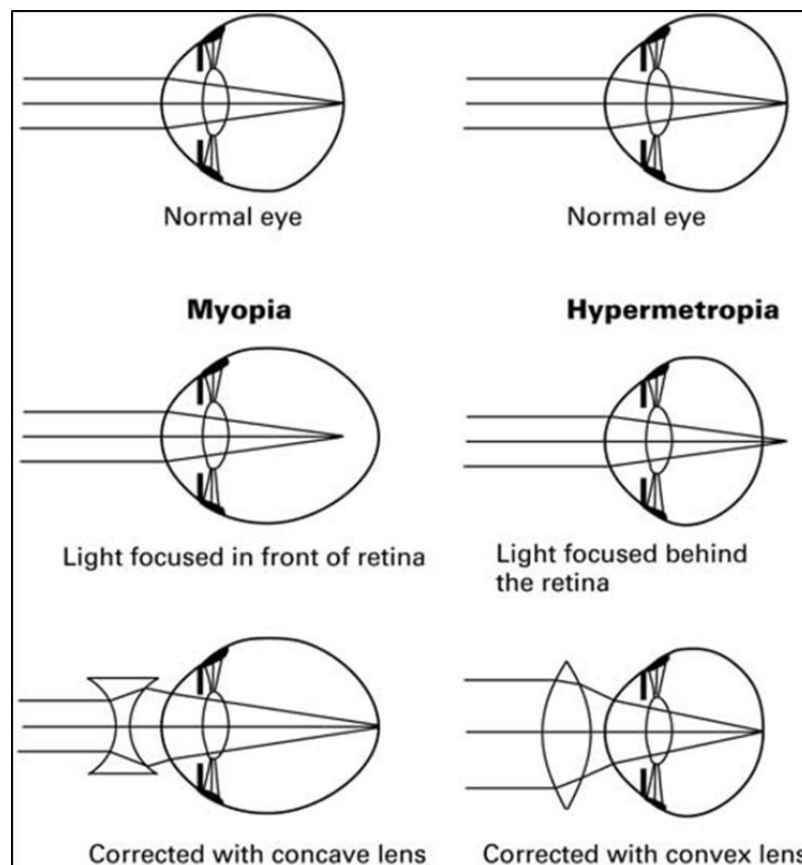


Figure 6-1: Examples of myopia (left) and hypermetropia (right) with correction using concave lens (for myopia) and convex lens (for hypermetropia). Image reproduced from <http://www.patient.co.uk/doctor/Refraction-and-Refractive-Errors.htm>

### 6.1.2.2 Cylindrical Refractive Error - Astigmatism

Astigmatism is caused by defects in the curvature of the cornea (corneal astigmatism) or lens (lenticular astigmatism) (Ansons and Davis 2000). Most astigmatic refractive errors are bilateral and symmetrical. If astigmatism appears as an isolated feature it is classed as simple astigmatism. However, if it is also associated with a spherical refractive error it is classed as compound myopic, compound hypermetropic or mixed astigmatism (Ansons and Davis 2000). The 3 main types of astigmatism that occur are with-the-rule, against-the-rule and oblique:

**With-the-rule astigmatism:** the steepest corneal meridian is vertical. The shape of the eye is like a rugby ball on its belly.

**Against-the-rule astigmatism:** the steepest corneal meridian is horizontal. The shape of the eye is like a rugby ball on its point edge.

**Oblique astigmatism:** is where the steepest corneal meridian is orientated at an oblique angle.

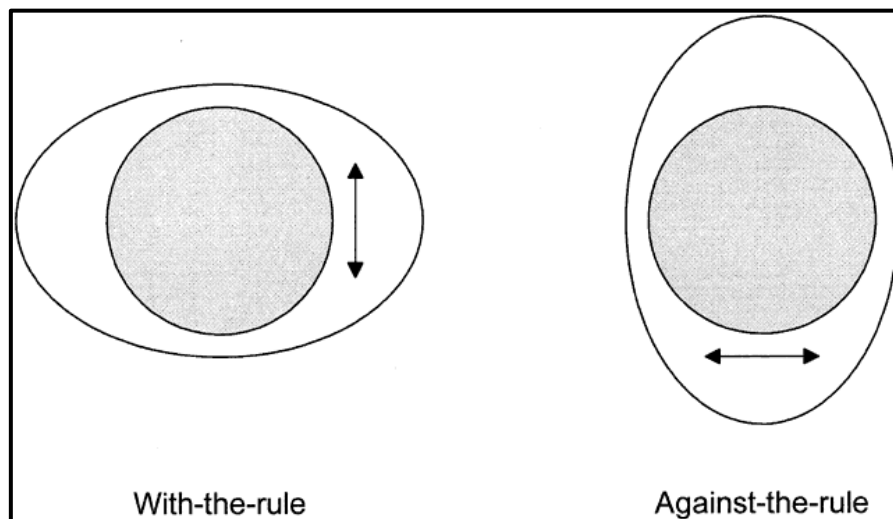


Figure 6-2: With-the-rule and against-the rule astigmatism. Figure reproduced from: <http://www.oculist.net>

### **6.1.3 Genetic and Environmental Factors Affecting Refractive Errors**

The development of refractive errors relies on a combination of genetic and environmental factors (Hung and Ciuffreda 1999). Environmental factors influence the corneal and lens power and also the axial length of the eye (Hung and Ciuffreda 1999). One of the most commonly known environmental factors that can cause myopia is increased periods of close work (Ip, Saw et al. 2008, Schaeffel 2012).

### **6.1.4 Refractive Error in Albinism**

The refractive profiles in albinism are generally found to be abnormal with high refractive errors frequently occurring (Dickinson and Abadi 1984, Abadi and Dickinson 1986, Wildsoet, Oswald et al. 2000, Sampath and Bedell 2002, Anderson, Lavoie et al. 2004, Yahalom, Tzur et al. 2012). However, there continues to be a debate between authors as to whether individuals with albinism demonstrate predominantly myopia (Dickinson and Abadi 1984) or hypermetropia (Loshin and Browning 1983, Dickinson and Abadi 1984, Wildsoet, Oswald et al. 2000). Individuals with albinism predominantly show with-the-rule astigmatism (Wildsoet, Oswald et al. 2000).

Wildsoet, Oswald et al (2000) evaluated the refractive status of 25 individuals with albinism. This cohort of individuals with albinism included both high hypermetropia and high myopia, but they found a slight bias towards hypermetropia. They could not distinguish any differences between the different genetic types of albinism. The authors also found a correlation between refractive errors and axial length. As refractive error became more myopic the axial length increased. They found the refractive astigmatism was highly correlated with corneal astigmatism in albinism (Wildsoet, Oswald et al. 2000). Wildsoet et al (2000) found all 25 individuals with albinism to have with-the-rule astigmatism.

Although the majority of research claims there is no relationship within albinism subtype and type of refractive defect present (Dickinson and Abadi 1984, Wildsoet, Oswald et al. 2000), there are some authors that argue the contrary (Kassmann and Ruprecht 1996, Yahalom, Tzur et al. 2012).

Kässmann and Ruprecht (1996) describe a weak association between tyrosinase negative albinism (OCA1) and myopia, and between tyrosinase positive albinism (OCA2) and hypermetropia. However, there were not enough patients in their study to statistically assess for correlations. Yahalom et al (2012) separated albinism into four categories genetically (OCA1A, OCA1B, OCA1C and OCA2) to assess whether spherical refractive error varied based on genetic diagnosis and pigmentation in albinism. Their findings appear at odds with Kässmann and Ruprecht (1996). Yahalom et al (2012) found those with OCA1A (no pigmentation) showed the highest level of hypermetropia when compared with other groups ( $P=0.007$ ), whereas those with OCA2 demonstrated the highest level of myopia (although not statistically significant). Those with OCA1A also demonstrated the poorest BCVA compared to the other groups, however, not to significant levels. (Yahalom, Tzur et al. 2012). The studies from Kässmann and Ruprecht (1996) and Yahalom et al (2012) exhibit conflicting views and also present us with a further question on pigmentation and whether this may have a bearing upon the development of refractive error.

Another interesting study by Sampath and Bedell (2002) compared the refractive errors in a group of individuals with albinism ( $n=19$ ) to a group with IIN (46 patients). They assessed the kurtosis of each group and found that distribution of refractive profiles was significantly less broad for the IIN group in comparison to the albinism group. Sampath and Bedell (2002) found albinism and IIN refractive profiles are more spread out (further away from 0 spherical equivalent) compared to normals and did not show any kurtosis when compared to the kurtosis for normals individuals who show a leptokurtic distribution (from a previous paper (Sorsby et al 1960)).

More recently (as stated in the general introduction), Healey et al (2013) published a study to gain a better understanding of how foveal morphology can affect refractive errors in infantile nystagmus.

The authors found that when grouping all participants together (33 with albinism and 17 with NAIN) there was a significant association between grade of foveal hypoplasia and SER ( $P=0.008$ ) and MAM ( $P=0.005$ ). However, when the groups were analysed separately there were no statistically significant correlations. The authors concluded that for individuals without albinism but with nystagmus the fovea has a limited impact on refractive outcome and further supports the idea that the fovea does not play a central role in the emmetropisation process (Healey, McLoone et al. 2013).

From these previous findings in albinism, various questions remain unanswered and provide scope for further research into refractive errors in albinism in comparison to other conditions. The present study has a primary aim of assessing how foveal hypoplasia affects refractive error not only in albinism but also other conditions associated with nystagmus in order to assess whether the effect of foveal development on refractive error is disease specific. For the first time we also compare the subjective clinically available foveal hypoplasia grading scheme to an objective measure of foveal hypoplasia to assess efficacy.

## 6.1.5 Aims and Rationale for Study 4

The main aim for this study is to assess the relationship between foveal hypoplasia and refractive error. In addition, there are a number of sub-aims:

1. Assess how objective (foveal development index) and subjective (foveal hypoplasia grading) measures of foveal hypoplasia compare with each other as well as with best corrected visual acuity.
2. Assess how the refractive error relates to foveal hypoplasia in each group with nystagmus, separately.
3. Assess the effect of axial length on refractive error and foveal hypoplasia in albinism.
4. Assess how PEL (pigment epithelium layer of the iris) thickness affects axial length in albinism.

## 6.1.6 Hypotheses

These are the three main hypotheses to be addressed in **Study 4**.

- Foveal hypoplasia grading and foveal development index will provide a strong correlation between subjective and objective measures of foveal hypoplasia.
- Refractive error will correlate with foveal hypoplasia for all groups with nystagmus.
- Axial length (eye growth) and pigmentation (PEL thickness-measure of iris pigmentation) will correlate with refractive error.

## 6.2 Methodology for Study 4

### 6.2.1 Participants and Data Collection

Participants were only used if a refractive assessment was conducted within 3 months of OCT imaging to ensure the current refractive status matched the OCT timeframe. The participants recruited to this study were 33 individuals with albinism, 18 individuals with IIN, 9 individuals with *PAX6* mutation and 12 individuals with achromatopsia.

### 6.2.2 Refraction

All individuals in this study had an up to date refraction from a high-street optometrist or were subjectively refracted at the Leicester Royal Infirmary optometry department on the same day as their OCT assessment. All included subjects were over the age of 7 years and therefore did not require any pupillary dilation. All refractive assessments were carried out by experienced optometrists.

### 6.2.3 OCT Imaging and Analysis

OCT imaging methods for the fovea are the same as the previous studies described in **Section**

**2.2.2.4.3**. OCT imaging was successful in all but two participants with *PAX6* mutation who demonstrated refractive error over -10 dioptres and were therefore unable to be scanned.

From the foveal layer thicknesses we calculated the foveal development index (FDI) which provides an objective quantitative measure of foveal hypoplasia as a number between 0 and 1. A FDI at or close to zero indicates no foveal hypoplasia. The FDI was calculated using the following formula:

$$\text{Foveal Development Index} = \frac{\text{Inner Foveal Layers Thickness}}{\text{Total Foveal Layers Thickness}}$$

## 6.2.4 Clinical Grading of Foveal Hypoplasia

A subjective measure of foveal hypoplasia can be provided using the foveal hypoplasia grading (FHG) scheme as proposed by Thomas et al (2011). The grading scheme is shown in **Figure 6-3** (Thomas, Kumar et al. 2011). The FHG scheme provides a quick and easy method to assess the structure of a fovea and provides a severity score between 1 and 4. Those who do not have any foveal hypoplasia can be classed as grade 0 and those who have an abnormal lining of retinal layers are classified as atypical (e.g. achromatopsia). For a subjective comparison of foveal hypoplasia we also used this categorisation for our analysis.

(A) Normal foveal structural features detectable using optical coherence tomography		Illustration	
(a) Extrusion of plexiform layers (b) Foveal pit (c) OS lengthening (d) ONL widening		RNFL GCL IPL INL OPL ONL ELM IS/OS RPE	
(B) Grade of foveal hypoplasia	Structural features detected on optical coherence tomography	Present or absent	Illustration
1	(a) Extrusion of plexiform layers (b) Foveal pit – Shallow (c) OS lengthening (d) ONL widening	(a) Absent (b) Present (c) Present (d) Present	
2	(a) Extrusion of plexiform layers (b) Foveal pit (c) OS lengthening (d) ONL widening	(a) Absent (b) Absent (c) Present (d) Present	
3	(a) Extrusion of plexiform layers (b) Foveal pit (c) OS lengthening (d) ONL widening	(a) Absent (b) Absent (c) Absent (d) Present	
4	(a) Extrusion of plexiform layers (b) Foveal pit (c) OS lengthening (d) ONL widening	(a) Absent (b) Absent (c) Absent (d) Absent	
Atypical	(a) Extrusion of plexiform layers (b) Foveal pit – Shallow (e) IS/OS disruption	(a) Absent (b) Present (e) Present	

Figure 6-3 (A) Illustration of the unique features of a normal fovea on optical coherence tomography. (B) Typical and atypical grades of foveal hypoplasia. Image reproduced from Thomas et al (2011).

## 6.2.5 Axial Length Measurement

Axial length measures were taken on individuals with albinism as we wanted to assess the relationship between eye growth and pigmentation (objectively measured) within the eye (iris specifically).

**Figure 6-4** shows the IOLmaster which is used to obtain an axial length measurement. The principle behind obtaining these readings is partial coherence interferometry (PCI) which is similar to OCT. A dual beam of infrared light is emitted from a laser diode. The eye to be measured and the photodetector are situated at opposite ends of the interferometer. The partial beams are reflected at the cornea and retina and this allows measurement of axial length. The method requires a Michelson interferometer.

An axial length reading takes 0.5 seconds per reading. For all readings to be clinically useable and accurate, repeatability must be ensured. The axial length measurement is taken a minimum of 10 times with at least 5 concordant results (within 0.1mm).



**Figure 6-4: (Left) IOLmaster, (Right) IOLmaster in use.**

## 6.3 Results

### 6.3.1 Patient Demographics

	<b>Albinism</b>	<b>IIN</b>	<b>Pax6</b>	<b>Ach</b>
<b>N</b>	33	18	9	12
<b>Age (±SD)</b>	36.27 (±15.70)	29.72 (±13.91)	40.11(±19.66)	25.08(±18.55)
<b>LogMAR BCVA (±SD)</b>	0.45 (±0.18)	0.20 (±0.11)	0.33(±0.12)	0.91(±0.10)
<b>FDI (±SD)</b>	0.34 (±0.06)	0.06 (±0.04)	0.26(±0.13)	0.22(±0.10)
<b>FH Grade (±SD)</b>	2.73 (±0.94)	0.33 (±0.48)	1.89(±0.60)	Atypical

**Table 6-1: Patient demographics for all 4 groups. BCVA=Best Corrected Visual Acuity, FDI=Foveal Development Index, FH Grade=Foveal Hypoplasia Grade, Ach=Achromatopsia.**

#### 6.3.1.1 Statistical Tests

As the data was not normally distributed we used non-parametric Kruskal Wallis statistical tests to compare each group for the following comparisons. A Bonferroni correction was used to adjust for multiple comparisons.

See next page for results.

## 6.3.2 Foveal Hypoplasia

### 6.3.2.1 Foveal Hypoplasia Grading (FHG)

The mean grade of foveal hypoplasia for each group was: albinism (2.73), IIN (0.33), *PAX6* (1.89) and achromatopsia (atypical). As evident in **Figure 6-5**, the only significant finding was the FHG in the IIN group was significantly lower than the albinism group ( $P < 0.001$ ). Achromatopsia was not included in this analysis as it is graded “atypical” due to the structure of the fovea in this condition.

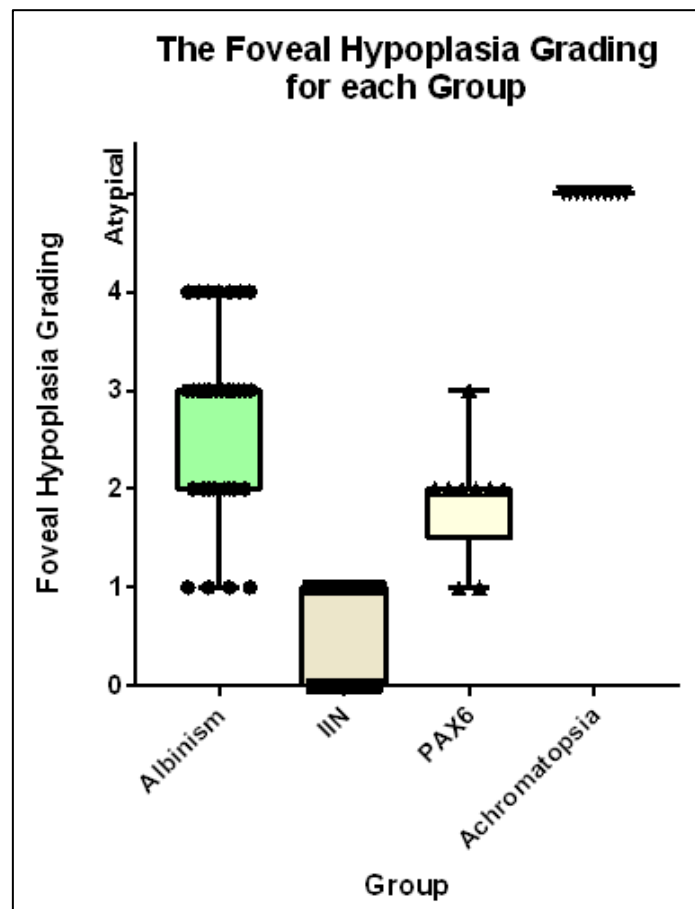
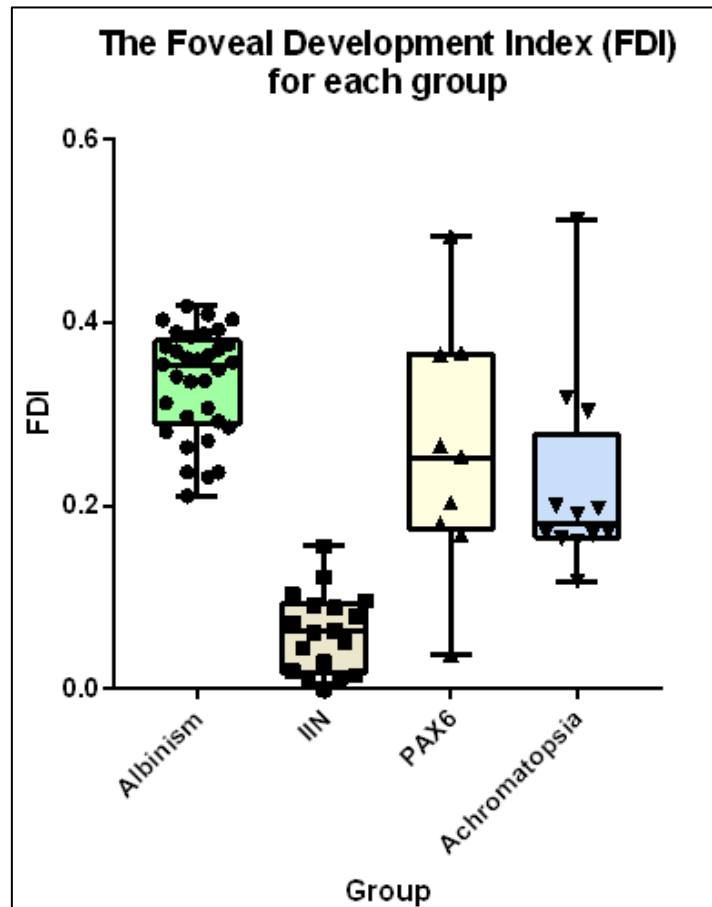


Figure 6-5: Foveal hypoplasia grade for each group with nystagmus. Data for each participant is shown.

### 6.3.2.2 Foveal Development Index (FDI)

The FDI was calculated for each group to provide an objective continuous measure of foveal hypoplasia based on the thickness of foveal layers. The mean FDI for each group was: albinism (0.34), IIN (0.06), *PAX6* (0.26) and achromatopsia (0.22). **Figure 6-6** illustrates this data.



**Figure 6-6: Foveal development index (FDI) for each group and data for each participant is shown.**

The FDI in the IIN group was significantly lower than in albinism ( $P < 0.0001$ ), *PAX6* ( $P < 0.01$ ) and the achromatopsia group ( $P < 0.01$ ). The FDI in the achromatopsia group was also significantly lower than the albinism group ( $P < 0.05$ ).

### 6.3.2.3 The Relationship between Foveal Development Index (FDI) and Foveal Hypoplasia Grading (FHG)

Figure 6-7 shows how the measures of foveal hypoplasia correspond for FHG (subjective measure) and FDI (objective measure). Those with IIN who demonstrate FHG 0-1 correspond to the lower end of the FDI. Those with albinism who demonstrate FHG 1-4 correspond to the lower end of the FDI. Those with albinism show a wide range of FHG (1-4), the group with PAX6 appear to exhibit grades 1-3.

There is a highly significant association between FDI and FHG ( $P < 0.0001$ ,  $F = 205.36$ ) (achromatopsia omitted from analysis as grading classified as “atypical”).

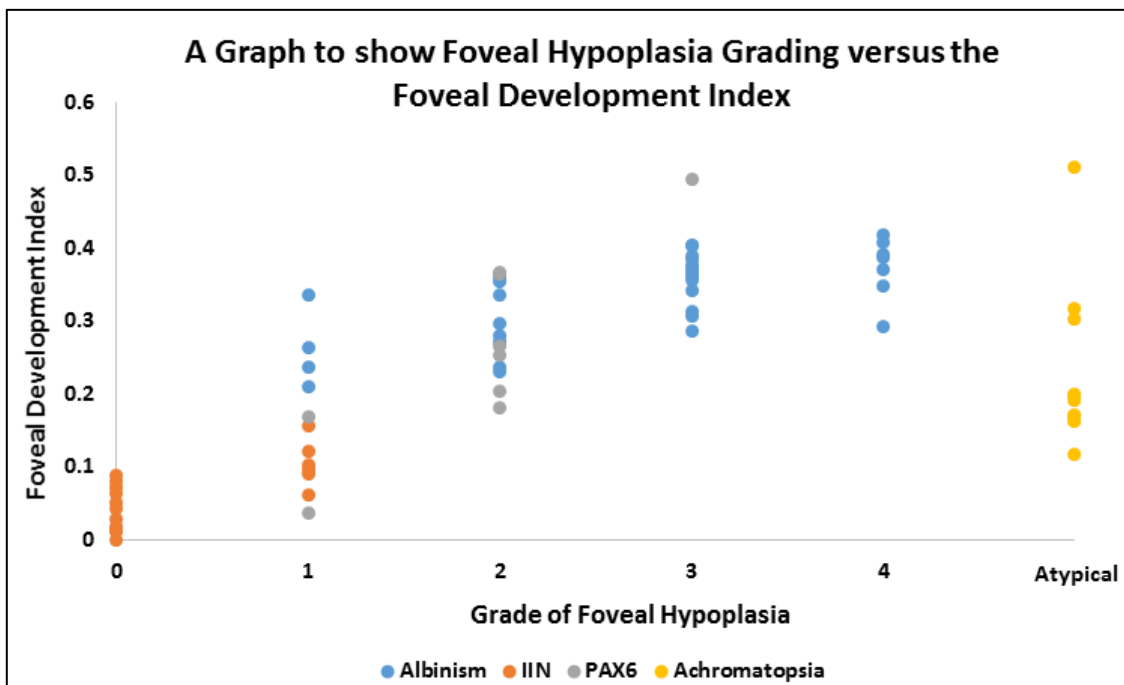
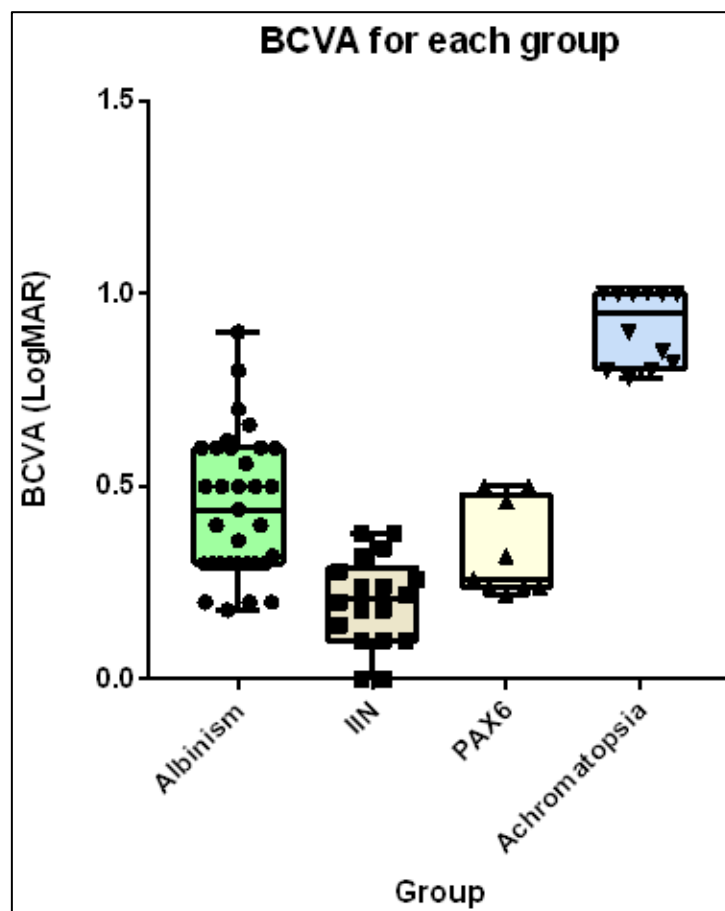


Figure 6-7: The relationship between foveal hypoplasia grading and foveal development index each colour represents a different group.

## 6.3.3 Best Corrected Visual Acuity (BCVA)

### 6.3.3.1 BCVA for Each Group

The BCVA varies considerably for each group. The mean BCVA for the IIN group was the best at 0.20 ( $\pm 0.11$ ) logMAR, followed by the *PAX6* group at 0.33 ( $\pm 0.12$ ) logMAR, then the albinism group at 0.45 ( $\pm 0.18$ ) logMAR. The group with achromatopsia had the worst mean BCVA compared to all other groups at 0.91 ( $\pm 0.10$ ) logMAR. This is illustrated in **Figure 6-8**.



**Figure 6-8: BCVA for each group which includes data for each participant.**

The BCVA in the achromatopsia group was significantly poorer than the albinism group ( $P < 0.001$ ), the IIN group ( $P < 0.0001$ ) and the *PAX6* group ( $P < 0.001$ ). The BCVA in the albinism group was also significantly worse than the IIN group ( $P < 0.001$ ).

### 6.3.3.2 The Relationship between BCVA and Foveal Hypoplasia Grading (FHG)

Figure 6-9 shows the comparison of BCVA to FHG (0-4) for the groups (excluding achromatopsia as this group is classified as “atypical” foveal hypoplasia). Regression analysis reveals a significant correlation between BCVA and subjective FHG. As the FHG increases the BCVA becomes worse ( $P < 0.001$ ,  $F = 32.74$ ).

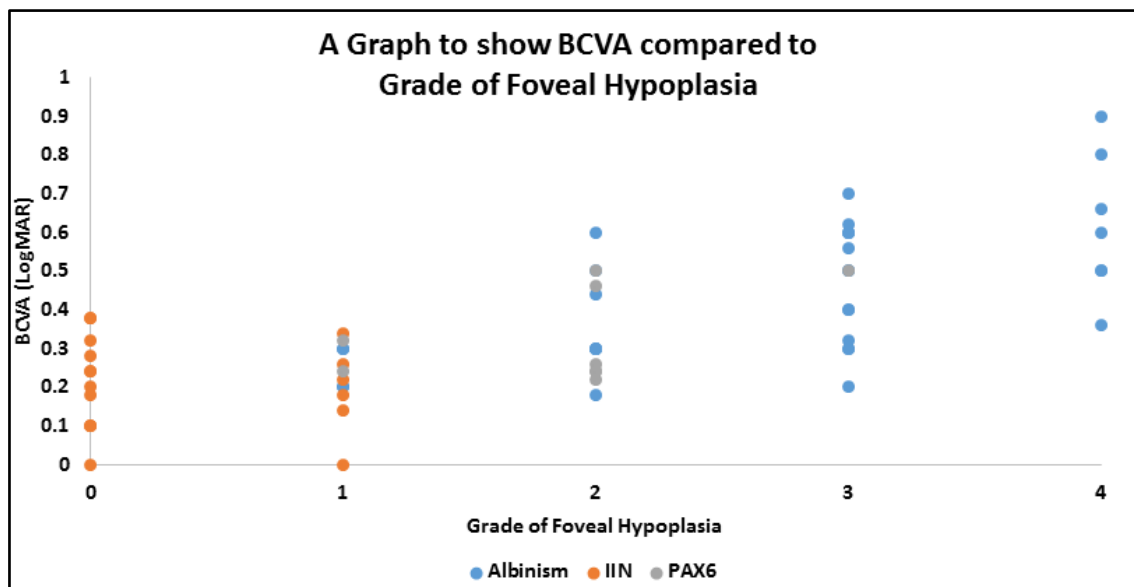


Figure 6-9: The relationship between BCVA and foveal hypoplasia grading for albinism, IIN and PAX6.

### 6.3.3.3 The Comparison of BCVA to Foveal Development Index (FDI)

Figure 6-10 illustrates the comparison of BCVA to FDI for the groups (except achromatopsia as this group is classified as “atypical” foveal hypoplasia). Using regression analysis we see a significant positive correlation between BCVA and FDI ( $P < 0.001$ ,  $F = 43.59$ ).

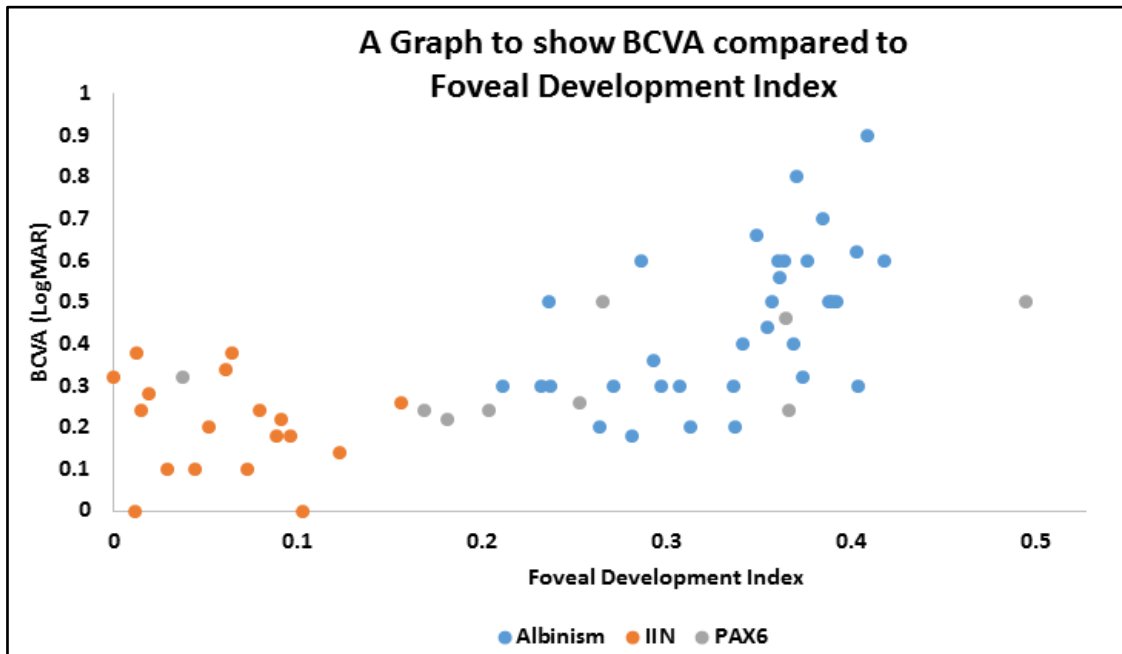


Figure 6-10: The relationship between BCVA and FDI for albinism, IIN and PAX6.

## 6.3.4 Refractive Differences between Groups

The next section presents differences in refractive error for the groups with nystagmus investigating spherical and cylindrical refractive error in each group first, followed by the spherical equivalent (SE) and the most ametropic meridian (MAM).

### 6.3.4.1 Spherical Refractive Error

Figure 6-11 illustrates the spherical refractive error for each group: there are no significant differences for comparisons of all groups. However, all groups show a wide variety of spherical refractive errors.

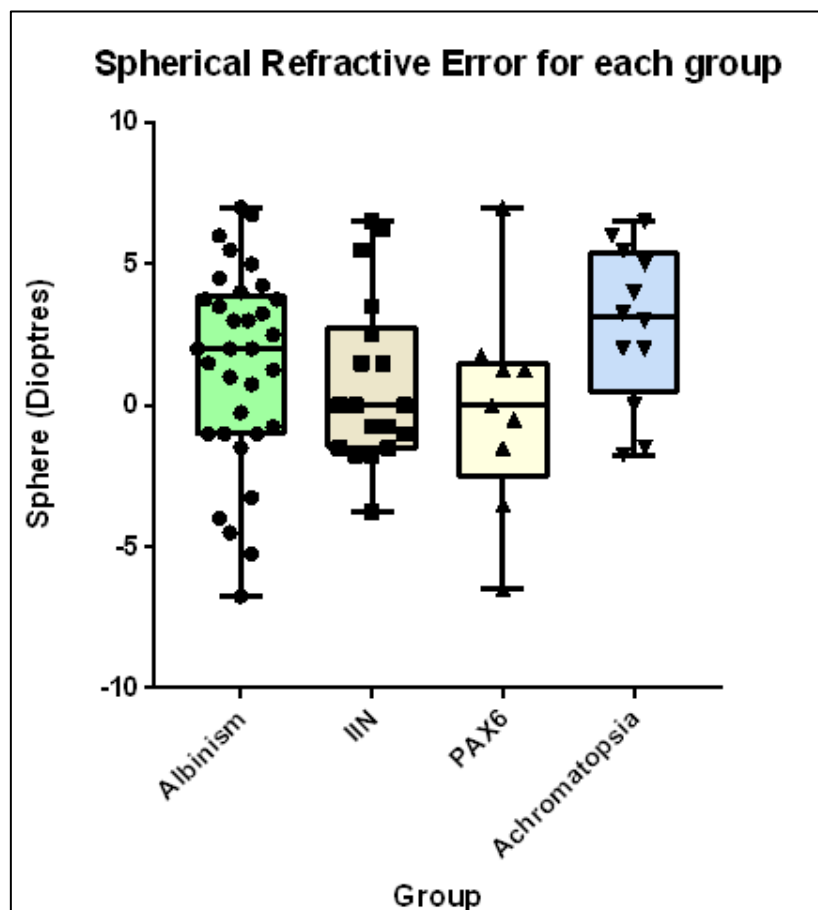


Figure 6-11: Spherical refractive error for each group and data for each participant.

### 6.3.4.2 Cylindrical Refractive Error

Figure 6-12 shows the spherical refractive error for each group. There was only one significant difference between groups. The cylindrical refractive error in albinism was found to be significantly lower than that in *PAX6* mutation ( $P < 0.05$ ).

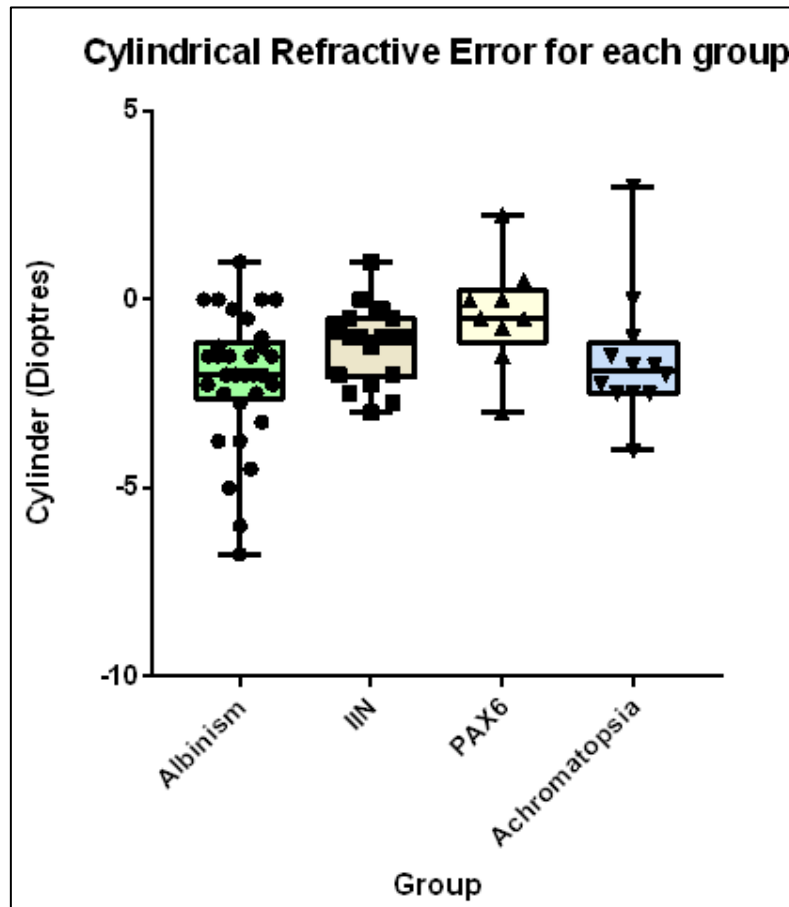


Figure 6-12: Cylindrical refractive error for each group and data for each participant.

### 6.3.4.3 Spherical Equivalent

Figure 6-13 shows the spherical equivalent refractive error for each group, there are no significant findings for comparisons of all groups.

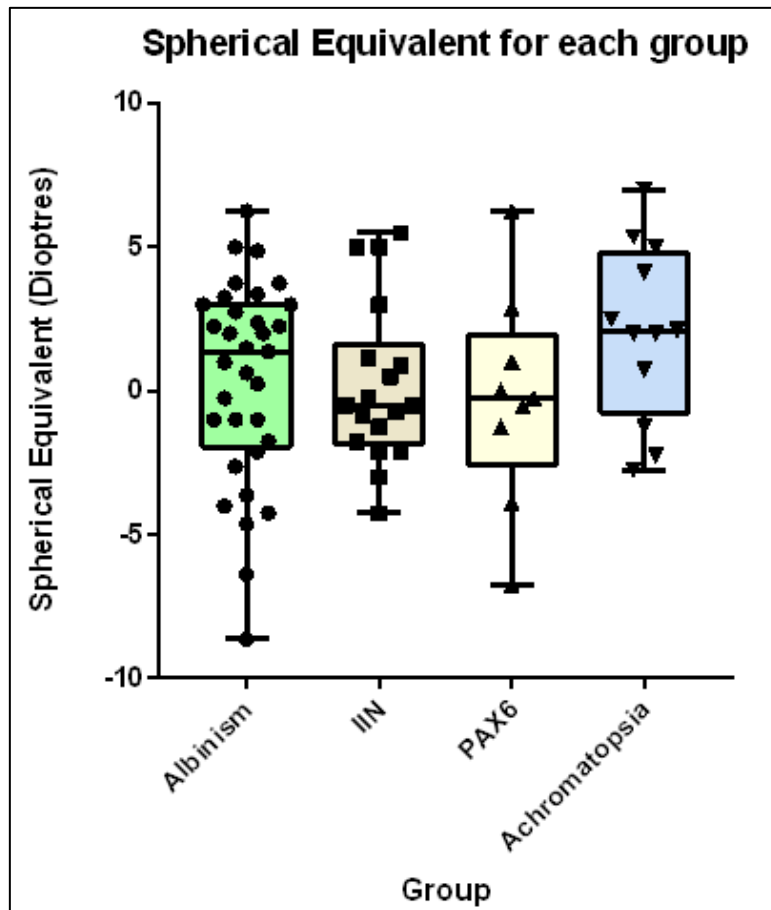


Figure 6-13: The spherical equivalent for each group and data for each participant.

### 6.3.4.4 Most Ametropic Meridian

Figure 6-14 shows the most ametropic meridian refractive error for each group, there are no significant differences for comparisons of all groups.

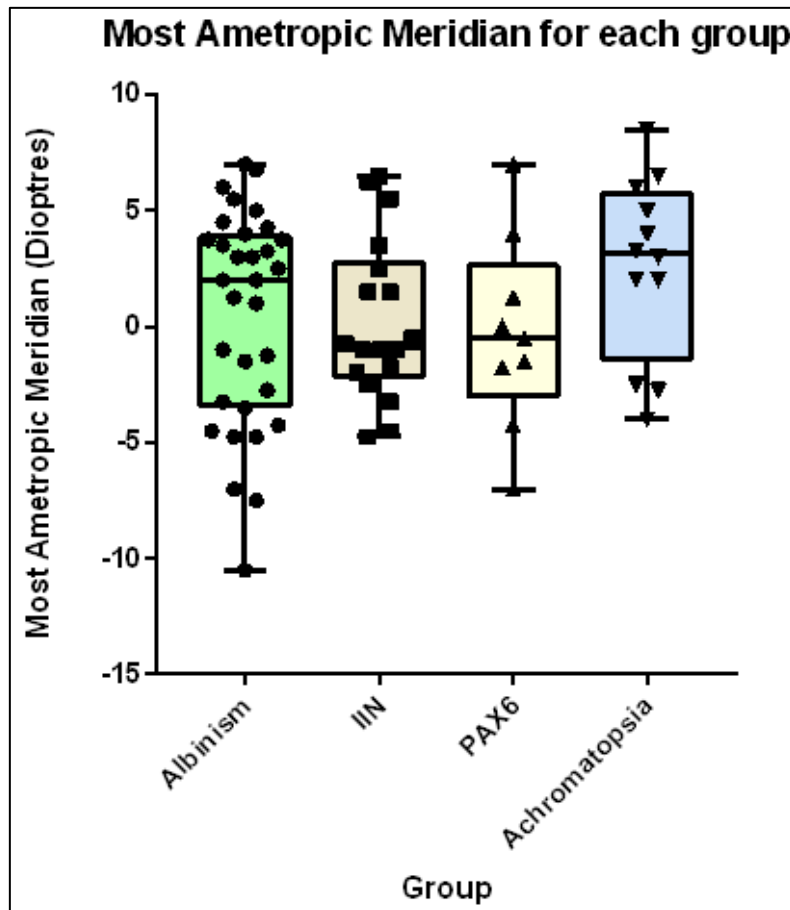


Figure 6-14: The most ametropic meridian for each group and data for each participant.

### **6.3.5 The Comparison of Refractive Measures with Foveal Hypoplasia Grading and Foveal Development Index**

Our main question for this chapter was to determine whether foveal development was associated to refractive error. Here, we compare the refractive measures to both subjective (FHG) and objective (FDI) measures of foveal hypoplasia. Graphs to show these comparisons for each group separately are on the next page.

### 6.3.5.1 Refractive Measures Compared to FHG

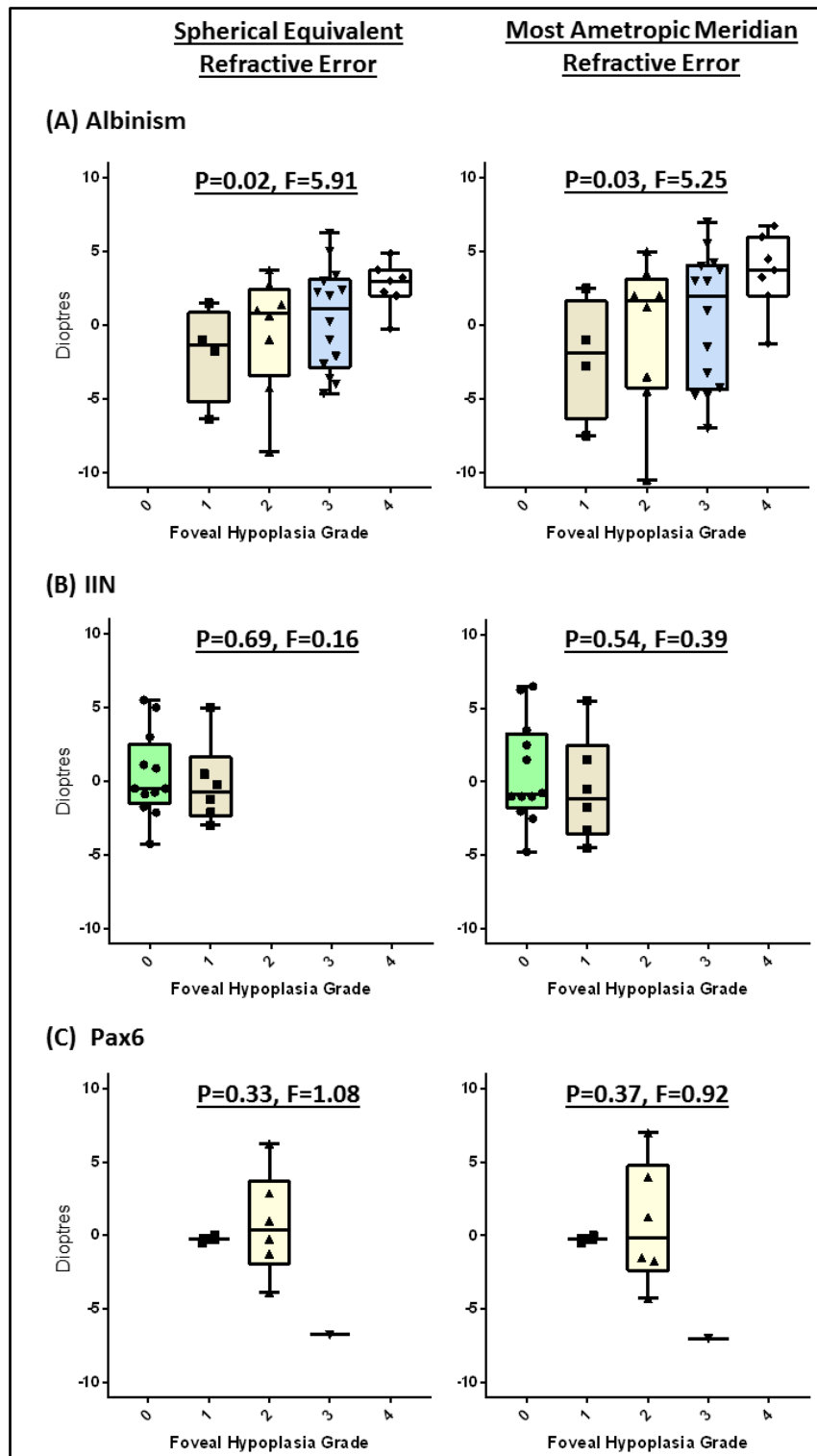


Figure 6-15: The comparison of foveal hypoplasia grade and (left) spherical equivalent refractive error and (right) most ametropic meridian. At the top (A) these comparisons for the albinism group is shown, in the middle (B) these comparison for the IIN group is shown and at the bottom (C) these comparisons for the *PAX6* group is shown. Above each graph values from regression analysis are shown as P and F values.

From **Figure 6-15** only the albinism group demonstrate a significant relationship between FHG and spherical equivalent refractive error ( $P=0.02$ ,  $F=5.91$ ) and most ametropic meridian refractive error ( $P=0.03$ ,  $F=5.24$ ). As the FHG increases the refractive error moves in a hypermetropic direction.

All comparisons, for IIN and *PAX6*, did not demonstrate any significant relationships between FHG and refractive error, however, both IIN and *PAX6* do not show a wide range of foveal hypoplasia grades which may account for this finding.

### 6.3.5.2 Refractive Measures Compared to FDI

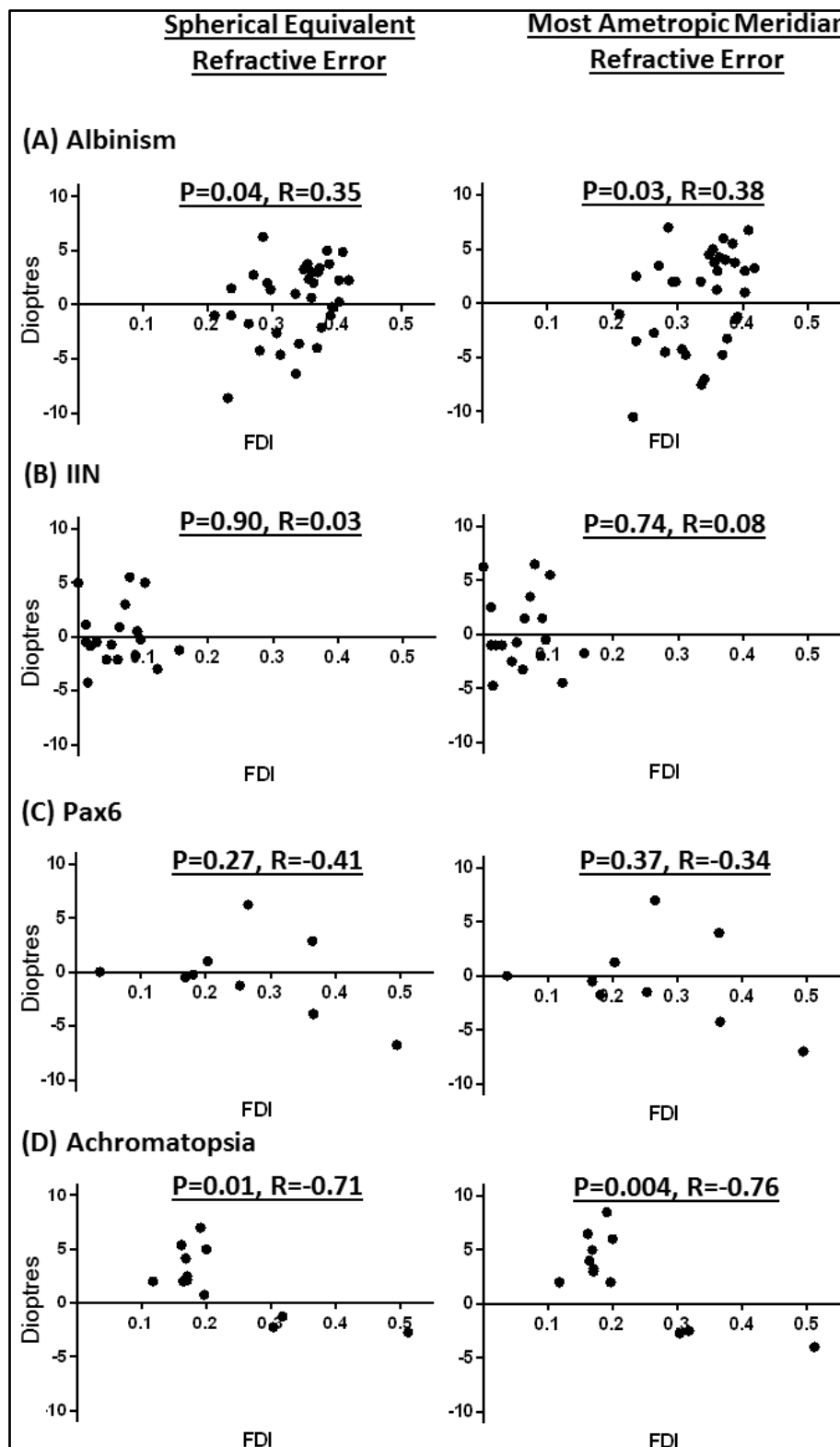
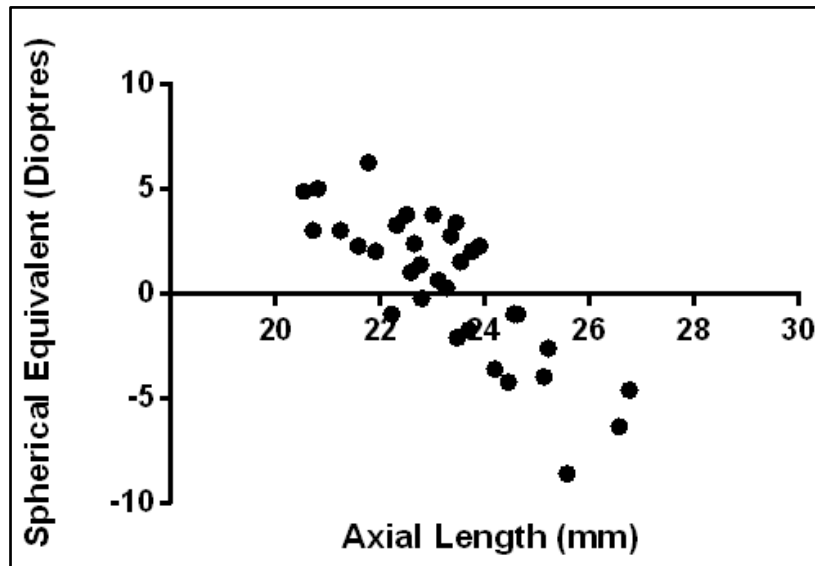


Figure 6-16: The comparison of foveal development index and (left) spherical equivalent refractive error and (right) most ametropic meridian. (A) Albinism, (B) IIN, (C) PAX6 and (D) Achromatopsia. Above each graph, Pearson's correlation values are shown as P and R.

From **Figure 6-16** the albinism group demonstrated a significant positive relationship between foveal development index and spherical equivalent refractive error ( $P=0.04$ ,  $r=0.35$ ) and most ametropic meridian refractive error ( $P=0.03$ ,  $r=0.38$ ). There were no significant relationships noted for IIN or *PAX6*. Interestingly, the achromatopsia group demonstrate a significant negative relationship between foveal development index and spherical equivalent refractive error ( $P=0.01$ ,  $r=-0.71$ ) and most ametropic meridian refractive error ( $P=0.004$ ,  $r=-0.76$ ). As the FDI increases the refractive error moves in a myopic direction.

## 6.3.6 The Importance of Axial Length on Foveal Hypoplasia and Refractive Error

### 6.3.6.1 The Relationship between Axial Length and Spherical Equivalent in Albinism



**Figure 6-17: The correlation between axial length and spherical equivalent refractive error in albinism.**

There was a very strong significant negative correlation between spherical equivalent and axial length ( $P < 0.0001$ ,  $r = -0.82$ ) (**Figure 6-17**). Therefore, as expected, as eye size increases the refractive error (spherical equivalent) moves from hypermetropic to myopic.

### 6.3.6.2 The Relationship between Axial Length and FHG in Albinism

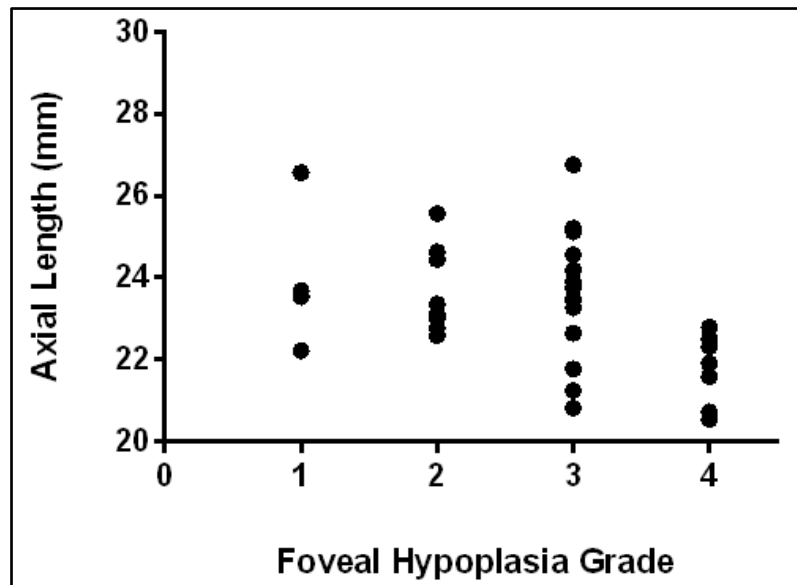


Figure 6-18: Correlation between axial length and foveal hypoplasia grading in albinism.

A significant correlation between FHG and axial length ( $P=0.02$ ,  $r=-0.42$ ) can be observed in **Figure 6-18**. From this finding it appears that as the grade of foveal hypoplasia increases the axial length decreases postulating that foveal hypoplasia may be leading to a lack of successful emmetropisation/growth in albinism. Those with grade 4 appear tightly clustered with very low axial lengths demonstrating lack of axial eye growth with high grade foveal hypoplasia.

### 6.3.6.3 The Relationship between Axial Length and FDI in Albinism

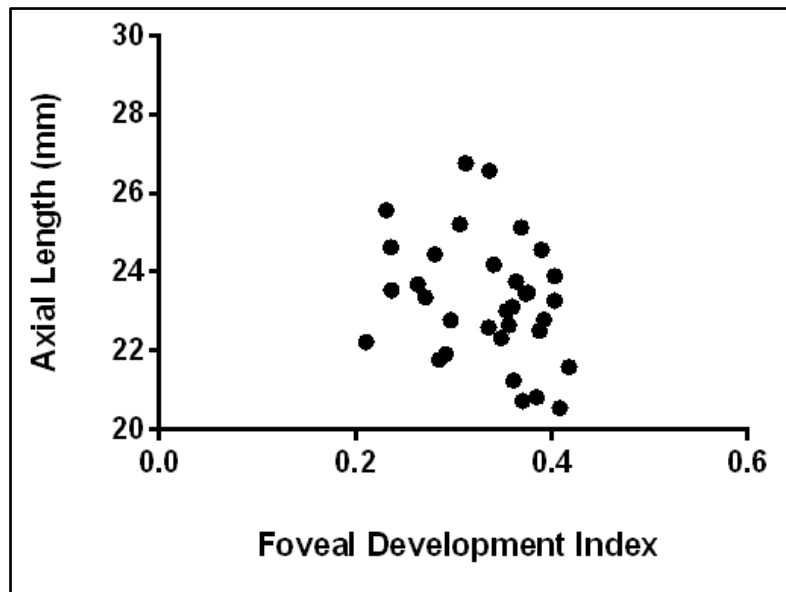


Figure 6-19: The relationship between axial length and foveal development index (FDI).

For the comparison of axial length and foveal development index in albinism there was no significant relationship observed ( $P=0.09$ ,  $r=-0.29$ ) (Figure 6-19).

### 6.3.6.4 The Relationship between Axial Length and BCVA in Albinism

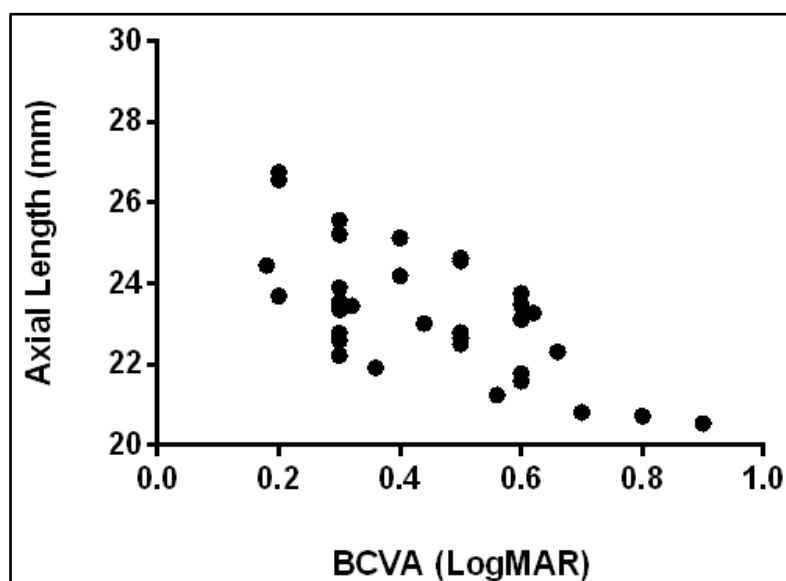


Figure 6-20: The correlation between axial length and BCVA in albinism.

A striking correlation was observed when comparing BCVA and axial length in albinism ( $P < 0.0001$ ,  $r = -0.67$ ) (**Figure 6-20**). This indicates that shorter axial lengths (shorter eyes) are associated with poorer BCVA. From this finding a, an additional correlation was conducted to compare BCVA to spherical equivalent refractive error in albinism. Interestingly, we also observed a highly significant positive association for this comparison ( $P < 0.005$ ,  $r = 0.572$ ), indicating those who demonstrate myopia have better BCVA and those who have hypermetropia have poorer BCVA.

### 6.3.6.5 The Relationship between Axial Length (Eye Growth) and PEL Thickness (Iris Pigmentation)

The comparison of axial length and PEL thickness (findings from **Study 1**) was made to assess how eye growth may be related to melanin pigment production/accumulation.

We found that axial length and PEL show a significant positive correlation ( $P = 0.006$ ,  $r = 0.52$ ) (with 0 values omitted ( $P < 0.05$ ,  $r = 0.41$ )) demonstrating as PEL thickness (pigmentation) increases, axial length (eye growth) also increases (**Figure 6-21**).

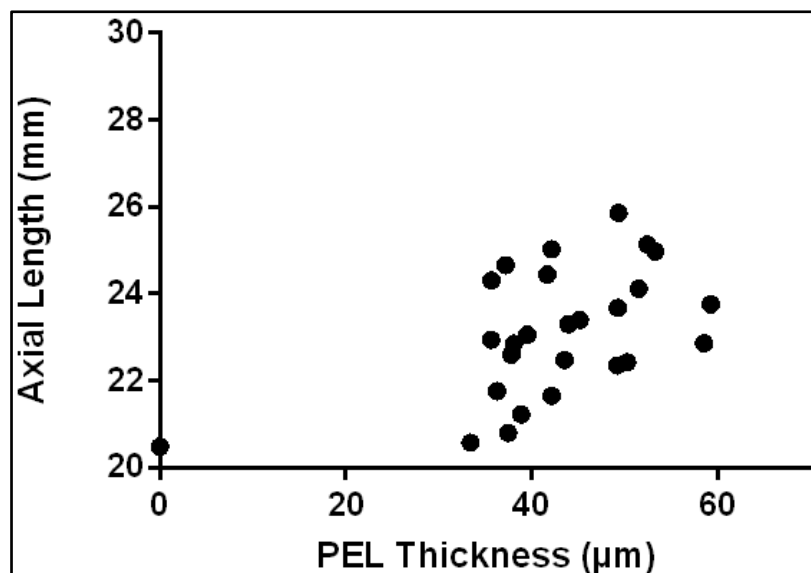


**Figure 6-21: Correlation between axial length and PEL thickness in albinism.**

## 6.4 Discussion

This chapter aims to assess for relationships between foveal hypoplasia (subjective and objective) and refractive error. The main findings were:

1. Foveal hypoplasia (FHG and FDI) was significantly related to refractive error in albinism. Higher levels of foveal hypoplasia are related to hypermetropia whereas lower levels of foveal hypoplasia are related to myopia.
2. There is a relationship between foveal hypoplasia (FDI) and refractive error in achromatopsia, however, predominantly in the opposite direction to albinism. Higher levels of foveal hypoplasia are related to myopia and lower levels are related to hypermetropia
3. Comparison of FDI (objective method) and FHG (subjective method) suggest that both measures reliably quantify FH.
4. Axial length is strongly correlated with refractive error in albinism
5. Axial length is strongly correlated with the level of pigmentation within the iris (PEL specifically).

These principal findings are discussed further in the sections below.

### 6.4.1 Albinism

#### 6.4.1.1 The Relationship between Foveal Hypoplasia and Refractive Error

Healey et al (2013) found that FHG was only correlated to refractive error when combining all participants (albinism and NAIN) in their study together for analysis but this relationship was found not to be disease specific when assessing the groups individually. Our study argues the contrary. When exploring the relationship between foveal hypoplasia and refractive error we see obvious correlations in albinism for both spherical equivalent refractive error and most ametropic meridian

in comparison to FHG and FDI. Unlike Healey et al (2013), when all groups (albinism, IIN, PAX6 and achromatopsia) were grouped together this association was no longer significant.

Our study differed in several aspects from Healey et al (2013). Firstly, our data set included a wide range of FHG in albinism ranging from 1-4 demonstrating the diverse spectrum of this condition, whereas Healey et al (2013) only encountered individuals with albinism who were more severely affected with grades 3 and 4 foveal hypoplasia. Also, within our study we have separated the four different diagnoses associated with nystagmus whereas Healey et al (2013) combined all non-albinotic types of infantile nystagmus as NAIN (non albinotic idiopathic nystagmus). This included IIN, isolated foveal hypoplasia and *PAX6* patients and thus comparisons to such a group must be treated with caution.

Interestingly, for the first time, our results also demonstrate that foveal hypoplasia is related to the length of the eye in albinism. A significant positive correlation is found between axial length and foveal hypoplasia grade demonstrating the eye is likely to be myopic (longer) in lower grades of foveal hypoplasia and hypermetropic (shorter) in higher grades of foveal hypoplasia.

### **6.4.1.2 Proposed Mechanisms for our Findings**

Here we discuss possible mechanisms which help explain our findings in albinism.

#### **1. Form Deprivation Hypothesis:**

Form deprivation myopia occurs when the eyes are deprived of sufficient visual stimulation leading to an increase in axial length (Stone, Lin et al. 1989, Bowrey, Metse et al. 2015). The mechanism by which this occurs is thought to be due to a reduction in dopamine activity. Dopamine signalling in the retina is critical for the normal development of axial length.

In our participants with albinism, although there is degradation of image quality most likely due to foveal hypoplasia, we find the opposite trend to that expected for the form deprivation theory. As

shown in **Figure 6-15** and **Figure 6-20** worsening foveal hypoplasia and BCVA are associated with increasing hypermetropia and lower axial lengths. Since myopia is associated with the participants with albinism with better vision rather than emmetropia, the form deprivation theory could account for the pattern observed in these individuals (**Figure 6-20**).

## **2. Increased Light Scatter Hypothesis (Hyper-illumination):**

Individuals with albinism are more likely to be exposed to higher intensities of light due to the lack of melanin within the eye leading to iris transillumination and fundus hypopigmentation. Our data illustrates a significant positive correlation between eye pigmentation, specifically the PEL thickness of the iris, and axial length which suggests that hyperillumination in the retina may be the cause of hypermetropia.

Interestingly, Yahalom et al (2012) also found their participants with albinism who had profound hypopigmentation (OCA1A) were most likely to be hypermetropic, have severe levels of foveal hypoplasia and demonstrate the poorest BCVA (Gronskov, Ek et al. 2007, Yahalom, Tzur et al. 2012).

The hyperillumination theory may explain the trend of increasing hypermetropia (caused by decreasing axial length) with increasing severity of the albinism phenotype reflected by foveal hypoplasia, BCVA and PEL thickness. A recent study by Chen et al (2017) found that bright light exposure (2500-5000 lux) in mice, over a period of a month, inhibited form deprivation myopia development by reducing ocular elongation and shifting refraction towards hypermetropia as compared with changes occurring in normal light (100-200 lux) (Chen, Zhi et al. 2017). The authors hypothesise that bright light increases the dopamine receptor activity in the bipolar cells and is associated with less myopic shift and ocular elongation than those occurring in normal light. Retinal dopamine is also released in response to light and is a stop signal for the homeostatic control of eye growth (Iuvone, Tigges et al. 1991). Previous work in chicks (Cohen, Belkin et al. 2011) and rhesus monkeys (Iuvone, Tigges et al. 1991) also agree that high illumination levels inhibit form deprivation

myopia and lead to hypermetropia. A study by Cohen et al (2008) also suggests that ocular growth is controlled by the intrinsic circadian clock (endogenous oscillator) which controls the action of melatonin and dopamine based on a light-dark cycle. They postulate that the chicks who are exposed to a high intensity of light do not get sufficient “dark time” which reduces the release of melatonin and increases dopamine and thus leads to a lack of eye growth (Cohen, Belkin et al. 2008). Similarly, in albinism transillumination of the iris and lack of pigment in eye may cause hyperillumination and lack of “dark time” which could lead to increased dopamine production and thus reduce eye growth. Future studies assessing sleep patterns in albinism and light/dark time are worth consideration.

### **3. Retinal Crowding Hypothesis:**

Another potential hypothesis explaining the relationship between axial length and foveal hypoplasia is that of the crowded retina. This can be illustrated using a condition known as nanophthalmus. In nanophthalmus there is arrested development of the globe in all directions. It is characterised by a small eye with short axial length (<20mm) and high levels of hypermetropia. Amongst other clinical features, foveal hypoplasia is always demonstrated within this cohort of patients (Walsh and Goldberg 2007, Bijlsma, van Schooneveld et al. 2008, Helvacioğlu, Kapran et al. 2014). It has been hypothesised that this could be due to the lack of space for the fovea to develop leaving it hypoplastic.

In albinism a reduction in melanin and dopamine production is likely to lead to the reduced growth of the eye causing a shorter axial length which in turn could lead to foveal hypoplasia as there is not enough space structurally within the eye for the development of a fovea and successful foveal pit. Walsh and Goldberg (2007) state all of their cases with nanophthalmus demonstrate foveal hypoplasia, high hypermetropia and reduced vision (Walsh and Goldberg 2007).

This retinal crowding theory is likely to only relate to the smallest of eyes since most of the axial lengths in the albinism group fall within normal ranges (22-25mm) (Bhardwaj and Rajeshbhai 2013).

Mohammad et al (2015) assessed a wider range of optic nerve parameters and found a significant negative correlation between refractive error and optic disc, cup and rim size which means the higher the spherical refractive error (more hypermetropic), the smaller the eyes and this leads to a smaller and more crowded optic disc as there is not enough space for sufficient optic nerve development (Mohammad, Gottlob et al. 2015).

#### **4. Genetic Subtype:**

Unfortunately, within our data set, participants with albinism were not genetically classified due to cost implications. Genetic subtypes within the albinism group could further elucidate whether in fact pigmentation and development of pigmentation plays a large part in the development of refractive error and foveal hypoplasia in albinism. Previous literature has found that those individuals with albinism who were diagnosed with OCA1A demonstrated high levels of hypermetropia and the poorest vision (Yahalom, Tzur et al. 2012). This could potentially be the case for our patients if we divided them using genotyping.

We hope, with the introduction of genetic panels and the reducing cost of genetic testing, we may be able to do this in the future. However, using genetic testing to diagnose albinism may still be challenging because not all mutations have yet been discovered.

## **6.4.2 Other Groups**

### **6.4.2.1 IIN and *PAX6***

Healey et al (2013) created a group of NAIN patients to compare to their albinism group. However, they had a mixture of IIN, isolated foveal hypoplasia and *PAX6* in this group (Healey, McLoone et al. 2013). Due to the variation in phenotype within the groups we divided ours into IIN and *PAX6*.

For both IIN *and* PAX6 there were no significant associations when correlating refractive error with foveal hypoplasia (FHG or FDI). This could be for various reasons. Firstly, our data set only consisted of 18 individuals with IIN and 9 individuals with PAX6 which may be underpowered to identify correlations. Furthermore, the narrow range of grades of foveal hypoplasia encountered within the groups (IIN (grade 0 (n=12), grade 1 (n= 6)) and PAX6 (grade 1 (n=2), grade 2 (n=6), grade 3 (n=1)) mean there is little variability in foveal hypoplasia within these groups limiting correlation analysis. We used FDI to circumvent this issue since it provides a continuous scale. However, FDI did not reveal any relationships for refractive error and foveal hypoplasia.

### 6.4.2.2 Achromatopsia

There is no previous comparison of refractive errors to foveal development in achromatopsia (not included by Healey et al (2013) either). Within the grading scheme individuals with achromatopsia fall into the category of “atypical” and thus it is not possible to compare FHG to refractive error since there is only one grade. As mentioned above, using FDI circumvents this problem. Using this method we find a very interesting pattern between foveal hypoplasia and refractive error (SER and MAM) which is opposite to the pattern found in albinism. There is a negative correlation between refractive error and FDI meaning that as the FDI increases, the refractive errors become more myopic. The most likely explanation for this finding is the form deprivation hypothesis (without the interference of hyperillumination) in this case as greater foveal hypoplasia will lead to poorer foveal vision and form deprivation, leading to a myopic shift in refractive error as demonstrated in **Figure 6-16**.

## 6.4.3 Intergroup Differences

### 6.4.3.1 Foveal Hypoplasia

For FHG our four groups (albinism, IN, PAX6 and achromatopsia) exhibit different degrees of foveal hypoplasia. Those with albinism show the highest degree of FHG (subjective method) and also show

the most variability: this is likely to be due to the clinical variability of the phenotype. Interestingly, our FDI (objective method) demonstrated similar results. When we correlated FHG and FDI we found a highly significant correlation ( $P < 0.0001$ ) validating the reliability and accuracy of each measure when assessing foveal hypoplasia. This has not been demonstrated before.

### **6.4.3.2 BCVA**

The BCVA varies amongst all groups with nystagmus. Those with achromatopsia have the poorest BCVA, followed by the albinism group, *PAX6* group and then the IIN group. When comparing BCVA with FHG we found a significant positive correlation which corresponds to the findings from Thomas et al (2011) and Healey et al (2013). Those with better BCVA were found to have lower grades of FHG and vice versa for those with poorer BCVA. Similarly, when we conducted the same comparison for FDI with BCVA, we found a significant positive correlation.

### **6.4.3.3 Refractive Error**

When comparing all groups (albinism, IIN, *PAX6* and achromatopsia) spherical equivalent refractive errors (SER) or most ametropic meridian (MAM) there are no significant differences found between the groups.

Our findings demonstrate that refractive errors in albinism pull in both directions (myopia and hypermetropia) whereas in achromatopsia they are found to be going in a myopic direction.

In albinism it appears our results are affected by form deprivation and retinal crowding but the overarching factor is the hyperillumination which is caused by the lack of pigment throughout the eye, especially the iris. There doesn't seem to be a single cause to refractive error in albinism, it appears multi-factorial. In achromatopsia, from our results, it appears foveal structure leads to form deprivation and impacts refractive error.

## 6.5 Limitations of Study

Study limitations are listed below:

- Individuals with higher than + or - 10 dioptres were excluded from the study as OCT in these individuals was not possible. This led to two participants from the *PAX6* group to be excluded from this study who had refractions higher than this limit.
- Subjective refraction often relies on the examiner's opinions of refractive error and these can occasionally vary between examiners: this factor is unlikely to be controlled unless all refractions are carried out by one experienced optometrist.
- Lack of genetic diagnosis in albinism makes it difficult to assess whether specific refractive errors in albinism are linked to a specific genotype.

## 6.6 Future Direction

Following on from this study comparing refractive error and foveal hypoplasia it appears the relationship between foveal structure and refractive error could be disease-specific. Taking this one step further, it would be prudent to assess the genotype of these patients to assess whether exact genetic diagnosis lead to specific refractive errors.

In addition, in the future, if OCT allows successful scanning in patients who are more than +10 or -10 spherical refractive error, it would provide the ability to assess those with extremely high refractive errors (two individuals with *PAX6* mutation were excluded due to the inability to obtain OCT images due to high refractive error).

Although not the principal aim of this study, we could also factor in nystagmus and the effect of nystagmus on refractive error.

# **Chapter 7**

# **Conclusion**

## Chapter 7 Conclusion

The main aim of this thesis was to characterise the phenotypic features of the visual pathway in albinism using novel and established methods.

### 7.1 Principal Findings

#### **Study 1: Iris Cross-Sectional Imaging in Albinism using Optical Coherence Tomography**

- Significant iris thinning occurs in albinism, with the posterior epithelial layer (PEL) being the principally affected layer.
- AS-OCT imaging of the iris can be used to assist the diagnosis of albinism.

#### **Study 2: Visual Fields in Albinism and IIN**

- The upper nasal VF in albinism demonstrated significantly worse detection thresholds compared to the other quadrants.
- Nasal/temporal asymmetries exist in the VFs in albinism but not in IIN and we see a positive correlation between this asymmetry and the VEP asymmetry (measured using Apkarian's method) for the left eye but not the right eye.
- The left eye showed significantly poorer detection thresholds compared to the right eye and this was found to be significantly influenced by eye dominance.

#### **Study 3: The Comparison of Visual Field to Foveal and Optic Nerve OCT Parameters in Albinism**

- There were correlations between central VF detection threshold and foveal OCT layers with increasing foveal hypoplasia being associated with worse central detection threshold in albinism.
- There was a lack of any significant correlation between VF quadrant detection thresholds and ppRNFL thickness around the optic nerve.

## **Study 4: Investigating the Relationship between Foveal Morphology and Refractive Error in**

### **Infantile Nystagmus**

- Foveal hypoplasia (FHG and FDI) is significantly related to refractive error in albinism. Higher levels of foveal hypoplasia are related to hypermetropia whereas lower levels of foveal hypoplasia are related to myopia.
- The axial length is strongly correlated with refractive error, level of pigmentation in the iris (PEL thickness) and BCVA in albinism.
- The subjective (FHG) and objective (FDI) measures of foveal hypoplasia have shown to reliably quantify foveal hypoplasia and FDI allows further intergrade analysis of foveal hypoplasia.
- FDI is significantly related to refractive error in achromatopsia, however in the opposite direction to albinism (higher levels of foveal hypoplasia lead to myopia).

## 7.2 The Significance of Study Findings

Figure 7-1 outlines different phenotyping measures and the modes of assessment used to evaluate visual pathway anomalies.

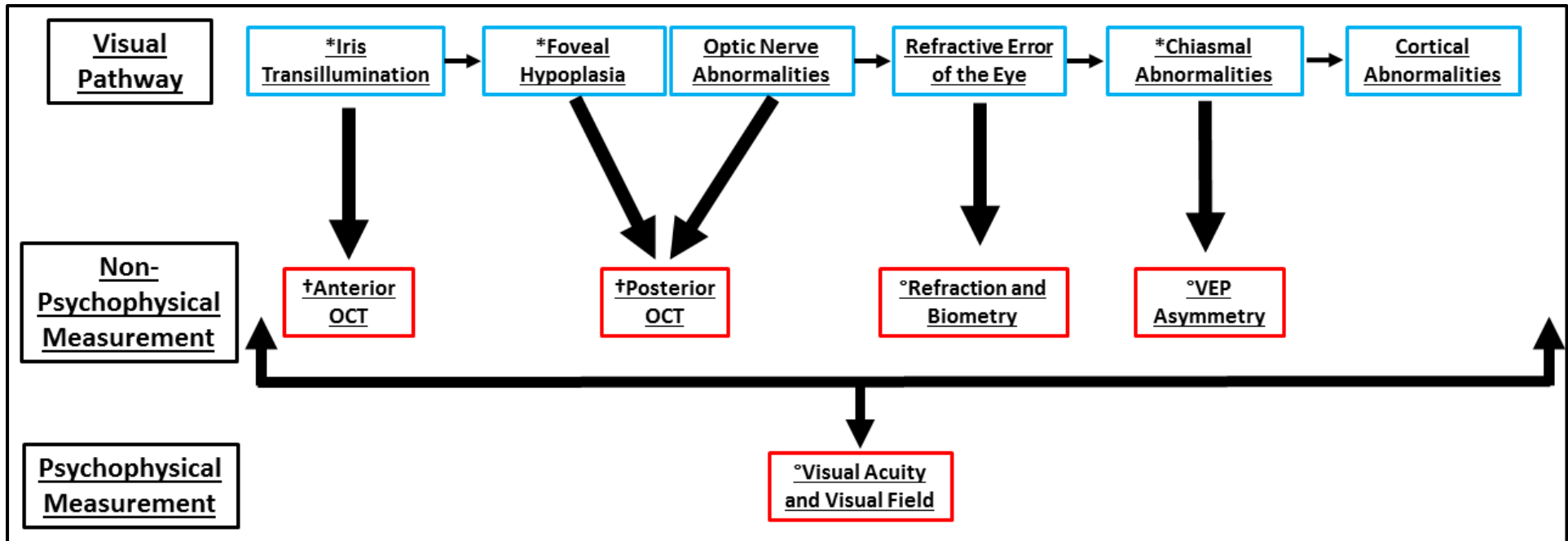


Figure 7-1: Visual pathway anomalies observed in albinism and mode of assessment used. Visual acuity and visual field measures are the cumulative effect of visual deficits along the whole visual pathway since they are psychophysical methods that require a response. Nystagmus is another visual pathway anomaly but was not the focus of this thesis. \*Signs used to diagnose albinism. †New OCT assessment techniques. °Conventional assessment techniques.

Associated with the assessment of various visual pathway anomalies in albinism, numerous themes developed throughout the thesis. These were (i) the development of diagnostic signs in albinism, (ii) use of assessments of local visual pathway deficits to understand psychophysical measures which evaluate the whole visual pathway (i.e. visual fields and visual acuity), (iii) exploring causal relationships between visual pathway deficits, and (iv) correlation between related and unrelated phenotypical features in albinism.

**(i) Diagnosis of albinism**

The diagnosis of albinism is often difficult. Genetic testing is currently very expensive and therefore it is not routinely offered in healthcare, in addition, all genes associated with albinism have not yet been identified. For example, Gronskov et al (2007) estimates that 50% of OCA mutations remain undetected (Gronskov, Ek et al. 2007). With the introduction of gene panels there is hope that the cost of genetic assessment will become more affordable in the coming years (Thomas, Maconachie et al. 2017).

When using phenotypic signs to diagnose albinism, the co-existence of three signs: (i) iris transillumination, (ii) foveal hypoplasia, and (iii) chiasmal misrouting are the standard procedure used in reaching an accurate diagnosis. These three signs constitute the diagnostic criteria used in this study. Additionally, the majority of individuals with albinism also have nystagmus. This included all of the participants in this study.

Posterior (foveal and optic nerve) OCT has been recently identified as a new tool in the diagnosis of all participants with nystagmus (Mohammad, Gottlob et al. 2011, Thomas and Gottlob 2012), especially in children where other diagnostic tests (e.g. VEP) can be challenging (Lee, Sheth et al. 2013). A new adjunct to this was added in **Chapter 3** using iris AS-OCT which has proven to be effective as a diagnostic aid in albinism. This novel imaging and analysis technique can be used in any study considering the iris and is not confined to use with just albinism. This now moves all of the three diagnostic signs for albinism from the realm of

subjective clinical grading methods to quantifiable methods for which criteria can be defined and tested.

In addition, the correspondence between FDI and FHG in **Chapter 6 (Figure 6-7)** indicates that there is more than one way to observe and quantify foveal hypoplasia. This is especially useful for conditions where the foveal hypoplasia grading falls within one grade as occurs in participants with achromatopsia.

(ii) **Assessment of local visual pathway deficits to understand measures of the whole visual pathway**

We were able to identify newly described VF anomalies in albinism as discussed in **Chapter 4**. The upper nasal VF quadrant demonstrated a significantly lower detection threshold compared to all other quadrants. One difficulty in interpreting these results is that VF measures represent the cumulative effect of visual deficits along the whole visual pathway (as shown in **Figure 7-1**). Psychophysical measures such as VF and visual acuity both require perception of stimuli at a cortical level since they require a voluntary response from the participant.

In **Chapter 5** we correlated objective structural measurements of the fovea and optic nerve (ppRNFL) using OCT to determine if early pathway deficits are the likely cause of some of our findings within **Chapter 4**. Essentially, our correlations between ppRNFL thickness around the optic nerve and sectoral VF detection thresholds were negative. A potential reason for the lack of any significant correlation between ppRNFL and VF quadrants could be that the exact route of ppRNFL fibres entering the optic nerve in albinism is unknown and thus assumptions were made about the VF locations and their projections based on anatomy and previous work in glaucoma. However, the differences found on the VF may be due to localised functional abnormalities of retinal ganglion cells or their inputs which do not manifest as structural changes. Alternatively they may be due to retrobulbar changes such as changes in cortical connectivity.

In contrast, our correlations between foveal layers and central detection threshold proved informative. The degree of foveal hypoplasia correlated significantly to central VF detection threshold indicating that the degree of central VF attenuation reflects the degree of foveal hypoplasia suggesting some clinical utility of VF for detecting central abnormalities if OCT is unavailable.

We also discovered significant positive correlations when comparing VEP asymmetry (using Apkarian's method) to nasal/temporal and upper nasal quadrant asymmetry on VF, for the left eye only but not the right eye. These correlations between VEP asymmetry and VF might suggest retrobulbar connectivity at the LGN or the visual cortex may underlie the quadrant deficits seen. Hoffman and Dumoulin (2015) summarise differing patterns of visual representation in albinism at a cortical level (Hoffmann and Dumoulin 2015). In humans with albinism this pattern was considered as the interleaved representation pattern (formerly "True Albino pattern") which allows the use of VF stimuli from both eyes without suppressing it (Hoffmann, Tolhurst et al. 2003), Welton et al (2017) have also recently shown that there are differences in white matter and interhemispheric hyper-connectivity in albinism (Welton, Ather et al. 2017).

Along with VFs, visual acuity, being a psychophysical measure represents the cumulative effect of visual pathway deficits and can be affected by numerous anomalies associated with albinism.

We found significant negative correlations for both total iris thickness and PEL thickness with BCVA. Thicker layers for both AS-OCT measures are associated with better visual acuity which indicate that in albinism, less iris transillumination is related to better vision. This adds to the growing literature explaining the cause of visual acuity deficits in albinism. Previously, Mohammad et al (2011) has shown that OS length is inversely correlated with visual acuity in albinism. This is due to albinism interfering with the specialisation of cones at the fovea where

they are normally longer and thinner to facilitate dense packing (Mohammad, Gottlob et al. 2011). In contrast, Dunn et al (2017) measured visual acuity in patients with nystagmus at different gaze angles (causing different intensity of nystagmus) and found this did not change visual acuity significantly (Dunn, Wiggins et al. 2017). This would suggest that nystagmus in general is not a significant factor in the visual acuity in albinism.

**(iii) Exploring causal relationships between pathway deficits**

In **Chapter 6** we explored whether foveal hypoplasia (FHG and FDI) was related to refractive error in four distinctly diagnosed groups with nystagmus. We also explored how iris pigmentation was associated with refractive error in albinism due to the iris transillumination defect. Two principal theories exist which are likely to lead to refractive errors in our groups. These are form deprivation, caused by foveal hypoplasia, which leads to myopia (larger eyes) and hyperillumination which leads to hypermetropia (smaller eyes). In addition, nystagmus may lead to astigmatism. All four groups with nystagmus display a differing phenotype. Individuals with albinism exhibit foveal hypoplasia, iris transillumination, fundus hypopigmentation and chiasmal misrouting. Individuals with IIN show minimal foveal hypoplasia but no phenotypic signs. Those with *PAX6* mutation have foveal hypoplasia and additional anterior segment dysgenesis and those with achromatopsia have foveal hypoplasia (with a hypo-reflective zone), abnormal ERG response but no other eye signs. The iris transillumination and fundus hypopigmentation only significantly affects our albinism group and so hyperillumination is likely to have the biggest impact in this group.

All individuals with nystagmus have been shown to have astigmatism which has been predominantly with-the-rule; this is shown predominantly in literature for albinism (Wildsoet, Oswald et al. 2000, Wang, Wyatt et al. 2010). The main reason underlying this finding appears to be the horizontal nature of nystagmus in these patients (Wildsoet, Oswald et al. 2000, Wang, Wyatt et al. 2010). A study in chicks with albinism, but without nystagmus, found most

chicks exhibited against-the-rule astigmatism, postulating the importance of constant rhythmic side to side oscillations of the eye in the moulding of the shape of the eye (Rymer, Choh et al. 2007).

When assessing the development of spherical refractive error in relation to foveal hypoplasia we found significant and contrasting patterns between refractive errors and foveal hypoplasia in albinism and achromatopsia.

In achromatopsia, we also found a significant relationship between foveal hypoplasia (FDI) and refractive error in the expected direction where more foveal hypoplasia led to greater myopia presumably due to form deprivation.

Foveal hypoplasia (FHG and FDI) was significantly correlated to refractive error in albinism, but higher levels of foveal hypoplasia were associated to hypermetropia whereas lower levels of foveal hypoplasia were associated to myopia. The expected pattern of form deprivation is reversed here and the potential reason for this is that the iris transillumination defect is proportional to foveal hypoplasia in albinism. It appears that in albinism the hyperillumination caused by iris transillumination is the overarching factor in the development of refractive error and dominates the pattern of eye development in more severe forms of albinism. We also found a strong correlation between spherical refractive error and PEL thickness which supports this theory.

(iv) **Correlations between related and unrelated phenotypic features seen in albinism**

Throughout the course of this thesis there are numerous correlations that were seen, some expected and some unexpected. These are described in detail.

### **Expected correlations**

The correlation between total iris thickness, PEL thickness and subjective skin and hair pigmentation were expected as both measures relate to the level of pigmentation. Similarly the correlation between BCVA and total iris thickness and PEL thickness were also expected indicating better BCVA for those with thicker irides and less iris transillumination.

We also found a significant positive correlation between PEL thickness and axial length as well as also BCVA and axial length. These findings indicate a close association between the amount of light entering the eye and both axial length and visual acuity. We hypothesise that in albinism foveal hypoplasia may not be the key factor in the causation of refractive errors and that hyperillumination overrides form deprivation caused by foveal hypoplasia.

Another expected correlation was between RPE (retinal pigment epithelium) and PEL thickness, since these are both pigmented epithelial layers, however, surprisingly no correlation was evident. Both of these measures have the same origin and thus it was assumed would develop similarly. A recent study by Wilk et al (2017) provides a plausible explanation for the lack of correlation between RPE and PEL in describing the difficulty in delineating outer retinal layers below the outer segment layer using OCT. This investigation reports that higher levels of melanin below the outer segment layer leads to difficulties in separating out retinal layers (Wilk, Huckenpahler et al. 2017).

### **Unexpected correlations**

There are some surprising correlations noted within this thesis where the relationship between two separate measures were difficult to interpret. An example of this is the negative correlation between nystagmus intensity and PEL thickness which indicates the nystagmus is of a higher intensity in individuals where the PEL is thinner. The reasons for this are unclear.

A recent study by Yonehara et al (2016) has found that horizontal retinal motion sensitivity abnormalities in the retina are causative of nystagmus. They found that in mice with *FRMD7* mutations, known to cause horizontal nystagmus in humans, there is a selective loss of horizontal direction selectivity in RGCs. In wild-type retinas the *FRMD7* was specifically expressed in starburst amacrine cells which is the interneuron that provides asymmetric inhibition to direction-selective retinal ganglion cells (Yonehara, Fiscella et al. 2016). This study suggests involvement of a specific inhibitory neuron type in *FRMD7*. It is not presently known if this is the cause of nystagmus in albinism. However, structural abnormalities of RGCs clearly exist in albinism in terms of their projections (crossed or uncrossed) and also their arrangement around the fovea. The function of motion sensitive RGCs and starburst amacrine cells in albinism provide a fascinating area for elucidating mechanisms underlying nystagmus.

## 7.3 Clinical, Scientific and Methodological Advancement

This thesis shows how the phenotypic features in albinism can affect the visual pathway and have a cascading effect on visual potential. Novel findings are summarised below.

### 7.3.1 Clinical and Scientific Advances

We have, for the first time, investigated ultra-structural iris changes underlying iris transillumination defects in albinism and have found that the iris pigment epithelial layer (PEL) is responsible for the abnormality. We have also demonstrated the potential of iris OCT to aid the diagnosis of albinism and its potential role for objective measurements of pigmentation for future clinical trials.

With respect to the visual fields in albinism, there is disagreement in findings from previous authors as to whether nasal/temporal asymmetry exists in visual fields in albinism (St John and Timney 1981, Abadi and Pascal 1993, Hoffmann, Seufert et al. 2007). Our study, which incorporates a large cohort of albinism patients (n=61), finds a significant nasal/temporal asymmetry in albinism but even more interestingly finds a novel vertical visual field deficit. The upper nasal visual field in albinism has a significantly worse detection threshold compared to all other quadrants. We conducted a correlation with OCT changes to help understand the visual field differences found in albinism. We observed that the foveal changes in retinal layers help explain differences in central detection threshold in albinism. However, the changes in ppRNFL thickness around the optic nerve were not correlated to visual field deficits.

For the assessment of relationships between foveal structure and refractive error in nystagmus our findings are at odds with previous work by Healey et al (2013) (Healey, McLoone et al. 2013). We find relationships between foveal structure and refractive error are disease-specific with significant correlations found for albinism and achromatopsia. In albinism we find that

foveal hypoplasia is related to refractive error although hyperillumination (due to the iris transillumination defect) is likely to be the overriding factor pushing refractive error in the hypermetropic direction. In contrast, in achromatopsia it appears that form deprivation (due to the hyper-reflective zone) causes myopia that is related to the degree of foveal hypoplasia.

We also compare an objective (foveal development index (FDI)) and subjective (foveal hypoplasia grading (FHG)) measure of foveal hypoplasia and find they correlate significantly to one another, indicating both as useful scientific and clinical measures of foveal hypoplasia.

### **7.3.2 Methodological advances**

Our studies have provided advancements in methodology which are already being implemented in ophthalmology clinics as well as in clinical research.

Using the ultra-high resolution OCT, we have developed methodology for the objective measurement of the iris using AS-OCT for the first time. This can be used in albinism as well as any other condition where the iris structure is of importance.

Our method of visual field analysis is also different to previous literature as we have divided the visual field into 4 defined quadrants, which has allowed us to ascertain vertical visual field deficit asymmetries in albinism.

We have developed an objective means of assessment for foveal hypoplasia termed the foveal development index (FDI). In the future automated analysis of the FDI should be available and we have proven this to be an important tool in understanding how refractive error relates to foveal maldevelopment in achromatopsia and albinism.

## 7.4 Final Thoughts

To further understand the phenotypic features in albinism as well as other nystagmus associated conditions, one must consider phenotype and genotype correlations. Albinism is a spectrum disease where some genotypes show an accumulation of pigmentation through time whereas others do not. It is important to differentiate these to understand the condition further. It would be particularly interesting to determine whether some of these trends exist within an albinism genetic subtype or whether in fact some of the power is lost when analysing across groups since the pattern may only be group specific. In recent years the cost for genetic analysis has started to reduce and with the introduction of gene panels, this has made genotype-phenotype correlations for our patients a distinct possibility. The author has collaboratively assisted with one such panel for nystagmus (Thomas, Maconachie et al. 2017).

## 7.5 Future Research

Research leading on from our findings is prudent. Important areas of future research are as follows:

1. Phenotype/genotype correlations in albinism
2. The comparison of visual field asymmetry to the optic chiasm and cortical measures in albinism
3. Investigate refractive error and biometrical measures in other early onset eye disease which leads to poor vision.
4. Conduct dark therapy in mice with albinism to aid eye growth to assess whether this improves visual prognosis.
5. Assess the development of retina, optic nerve and iris in children with albinism using Hand-Held OCT (HH-OCT)
6. Directional sensitivity of RGCs in albinism

## 7.6 Publication Plan

A current publication list and future publication plan is described in Appendix B.



# **Appendices**

## **Appendix A:**

### **Example Participant Information Leaflet and Consent Form (up to date)**

Please see next page

## ADULT PATIENT INFORMATION LEAFLET

### **Genetic studies of common and complex strabismus and their associated anomalies**

We invite you to consider taking part in a research project. Before you decide it is important for you to understand why the research is being done and what it will involve. Please take time to read the following information carefully and discuss it with others if you wish. Ask us if there is anything that is not clear or if you would like more information. Take time to decide whether or not you wish to take part.

#### **What is the purpose of the study?**

Genes are found in the cells of our body and are the instructions that tell our body how to grow and develop. They are passed on to us (inherited) from our parents. The DNA sequence that makes up our genes is remarkably similar from one person to the next, but tiny variations do occur, making each of us a unique individual. Most of these changes in our genes are harmless and cause such variation as eye colour and height. There can also be changes in genes that cause them not to work properly and lead to health problems or disease. We wish to determine and understand which genes are important for brain development by studying the changes in genes of individuals who have disorders affecting their eye movement, cranial nerve abnormalities (nerves at the back of the brain which control how the eyes move), optic nerve and their associated anomalies including nystagmus (an involuntary, to-and-fro movement of the eyes). We hope that the knowledge we gain from this research will lead to improved diagnosis, management and treatment of these conditions.

#### **What will be involved if I take part in the study?**

Firstly, we will ask you to fill out a questionnaire about your medical history or ask for information about it. We will next ask for details of your relatives, whether you were born or married into the family, so we can construct a family tree. We will then carry out an eye examination. We may record your eye movements using videotapes, infrared video cameras and/or photography. All these examinations are completely harmless. We may also need to put drops in your eyes to dilate pupil to examine the back of eyes and also take photographs of the back of the eye with a camera or using a scanning light with equipment called optical coherence tomography to compare the retinal thickness at various levels. The eye drops will blur your vision for several hours after they have been used and you will be unable to drive.

We will also take a saliva or blood sample to test for DNA. If we perform all the examinations it will take up to a maximum of ninety minutes but in the majority of cases not

all the test will be required. In addition we would normally only need to see you once. Should you be unwilling to provide a saliva or blood sample, we can also take a swab from the inner lining of your cheek. However, this might give us less information.

**Why have I been chosen?**

You have been chosen for this study as your eye muscles are not working fully and as a result have a lazy/turn of the one eye or associated problem.

**What is the benefit of this study to others and me?**

We hope to identify the genes, which are responsible for disorders of common and complex strabismus (a turn in one eye or “lazy eye”) and any defects in the muscle associated with it for example nystagmus. This may not lead to direct benefits for patients or their relatives. However, some families may wish to consider a gene test in the future. Knowledge of the way the gene works may lead to new approaches to both treatment and prevention of the eye problems.

**Will information obtained in the study be confidential?**

Any personal information and individual results will be kept confidential. The tests will be recorded in your medical records and will be treated with the usual degree of confidentiality under the data protection act. You will not be identified in any documents relating to the study. Any information will be accessible by research staff only and will be stored within the research department in a secure and locked location and/or on a password-protected database

**What will happen to the DNA obtained in this study?**

In order to obtain the results from your DNA we are collaborating with Harvard University in Boston, USA and other collaborators who specialise in certain eye conditions relating to this study. As part of this process we will allocate your DNA samples and any clinical information, collected during this study, a unique coding number. It is this unique code that will be given to collaborators along with your DNA and clinical information and not your personal details. This is to ensure that only those which have a direct link to the project within this department will have access to personal data.

DNA obtained from your sample may be used to search, identify and study genes involved in complex and common strabismus and their associated anomalies. They may use techniques that study all of your genes, only some of your genes and/or parts of your genetic material that do not have a currently known purpose or function. We may also use a technique called linkage analysis which involves comparing your DNA with other members of the family to look for similarities and differences in your genetic make-up. These will then be compared with other families who have a similar eye condition in order to find the causative gene.

Other techniques may include whole genome analysis in which all or most of your genetic code is studied and used to find the causes of your disorder, or the disorder in your family. In some cases we may use blood, if a sample has been taken, that has already been drawn to grow your blood cells in a dish. Blood cells grown in this manner can survive indefinitely, providing a greater source of genetic material. We may also use your blood to examine your chromosomes for abnormalities that may cause the eye movement disorder.

As part of this research we would like to store any remaining samples for future use. The remaining samples may be stored indefinitely and may be used for further studies on complex and common strabismus and their associated anomalies. If shared with any outside collaborator, which often occurs in order to analysis the DNA, your identity will not be shared. Your samples will be held in accordance with appropriate legislation and will remain in the possession of Dr. Engle or her successors at Children's Hospital Boston at our other collaborators site under their unique code. If at any time you would like to have your sample removed from storage, please let us know and it will be transferred or destroyed according to your wishes.

Results obtained prior to your sample removal will remain part of the study. In order to allow researchers to share results, the National Institutes of Health (NIH) and other organisations have developed special data/information banks that collect and analyze DNA samples and results of whole genome studies. If provided to them, these central banks would store your DNA and sample (s) and give them to other researchers to do more studies. Your sample(s) and data would be sent with your unique code number; no identifiable information about you would ever be given to central banks. We do not think there will be further risks to your privacy and confidentiality by sharing your samples and whole genome information with these banks. There are many safeguards in place to protect your information and sample(s) while they are stored in these banks and used for research.

You should be aware that they may detect instances of non-paternity (the discovery through the analysis of genetic testing that the father is someone other than who he was thought to be), and such information may interfere with our analysis. This non-paternity information will be kept in the strictest confidence and will not be divulged to anyone.

#### **What if I am harmed by the study?**

All the tests within this study have minimal risk but if you are harmed by taking part in this research project, there are no special compensation arrangements. If you are harmed due to someone's negligence, then you may have grounds for a legal action but you may have to pay for it. Regardless of this, if you wish to complain, or have any concerns about any aspect of the way you have been approached or treated during the course of this study, the normal National Health Service complaints mechanisms should be available to you. This can be done by contacting the NHS Patient information and Liaison Service (PILS) on 0808178 8337 or by writing to:

The Chief Executive  
Trust Headquarters  
Gwendolen House  
Gwendolen Road  
Leicester, LE5 4QF

#### **Who is organising and funding the research?**

The National Institute of Health (NIH) is funding this project.

**Who has reviewed the study?**

All research in the NHS is looked at by an independent group of people called a Research Ethics Committee to protect your safety, rights, wellbeing and dignity. This study has been reviewed and given favourable opinion by a Research Ethics Committee.

**What happens if I do not wish to participate in this study or wish to withdraw from the study?**

You are not under any obligation to participate in these studies. If you do enter the study and subsequently wish to withdraw please inform the Ophthalmology Department at University of Leicester NHS trust. You need give no reason for doing so. Medical care of both yourself and other members of your family will not be affected if you decide not to participate in the study.

**Will I receive out of pocket expenses for taking part in the study?**

Return travel expenses from your home to the Leicester Royal Infirmary will be reimbursed if you come especially for the research. You will not receive any payment for the tissue. The tissue is a gift - neither you nor your relatives will benefit from any inventions that result from the use of the tissue.

**What will happen to the results of the research study?**

The blood sample and the tissue sample that you provide are for research purposes only, to help us find the gene that may cause problems of eye movements. This study may take two to five years to complete; the results will be published in medical journals.

**Who do I contact for further information?**

Professor Irene Gottlob  
Ophthalmology  
The Robert Kilpatrick Clinical Sciences Building  
PO Box 65, The Leicester Royal Infirmary  
Leicester, LE2 7LX.

Tel: 0116 2586291

Fax: 0116 2558810

**Thank you for reading this**

Centre Number:  
Study Number:  
Patient Identification Number for this trial:

### ADULT PATIENT CONSENT FORM

Genetic studies of common and complex strabismus and their associated anomalies.

Name of Researcher/Principal Investigator: Professor Irene Gottlob  
Professor of Ophthalmology  
Tel: 0116 2586291

Name of adult: \_\_\_\_\_

Address of adult: \_\_\_\_\_  
\_\_\_\_\_

DOB of adult: \_\_\_\_\_

This form shall be read in conjunction with the Adult Information Leaflet, Version 4, dated 24<sup>th</sup> April 2012.

**Please initial the following box(es):**

1. I confirm that I have read and understand the Adult Patient Information Leaflet dated 24<sup>th</sup> April 2012, Version 4, for the above study and have had the opportunity to ask questions.
2. I understand that I may withdraw my consent to my tissue being used at any time without justifying my decision and without affecting my normal care and medical management.
3. I agree to donate the tissue (DNA) samples as detailed below and allow their use in medical research as described in the Adult Information Leaflet.
4. I understand that the tissue is a gift and that I will not benefit from any intellectual properties that result from the use of the tissue.
5. **I agree /do not agree** to my saliva samples/ mouth swab/ blood being used to undertake genetic research as described in the Adult Patient Information Leaflet.   
**(Patient to delete as applicable)**

6. **I agree / do not agree** to my tissue samples being used to undertake genetic research as described in the Adult Information Leaflet.
- (Patient to delete as applicable)**
7. **I agree/do not agree** for my tissue samples to be used in future studies associated with complex and common strabismus and their associated anomalies.
8. I understand that if research using my tissues produces information, which has immediate clinical relevance to me, I will be informed by my hospital consultant or GP and be given an opportunity to discuss the results.
9. I understand that sections of any of my medical notes may be looked at by responsible individuals from the research team, [Ophthalmology, University of Leicester], Sponsor and NHS Trust, or from regulatory authorities where it is relevant to my taking part in research. I give permission for these individuals to have access to my records.
10. I understand that tissue samples and associated clinical data may be transferred to non-commercial research partners of the University Hospitals of Leicester NHS Trust and Ophthalmology, University of Leicester, but that the personal information will be removed prior to transfer.
11. I agree to taking part in the following eye examinations:  
**(please tick if possible in box(es) below)**
- Eye examination
  - Video recording
  - Photography
  - Eye movement recording
12. The samples which I hereby consent to donate are:  
**(please tick if possible in box(es) below)**
- Saliva, Mouth Swabs
  - Blood
  - Nail clipping, hair
  - Muscle tissue from outside the eye
13. I agree to take part in the above study.

Signature of adult \_\_\_\_\_

(Name in BLOCK LETTERS): \_\_\_\_\_

Date: \_\_\_\_\_

I confirm I have explained the nature of the Study, as detailed in the Adult Information Leaflet, in terms, which in my judgment are suited to the understanding of the adult.

Signature of investigator: \_\_\_\_\_

(Name in BLOCK LETTERS): \_\_\_\_\_

Date: \_\_\_\_\_

## Appendix B:

### Publications as first author

Sheth V, Gottlob I, Mohammad S, McLean RJ, Maconachie GD, Kumar A, Degg C, Proudlock FA. Diagnostic potential of iris cross-sectional imaging in albinism using optical coherence tomography. *Ophthalmology*. 2013 Oct; 120(10):2082-90. doi:10.1016/j.ophtha.2013.03.018. Epub 2013 May 29. PubMed PMID: 23725737.

### Collaborative publications related to thesis

Thomas MG, Maconachie G, Sheth V, McLean RJ, Gottlob I. Development and clinical utility of a novel diagnostic nystagmus gene panel using targeted next-generation sequencing. *Eur J Hum Genet*. 2017 Jun;25(6):725-734. doi: 10.1038/ejhg.2017.44. Epub 2017 Apr 5. PubMed PMID: 28378818; PubMed Central PMCID: PMC5477371.

Mohammad S, Gottlob I, Sheth V, Pilat A, Lee H, Pollheimer E, Proudlock FA. Characterization of Abnormal Optic Nerve Head Morphology in Albinism Using Optical Coherence Tomography. *Invest Ophthalmol Vis Sci*. 2015 Jul;56(8):4611-8. doi: 10.1167/iovs.15-16856. PubMed PMID: 26200501.

Mohammad S, Gottlob I, Kumar A, Thomas M, Degg C, Sheth V, Proudlock FA. The functional significance of foveal abnormalities in albinism measured using spectral-domain optical coherence tomography. *Ophthalmology*. 2011 Aug;118(8):1645-52. doi: 10.1016/j.ophtha.2011.01.037. Epub 2011 May 12. PubMed PMID: 21570122.

Lee H, Purohit R, Sheth V, Papageorgiou E, Maconachie G, McLean RJ, Patel A, Pilat A, Anwar S, Sarvanathan N, Proudlock FA, Gottlob I. Retinal development in albinism: a prospective study using optical coherence tomography in infants and young children. *Lancet*. 2015 Feb 26;385 Suppl 1:S14. doi: 10.1016/S0140-6736(15)60329-4. PubMed PMID: 26312836.

Lee H, Sheth V, Bibi M, Maconachie G, Patel A, McLean RJ, Michaelides M, Thomas MG, Proudlock FA, Gottlob I. Potential of handheld optical coherence tomography to determine cause of infantile nystagmus in children by using foveal morphology. *Ophthalmology*. 2013 Dec;120(12):2714-24. doi: 10.1016/j.ophtha.2013.07.018. Epub 2013 Oct 22. PubMed PMID: 24161406.

**Publications as first author in preparation**

Novel Visual Field Deficits in Albinism. Sheth V, Gottlob I, Proudlock FA.

The role of foveal hypoplasia and iris transillumination in determining Refractive Error in Infantile Nystagmus? Sheth V, Gottlob I, Proudlock FA

## References

- (2016). "In vivo features of Fox-Fordyce disease in high-definition optical coherence tomography." *J Dtsch Dermatol Ges* **14**(3): 340.
- Abadi, R. V. and C. M. Dickinson (1986). "Waveform characteristics in congenital nystagmus." *Doc Ophthalmol* **64**(2): 153-167.
- Abadi, R. V. and E. Pascal (1993). "Incremental light detection thresholds across the central visual field of human albinos." *Invest Ophthalmol Vis Sci* **34**(5): 1683-1690.
- Abadi, R. V. and E. Pascal (1994). "Ocular motor behaviour of monozygotic twins with tyrosinase negative oculocutaneous albinism." *Br J Ophthalmol* **78**(5): 349-352.
- Abadi, R. V. and E. Pascal (1994). "Periodic alternating nystagmus in humans with albinism." *Invest Ophthalmol Vis Sci* **35**(12): 4080-4086.
- Abadi, R. V. and C. J. Scallan (2000). "Waveform characteristics of manifest latent nystagmus." *Invest Ophthalmol Vis Sci* **41**(12): 3805-3817.
- Abe, T., M. Yoshida, Y. Yoshioka, R. Wakusawa, Y. Tokita-Ishikawa, H. Seto, M. Tamai and K. Nishida (2007). "Iris pigment epithelial cell transplantation for degenerative retinal diseases." *Prog Retin Eye Res* **26**(3): 302-321.
- Akeo, K., S. Shirai, S. Okisaka, H. Shimizu, H. Miyata, A. Kikuchi, T. Nishikawa, K. Suzumori, T. Fujiwara and A. Majima (1996). "Histology of fetal eyes with oculocutaneous albinism." *Arch Ophthalmol* **114**(5): 613-616.
- Akerman, C. J., D. J. Tolhurst, J. E. Morgan, G. E. Baker and I. D. Thompson (2003). "Relay of visual information to the lateral geniculate nucleus and the visual cortex in albino ferrets." *J Comp Neurol* **461**(2): 217-235.
- Al-Araimi, M., B. Pal, J. A. Poulter, M. M. van Genderen, I. Carr, T. Cudrnak, L. Brown, E. Sheridan, M. D. Mohamed, J. Bradbury, M. Ali, C. F. Inglehearn and C. Toomes (2013). "A new recessively inherited disorder composed of foveal hypoplasia, optic nerve decussation defects and anterior segment dysgenesis maps to chromosome 16q23.3-24.1." *Mol Vis* **19**: 2165-2172.
- Anderson, J., J. Lavoie, K. Merrill, R. A. King and C. G. Summers (2004). "Efficacy of spectacles in persons with albinism." *J AAPOS* **8**(6): 515-520.
- Ansons, A. M. and H. Davis. (2000). "Diagnosis and Management of Ocular Motility Disorders." from <http://public.eblib.com/EBLPublic/PublicView.do?ptiID=470241>.
- Apkarian, P. (1992). "A practical approach to albino diagnosis. VEP misrouting across the age span." *Ophthalmic Paediatr Genet* **13**(2): 77-88.
- Apkarian, P. (1993). "Temporal frequency responsivity shows multiple maturational phases: state-dependent visual evoked potential luminance flicker fusion from birth to 9 months." *Vis Neurosci* **10**(6): 1007-1018.
- Apkarian, P., D. Reits and H. Spekreijse (1984). "Component specificity in albino VEP asymmetry: maturation of the visual pathway anomaly." *Exp Brain Res* **53**(2): 285-294.
- Apkarian, P., D. Reits, H. Spekreijse and D. Van Dorp (1983). "A decisive electrophysiological test for human albinism." *Electroencephalogr Clin Neurophysiol* **55**(5): 513-531.
- Apkarian, P. and J. Shallo-Hoffmann (1991). "VEP projections in congenital nystagmus; VEP asymmetry in albinism: a comparison study." *Invest Ophthalmol Vis Sci* **32**(9): 2653-2661.
- Asuquo, M. E., O. Ngim, G. Ebughe and E. E. Basse (2009). "Skin cancers amongst four Nigerian albinos." *Int J Dermatol* **48**(6): 636-638.
- Bhansali, P., I. Rayport, A. Rebsam and C. Mason (2014). "Delayed neurogenesis leads to altered specification of ventrotemporal retinal ganglion cells in albino mice." *Neural Development* **9**(11): 1749-8104.
- Bengtsson, B., A. Heijl and J. Olsson (1998). "Evaluation of a new threshold visual field strategy, SITA, in normal subjects. Swedish Interactive Thresholding Algorithm." *Acta Ophthalmol Scand* **76**(2): 165-169.

Bengtsson, B., J. Olsson, A. Heijl and H. Rootzen (1997). "A new generation of algorithms for computerized threshold perimetry, SITA." *Acta Ophthalmol Scand* **75**(4): 368-375.

Bergen, A. A., C. Samanns, D. B. Van Dorp, M. A. Ferguson-Smith, A. Gal and E. M. Bleeker-Wagemakers (1990). "Localization of the X-linked ocular albinism gene (OA1) between DXS278/DXS237 and DXS143/DXS16 by linkage analysis." *Ophthalmic Paediatr Genet* **11**(3): 165-170.

Bezerra, H. G., M. A. Costa, G. Guagliumi, A. M. Rollins and D. I. Simon (2009). "Intracoronary optical coherence tomography: a comprehensive review clinical and research applications." *JACC Cardiovasc Interv* **2**(11): 1035-1046.

Bhardwaj, V. and G. P. Rajeshbhai (2013). "Axial length, anterior chamber depth-a study in different age groups and refractive errors." *J Clin Diagn Res* **7**(10): 2211-2212.

Bijlsma, W. R., M. J. van Schooneveld and A. Van der Lelij (2008). "Optical coherence tomography findings for nanophthalmic eyes." *Retina* **28**(7): 1002-1007.

Boissy, R. E. and J. J. Nordlund (1997). "Molecular basis of congenital hypopigmentary disorders in humans: a review." *Pigment Cell Res* **10**(1-2): 12-24.

Bowrey, H. E., A. P. Metse, A. J. Leotta, G. Zeng and S. A. McFadden (2015). "The relationship between image degradation and myopia in the mammalian eye." *Clin Exp Optom* **98**(6): 555-563.

Boycott KM, P. W., Bech-Hansen NT. (2000). "Clinical variability among patients with incomplete X-linked congenital stationary night blindness and a founder mutation in CACNA1F." *Can J Ophthalmol*. **35**(4): 204-213.

Brodsky, M. C. (2008). "Positive angle kappa: a confounding variable in the diagnostic testing of patients with albinism." *Br J Ophthalmol* **92**(4): 577-578.

Brodsky, M. C. and K. J. Fray (1997). "The prevalence of strabismus in congenital nystagmus: the influence of anterior visual pathway disease." *J AAPOS* **1**(1): 16-19.

Brodsky, M. C. and K. J. Fray (2004). "Positive angle kappa: a sign of albinism in patients with congenital nystagmus." *Am J Ophthalmol* **137**(4): 625-629.

Bruce, A., I. E. Pacey, J. A. Bradbury, A. J. Scally and B. T. Barrett (2013). "Bilateral changes in foveal structure in individuals with amblyopia." *Ophthalmology* **120**(2): 395-403.

Bussel, II, G. Wollstein and J. S. Schuman (2014). "OCT for glaucoma diagnosis, screening and detection of glaucoma progression." *Br J Ophthalmol* **98 Suppl 2**: ii15-19.

Carnide, E. M., C. M. Jacob, A. C. Pastorino, R. Bellinati-Pires, M. B. Costa and A. S. Grumach (1998). "Chediak-Higashi syndrome: presentation of seven cases." *Sao Paulo Med J* **116**(6): 1873-1878.

Charles, S. J., J. S. Green, J. W. Grant, J. R. Yates and A. T. Moore (1993). "Clinical features of affected males with X linked ocular albinism." *Br J Ophthalmol* **77**(4): 222-227.

Charles, S. J., A. T. Moore, J. W. Grant and J. R. Yates (1992). "Genetic counselling in X-linked ocular albinism: clinical features of the carrier state." *Eye (Lond)* **6 ( Pt 1)**: 75-79.

Chen, S., Z. Zhi, Q. Ruan, Q. Liu, F. Li, F. Wan, P. S. Reinach, J. Chen, J. Qu and X. Zhou (2017). "Bright Light Suppresses Form-Deprivation Myopia Development With Activation of Dopamine D1 Receptor Signaling in the ON Pathway in Retina." *Invest Ophthalmol Vis Sci* **58**(4): 2306-2316.

Cheng, W., D. K. Au, C. H. Knowles, P. Anand and P. K. Tam (2001). "Hirschsprung's disease: a more generalised neuropathy?" *J Pediatr Surg* **36**(2): 296-300.

Choi, J. A., J. S. Kim, H. Y. Park, H. Park and C. K. Park (2014). "Retinal nerve fiber layer thickness profiles associated with ocular laterality and dominance." *Neurosci Lett* **558**: 197-202.

Chong, G. T., S. Farsiu, S. F. Freedman, N. Sarin, A. F. Koreishi, J. A. Izatt and C. A. Toth (2009). "Abnormal foveal morphology in ocular albinism imaged with spectral-domain optical coherence tomography." *Arch Ophthalmol* **127**(1): 37-44.

Cohen, Y., M. Belkin, O. Yehezkel, I. Avni and U. Polat (2008). "Light intensity modulates corneal power and refraction in the chick eye exposed to continuous light." Vision Res **48**(21): 2329-2335.

Cohen, Y., M. Belkin, O. Yehezkel, A. S. Solomon and U. Polat (2011). "Dependency between light intensity and refractive development under light-dark cycles." Exp Eye Res **92**(1): 40-46.

Collewijn, H., P. Apkarian and H. Spekreijse (1985). "The oculomotor behaviour of human albinos." Brain **108 ( Pt 1)**: 1-28.

Cooymans, P., S. Al-Zuhaibi, R. Al-Senawi and A. Ganesh (2010). "Congenital fibrosis of the extraocular muscles." Oman J Ophthalmol **3**(2): 70-74.

Creel, D., A. E. Hendrickson and A. G. Leventhal (1982). "Retinal projections in tyrosinase-negative albino cats." J Neurosci **2**(7): 907-911.

Creel, D., C. J. Witkop, Jr. and R. A. King (1974). "Asymmetric visually evoked potentials in human albinos: evidence for visual system anomalies." Invest Ophthalmol **13**(6): 430-440.

Cruz-Inigo, A. E., B. Ladizinski and A. Sethi (2011). "Albinism in Africa: stigma, slaughter and awareness campaigns." Dermatol Clin **29**(1): 79-87.

De Moraes, C. G., V. J. Juthani, J. M. Liebmann, C. C. Teng, C. Tello, R. Susanna, Jr. and R. Ritch (2011). "Risk factors for visual field progression in treated glaucoma." Arch Ophthalmol **129**(5): 562-568.

Dell'Osso, L. F. (1985). "Congenital, latent and manifest latent nystagmus--similarities, differences and relation to strabismus." Jpn J Ophthalmol **29**(4): 351-368.

Dell'Osso, L. F. and R. B. Daroff (1975). "Congenital nystagmus waveforms and foveation strategy." Doc Ophthalmol **39**(1): 155-182.

Dessinioti, C., A. J. Stratigos, D. Rigopoulos and A. D. Katsambas (2009). "A review of genetic disorders of hypopigmentation: lessons learned from the biology of melanocytes." Exp Dermatol **18**(9): 741-749.

Dickinson, C. M. and R. V. Abadi (1984). "Corneal topography of humans with congenital nystagmus." Ophthalmic Physiol Opt **4**(1): 3-13.

Dunn, M. J., D. Wiggins, J. M. Woodhouse, T. H. Margrain, C. M. Harris and J. T. Erichsen (2017). "The Effect of Gaze Angle on Visual Acuity in Infantile Nystagmus." Invest Ophthalmol Vis Sci **58**(1): 642-650.

Eagle, R. C., Jr. (1988). "Iris pigmentation and pigmented lesions: an ultrastructural study." Trans Am Ophthalmol Soc **86**: 581-687.

Ezeilo, B. N. (1989). "Psychological aspects of albinism: an exploratory study with Nigerian (Igbo) albino subjects." Soc Sci Med **29**(9): 1129-1131.

Fercher, A. F. (2010). "Optical coherence tomography - development, principles, applications." Z Med Phys **20**(4): 251-276.

Fercher, A. F., C. K. Hitzenberger, W. Drexler, G. Kamp and H. Sattmann (1993). "In vivo optical coherence tomography." Am J Ophthalmol **116**(1): 113-114.

Fiergang, D. L., K. W. Wright and J. A. Foster (1999). "Unilateral or asymmetric congenital ptosis, head posturing, and amblyopia." J Pediatr Ophthalmol Strabismus **36**(2): 74-77.

Freddo, T. F. (1996). "Ultrastructure of the iris." Microsc Res Tech **33**(5): 369-389.

Fukai, K., S. A. Holmes, N. J. Lucchese, V. M. Siu, R. G. Weleber, R. E. Schnur and R. A. Spritz (1995). "Autosomal recessive ocular albinism associated with a functionally significant tyrosinase gene polymorphism." Nat Genet **9**(1): 92-95.

Fulton, A. B., D. M. Albert and J. L. Craft (1978). "Human albinism. Light and electron microscopy study." Arch Ophthalmol **96**(2): 305-310.

Gad, A., M. Laurino, K. R. Maravilla, M. Matsushita and W. H. Raskind (2008). "Sensorineural deafness, distinctive facial features, and abnormal cranial bones: a new variant of Waardenburg syndrome?" Am J Med Genet A **146A**(14): 1880-1885.

Galvao Filho, R. P., R. M. Vessani and R. Susanna, Jr. (2005). "Comparison of retinal nerve fibre layer thickness and visual field loss between different glaucoma groups." Br J Ophthalmol **89**(8): 1004-1007.

Garipis, N. and K. P. Hoffmann (2003). "Visual field defects in albino ferrets (*Mustela putorius furo*)."  
*Vision Res* **43**(7): 793-800.

Garway-Heath, D. F., G. E. Holder, F. W. Fitzke and R. A. Hitchings (2002). "Relationship between electrophysiological, psychophysical, and anatomical measurements in glaucoma."  
*Invest Ophthalmol Vis Sci* **43**(7): 2213-2220.

Garway-Heath, D. F., D. Poinoosawmy, F. W. Fitzke and R. A. Hitchings (2000). "Mapping the visual field to the optic disc in normal tension glaucoma eyes."  
*Ophthalmology* **107**(10): 1809-1815.

Gettys, L. A. and D. S. Wofford (2007). "Genetic control of albinism in pickerelweed (*Pontederia cordata* L.)."  
*J Hered* **98**(4): 356-359.

Giebel, L. B., R. K. Tripathi, R. A. King and R. A. Spritz (1991). "A tyrosinase gene missense mutation in temperature-sensitive type I oculocutaneous albinism. A human homologue to the Siamese cat and the Himalayan mouse."  
*J Clin Invest* **87**(3): 1119-1122.

Gronskov, K., C. M. Dooley, E. Ostergaard, R. N. Kelsh, L. Hansen, M. P. Levesque, K. Vilhelmsen, K. Mollgard, D. L. Stemple and T. Rosenberg (2013). "Mutations in *c10orf11*, a melanocyte-differentiation gene, cause autosomal-recessive albinism."  
*Am J Hum Genet* **92**(3): 415-421.

Gronskov, K., J. Ek and K. Brondum-Nielsen (2007). "Oculocutaneous albinism."  
*Orphanet J Rare Dis* **2**: 43.

Guibal, C. and G. E. Baker (2009). "Abnormal axons in the albino optic tract."  
*Invest Ophthalmol Vis Sci* **50**(12): 5516-5521.

Guillery, R. W., T. L. Hickey, J. H. Kaas, D. J. Felleman, E. J. Debruyne and D. L. Sparks (1984). "Abnormal central visual pathways in the brain of an albino green monkey (*Cercopithecus aethiops*)."  
*J Comp Neurol* **226**(2): 165-183.

Guillery, R. W. and J. H. Kaas (1971). "A study of normal and congenitally abnormal retinogeniculate projections in cats."  
*J Comp Neurol* **143**(1): 73-100.

Guillery, R. W., A. N. Okoro and C. J. Witkop, Jr. (1975). "Abnormal visual pathways in the brain of a human albino."  
*Brain Res* **96**(2): 373-377.

Haegerstrom-Portnoy, G., M. E. Schneck, W. A. Verdon and S. E. Hewlett (1996). "Clinical vision characteristics of the congenital achromatopsias. I. Visual acuity, refractive error, and binocular status."  
*Optom Vis Sci* **73**(7): 446-456.

Harwerth, R. S., A. S. Vilupuru, N. V. Rangaswamy and E. L. Smith, 3rd (2007). "The relationship between nerve fiber layer and perimetry measurements."  
*Invest Ophthalmol Vis Sci* **48**(2): 763-773.

Harwerth, R. S., J. L. Wheat, M. J. Fredette and D. R. Anderson (2010). "Linking structure and function in glaucoma."  
*Prog Retin Eye Res* **29**(4): 249-271.

Havertape, S. A. and O. A. Cruz (1998). "Abnormal head posture associated with high hyperopia."  
*J AAPOS* **2**(1): 12-16.

Healey, N., E. McLoone, G. Mahon, A. J. Jackson, K. J. Saunders and J. F. McClelland (2013). "Investigating the relationship between foveal morphology and refractive error in a population with infantile nystagmus syndrome."  
*Invest Ophthalmol Vis Sci* **54**(4): 2934-2939.

Helvacioglu, F., Z. Kapran, S. Sencan, M. Uyar and O. Cam (2014). "Optical coherence tomography of bilateral nanophthalmos with macular folds and high hyperopia."  
*Case Rep Ophthalmol Med* **2014**: 173853.

Helveston, E. M. (1990). "The value of strabismus surgery."  
*Ophthalmic Surg* **21**(5): 311-317.

Hewitt, A. W., L. S. Kearns, R. V. Jamieson, K. A. Williamson, V. van Heyningen and D. A. Mackey (2007). "PAX6 mutations may be associated with high myopia."  
*Ophthalmic Genet* **28**(3): 179-182.

Hingorani, M., K. A. Williamson, A. T. Moore and V. van Heyningen (2009). "Detailed ophthalmologic evaluation of 43 individuals with PAX6 mutations."  
*Invest Ophthalmol Vis Sci* **50**(6): 2581-2590.

Hoffmann, M. B. and S. O. Dumoulin (2015). "Congenital visual pathway abnormalities: a window onto cortical stability and plasticity." *Trends Neurosci* **38**(1): 55-65.

Hoffmann, M. B., B. Lorenz, A. B. Morland and L. C. Schmidtborn (2005). "Misrouting of the optic nerves in albinism: estimation of the extent with visual evoked potentials." *Invest Ophthalmol Vis Sci* **46**(10): 3892-3898.

Hoffmann, M. B., P. S. Seufert and L. C. Schmidtborn (2007). "Perceptual relevance of abnormal visual field representations: static visual field perimetry in human albinism." *Br J Ophthalmol* **91**(4): 509-513.

Hoffmann, M. B., D. J. Tolhurst, A. T. Moore and A. B. Morland (2003). "Organization of the visual cortex in human albinism." *J Neurosci* **23**(26): 8921-8930.

Horn, F. K., C. Y. Mardin, R. Laemmer, D. Baleanu, A. M. Juenemann, F. E. Kruse and R. P. Tornow (2009). "Correlation between local glaucomatous visual field defects and loss of nerve fiber layer thickness measured with polarimetry and spectral domain OCT." *Invest Ophthalmol Vis Sci* **50**(5): 1971-1977.

Huang, D., E. A. Swanson, C. P. Lin, J. S. Schuman, W. G. Stinson, W. Chang, M. R. Hee, T. Flotte, K. Gregory, C. A. Puliafito and et al. (1991). "Optical coherence tomography." *Science* **254**(5035): 1178-1181.

Hung, G. K. and K. J. Ciuffreda (1999). "Model of human refractive error development." *Curr Eye Res* **19**(1): 41-52.

Hutton, S. M. and R. A. Spritz (2008). "A comprehensive genetic study of autosomal recessive ocular albinism in Caucasian patients." *Invest Ophthalmol Vis Sci* **49**(3): 868-872.

Imes, D. L., L. A. Geary, R. A. Grahn and L. A. Lyons (2006). "Albinism in the domestic cat (*Felis catus*) is associated with a tyrosinase (TYR) mutation." *Anim Genet* **37**(2): 175-178.

Imesch, P. D., C. D. Bindley, Z. Khademian, B. Ladd, R. Gangnon, D. M. Albert and I. H. Wallow (1996). "Melanocytes and iris color. Electron microscopic findings." *Arch Ophthalmol* **114**(4): 443-447.

Inagaki, K., T. Suzuki, H. Shimizu, N. Ishii, Y. Umezawa, J. Tada, N. Kikuchi, M. Takata, K. Takamori, M. Kishibe, M. Tanaka, Y. Miyamura, S. Ito and Y. Tomita (2004). "Oculocutaneous albinism type 4 is one of the most common types of albinism in Japan." *Am J Hum Genet* **74**(3): 466-471.

Ip, J. M., S. M. Saw, K. A. Rose, I. G. Morgan, A. Kifley, J. J. Wang and P. Mitchell (2008). "Role of near work in myopia: findings in a sample of Australian school children." *Invest Ophthalmol Vis Sci* **49**(7): 2903-2910.

Iuvone, P. M., M. Tigges, R. A. Stone, S. Lambert and A. M. Laties (1991). "Effects of apomorphine, a dopamine receptor agonist, on ocular refraction and axial elongation in a primate model of myopia." *Invest Ophthalmol Vis Sci* **32**(5): 1674-1677.

Izquierdo, N. J., W. Townsend and I. E. Hussels (1995). "Ocular findings in the Hermansky-Pudlak syndrome." *Trans Am Ophthalmol Soc* **93**: 191-200; discussion 200-192.

Jeffery, G., G. Schutz and L. Montoliu (1994). "Correction of abnormal retinal pathways found with albinism by introduction of a functional tyrosinase gene in transgenic mice." *Dev Biol* **166**(2): 460-464.

Kasmann-Kellner, B., T. Schafer, C. M. Krick, K. W. Ruprecht, W. Reith and B. L. Schmitz (2003). "[Anatomical differences in optic nerve, chiasma and tractus opticus in human albinism as demonstrated by standardised clinical and MRI evaluation]." *Klin Monbl Augenheilkd* **220**(5): 334-344.

Kasmann, B. and K. W. Ruprecht (1996). "Might the refractive state in oculocutaneous albino patients be a clue for distinguishing between tyrosinase-positive and tyrosinase-negative forms of oculocutaneous albinism?" *Ger J Ophthalmol* **5**(6): 422-427.

Kausar, T., M. A. Bhatti, M. Ali, R. S. Shaikh and Z. M. Ahmed (2013). "OCA5, a novel locus for non-syndromic oculocutaneous albinism, maps to chromosome 4q24." *Clin Genet* **84**(1): 91-93.

King, R. A. (1993). Oculocutaneous Albinism Type 1. *GeneReviews*. R. A. Pagon, T. D. Bird, C. R. Dolan, K. Stephens and M. P. Adam. Seattle (WA).

King, R. A. (2000). "Oculocutaneous Albinism Type 1."

King, R. A., Hearing, V.J., Creel, D.J., Oetting, W.S, (1995). "Albinism. In the metabolic and molecular bases of inherited disease." New York , McGraw-Hill: 4353–4392.

King, R. A., R. A. Lewis, D. Townsend, A. Zelickson, D. P. Olds and J. Brumbaugh (1985). "Brown oculocutaneous albinism. Clinical, ophthalmological, and biochemical characterization." Ophthalmology **92**(11): 1496-1505.

King, R. A. and W. S. Oetting (2003). "Oculocutaneous Albinism Type 2."

King, R. A., J. Pietsch, J. P. Fryer, S. Savage, M. J. Brott, I. Russell-Eggitt, C. G. Summers and W. S. Oetting (2003). "Tyrosinase gene mutations in oculocutaneous albinism 1 (OCA1): definition of the phenotype." Hum Genet **113**(6): 502-513.

King, R. A. and C. G. Summers (1988). "Albinism." Dermatol Clin **6**(2): 217-228.

King, R. A., D. Townsend, W. Oetting, C. G. Summers, D. P. Olds, J. G. White and R. A. Spritz (1991). "Temperature-sensitive tyrosinase associated with peripheral pigmentation in oculocutaneous albinism." J Clin Invest **87**(3): 1046-1053.

King, R. A., J. D. Wirtschafter, D. P. Olds and J. Brumbaugh (1986). "Minimal pigment: a new type of oculocutaneous albinism." Clin Genet **29**(1): 42-50.

Kohl S, J. H., Sharpe LT, Wissinger B. (2004). "Achromatopsia - Rod Monochromatism, Total Color Blindness. Includes: Achromatopsia 1, Achromatopsia 2, Achromatopsia 3, Achromatopsia 4, Achromatopsia 5." Gene Reviews.

Kriss, A., I. Russell-Eggitt and D. Taylor (1990). "Childhood albinism. Visual electrophysiological features." Ophthalmic Paediatr Genet **11**(3): 185-192.

Kromberg, J. G., D. Castle, E. M. Zwane and T. Jenkins (1989). "Albinism and skin cancer in Southern Africa." Clin Genet **36**(1): 43-52.

Kromberg, J. G., D. J. Castle, E. M. Zwane, J. Bothwell, S. Kidson, P. Bartel, J. I. Phillips and T. Jenkins (1990). "Red or rufous albinism in southern Africa." Ophthalmic Paediatr Genet **11**(3): 229-235.

Kromberg, J. G. and T. Jenkins (1982). "Prevalence of albinism in the South African negro." S Afr Med J **61**(11): 383-386.

Kumar, A., I. Gottlob, R. J. McLean, S. Thomas, M. G. Thomas and F. A. Proudlock (2010). "Clinical and oculomotor characteristics of albinism compared to FRMD7 associated infantile nystagmus." Invest Ophthalmol Vis Sci **52**(5): 2306-2313.

Kumar, A., I. Gottlob, R. J. McLean, S. Thomas, M. G. Thomas and F. A. Proudlock (2011). "Clinical and oculomotor characteristics of albinism compared to FRMD7 associated infantile nystagmus." Invest Ophthalmol Vis Sci **52**(5): 2306-2313.

Lahiri, K. and S. R. Sengupta (1998). "A regionwise comparative study of the extent of post punch graft surgical repigmentation in cutaneous achromia." Indian J Dermatol Venereol Leprol **64**(4): 173-175.

Lam, B. L., J. H. Fingert, B. C. Shutt, E. M. Singleton, L. M. Merin, H. H. Brown, V. C. Sheffield and E. M. Stone (1997). "Clinical and molecular characterization of a family affected with X-linked ocular albinism (OA1)." Ophthalmic Genet **18**(4): 175-184.

Lamason, R. L., M. A. Mohideen, J. R. Mest, A. C. Wong, H. L. Norton, M. C. Aros, M. J. Juryneec, X. Mao, V. R. Humphreville, J. E. Humbert, S. Sinha, J. L. Moore, P. Jagadeeswaran, W. Zhao, G. Ning, I. Makalowska, P. M. McKeigue, D. O'Donnell, R. Kittles, E. J. Parra, N. J. Mangini, D. J. Grunwald, M. D. Shriver, V. A. Canfield and K. C. Cheng (2005). "SLC24A5, a putative cation exchanger, affects pigmentation in zebrafish and humans." Science **310**(5755): 1782-1786.

Lauronen, L., R. Jalkanen, J. Huttunen, E. Carlsson, S. Tuupanen, S. Lindh, H. Forsius, E. M. Sankila and T. Alitalo (2005). "Abnormal crossing of the optic fibres shown by evoked magnetic fields in patients with ocular albinism with a novel mutation in the OA1 gene." Br J Ophthalmol **89**(7): 820-824.

Lavado, A., G. Jeffery, V. Tovar, P. de la Villa and L. Montoliu (2006). "Ectopic expression of tyrosine hydroxylase in the pigmented epithelium rescues the retinal abnormalities and visual function common in albinos in the absence of melanin." J Neurochem **96**(4): 1201-1211.

Lee, H., V. Sheth, M. Bibi, G. Maconachie, A. Patel, R. J. McLean, M. Michaelides, M. G. Thomas, F. A. Proudlock and I. Gottlob (2013). "Potential of handheld optical coherence tomography to determine cause of infantile nystagmus in children by using foveal morphology." *Ophthalmology* **120**(12): 2714-2724.

Lee, K. A., R. A. King and C. G. Summers (2001). "Stereopsis in patients with albinism: clinical correlates." *J AAPOS* **5**(2): 98-104.

Leigh, R. J. and D. S. Zee (2006). *The neurology of eye movements*. Oxford, Oxford University Press.

Levin, A. V. and E. Stroh (2011). "Albinism for the busy clinician." *J AAPOS* **15**(1): 59-66.

Lewis, R. A. (1993). Ocular Albinism, X-Linked. *GeneReviews*. R. A. Pagon, T. D. Bird, C. R. Dolan, K. Stephens and M. P. Adam. Seattle (WA).

Lopez, V. M., C. L. Decatur, W. D. Stamer, R. M. Lynch and B. S. McKay (2008). "L-DOPA is an endogenous ligand for OA1." *PLoS Biol* **6**(9): e236.

Loshin, D. S. and R. A. Browning (1983). "Contrast sensitivity in albinotic patients." *Am J Optom Physiol Opt* **60**(3): 158-166.

Luande, J., C. I. Henschke and N. Mohammed (1985). "The Tanzanian human albino skin. Natural history." *Cancer* **55**(8): 1823-1828.

Lund, P. M. (2005). "Oculocutaneous albinism in southern Africa: population structure, health and genetic care." *Ann Hum Biol* **32**(2): 168-173.

Lund, R. D. (1965). "Uncrossed Visual Pathways of Hooded and Albino Rats." *Science* **149**(3691): 1506-1507.

Manga, P., J. Kromberg, A. Turner, T. Jenkins and M. Ramsay (2001). "In Southern Africa, brown oculocutaneous albinism (BOCA) maps to the OCA2 locus on chromosome 15q: P-gene mutations identified." *Am J Hum Genet* **68**(3): 782-787.

Manga, P., J. G. Kromberg, N. F. Box, R. A. Sturm, T. Jenkins and M. Ramsay (1997). "Rufous oculocutaneous albinism in southern African Blacks is caused by mutations in the TYRP1 gene." *Am J Hum Genet* **61**(5): 1095-1101.

McCartney, A. C., D. J. Spalton and T. B. Bull (1985). "Type IV melanosomes of the human albino iris." *Br J Ophthalmol* **69**(7): 537-541.

McMenamin, P. G. (1997). "The distribution of immune cells in the uveal tract of the normal eye." *Eye (Lond)* **11** ( Pt 2): 183-193.

Medeiros, F. A., L. M. Zangwill, C. Bowd, K. Mansouri and R. N. Weinreb (2012). "The structure and function relationship in glaucoma: implications for detection of progression and measurement of rates of change." *Invest Ophthalmol Vis Sci* **53**(11): 6939-6946.

Menasche, G., C. H. Ho, O. Sanal, J. Feldmann, I. Tezcan, F. Ersoy, A. Houdusse, A. Fischer and G. de Saint Basile (2003). "Griscelli syndrome restricted to hypopigmentation results from a melanophilin defect (GS3) or a MYO5A F-exon deletion (GS1)." *J Clin Invest* **112**(3): 450-456.

Merrill, K. S., J. D. Lavoie, R. A. King and C. G. Summers (2004). "Positive angle kappa in albinism." *J AAPOS* **8**(3): 237-239.

Michaelides, M., G. Jeffery and A. T. Moore (2012). "Developmental macular disorders: phenotypes and underlying molecular genetic basis." *Br J Ophthalmol* **96**(7): 917-924.

Miyake, Y., M. Horiguchi, H. Terasaki and M. Kondo (1994). "Scotopic threshold response in complete and incomplete types of congenital stationary night blindness." *Invest Ophthalmol Vis Sci* **35**(10): 3770-3775.

Mohammad, S., I. Gottlob, A. Kumar, M. Thomas, C. Degg, V. Sheth and F. A. Proudlock (2011). "The functional significance of foveal abnormalities in albinism measured using spectral-domain optical coherence tomography." *Ophthalmology* **118**(8): 1645-1652.

Mohammad, S., I. Gottlob, V. Sheth, A. Pilat, H. Lee, E. Pollheimer and F. A. Proudlock (2015). "Characterization of Abnormal Optic Nerve Head Morphology in Albinism Using Optical Coherence Tomography." *Invest Ophthalmol Vis Sci* **56**(8): 4611-4618.

Montoliu, L., K. Gronskov, A. H. Wei, M. Martinez-Garcia, A. Fernandez, B. Arveiler, F. Morice-Picard, S. Riazuddin, T. Suzuki, Z. M. Ahmed, T. Rosenberg and W. Li (2014). "Increasing the complexity: new genes and new types of albinism." *Pigment Cell Melanoma Res* **27**(1): 11-18.

Neveu, M. M. and G. Jeffery (2007). "Chiasm formation in man is fundamentally different from that in the mouse." *Eye (Lond)* **21**(10): 1264-1270.

Newkirk, M. R., S. K. Gardiner, S. Demirel and C. A. Johnson (2006). "Assessment of false positives with the Humphrey Field Analyzer II perimeter with the SITA Algorithm." *Invest Ophthalmol Vis Sci* **47**(10): 4632-4637.

Nowomiejska, K., R. Vonthein, J. Paetzold, Z. Zagorski, R. Kardon and U. Schiefer (2010). "Reaction time during semi-automated kinetic perimetry (SKP) in patients with advanced visual field loss." *Acta Ophthalmol* **88**(1): 65-69.

Nucci, P., B. J. Kushner, M. Serafino and N. Orzalesi (2005). "A multi-disciplinary study of the ocular, orthopedic, and neurologic causes of abnormal head postures in children." *Am J Ophthalmol* **140**(1): 65-68.

O'Donnell, F. E., Jr., W. R. Green, J. A. Fleischman and G. W. Hambrick (1978). "X-linked ocular albinism in Blacks. Ocular albinism cum pigmento." *Arch Ophthalmol* **96**(7): 1189-1192.

Odom, J. V., M. Bach, M. Brigell, G. E. Holder, D. L. McCulloch, A. P. Tormene and Vaegan (2010). "ISCEV standard for clinical visual evoked potentials (2009 update)." *Doc Ophthalmol* **120**(1): 111-119.

Oetting, W. S. and R. A. King (1999). "Molecular basis of albinism: mutations and polymorphisms of pigmentation genes associated with albinism." *Hum Mutat* **13**(2): 99-115.

Onojafe, I. F., D. R. Adams, D. R. Simeonov, J. Zhang, C. C. Chan, I. M. Bernardini, Y. V. Sergeev, M. B. Dolinska, R. P. Alur, M. H. Brilliant, W. A. Gahl and B. P. Brooks (2011). "Nitisinone improves eye and skin pigmentation defects in a mouse model of oculocutaneous albinism." *J Clin Invest* **121**(10): 3914-3923.

Orlow, S. J. (1997). "Albinism: an update." *Semin Cutan Med Surg* **16**(1): 24-29.

Orlow, S. J. (1998). "The biogenesis of melanosomes." *The Pigmentary system*: 97-106.

Pal, B., M. D. Mohamed, T. J. Keen, G. A. Williams, J. A. Bradbury, E. Sheridan and C. F. Inglehearn (2004). "A new phenotype of recessively inherited foveal hypoplasia and anterior segment dysgenesis maps to a locus on chromosome 16q23.2-24.2." *J Med Genet* **41**(10): 772-777.

Podkrajsek, K. T., B. S. Kranjc, T. Hovnik, J. Kovac and T. Battelino (2012). "GPR143 Gene Mutation Analysis In Pediatric Patients With Albinism." *Ophthalmic Genet*.

Poulter, J. A., M. Al-Araimi, I. Conte, M. M. van Genderen, E. Sheridan, I. M. Carr, D. A. Parry, M. Shires, S. Carrella, J. Bradbury, K. Khan, P. Lakeman, P. I. Sergouniotis, A. R. Webster, A. T. Moore, B. Pal, M. D. Mohamed, A. Venkataramana, V. Ramprasad, R. Shetty, M. Saktivel, G. Kumaramanickavel, A. Tan, D. A. Mackey, A. W. Hewitt, S. Banfi, M. Ali, C. F. Inglehearn and C. Toomes (2013). "Recessive mutations in SLC38A8 cause foveal hypoplasia and optic nerve misrouting without albinism." *Am J Hum Genet* **93**(6): 1143-1150.

Prieur, D. S. and A. Rebsam (2017). "Retinal axon guidance at the midline: Chiasmatic misrouting and consequences." *Dev Neurobiol* **77**(7): 844-860.

Raviola, G., M. J. Sagatias and C. Miller (1987). "Intercellular junctions between fibroblasts in connective tissues of the eye of macaque monkeys. A thin section and freeze fracture analysis." *Invest Ophthalmol Vis Sci* **28**(5): 834-841.

Reddy, R. R., B. M. Babu, B. Venkateshwaramma and C. Hymavathi (2011). "Silvery hair syndrome in two cousins: Chediak-Higashi syndrome vs Griscelli syndrome, with rare associations." *Int J Trichology* **3**(2): 107-111.

Rittig, M., E. Lutjen-Drecoll, J. Rauterberg, R. Jander and J. Mollenhauer (1990). "Type-VI collagen in the human iris and ciliary body." *Cell Tissue Res* **259**(2): 305-312.

Roffler-Tarlov, S., J. H. Liu, E. N. Naumova, M. M. Bernal-Ayala and C. A. Mason (2013). "L-Dopa and the albino riddle: content of L-Dopa in the developing retina of pigmented and albino mice." *PLoS One* **8**(3): e57184.

Roggen, X., K. Herman, L. Van Malderen, M. Devos and W. Spileers (2001). "Different strategies for Humphrey automated perimetry: FASTPAC, SITA standard and SITA fast in normal subjects and glaucoma patients." Bull Soc Belge Ophtalmol(279): 23-33.

Rosenberg, T. and M. Schwartz (1998). "X-linked ocular albinism: prevalence and mutations--a national study." Eur J Hum Genet **6**(6): 570-577.

Roudybush, T. E. (1999). "Psittacine nutrition." Vet Clin North Am Exot Anim Pract **2**(1): 111-125, vi-vii.

Rundshagen, U., C. Zuhlke, S. Opitz, E. Schwinger and B. Kasmann-Kellner (2004). "Mutations in the MATP gene in five German patients affected by oculocutaneous albinism type 4." Hum Mutat **23**(2): 106-110.

Rymer, J., V. Choh, S. Bharadwaj, V. Padmanabhan, L. Modilevsky, E. Jovanovich, B. Yeh, Z. Zhang, H. Guan, W. Payne and C. F. Wildsoet (2007). "The albino chick as a model for studying ocular developmental anomalies, including refractive errors, associated with albinism." Exp Eye Res **85**(4): 431-442.

Sames, K. and J. W. Rohen (1978). "Histochemical studies on the glycosaminoglycans in the normal and glaucomatous iris of human eyes." Albrecht Von Graefes Arch Klin Exp Ophthalmol **207**(3): 157-167.

Sampath, V. and H. E. Bedell (2002). "Distribution of refractive errors in albinos and persons with idiopathic congenital nystagmus." Optom Vis Sci **79**(5): 292-299.

Santiago Borrero, P. J., Y. Rodriguez-Perez, J. Y. Renta, N. J. Izquierdo, L. Del Fierro, D. Munoz, N. L. Molina, S. Ramirez, G. Pagan-Mercado, I. Ortiz, E. Rivera-Caragol, R. A. Spritz and C. L. Cadilla (2006). "Genetic testing for oculocutaneous albinism type 1 and 2 and Hermansky-Pudlak syndrome type 1 and 3 mutations in Puerto Rico." J Invest Dermatol **126**(1): 85-90.

Sarvananthan, N., M. Surendran, E. O. Roberts, S. Jain, S. Thomas, N. Shah, F. A. Proudlock, J. R. Thompson, R. J. McLean, C. Degg, G. Woodruff and I. Gottlob (2009). "The prevalence of nystagmus: the Leicestershire nystagmus survey." Invest Ophthalmol Vis Sci **50**(11): 5201-5206.

Schaeffel, F. (2012). "[Clinical risk factors for progressive myopia]." Ophthalmologe **109**(8): 738-748.

Schmitz, B., B. Kasmann-Kellner, T. Schafer, C. M. Krick, G. Gron, M. Backens and W. Reith (2004). "Monocular visual activation patterns in albinism as revealed by functional magnetic resonance imaging." Hum Brain Mapp **23**(1): 40-52.

Schmitz, B., T. Schaefer, C. M. Krick, W. Reith, M. Backens and B. Kasmann-Kellner (2003). "Configuration of the optic chiasm in humans with albinism as revealed by magnetic resonance imaging." Invest Ophthalmol Vis Sci **44**(1): 16-21.

Schmolesky, M. T., Y. Wang, D. J. Creel and A. G. Leventhal (2000). "Abnormal retinotopic organization of the dorsal lateral geniculate nucleus of the tyrosinase-negative albino cat." J Comp Neurol **427**(2): 209-219.

Schnur, R. E., R. L. Nussbaum, L. Anson-Cartwright, C. McDowell, R. G. Worton and M. A. Musarella (1991). "Linkage analysis in X-linked ocular albinism." Genomics **9**(4): 605-613.

Seo, J. H., Y. S. Yu, J. H. Kim, H. K. Choung, J. W. Heo and S. J. Kim (2007). "Correlation of visual acuity with foveal hypoplasia grading by optical coherence tomography in albinism." Ophthalmology **114**(8): 1547-1551.

Seyal, M., S. Sato, B. G. White and R. J. Porter (1981). "Visual evoked potentials and eye dominance." Electroencephalogr Clin Neurophysiol **52**(5): 424-428.

Shallo-Hoffmann, J., M. Faldon and R. J. Tusa (1999). "The incidence and waveform characteristics of periodic alternating nystagmus in congenital nystagmus." Invest Ophthalmol Vis Sci **40**(11): 2546-2553.

Shatz, C. (1977). "A comparison of visual pathways in Boston and Midwestern Siamese cats." J Comp Neurol **171**(2): 205-228.

Shiono, T., M. Tsunoda, Y. Chida, M. Nakazawa and M. Tamai (1995). "X linked ocular albinism in Japanese patients." Br J Ophthalmol **79**(2): 139-143.

Smith, S. D., P. M. Kelley, J. B. Kenyon and D. Hoover (2000). "Tietz syndrome (hypopigmentation/deafness) caused by mutation of MITF." *J Med Genet* **37**(6): 446-448.

Snell, R. S. and M. A. Lemp (1989). *Clinical anatomy of the eye*, Blackwell Scientific.

Soong, F., A. V. Levin and C. A. Westall (2000). "Comparison of techniques for detecting visually evoked potential asymmetry in albinism." *J AAPOS* **4**(5): 302-310.

St John, R. and B. Timney (1981). "Sensitivity deficits consistent with aberrant crossed visual pathways in human albinos." *Invest Ophthalmol Vis Sci* **21**(6): 873-877.

Stevens, D. J. and R. W. Hertle (2003). "Relationships between visual acuity and anomalous head posture in patients with congenital nystagmus." *J Pediatr Ophthalmol Strabismus* **40**(5): 259-264; quiz 297-258.

Stone, R. A., T. Lin, A. M. Laties and P. M. Iuvone (1989). "Retinal dopamine and form-deprivation myopia." *Proc Natl Acad Sci U S A* **86**(2): 704-706.

Sturm, R. A. and T. N. Frudakis (2004). "Eye colour: portals into pigmentation genes and ancestry." *Trends Genet* **20**(8): 327-332.

Sturm, R. A. and M. Larsson (2009). "Genetics of human iris colour and patterns." *Pigment Cell Melanoma Res* **22**(5): 544-562.

Summers, C. G. (1996). "Vision in albinism." *Trans Am Ophthalmol Soc* **94**: 1095-1155.

Summers, C. G., J. E. Connett, A. M. Holleschau, J. L. Anderson, I. De Becker, B. S. McKay and M. H. Brilliant (2014). "Does levodopa improve vision in albinism? Results of a randomized, controlled clinical trial." *Clin Exp Ophthalmol* **42**(8): 713-721.

Summers, C. G., W. H. Knobloch, C. J. Witkop, Jr. and R. A. King (1988). "Hermansky-Pudlak syndrome. Ophthalmic findings." *Ophthalmology* **95**(4): 545-554.

Suzuki, T. and M. Hayashi (2005). "Oculocutaneous Albinism Type 4."

Swanson, E. A., J. A. Izatt, M. R. Hee, D. Huang, C. P. Lin, J. S. Schuman, C. A. Puliafito and J. G. Fujimoto (1993). "In vivo retinal imaging by optical coherence tomography." *Opt Lett* **18**(21): 1864-1866.

Tarpey, P., S. Thomas, N. Sarvananthan, U. Mallya, S. Lisgo, C. J. Talbot, E. O. Roberts, M. Awan, M. Surendran, R. J. McLean, R. D. Reinecke, A. Langmann, S. Lindner, M. Koch, S. Jain, G. Woodruff, R. P. Gale, A. Bastawrous, C. Degg, K. Droutsas, I. Asproudis, A. A. Zubcov, C. Pieh, C. D. Veal, R. D. Machado, O. C. Backhouse, L. Baumber, C. S. Constantinescu, M. C. Brodsky, D. G. Hunter, R. W. Hertle, R. J. Read, S. Edkins, S. O'Meara, A. Parker, C. Stevens, J. Teague, R. Wooster, P. A. Futreal, R. C. Trembath, M. R. Stratton, F. L. Raymond and I. Gottlob (2006). "Mutations in FRMD7, a newly identified member of the FERM family, cause X-linked idiopathic congenital nystagmus." *Nat Genet* **38**(11): 1242-1244.

Taylor, K., C. Powell, S. R. Hatt and C. Stewart (2012). "Interventions for unilateral and bilateral refractive amblyopia." *Cochrane Database Syst Rev*(4): CD005137.

Thomas, M. G., M. Crosier, S. Lindsay, A. Kumar, S. Thomas, M. Araki, C. J. Talbot, R. J. McLean, M. Surendran, K. Taylor, B. P. Leroy, A. T. Moore, D. G. Hunter, R. W. Hertle, P. Tarpey, A. Langmann, S. Lindner, M. Brandner and I. Gottlob (2011). "The clinical and molecular genetic features of idiopathic infantile periodic alternating nystagmus." *Brain* **134**(Pt 3): 892-902.

Thomas, M. G. and I. Gottlob (2012). "Optical coherence tomography studies provides new insights into diagnosis and prognosis of infantile nystagmus: a review." *Strabismus* **20**(4): 175-180.

Thomas, M. G., A. Kumar, S. Mohammad, F. A. Proudlock, E. C. Engle, C. Andrews, W. M. Chan, S. Thomas and I. Gottlob (2011). "Structural grading of foveal hypoplasia using spectral-domain optical coherence tomography a predictor of visual acuity?" *Ophthalmology* **118**(8): 1653-1660.

Thomas, M. G., G. Maconachie, V. Sheth, R. J. McLean and I. Gottlob (2017). "Development and clinical utility of a novel diagnostic nystagmus gene panel using targeted next-generation sequencing." *Eur J Hum Genet* **25**(6): 725-734.

Thomas, S., F. A. Proudlock, N. Sarvananthan, E. O. Roberts, M. Awan, R. McLean, M. Surendran, A. S. Kumar, S. J. Farooq, C. Degg, R. P. Gale, R. D. Reinecke, G. Woodruff, A.

Langmann, S. Lindner, S. Jain, P. Tarpey, F. L. Raymond and I. Gottlob (2008). "Phenotypical characteristics of idiopathic infantile nystagmus with and without mutations in FRMD7." Brain **131**(Pt 5): 1259-1267.

Thompson, I. D., J. E. Morgan and Z. Henderson (1993). "The effects of monocular enucleation on ganglion cell number and terminal distribution in the ferret's retinal pathway." Eur J Neurosci **5**(4): 357-367.

Tick, S., F. Rossant, I. Ghorbel, A. Gaudric, J. A. Sahel, P. Chaumet-Riffaud and M. Paques (2011). "Foveal shape and structure in a normal population." Invest Ophthalmol Vis Sci **52**(8): 5105-5110.

Timms, C., D. Thompson, I. Russell-Eggitt and R. Clement (2006). "Saccadic instabilities in albinism without nystagmus." Exp Brain Res **175**(1): 45-49.

Trantow, C. M., M. Mao, G. E. Petersen, E. M. Alward, W. L. Alward, J. H. Fingert and M. G. Anderson (2009). "Lyst mutation in mice recapitulates iris defects of human exfoliation syndrome." Invest Ophthalmol Vis Sci **50**(3): 1205-1214.

Ung, T., L. E. Allen, A. T. Moore, D. Trump, I. Zito, A. J. Hardcastle, J. Yates and K. Bradshaw (2005). "Is optic nerve fibre mis-routing a feature of congenital stationary night blindness?" Doc Ophthalmol **111**(3): 169-178.

van Genderen, M. M., F. C. Riemsdag, J. Schuil, F. P. Hoeben, J. S. Stilma and F. M. Meire (2006). "Chiasmal misrouting and foveal hypoplasia without albinism." Br J Ophthalmol **90**(9): 1098-1102.

Vingrys, A. J. and S. Demirel (1998). "False-response monitoring during automated perimetry." Optom Vis Sci **75**(7): 513-517.

Vogel, P., R. W. Read, R. B. Vance, K. A. Platt, K. Troughton and D. S. Rice (2008). "Ocular albinism and hypopigmentation defects in Slc24a5<sup>-/-</sup> mice." Vet Pathol **45**(2): 264-279.

Walsh, M. K. and M. F. Goldberg (2007). "Abnormal foveal avascular zone in nanophthalmos." Am J Ophthalmol **143**(6): 1067-1068.

Walsh, R. J. (1971). "A distinctive pigment of the skin in New Guinea indigenes." Ann Hum Genet **34**(4): 379-388.

Wang, B., L. M. Sakata, D. S. Friedman, Y. H. Chan, M. He, R. Lavanya, T. Y. Wong and T. Aung (2010). "Quantitative iris parameters and association with narrow angles." Ophthalmology **117**(1): 11-17.

Wang, C., F. Brancusi, Z. M. Valivullah, M. G. Anderson, D. Cunningham, A. Hedberg-Buenz, B. Power, D. Simeonov, W. A. Gahl, W. M. Zein, D. R. Adams and B. Brooks (2018). "A novel iris transillumination grading scale allowing flexible assessment with quantitative image analysis and visual matching." Ophthalmic Genet **39**(1): 41-45.

Wang, J., L. M. Wyatt, J. Felius, D. R. Stager, Jr., D. R. Stager, Sr., E. E. Birch and H. E. Bedell (2010). "Onset and progression of with-the-rule astigmatism in children with infantile nystagmus syndrome." Invest Ophthalmol Vis Sci **51**(1): 594-601.

Wang, T., C. T. Waters, T. Jakins, J. R. Yates, D. Trump, K. Bradshaw and A. T. Moore (2005). "Temperature sensitive oculocutaneous albinism associated with missense changes in the tyrosinase gene." Br J Ophthalmol **89**(10): 1383-1384.

Wei, A. H., D. J. Zang, Z. Zhang, X. Z. Liu, X. He, L. Yang, Y. Wang, Z. Y. Zhou, M. R. Zhang, L. L. Dai, X. M. Yang and W. Li (2013). "Exome sequencing identifies SLC24A5 as a candidate gene for nonsyndromic oculocutaneous albinism." J Invest Dermatol **133**(7): 1834-1840.

Welton, T., S. Ather, F. A. Proudlock, I. Gottlob and R. A. Dineen (2017). "Altered whole-brain connectivity in albinism." Hum Brain Mapp **38**(2): 740-752.

Wheat, J. L., N. V. Rangaswamy and R. S. Harwerth (2012). "Correlating RNFL thickness by OCT with perimetric sensitivity in glaucoma patients." J Glaucoma **21**(2): 95-101.

Wildsoet, C. F., P. J. Oswald and S. Clark (2000). "Albinism: its implications for refractive development." Invest Ophthalmol Vis Sci **41**(1): 1-7.

Wilkerson, C. L., N. A. Syed, M. R. Fisher, N. L. Robinson, I. H. Wallow and D. M. Albert (1996). "Melanocytes and iris color. Light microscopic findings." Arch Ophthalmol **114**(4): 437-442.

Wilk, M. A., A. L. Huckenpahler, R. F. Collery, B. A. Link and J. Carroll (2017). "The Effect of Retinal Melanin on Optical Coherence Tomography Images." *Transl Vis Sci Technol* 6(2): 8.

Willermain, F., C. Deflorenne, C. Bouffieux, X. Janssens, P. Koch and L. Caspers (2010). "Uveitis-like syndrome and iris transillumination after the use of oral moxifloxacin." *Eye (Lond)* 24(8): 1419; author reply 1419-1420.

Williams, K. M., V. J. Verhoeven, P. Cumberland, G. Bertelsen, C. Wolfram, G. H. Buitendijk, A. Hofman, C. M. van Duijn, J. R. Vingerling, R. W. Kuijpers, R. Hohn, A. Mirshahi, A. P. Khawaja, R. N. Luben, M. G. Erke, T. von Hanno, O. Mahroo, R. Hogg, C. Gieger, A. Cougnard-Gregoire, E. Anastasopoulos, A. Bron, J. F. Dartigues, J. F. Korobelnik, C. Creuzot-Garcher, F. Topouzis, C. Delcourt, J. Rahi, T. Meitinger, A. Fletcher, P. J. Foster, N. Pfeiffer, C. C. Klaver and C. J. Hammond (2015). "Prevalence of refractive error in Europe: the European Eye Epidemiology (E(3)) Consortium." *Eur J Epidemiol* 30(4): 305-315.

Wirtschafter, J. D., W. L. Becker, J. B. Howe and B. R. Younge (1982). "Glaucoma visual field analysis by computed profile of nerve fiber function in optic disc sectors." *Ophthalmology* 89(3): 255-267.

Witkop, C. J., M. Nunez Babcock, G. H. Rao, F. Gaudier, C. G. Summers, F. Shanahan, K. R. Harmon, D. Townsend, H. O. Sedano, R. A. King and et al. (1990). "Albinism and Hermansky-Pudlak syndrome in Puerto Rico." *Bol Asoc Med P R* 82(8): 333-339.

Yahalom, C., V. Tzur, A. Blumenfeld, G. Greifner, D. Eli, A. Rosenmann, S. Glanzer and I. Anteby (2012). "Refractive profile in oculocutaneous albinism and its correlation with final visual outcome." *Br J Ophthalmol* 96(4): 537-539.

Yip, L. W., N. Sothornwit, J. Berkowitz and F. S. Mikelberg (2009). "A comparison of interocular differences in patients with pigment dispersion syndrome." *J Glaucoma* 18(1): 1-5.

Yonehara, K., M. Fiscella, A. Drinnenberg, F. Esposti, S. Trenholm, J. Krol, F. Franke, B. G. Scherf, A. Kusnyerik, J. Muller, A. Szabo, J. Juttner, F. Cordoba, A. P. Reddy, J. Nemeth, Z. Z. Nagy, F. Munier, A. Hierlemann and B. Roska (2016). "Congenital Nystagmus Gene FRMD7 Is Necessary for Establishing a Neuronal Circuit Asymmetry for Direction Selectivity." *Neuron* 89(1): 177-193.

Zhao, H. and R. E. Boissy (1994). "Distinguishing between the catalytic potential and apparent expression of tyrosinase activities." *Am J Med Sci* 308(6): 322-330.

Zubko, M. K. and A. Day (1998). "Stable albinism induced without mutagenesis: a model for ribosome-free plastid inheritance." *Plant J* 15(2): 265-271.

Zuhlke, C., A. Stell and B. Kasmann-Kellner (2007). "[Genetics of oculocutaneous albinism]." *Ophthalmologie* 104(8): 674-680.

